DOCTOR OF PHILOSOPHY

The signalling pathways allowing hormonal regulation of Na+ transport in murine collecting duct cells

Mansley, Morag K.

Award date:
2010

DOCTOR OF PHILOSOPHY

The signalling pathways allowing hormonal regulation of Na+ transport in murine collecting duct cells

Morag K. Mansley

2010

University of Dundee

The Signalling Pathways Allowing Hormonal Regulation of Na^+ transport in Murine Collecting Duct Cells.

Morag K. Mansley

A dissertation submitted in fulfilment of the requirements for the degree of Doctor of Philosophy.

Centre for Cardiovascular and Lung Biology

University of Dundee

July 2010

Contents

List of Figures

Chapter 1

Chapter 2

Chapter 3

Chapter 4

Chapter 5

Chapter 6

List of Tables

Chapter 2

Chapter 3

Chapter 4

Chapter 5

Chapter 6

List of Abbreviations

11-βHSDH	11-beta Hydroxysteroid Dehydrogenase
AGC kinases	Protein Kinase A / Protein Kinase G / Protein Kinase C family
Akt	Protein Kinase B
AME	Apparent Mineralocorticoid Excess Syndrome
ANOVA	Analysis of Variance
AQP2	Aquaporin 2
ASDN	Aldosterone Sensitive Distal Nephron
ASIC	Acid Sensing Ion Channel
ATP	Adenosine Triphosphate
AVP	Arginine Vasopressin
BCS	Bovine Calf Serum
cAMP	Cyclic Adenosine Monophosphate
CCD	Cortical Collecting Duct
CFTR	Cystic Fibrosis Transmembrane Conducance Regulator
CK2	Casein Kinase 2
CREB	cAMP Response Element Binding Protein
Dex	Dexamethasone
DMEM	Dulbecco's Modified Eagle Media
DMSO	Dimethyl Sulfoxide
EDTA	Ethylenediaminetetraacetic Acid
EGF	Epidermal Growth Factor
EGTA	Ethylene Glycol-bis-N,N,N',N'-tetraacetic Acid
EIPA	5-(N-Ethyl-N-isopropyl) Amiloride

ENaC	Epithelial Sodium Channel
ERK	Extracellular Regulated Kinase
FBS	Foetal Bovine Serum
FDLE	Foetal Distal Lung Epithelial Cells
GILZ	Glucocorticoid-inducible Leucine Zipper Protein
GR	Glucocorticoid Receptor
GSK3	Glycogen Synthase Kinase 3
HIPK	Homeo-domain Interacting Protein Kinase
IC_{50}	Concentration Needed for 50% Inhibition
ΔI_{eq}	Change in Equivalent Short Circuit Current
I_{eq}	Equivalent Short Circuit Current
I_{SC}	Short Circuit Current
IRS	Insulin Receptor Substrates
Ki-Ras2A	Kirsten Ras GTP-binding protein 2A
MAPK	Mitogen-activated Protein Kinase
MDCK	Madine Darby Canine Kidney
mLST8	Mammalian Lethal with Sec Thirteen
MR	Mineralocorticoid Receptor
mRNA	Messenger Ribosomal Nucleic Acid
mSin1	Mammalian Stress-activated MAP Kinase Interacting Protein 1
mTOR	Mammalian Target of Rapamycin
mTORC1	Mammalian Target of Rapamycin Complex 1
mTORC2	Mammalian Target of Rapamycin Complex 2
N	Number of Channels

NDRG1	N-myc Downstream Regulated Gene 1
Nedd4-2	Neural Precursor Cell-Expressed Developmentally Down-regulated Protein 4
NHE_3	Na^+ / H^+ exchanger 3
NKCC2	$Na^+ / K^+ / 2Cl^-$ cotransporter 2
nSRE	Negative Steroid Response Element
P_o	Open Probability
P70-S6K	70 kDa Ribosomal S6 Kinase
PBS	Phosphate Buffered Saline
PH domain	Pleckstrin Homology Domain
PI3-kinase	Phosphoinositide-3-kinase
PDK1	Phosphoinositde-dependent Protein Kinase 1
PHA-I	Pseudohypoaldosteronism Type I
PIMK1	Provirus Integration Site for Moloney Murine Leukaemia Virus Kinase 1
PIP_2	Phosphatidylinositol 3,5-bisphosphate
PIP_3	Phosphatidylinositol 3,4,5-trisphosphate
PKA	Adenine Nucleotide-dependent Protein Kinase
PLK1	Polo-like Kinase 1
PPARγ	Peroxisome-proliferator Actviated Receptor Gamma
PRAS40	40 kDa Proline-rich Substrate of Akt
PROTOR	Protein Observed with Rictor
PY motif	Proline-rich Motif
RAPTOR	Regulatory-associated Protein of TOR

RICTOR	Rapamycin-insensitive Companion of TOR
R_t	Transepithelial Resistance
SDS	Sodium Dodecyl Sulphate
S.E.M.	Standard Error of the Mean
siRNA	Small Interefering Ribonucleic Acid
SGK1	Serum and Glucocorticoid-Regulated Kinase 1
SmMLCK	Smooth-muscle Myosin Light-chain Kinase
SRE	Steroid Response Element
TBS-T	Tris-buffered Saline with Tween
TEMED	Tetramethylethylenediamine
TZD	Thiazolidinediones
V_t	Transepithelial Voltage

Acknowledgements

Firstly I would like to thank my supervisor Dr. Stuart Wilson for giving me the chance to conduct my research in the Centre for Cardiovascular and Lung Biology at the University of Dundee. I would like to thank Stuart for his support and patience throughout my PhD project and for giving me the opportunity to travel to several international conferences to communicate my work as well as attending the Microelectrode Technique Workshop in Plymouth. I would also like to thank the Medical Research Council for providing the funding needed to carry out this research.

I would like to thank all of the past and present members of our lab group, particularly Dr. Sarah Inglis for help with the Ussing chamber technique. I would also like to thank all the staff in the Centre for Cardiovascular and Lung Biology.

I must also thank Sir Professor Phillip Cohen, Professor Dario Alessi and Professor Carol MacKintosh for providing the NDRG1 antibody which has been so useful as well as the plethora of other antibodies and inhibitors used in this research.

Finally special thanks must go to my family for providing unfaltering support and guidance whilst undertaking this degree. Thanks to the many friends I have met in Dundee as well as those from Aberdeen who I have made great memories with. Finally a particular thanks to Michael for all of his encouragement and support.

Declaration

I hereby declare this thesis to have been composed by myself, and has not been accepted in any previous application for a higher degree. The work of which this thesis is a record, has been carried out by myself, except where specifically acknowledged, and all sources of information have been acknowledged by means of reference.

Signature of Candidate

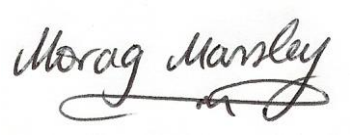

Morag K Mansley BSc (Hons)

Supervisor Statement

I certify that Morag Mansley has fulfilled the conditions of ordinance 39 and of the relevant regulations, such that she is qualified to submit this thesis in application for the higher degree of Doctor of Philosophy.

Signature of Supervisor

Dr. Stuart M Wilson

Abstract

The collecting duct of the distal nephron marks the final location where adjustments to Na^+ excretion can be made, therefore determining the final concentration of Na^+ conserved in the extracellular fluid which plays a role in governing overall blood volume and pressure. This transport of Na^+ is subject to hormonal regulation but the signalling pathways underpinning this regulation however, are not fully understood. In this thesis the signalling pathways allowing both basal and insulin-stimulated Na^+ absorption were explored in the murine collecting duct cell line, mpkCCDcl4. The effects of two insulin-sensitizing drugs, TZDs, on ENaC-mediated Na^+ transport were investigated and the signalling pathways underlying two other hormonal regulators of ENaC, dexamethasone and vasopressin, were also examined.

Unstimulated monolayers of mpkCCDcl4 cells generated spontaneous Na^+ absorption which was quantified by measuring equivalent short circuit current (I_{eq}). Selective inhibition of PI3-kinase, mTORC2 and SGK1 left ~80 % of the current intact, indicating these signalling molecules are not required for basal Na^+ transport. Acute addition of insulin stimulated I_{eq} and this occurred with a concomitant increase in mTORC2, SGK1 and Akt activity. Inhibition of PI3-kinase abolished the insulin-stimulated response as well as phosphorylation of downstream substrates, indicating a crucial role of PI3-kinase. Inhibition of mTORC1 with rapamycin did not alter basal or insulin-stimulated Na^+ transport. The mTOR inhibitors TORIN1 and PP242 could therefore be used to evaluate the role of mTORC2. These inhibitors greatly reduced insulin-stimulated ENaC-mediated Na^+ transport and also abolished SGK1 and mTORC2 activity, indicating a novel role of mTORC2. An inhibitor of SGK1, GSK650394A abolished insulin-stimulated Na^+ transport and specifically inhibited SGK1 acitivty demonstrating the importance of SGK1 in insulin signalling. The inhibitor Akti-1/2 also abolished insulin-mediated Na^+ transport but this compound inhibited both Akt and SGK1 activity. The TZDs pioglitazone and rosiglitazone

did not alter basal or insulin-stimulated Na^+ transport and had no effect on SGK1 activity indicating these drugs do not alter Na^+ absorption in this cell line.

Dexamethasone stimulated ENaC-mediated Na^+ transport in a similar manner to insulin and this could be blocked with rapamycin. This drug did not alter phosphorylation of NDRG1 indicating that dexamethasone stimulates Na^+ transport in an mTORC1-dependent manner but without altering SGK1 activity. Arginine vasopressin also stimulated I_{eq} but did so by reducing R_t with an associated depolarisation of V_t. I_{eq} could be blocked with amiloride and vasopressin-stimulated I_{eq} was insensitive to TORIN1 and PP242. Vasopressin suppressed SGK1 phosphorylation of NDRG1 but did stimulate protein kinase A (PKA) activity. Therefore vasopressin stimulates I_{eq} via a PKA-dependent but mTOR- and SGK1-independent pathway.

Chapter 1 - Introduction

1.1 Thesis overview

The regulation of body fluid and volume is fundamental to blood pressure regulation. The kidneys play a vital role in this by filtering blood and selectively absorbing and secreting electrolytes, water, nutrients and hormones as well as waste products. Alterations to electrolyte transport along the nephrons in the kidney, in particular Na^+ transport, have a critical effect on water movement. The final adjustments to Na^+ retention are made in the collecting duct of the nephron and are subject to hormonal control and these hormones alter the activity of epithelial sodium channels, ENaCs.

Whilst the natriferic effects of these hormones have been clearly demonstrated the signalling pathways underpinning these responses are not so clear. The scope of this thesis has been to investigate the signalling pathways allowing both spontaneous and insulin-stimulated Na^+ transport in the collecting duct cell line, mpkCCDcl4. The effects of two other hormones, dexamethasone and arginine vasopressin were also examined. The mpkCCDcl4 cell line has previously been shown to exhibit spontaneous Na^+ absorption that can be hormonally regulated (Bens *et al.*, 1999, Shane *et al.*, 2006, Nofziger *et al.*, 2005, Robert-Nicoud *et al.*, 2001). Here the basal properties of these cells have been confirmed as well as the effect of acute stimulation with insulin (Chapter 3). Furthermore the effects of two TZDs upon basal and insulin-stimulated Na^+ transport as well as SGK1 activity were investigated (Chapter 3). The role of PI3-kinase and mTORC1 under both basal and insulin-stimulated conditions were examined (Chapter 4). Using two novel inhibitors, Akti-1/2 and GSK650394A, the relative importance of both Akt

and SGK1 in spontaneous and insulin-stimulated Na^+ transport was investigated (Chapter 5). Finally, the novel inhibitors PP242 and TORIN1 were used to target mTORC2 to investigate the role of this signalling molecule in basal Na^+ absorption as well as under insulin-stimulated conditions (Chapter 6). The stimulatory effects of the glucocorticoid dexamethasone and the peptide hormone arginine vasopressin on basal Na^+ absorption were also quantified and the effects of TORIN1 and PP242 investigated (Chapter 6).

This introduction provides a brief and general overview of the structure and function of the kidneys as well as a description of salt transport that takes place across the epithelia lining the distal nephron. The epithelial Na^+ channel ENaC is then discussed in more detail, in particular previous studies regarding hormonal control of this channel and the signalling pathways proposed to be involved. Whilst this introduction provides a broad overview of previous work carried out, each chapter begins with a more specific introduction relevant to the particular signalling molecule(s) of interest. Similarly, each chapter closes with a specific discussion relevant to the data presented but an overall general discussion is given at the end of this thesis. Values of electrical parameters measured in larger scale experiments can be found in the appendix (Chapter 9).

1.2 Salt transport in the kidney

1.2.1 Structure and function of the kidneys

The kidneys are bean-shaped organs that lie behind the peritoneum of the abdominal cavity. They have several important functions in the body including excretion of metabolic breakdown products and toxins from the blood and the regulation of water and electrolyte balance (Koeppen and Stanton, 2007a). The kidneys also regulate acid base balance as well as the production or activation of hormones involved in erythropoeisis and the regulation of blood pressure and flow (Boron and Boulpaep, 2009b). Despite accounting for only 0.5 % of total body weight together, the kidneys receive ~ 25 % of the body's cardiac output (Koeppen and Stanton, 2007a). Blood enters the kidney via the renal artery at the hilus and subsequently splits into smaller arteries that extend into the medulla and cortex. These arteries finally split into afferent arterioles that feed blood into the nephrons of the kidney.

The nephron is the functional unit of a kidney and consists of a renal corpuscle (including a glomerulus, Bowman's capsule and Bowman's space) and a looped tubule. There are around one million nephrons in each human kidney and their function is to filter the blood across the glomerulus in the renal corpuscle into the Bowman's capsule leading to the tubule where urine is formed (Boron and Boulpaep, 2009b). The filtrate is mainly composed of electrolytes including Na^+, K^+ and Cl^- since larger proteins cannot permeate across the glomerulus. The kidney filters ~ 180 L of blood per day but only ~ 2 L of this will leave the body

as urine. Therefore one of the main functions of the renal tubule is the reabsorption of electrolytes and water (Koeppen and Stanton, 2007a). This reabsorption takes place along the tubule of the nephron which can be split up into different subsections starting with the proximal convoluted tubule which exits the Bowman's capsule followed by the proximal straight tubule (Koeppen and Stanton, 2007a). This leads into the loop of Henle which stretches down into the medulla and loops back up to the cortex where it becomes the distal convoluted tubule, the connecting tubule and collecting duct (cortical, outer medullary and inner medullary). The collecting duct stretches back down through the medulla and feeds into the renal pelvis leading to the ureter which connects to the bladder (Boron and Boulpaep, 2009b). The absorption of fluid and electrolytes along the tubule of the nephron occurs across epithelial cells lining the tubule.

1.2.2 Epithelia

Epithelial cells form a continuous sheet that lines the multiple segments of the renal tubules and it is across these cells that electrolytes and water are reabsorbed (Koeppen and Stanton, 2007b). Epithelia are characterised by tight junctions that couple cells together and this gives rise to polarised epithelia. Coupled cells have an apical membrane on one side of the tight junction facing the lumen of the tubule and a basolateral membrane on the other facing the extracellular fluid (Wills *et al.*, 1996). This polarity allows differential expression of transport proteins including ion channels and solute transporters. In the body it is the epithelium that comes into contact with the outside world, lining the airways and alveoli, oesophagus, stomach, intestine as well as the tubules of the kidney

(Butterworth *et al.*, 2009). These cells act as a barrier to the external environment but also allow selective movement of electrolytes and non-electrolytes between the external and internal compartments (Wills *et al.*, 1996). Epithelia can be classed as "leaky" or "tight" depending on the permeability of the tight junctions. Along the nephron beginning at the proximal convoluted tubule, epithelia are leaky but become tighter towards the distal nephron (Boron and Boulpaep, 2009c). This has bearing on transport since water and electrolytes can travel in both a transcellular (via transporters across the membrane) and a paracellular (via tight juntions) manner (Koeppen and Stanton, 2007b). The distal nephron is lined with tight epithelia which gives rise to transcellular electrolyte transport (Boron and Boulpaep, 2009c).

1.2.3 Salt transport along the nephron

The absorption of Na^+ in the kidney is the most important determinant of the extracellular fluid and blood volume. This is due to Na^+ movement creating a negative lumen which favours Cl^- absorption and the combined movement of NaCl creates an osmotic gradient that water will follow (Butterworth *et al.*, 2009). The kidney can alter how much salt and therefore water is reabsorbed and this will also determine urine concentration. Along the nephron Na^+ mainly moves across the epithelium in a transcellular manner, passively crossing the apical membrane of the epithelia via transporters specific to the segment of the tubule (Koeppen and Stanton, 2007b). This passive movement occurs due to a favourable electrochemical gradient for Na^+ entry into the cell, generated by a low intracellular concentration of Na^+ and a negatively charged cytosol with respect to

the lumen. Once inside the cell, Na^+ is extruded across the basolateral membrane by Na^+ / K^+ ATPase pumps where three Na^+ leave the cell in place of two K^+ entering; this action maintains the driving force for Na^+ entry (Boron and Boulpaep, 2009c). The intracellular K^+ then recycles out of the cell via ion channels in the basolateral and / or apical membrane depending on the segment of the nephron.

The bulk of Na^+ absorption along the nephron occurs across the proximal convoluted tubule, around 67 % of the filtered load, followed by a further 25 % in the thick ascending limb of the Loop of Henle. Only around 8 % of the filtrate remains as it moves into the distal tubule and collecting ducts (Boron and Boulpaep, 2009b). The proximal tubule and Loop of Henle are subject to tubuloglomerular feedback where increased fluid and Na^+ reaching the distal nephron will signal a decrease in the glomerular filtration rate. In contrast, transport across the distal nephron, in particular the collecting duct, are finely controlled by various hormones and bioactive factors (Koeppen and Stanton, 2007b). The transport of Na^+ across the collecting duct marks the final location where adjustments to Na^+ retention can be made (Pratt, 2005). The epithelium of this part of the tubule is characteristically very tight, and large potential differences across the membrane arise (Boron and Boulpaep, 2009c). The pathway for apical Na^+ entry in this part of the tubule is via the epithelial Na^+ channel, ENaC, and similar to the proximal parts of the tubule, Na^+ / K^+ ATPase pumps mediate extrusion of Na^+ out of the cell and into the blood (Kellenberger and Schild, 2002). Figure 1.1 shows the major ion transporters present in principal

cells of the collecting duct. The apically expressed ENaCs mark the rate-limiting step of Na^+ transport and are a target of hormones and other factors that regulate the fine control of Na^+ and fluid balance in the final segment of the tubule (Bhalla and Hallows, 2008). The importance of these channels in regulating blood pressure has been highlighted by the discovery that several monogenic forms of hypertension are caused by mutations in the genes encoding ENaC (Hummler and Horisberger, 1999), this is discussed in more detail below.

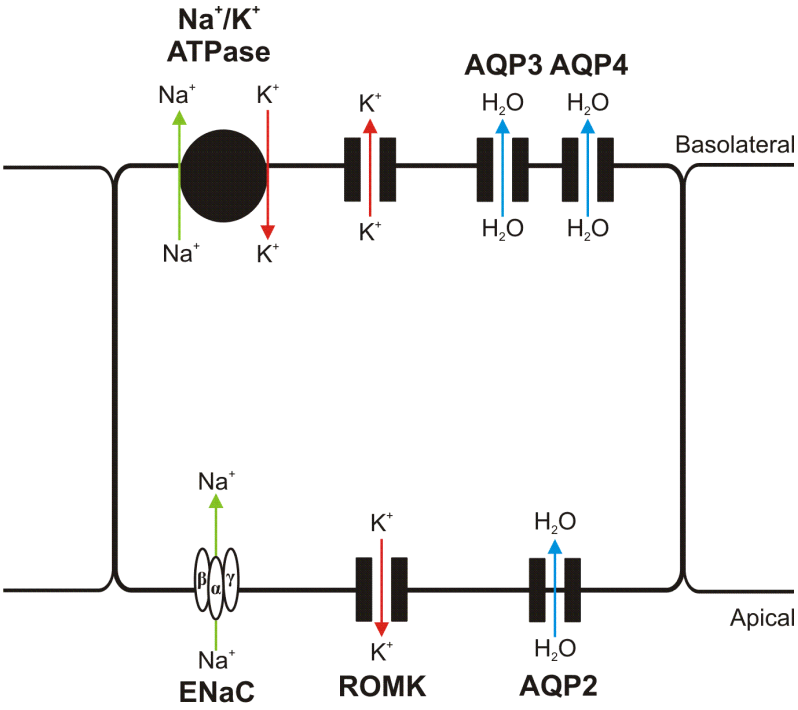

Figure 1.1 Ion transporters in principal cells of the collecting duct.

Simplified schematic showing ion transporters present in principal cells of the collecting duct. In the apical membrane ENaC mediates Na^+ entry into the cell and Na^+ is then extruded across the basolateral membrane via the Na^+ / K^+ ATPase. The K^+ that enters via the pump can leave via basolaterally expressed K^+ channels or via the Rat Outer Medullary K^+ channel (ROMK) in the apical membrane. Water is absorbed via the apically expressed Aquaporin 2 (AQP2) and the basolaterally expressed Aquaporin 3 (AQP3) and Aquaporin 4 (AQP4).

1.3 ENaC

1.3.1 Expression and function

The epithelial Na^+ channel, ENaC, is primarily expressed in lung, colon, sweat and salivary ducts as well as the distal nephron (Garty and Palmer, 1997). These channels are located in the apical membrane of the epithelia lining these tissues and mark the initial step of transcellular Na^+ transport. In the lung this Na^+ transport, in tandem with Cl^- secretion via the cystic fibrosis transmembrane conductance regulator (CFTR), maintains the surface liquid lining the airways allowing normal respiratory function (Kellenberger and Schild, 2002). Furthermore, these channels play a vital role in clearing the fluid-filled foetal lung at birth (Kamynina and Staub, 2002). ENaC also functions to absorb salt from the secretions of exocrine glands including sweat, mammary and salivary glands (Garty and Palmer, 1997). In the kidney, ENaC is responsible for salt reuptake from the filtrate in the lumen and therefore plays an important role in the maintenance of overall blood volume and pressure. ENaC is highly sensitive to the K^+-sparing diuretic amiloride (and its analogues) and triamterene (Snyder, 2002).

ENaC is composed of three subunits: α, β and γ which share ~ 30-35% amino acid sequence homology (Canessa *et al.*, 1994). α-ENaC was initially cloned from rat colon and generated a small, amiloride-sensitive current when expressed in oocytes (Canessa *et al.*, 1993, Lingueglia *et al.*, 1993). β- and γ-ENaC were identified through functional complementation of α-ENaC in oocytes (Canessa *et*

al., 1994). Only α-ENaC can form a functional channel on its own, but when expressed with both β- and γ-ENaC, a 100-fold potentiation in amiloride-sensitive current was observed over that recorded from α-ENaC expressed alone (Canessa *et al.*, 1994). Each subunit is made up of two membrane spanning domains, intracellular N- and C-termini and a large extracellular loop that contains several glycosylation sites (Snyder *et al.*, 1994).

Whilst α-, β- and γ-subunits are required to form a functional ENaC, the stoichiometry of this channel remains unclear. Several studies have concluded that there are twice as many α-subunits as β- and γ-subunits and the channel is tetrameric in structure with a stoichiometry of 2α:1β:1γ (Firsov *et al.*, 1998, Kosari *et al.*, 1998, Anantharam and Palmer, 2007). However, several other studies have found similar levels of all three subunits and propose a nonamer structure with a stoichiometry of 3α:3β:3γ (Snyder *et al.*, 1998, Eskandari *et al.*, 1999, Staruschenko *et al.*, 2005). The recent elucidation of the crystal structure of the acid-sensing ion channel 1 (ASIC1) in chicken, which is structurally related to ENaC, gives evidence that ENaC is in fact a heterotrimer with a stoichiometry of α:β:γ (Jasti *et al.*, 2007). A δ-ENaC subunit has also been discovered and can form functional amiloride-sensitive channels alone but similar to α-ENaC, is potentiated with co-expression of β- and γ-ENaC (Waldmann *et al.*, 1995). The expression of δ-ENaC is quite distinct from the other subunits, it is found in the testis, ovary, pancreas and to a lesser extent in the heart and brain (Waldmann *et al.*, 1995).

ENaC is highly selective for Na^+ over K^+ (100:1), whilst more selective for Li^+ over Na^+ (~1.5:1) (Palmer, 1992). The selectivity of the channel is partly due to the pore size allowing only the dehydrated form of Na^+ and Li^+ to be transported and not other larger cations. Therefore ENaC allows apical entry of Na^+ into a cell, down its electrochemical gradient but does not allow K^+ to leak back out of the cell (Snyder, 2002). The single channel conductance of ENaC is ~ 5 pS, it exhibits slow gating kinetics and is voltage-independent (Garty and Palmer, 1997).

1.3.2 The role of ENaC in maintaining blood pressure

Na^+ is the main component of the extracellular fluid and its movement can determine movement of water, therefore Na^+ absorption in the kidney is a key regulator of blood volume and pressure (Guyton *et al.*, 1972). With ENaC-mediated Na^+ transport in the collecting duct providing the final renal adjustment to Na^+ balance, dysregulation of this transport can give rise to increased blood pressure (Warnock and Rossier, 2005). The critical role that ENaC plays in the regulation of blood pressure is highlighted by the clinical conditions that arise with mutations to genes encoding ENaC subunits. Gain of function mutations in ENaC subunits lead to a rare form of hypertension known as Liddle's syndrome, whilst loss of function mutations produce pseudohypoaldosteronism type 1 (PHA-I) characterized by salt wasting and low blood pressure.

Liddle's syndrome is an autosomal dominant form of salt-sensitive hypertension and is characterised by early onset hypertension often accompanied by metabolic

alkalosis and hypokalaemia (Rossier and Schild, 2008). Plamsa renin activity is reduced and aldosterone levels are low, this condition is sometimes known as pseudoaldosteronism (Lifton *et al.*, 2001). The first study that linked Liddle's syndrome with ENaC showed that the original kindred had a truncation in the carboxy-terminal of the β-subunit (Shimkets *et al.*, 1994). Four additional kindreds revealed mutations in the same location on the β-subunit (Shimkets *et al.*, 1994) and truncation of this terminal in the γ-subunit has also been shown to cause this form of hypertension (Hansson *et al.*, 1995). The importance of the C-terminal truncation was further demonstrated in a study where ENaC activity was increased in oocytes expressing COOH-mutated ENaC subunits (Schild *et al.*, 1996). Another study showed that oocytes expressing a truncated β-ENaC displayed a five-fold increase in amiloride-sensitive current accompanied with a two-fold increase in surface expression, indicating an increased number of channels and individual channel activity giving rise to the response (Firsov *et al.*, 1996). Staub *et al.* proposed that deletion of a proline-rich motif (PPPxY) in the COOH terminal of either β- or γ-ENaC prevented binding of a ubiquitin ligase known as Nedd-4 (Staub *et al.*, 1996). This group demonstrated that the PPPxY motif, or PY motif, in the COOH terminal of ENaC subunits was a binding site for WW domains present in Nedd-4, thereby linking the ubiquitin ligase with ENaC (Staub *et al.*, 1996). Since ubiquitination of proteins promotes internalisation and degradation, an inhibition of this process would lead to reduced internalisation of the subunits resulting in an increase in the number of channels in the membrane and therefore increased Na^+ absorption (Rossier and Schild, 2008). A mouse model of Liddle's syndrome where the C-terminus of β-

ENaC has been deleted demonstrated that these mice developed normal blood pressure but when given a high salt diet developed high blood pressure and other symptoms synonymous with salt sensitive hypertension (Pradervand *et al.*, 1999b). An important feature of this mouse model is that mineralocorticoid regulation of ENaC was maintained, indicating that aldosterone exerts its actions via an alternate mechanism (Dahlmann *et al.*, 2003). Together these studies highlight the role of ENaC in the regulation of blood pressure as shown by the gain of function mutation that gives rise to Liddle's syndrome.

Loss of function mutations in genes encoding the subunits of ENaC have also been shown to give rise to pseudohypoaldosteronism type I (PHA-I) (Schafer, 2002). This disease is characterised by early onset salt-wasting, hypotension with hyperkalaemia and metabolic acidosis along with high levels of renin and aldosterone in the plasma (Lifton *et al.*, 2001). There are two forms of PHA-I: an autosomal dominant form which is less severe and most commonly caused by mutations in the mineralocorticoid receptor (Geller *et al.*, 1998); and an autosomal recessive form which has been linked to mutations in ENaC subunits (Hummler and Horisberger, 1999). Mutations have been found in the extracellular loop of the α- and γ-subunit (Firsov *et al.*, 1999, Strautnieks *et al.*, 1996) as well as in the N terminal of the α- and β-subunit (Chang *et al.*, 1996). Firsov *et al*. demonstrated that mutations in the two cysteine-rich domains of the extracellular loop of ENaC subunits expressed in oocytes caused inactivation of the channel thought to be due to abnormal trafficking of ENaCs to the membrane (Firsov *et al.*, 1999). Another group showed that expressing ENaC subunits with a mutated glycine in the N

terminal in ooctyes reduced amiloride-sensitive currents via alterations to open probability rather than channel surface expression (Gründer *et al.*, 1997). Unlike in Liddle's syndrome where the mutations were all in the PY motifs of the C terminus, the mutations that lead to PHA-I are not so conserved. Further investigation into the mechanism that allows these mutations of ENaC subunits to reduce Na^+ absorption is clearly warranted. These findings again highlight the importance of ENaC in maintaining blood volume and pressure.

Animal models where each of the subunits of ENaC were individually knocked out or disrupted have also revealed the importance of this Na^+ channel. α-ENaC$^{-/-}$ mice suffer from respiratory distress syndrome and neonatal death (Hummler *et al.*, 1996). Amiloride-sensitive currents were abolished revealing that functional ENaCs cannot be formed without the α-ENaC subunit. Due to the early death of these mice, determination of kidney function could not be fully addressed. However, in ENaC transgenic rescue mice where α-ENaC is expressed at a constitutively low level revealed that 50% of mice developed severe PHA-I and died within 2 weeks. The surviving mice displayed compensated PHA-I with normal acid / base and electrolyte values but had greatly increased plasma aldosterone levels (Hummler *et al.*, 1997). These provide further evidence for the role of ENaC in the regulation of blood pressure. Mice with disrupted β-ENaC expression displayed a mild PHA-I phenotype but when challenged with a low salt diet, developed acute clinical symptoms of PHA-I indicating a role of β-ENaC in salt conservation (Pradervand *et al.*, 1999a). γ-ENaC$^{-/-}$ mice die within 36 h due to severe PHA-I with urinary salt wasting and hyperkalaemia revealing that this

subunit plays a critical role in Na^+ transport in the kidney (Barker *et al.*, 1998). These data indicate that all three subunits of ENaC play an important role in regulating Na^+ transport in the kidney whereas only α-ENaC appears to be critical for respiratory function.

1.4 Mechanisms that regulate ENaC activity

There are several factors that can modulate ENaC activity and they do so either by changing the number of ENaCs in the membrane, N, or by changing the open probability of the channel, P_o (Butterworth *et al.*, 2009). The former can be due to insertion of new channels into the membrane; either from a subapical pool of pre-formed channels (Butterworth *et al.*, 2005) or from delivery of newly synthesised channels (Boyd and Náray-Fejes-Tóth, 2005). Changes to the internalisation and degradation of ENaC mark another mechanism that can alter the surface abundance of these channels (Flores *et al.*, 2003). Alterations to the open probability and the single channel conductance can also modulate ENaC activity (Tong *et al.*, 2004b). A number of hormones and factors act to increase ENaC activity by the above mechanisms and these will be discussed below.

1.4.1 Hormonal Regulation

In response to a drop in blood volume and pressure hormones are released by the body to stimulate the kidney to increase Na^+ absorption and subsequently fluid uptake (Boron and Boulpaep, 2009c). Two hormones most commonly associated with hormonal control of salt and water uptake in the distal nephron are the

mineralocorticoid aldosterone and the peptide hormone vasopressin (Kellenberger and Schild, 2002). The peptide hormone insulin has also been found to stimulate Na^+ absorption in the distal nephron but the physiological role for this remains uncertain (Shane *et al.*, 2006).

1.4.1.1 Aldosterone

Aldosterone is a steroid hormone synthesised in the adrenal cortex of the adrenal glands located above the kidneys. It is the final effector in the renin-angiotensin-aldosterone axis and is released into the blood in response to a decrease in blood volume and pressure (Booth *et al.*, 2002). Aldosterone exerts its effects in aldosterone-sensitive tissues including the renal distal tubule and collecting duct, the colon and the salivary ducts (Stockand, 2002). These tissues are lined with epithelia that contain ENaC in the apical membrane and it is modulation of this channel that aldosterone mainly targets. Aldosterone is thought to exert its effects by influencing gene expression although it has also been linked to the activation of certain signalling pathways. Aldosterone diffuses into the cell, binds the cytosolic mineralocorticoid receptor (MR) and the bound receptor complex then translocates into the nucleus. Here the bound receptor binds DNA binding sites, either steroid response elements (SREs) which promote activation of gene expression or negative steroid response elements (nSREs) which repress gene expression (Booth *et al.*, 2002). More recent studies have found that steroid-bound receptors can also exert their effects via protein-protein interactions rather than binding DNA directly (Stockand, 2002).

There are two types of steroid receptor in kidney tissue, one with a high affinity for mineralocorticoids (MR) and one with a high affinity for glucocorticoids (GR). MR are found in aldosterone-sensitive tissues whereas GR are ubiquitously expressed (Booth *et al.*, 2002). Glucocorticoids can bind both receptors and plasma levels of the endogenous glucocorticoid cortisol are nearly 100 fold greater than plasma levels of aldosterone. An enzyme present in aldosterone-sensitive tissues known as 11-β-hydroxysteroid dehydrogenase type 2 (11β-HSD2) acts to break down cortisol into cortisone which cannot bind MR and this action underpins the epithelial-specific action of aldosterone (Funder *et al.*, 1988). Certain forms of hypertension are caused either by increased concentrations of aldosterone or cortisol abnormally stimulating Na^+ transport by activating the MR. This is true in apparent mineralocorticoid excess (AME) syndrome, a clinical condition where patients present with early onset hypertension associated with hypokalaemia and metabolic alkalosis (New *et al.*, 1977). This disease was shown to be caused by an absence of 11β-HSD2, with mutations found in the genes encoding this enzyme in AME patients (Mune *et al.*, 1995). With a lack of 11β-HSD2 activity, cortisol cannot be converted to cortisone resulting in excess binding of the MR (Ulick *et al.*, 1979) and an abnormal stimulation of ENaC resulting in increased blood pressure.

The effects of aldosterone on Na^+ transport in the aldosterone-sensitive distal nephron (ASDN) can be split temporally into three phases: a lag period of 20-60 min; an early phase 1-3 h of increased Na^+ transport and a late phase after 3 h exposure of a maintained increase in Na^+ transport (Loffing *et al.*, 2001). The

early phase of increased Na^+ transport is thought to be due to the transcription of immediate early genes that act to traffic pre-made transport proteins, including ENaC, to the cell membrane (Stockand, 2002). The late phase is associated with the transcription of the transport machinery including ENaC, Na^+ / K^+ ATPase and energy producing enzymes (Loffing *et al.*, 2000, Masilamani *et al.*, 1999).

Whilst it has become clear that aldosterone can repress nearly as many genes as it can induce (Robert-Nicoud *et al.*, 2001), several proteins encoded by early induced genes have received a great deal of interest due to their role in the regulation of Na^+ transport. These include: the serum and glucocorticoid-regulated kinase, SGK1; the Kirsten Ras GTP-binding protein 2A, Ki-Ras2A; and the glucocorticoid-induced leucine zipper protein, GILZ. Expression of these proteins is upregulated in renal epithelia following exposure to aldosterone and co-expression of each of these proteins in oocytes expressing ENaC or in renal epithelia can increase ENaC activity (Stockand *et al.*, 1999, Chen *et al.*, 1999, Soundararajan *et al.*, 2005). The signalling molecules involved in the aldosterone response can be seen in the schematic in Figure 1.2 Signalling pathways allowing hormonal regulation of ENaC in the collecting duct.

.

Out of these three aldosterone-induced proteins, SGK1 has been the main focus of several studies, (for review see Loffing and Korbmacher, 2009, Lang *et al.*, 2009). Initially identified in a rat mammary tumour cell line, the expression of this kinase was shown to increase in response to both serum and glucocorticoid exposure

(Webster *et al.*, 1993a). Subsequently SGK1 expression was also shown to increase in response to aldosterone in renal epithelia (Chen *et al.*, 1999). Co-expression of SGK1 with ENaC subunits in oocytes led to a marked stimulation of ENaC-mediated Na^+ transport suggesting a role for this kinase in the regulation of ENaC (Chen *et al.*, 1999, Shigaev *et al.*, 2000). SGK1 activity requires phosphorylation of key residues by two kinases: phosphoinositide-dependent kinase 1, PDK1; and the mammalian target of rapamycin complex 2, mTORC2; both of which lie downstream of the phosphoinositide-3-kinase (PI3-kinase) (Kobayashi and Cohen, 1999, García-Martínez and Alessi, 2008). Aldosterone has been proposed to mediate its early effects on Na^+ transport by inducing expression of SGK1 which has been shown to phosphorylate, and therefore inhibit, the ubiquitin ligase Nedd4-2 (Flores *et al.*, 2005).

Ki-Ras2A stimulates ENaC activity by stabilizing the channel in an open state (Stockand *et al.*, 1999) however the mechanism by which it does this remains elusive. Ki-Ras2A can stimulate both PI3-kinase and mitogen-activated protein kinase (MAPK) signalling pathways, however only inhibition of PI3-kinase but not MAPK suppresses the natriferic response (Tong *et al.*, 2004a). It is important to note that as Ki-Ras2a stimulates PI3-kinase activity this mechanism could feed into the SGK1 pathway and mark a point of convergence between two aldosterone-induced proteins (Booth *et al.*, 2002).

GILZ was originally discovered as a glucocorticoid-induced early response gene in T-lymphocytes (D'Adamio *et al.*, 1997). It was subsequently shown to be an

aldosterone-induced protein in rat cortical collecting tubules as well as a murine collecting duct cell line (Muller *et al.*, 2003, Robert-Nicoud *et al.*, 2001). Overexpression of GILZ was found to increase ENaC-mediated Na^+ transport in oocytes expressing ENaC subunits as well as in a collecting duct cell line (Soundararajan *et al.*, 2005). This increase in Na^+ transport was demonstrated to be due to inhibition of the extracellular regulated kinase (ERK) pathway (Soundararajan *et al.*, 2005). The ERK pathway has been previously shown to play a role in ENaC-mediated Na^+ transport as the addition of epidermal growth factor (EGF), which activates the ERK pathway, inhibits amiloride-sensitive currents (Shen and Cotton, 2003). GILZ is thought to inhibit this effect and this was demonstrated by Soundararajan and colleagues who showed that overexpression of GILZ in a murine collecting duct cell line, pre-stimulated with EGF, increased Na^+ transport whilst at the same time decreased the phosphorylation of ERK (Soundararajan *et al.*, 2005). ERK has been shown to inhibit ENaC activity via different mechanisms including degradation of β- and γ-subunits downstream of protein kinase C (Booth and Stockand, 2003b) and downregulation of α-ENaC expression (Zentner *et al.*, 1998, Lin *et al.*, 1999). More recently ERK has been shown to phosphorylate residues on the PY motifs of both the β- and γ-subunits of ENaC which would facilitate their interaction with Nedd4 proteins and increase internalisation therefore reducing ENaC-mediated Na^+ transport (Shi *et al.*, 2002). Therefore, similar to SGK1, GILZ acts to disinhibit ENaC and it does this by preventing the effects of ERK on the Na^+ channel.

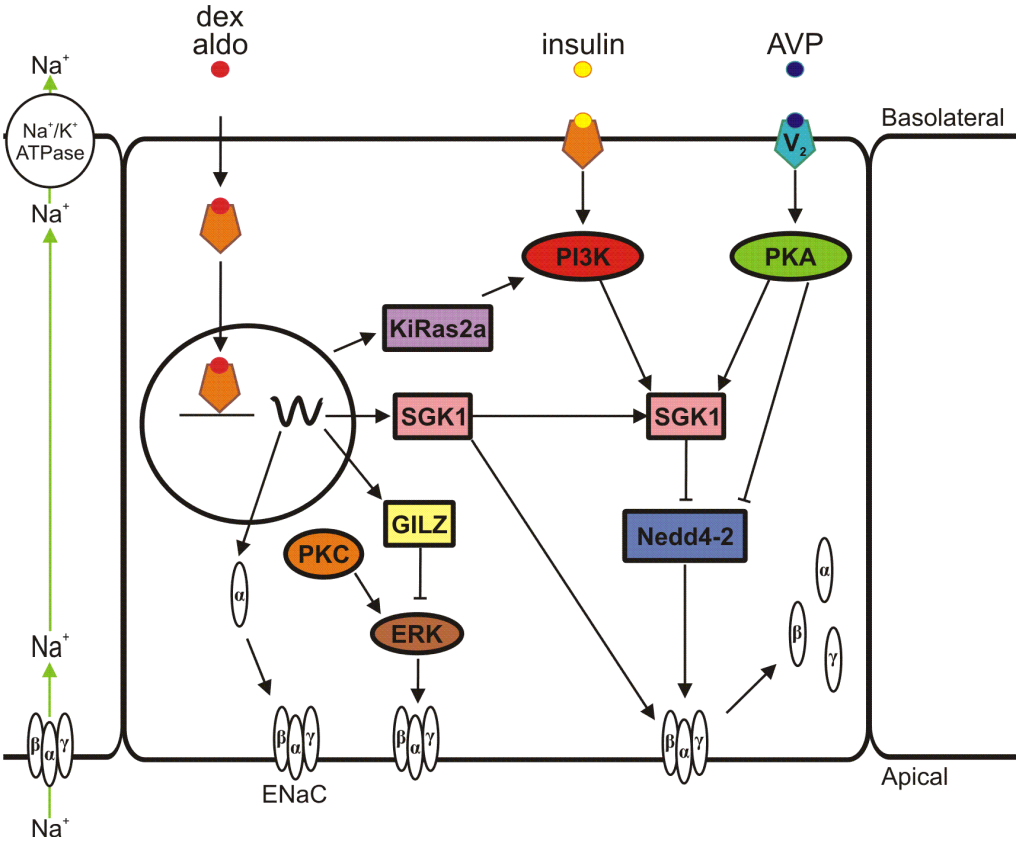

Figure 1.2 Signalling pathways allowing hormonal regulation of ENaC in the collecting duct. Schematic showing proposed signalling pathways allowing alterations to ENaC activity by the hormones: aldosterone (aldo), dexamethasone (dex), insulin and arginine vasopressin (AVP). Aldosterone and dexamethasone bind cytosolic receptors and migrate into the nucleus where they mediate expression of proteins including SGK1, KiRas2A and GILZ as well as increasing the transcription of α-ENaC. KiRas2a directly interacts with PI3-kinase therefore linking aldosterone action with the PI3K/SGK1/Nedd4-2 pathway; increased levels of SGK1 also feed into this pathway. GILZ inhibits the ERK pathway which lies downstream of protein kinase C (PKC) by downregulating expression of ENaC subunits but also by increasing the interaction of ENaC with Nedd4-2, thereby increasing internalisation. Insulin signals via PI3-kinase resulting in activation of SGK1 which phosphorylates Nedd4-2 preventing it from tagging membrane-bound ENaC for internalisation and degradation. AVP signals via protein kinase A (PKA) which has also been shown to phosphorylate SGK1 and inhibit Nedd4-2 marking SGK1 as a convergence point between aldosterone, insulin and AVP. Downstream of AVP, PKA has also been shown to phosphorylate Nedd4-2 marking a further convergence point.

1.4.1.2 Arginine Vasopressin (AVP)

Whilst aldosterone is the major hormonal regulator of salt transport in the distal nephron, the peptide hormone arginine vasopressin (AVP) is a major stimulus for water uptake in the distal nephron as well as increasing salt uptake. AVP, also known as anti-diuretic hormone, is synthesised in the hypothalamus and released from the posterior pituitary in response to hypovolaemia and increased plasma osmolality (Boron and Boulpaep, 2009d). When AVP is released into the systemic circulation it binds V_2 receptors in the basolateral membrane of the epithelia lining the collecting tubules and ducts (Loffing and Korbmacher, 2009). The bound G-protein coupled receptor stimulates adenylyl cyclase to produce cyclic adenosine monophosphate (cAMP) which in turn activates protein kinase A (PKA). PKA phosphorylates unidentified proteins that promote the trafficking and fusion of vesicles containing the aquaporin 2 (AQP2) water channels to the apical membrane, thus increasing water absorption from the filtrate (Boron and Boulpaep, 2009d). This cAMP-dependent pathway also increases the activity of ENaC by stimulating insertion of ENaCs into the apical membrane from a subapical pool rather than changes to P_o (Butterworth *et al.*, 2005). It has been proposed that PKA phosphorylates SGK1 (Perrotti *et al.*, 2001) to exert its effects, marking a convergence point with aldosterone signalling (see Figure 1.2). It has also been proposed that PKA can phosphorylate Nedd4-2 in a similar manner to SGK1 and this provides another mechanism by which PKA could stimulate ENaC activity by increasing internalisation of the channel (Snyder *et al.*, 2004b).

1.4.1.3 Insulin

Insulin is a peptide hormone synthesised in the pancreas and is released in response to increased blood glucose levels and acts to stimulate the uptake of glucose from the blood into the liver, muscle and fat (Boron and Boulpaep, 2009a). Insulin has also been found to stimulate Na^+ absorption in the distal nephron, first discovered in diabetic patients where Na^+ content in urine was increased when insulin treatment was halted (Atchley *et al.*, 1933). Insulin-induced Na^+ transport was subsequently demonstrated to be mediated via apical ENaCs in the distal nephron, in particular in the collecting duct (Marunaka *et al.*, 1992, Shane *et al.*, 2006). Insulin binds its tyrosine kinase receptor in the basolateral membrane of the epithelia lining the distal nephron which stimulates a PI3-kinase signalling cascade. It is stimulation of this pathway that leads to increased Na^+ absorption as inhibiting PI3-kinase abolishes the response as demonstrated in renal epithelia cell lines (Staruschenko *et al.*, 2007, Blazer-Yost *et al.*, 2003). PI3-kinase phosphorylates phosphatidylinositol- 4,5-bisphosphate (PIP_2) to generate phosphatidylinositol 3,4,5-trisphosphate (PIP_3) which triggers a signalling cascade leading to the phosphorylation mTORC2 (Mora *et al.*, 2004). mTORC2 phosphorylates SGK1-Ser^{422} on the hydrophobic domain and this phosphorylated residue becomes a substrate for PDK1 which then phosphorylates SGK-Thr^{256} thereby activating SGK1 (Pearce *et al.*, 2010). As described above, SGK1 has been shown to phosphorylate residues on the ubiquitin ligase Nedd4-2 which then prevents it tagging membrane-bound ENaCs for internalisation and degradation (Flores *et al.*, 2005). Lee and colleagues have also proposed that downstream of PI3-kinase, activated Akt (Lee *et al.*, 2007) can also phosphorylate

Nedd4-2 and reduce ubiquitination of ENaC (see Figure 1.3 for a more detailed diagram of insulin signalling). Whilst decreased ENaC removal from the membrane provides a mechanism to account for the increase in ENaC-mediated Na^+ transport, several other studies have reported that insulin exerts its effects on ENaC by insertion of channels from an intracellular pool (Blazer-Yost *et al.*, 2004) or by increasing P_o of the channel (Marunaka *et al.*, 1992).

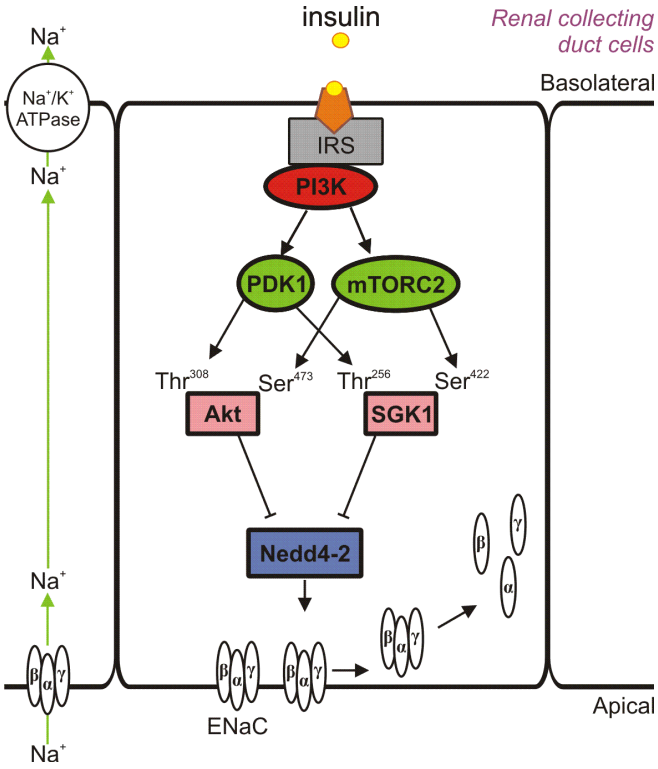

Figure 1.3 Schematic of insulin signalling in the collecting duct.

Insulin binds its receptor in the basolateral membrane of a principal cell. This results in autophosphorylation of the receptor / ligand complex which recruits PI3-kinase to the membrane. PI3-kinase generates PIP_3 triggering a signalling cascade leading to phosphorylation of mTORC2. SGK1 is phosphorylated by mTORC2 then by PDK1, activating SGK1 which can phosphorylate and therefore prevent the ubiquitin ligase Nedd4-2 targeting ENaCs for degradation resulting in increased Na^+ transport. It has also been proposed that Akt can be phosphorylated and activated in a similar manner to SGK1 and also phosphorylate Nedd4-2.

Whilst the signalling pathway underpinning the natriferic response to insulin in the distal nephron remains uncertain, it is clear that insulin can stimulate Na^+ uptake. Patients suffering type II diabetes, where cells lose responsiveness to insulin and can no longer clear increased blood glucose levels following a meal, can be treated with thiazolidinediones, TZDs, (Stumvoll and Häring, 2002). These drugs sensitize cells to insulin, but as the disease progresses this can be supplemented with insulin itself. Recently, side-effects of these drugs have been discovered, including fluid retention which can lead to oedema and congestive heart failure (Tang and Maroo, 2007). Initial studies proposed that abnormal stimulation of ENaC was the cause of this fluid retention (Guan *et al.*, 2005) via an SGK1-dependent pathway (Hong *et al.*, 2003). However, further studies have not found data consistent with this idea (Nofziger *et al.*, 2005) and the roles that SGK1 and ENaC play in mediating these complications is undecided.

1.4.2 Other factors

As well as hormonal regulation, ENaC activity can be modulated by several other factors. These include self-inhibition by increases in either $[Na^+]_i$ (Awayda, 1999) or $[Na^+]_o$ (Van Driessche and Lindemann, 1979), changes in $[H^+]_i$ (Harvey *et al.*, 1988) and intracellular levels of nucleotides (Thomas *et al.*, 2001). The phosphoinositides phosphatidylinositide 4,5-bisphosphate (PIP_2) and phosphatidylinoside 3,4,5-trisphosphate (PIP_3) (Record *et al.*, 1998) have also been shown to modulate ENaC activity. These lipid second messengers have been shown to directly bind ENaC and alter open probability as well as altering the

number of channels in the membrane (He-Ping *et al.*, 2002). Bioactive factors including prostaglandins and endothelin have also been shown to alter ENaC activity (Guan *et al.*, 1998, Bugaj *et al.*, 2008). Protein kinase C (PKC) has also been proposed to regulate ENaC activity, the first such evidence came from a study that demonstrated acute addition of phorbol esters, activators of PKC, inhibited ENaC-mediated Na^+ transport in A6 cells (Yanase and Handler, 1986). PKC has been reported to exert acute effects on ENaC activity due to either decreased P_o or increased internalisation of the channels, as well as long term effects due to a decrease in levels of ENaC subunits (Stockand *et al.*, 2000). Booth and Stockand proposed that long-term inhibition of ENaC activity by PKC is due to activation of the MAPK pathway as inhibitors of MAPK prevented inhibition of ENaC activity by PKC (Booth and Stockand, 2003a). Furthermore MAPK has been shown to phosphorylate residues on β- and γ-ENaC just proximal to the PY motif that increases the subunits interation with Nedd4-2 (Shi *et al.*, 2002). Another mode of regulation which has been the focus of recent research is the role of protealytic cleavage in the activation of ENaC (Vuagniaux *et al.*, 2000, Hughey *et al.*, 2003). Several studies have demonstrated that proteolytic cleavage of the extracellular loops of both α- and γ-subunits of ENaC results in an increase in P_o (Hughey *et al.*, 2003, Diakov *et al.*, 2008).

Trafficking and degradation of ENaCs encompasses another important regulation of ENaC activity. Following the discovery that mutation or deletion of the PY motif on β- or γ-ENaC caused Liddle's syndrome (Shimkets *et al.*, 1994, Hansson *et al.*, 1995), a severe monogenic form of salt-sensitive hypertension, several

studies carried out investigations into the mechanism by which ubiquitination could modulate ENaC activity (Staub *et al.*, 1996, Debonneville *et al.*, 2001, Kamynina *et al.*, 2001b). The E3 ubiquitin ligase Nedd4 was found to interact with ENaC subunits *in vitro* (Staub *et al.*, 1996) and *in vivo* (Staub *et al.*, 1997) via their WW domains. This suggested that ENaC was subject to ubiquitination and that this could regulate the number of channels in the plasma membrane and therefore ENaC activity. This was demonstrated in expression studies where co-expression of ENaC subunits with Nedd-4 in oocytes inhibited amiloride-sensitive currents (Goulet *et al.*, 1998). Oocytes expressing a mutated β-ENaC with a truncated C-terminus displayed increased amiloride-sensitive currents that were not inhibited by co-expression of Nedd-4 (Goulet *et al.*, 1998). This demonstrated that Nedd-4 requires the C-terminal of β-ENaC to exert its inhibitory effects which supports the hypothesis that Nedd-4 interacts with PY motif in the C-terminus of ENaC targeting it for degradation. Indeed inhibitors of the proteosomal and lysosomal pathways were found to increase the half life of ENaC subunits expressed in MDCK cells; demonstrating that both the proteasome and the lysosome play a role in ENaC degradation (Staub *et al.*, 1997). In humans there are two related Nedd-4 proteins: hNedd4-1 and hNedd4-2 and Kamynina *et al*. demonstrated that only Nedd4-2 interacts with PY motifs on ENaC subunits and not Nedd4-1 (Kamynina *et al.*, 2001b)

SGK1 via its own PY motif was found to interact with Nedd4-2 and phosphorylate it at two conserved sites. If these sites were mutated, SGK1 could no longer stimulate ENaC activity suggesting SGK1 modulates ENaC via

interactions with Nedd4-2 (Debonneville *et al.*, 2001). This would suggest that both the early action of aldosterone, which increases the abundance of SGK1 (Chen *et al.*, 1999, Náray-Fejes-Tóth *et al.*, 1999); and the action of insulin, which stimulates a PI3-kinase pathway giving rise to increased SGK1 activity (Shane *et al.*, 2006); is due to decreased Nedd4-2 interaction with ENaC giving rise to an increase in ENaC activity. Another hormonal regulator of ENaC vasopressin is known to bind basolateral V_2 receptors and increase cellular levels of cAMP which activates PKA and stimulates ENaC activity by increasing the number of channels in the plasma membrane (Snyder, 2000). In transfected FRT cells cAMP was found to prevent Nedd4-2 inhibition of ENaC-mediated Na^+ transport and when Nedd4-2 was silenced, cAMP could no longer stimulated amiloride-sensitive currents (Snyder *et al.*, 2004a). PKA was shown to phosphorylate Nedd4-2 at the same residues that SGK1 phosphorylated it and this provided evidence that aldosterone-, insulin- and vasopressin-mediated regulation of ENaC converge at the ubiquitin ligase Nedd4-2.

The mechanism by which phosphorylation of Nedd4-2 reduces interaction with ENaC subunits was subsequently shown to be due to 14-3-3 binding proteins preferentially binding the phosphorylated Nedd4-2 (Bhalla *et al.*, 2005). In oocytes expressing ENaC subunits, co-expression with Nedd4-2 abolished phenamil-sensitive currents and this was relieved by expressing SGK1 and further potentiated by including 14-3-3 (Bhalla *et al.*, 2005). Furthermore, oocytes expressing a mutant 14-3-3 protein in oocytes with ENaC and SGK1 abolished SGK1-stimulated ENaC activity (Ichimura *et al.*, 2005). In murine collecting duct

cells, silencing of the 14-3-3β isoform prevented aldosterone-induced amiloride-sensitive currents and was the first study showing the regulation of ENaC by 14-3-3 proteins in a native collecting duct cell line (Liang *et al.*, 2006). This study provided further evidence that SGK1-induced phosphorylation of Nedd4-2 increases its interaction with 14-3-3 proteins thereby reducing its interaction with ENaC. Together these data highlight a model by which hormones act to regulate ENaC activity and do so by preventing internalisation and degradation of the channel.

As well as Nedd4-2 tagging ENaC with ubiquitin to target it for internalisation and degradation, it has been proposed that ENaC once internalised can be recycled and returned to the membrane (Butterworth *et al.*, 2009). In murine collecting duct cells Butterworth *et al.* demonstrated that increased ENaC activity in response to AVP was due to insertion of channels from a subapical pool since inhibition of both exocytosis and endocytosis abolished this response whereas inhibition of translation did not (Butterworth *et al.*, 2005). Endocytosis of ENaC was shown to be clathrin-mediated as ENaC immunoprecipitated with both epsin and adaptor proteins in mpkCCDcl4 cells and epsin also downregulated ENaC activity when co-expressed in oocytes (Wang *et al.*, 2006). A study using MDCK cells stably expressing ENaC with various PY motif mutations demonstrated via immunofluorescence and live-imaging that Nedd4-2 and its interaction with the PY motif is critical for endocytosis and subsequent recycling of ENaC at the cell membrane (Lu *et al.*, 2007). Therefore ubiquitination of ENaC not only results in degradation of the channel, it also acts as a signal for the channel to be

endocytosed to a subapical pool which can then be recycled back to the cell membrane.

Clearly there are many factors that govern ENaC activity including hormonal and non-hormonal mediators. These agents act by altering either the number of channels in the membrane or the open probability of ENaC giving rise to a channel that has many levels of regulation.

1.5 Signalling pathways underpinning hormonal control of ENaC

Both aldosterone and insulin have been proposed to mediate increases in Na^+ transport in a PI3-kinase dependent manner. Studies in renal epithelial cell lines where PI3-kinase was inhibited using chemical agents prevented the increase in Na^+ transport brought about by these hormones (Blazer-Yost *et al.*, 1999, Blazer-Yost *et al.*, 2003). These studies highlighted that the spontaneous absorption of Na^+ also appeared to be dependent on the activity of PI3-kinase since these inhibitors blocked basal currents (Păunescu *et al.*, 2000). In the H441 human airway epithelial cell line and A6 toad kidney cell line, AVP-stimulated Na^+ transport was also shown to be PI3-kinase dependent since LY-294002 inhibited the natriferic response (Thomas *et al.*, 2004, Edinger *et al.*, 1999).

Vasopressin exerts its effects on ENaC activity in the collecting duct by binding basolateral receptors which stimulates an increase in levels of intracellular cAMP

which in turn activates PKA resulting in an increase in ENaCs in the apical membrane (Snyder *et al.*, 2004a, Morris and Schafer, 2002). Studies looking at the regulation of Na^+ transport by AVP have proposed that similar to insulin, AVP increases SGK1 activity (Perrotti *et al.*, 2001) which would then increase phosphorylation of Nedd4-2 and decrease its interaction with the subunits of ENaC. In contrast to this, Thomas *et al.* found that in H441 cells PKA did not increase SGK1 abundance indicating a lack of a role for this signalling molecule (Thomas *et al.*, 2004). Another study also showed that in MDCK cells expressing SGK1, cAMP did not increase SGK1 activity but did increase cAMP activity shown by an increase in CREB phosphorylation (Shelly and Herrera, 2002). Snyder *et al.* showed that PKA could phosphorylate Nedd4-2 at the same residues that SGK1 could and that Nedd4-2 marked the convergence point between AVP and insulin.

Whilst the evidence supporting the involvement of SGK1 in mediating the natriferic response to AVP is inconclusive, the evidence supporting a role for SGK1 in mediating the effects of both aldosterone and insulin is strong (Wang *et al.*, 2001, Faletti *et al.*, 2002, Shane *et al.*, 2006). Wang *et al.* showed that in A6 cells, the glucocorticoid dexamethasone increased SGK1 phosphorylation and this was potentiated with the addition of insulin indicating that both these hormones could increase the activity of this signalling molecule (Wang *et al.*, 2001). Similarly Tong *et al*. found that aldosterone increased phosphorylated SGK1 indicating an increase in active levels of this kinase (Tong *et al.*, 2004a). As well as clearly increasing SGK1 activity, both aldosterone and insulin increase ENaC-

mediated Na^+ transport which can be mimicked with expression studies using SGK1. Overexpression of wild-type SGK1 in A6 cells greatly potentiated amiloride-sensitive short circuit current compared to control cells (Faletti *et al.*, 2002). The addition of insulin to control cells significantly stimulated the current; however in cells overexpressing a kinase dead form of SGK1, insulin could not stimulate the current demonstrating a role for SGK1 in the natriferic response to insulin (Faletti *et al.*, 2002). Furthermore in FRT cells expressing ENaC subunits, silencing SGK1 expression abolished the insulin-induced amiloride-sensitive current (Lee *et al.*, 2007). Similar to PI3-kinase, SGK1 has also been shown to be required for spontaneous Na^+ absorption since a kinase-dead form represses all ENaC-mediated Na^+ transport (Alvarez De La Rosa and Canessa, 2003). Whilst these studies provide convincing data concerning the crucial involvement of SGK1 in Na^+ transport across the distal nephron, studies examining $SGK1^{-/-}$ mice do not support this hypothesis. These mice do not show any overt phenotype until they are exposed to a low-salt diet where they then develop salt-sensitive hypertension (Wulff *et al.*, 2002). The role that SGK1 plays in mediating both basal and hormone-stimulated Na^+ transport therefore remains uncertain and warrants further investigation.

The activity of SGK1 has been demonstrated to require phosphorylation of two residues by the kinases PDK1 and mTORC2 (Kobayashi and Cohen, 1999). Importantly, phosphorylation of SGK1 by mTORC2 is absolutely crucial for its activity (García-Martínez and Alessi, 2008). Whilst the role that mTORC2 plays in SGK1 activity seems clear, the importance of mTORC2 in mediating signalling

pathways involved in Na^+ transport is not understood. If SGK1 is required for hormonal stimulation of Na^+ transport then mTORC2 should equally be so, therefore further work on this kinase is clearly warranted. mTORC2 and PDK1 also phosphorylate and activate Akt, a downstream target of PI3-kinase (Alessi *et al.*, 1996, Sarbassov *et al.*, 2005). Recently, Akt has also been proposed to mediate Na^+ transport in a similar manner to SGK1 by phosphorylating the ubiquitin ligase Nedd4-2 (Lee *et al.*, 2007). However, conflicting data does not support a role for Akt in either basal or insulin-stimulated Na^+ transport (Arteaga and Canessa, 2005). Clearly the signalling pathways underpinning both spontaneous and hormonally stimulated Na^+ transport are not fully understood. With the unmistakable importance of ENaC-mediated Na^+ transport as a factor in blood pressure regulation as well as possible side effects in the treatment of type II diabetes, understanding these signalling pathways is of crucial importance.

1.6 Thesis Aims

Na^+ transport in the distal nephron, in particular the collecting duct is subject to hormonal regulation by aldosterone, vasopressin and insulin. Whilst these responses have been demonstrated (Shane *et al.*, 2006), the underlying signalling pathways involved in mediating these responses are not as clear. The role of insulin particularly has received less attention, yet for type II diabetic patients abnormal stimulation of Na^+ transport through treatment with insulin is a serious side effect worth consideration. Further understanding of how insulin could produce side effects of increased blood pressure as a function of stimulating Na^+

transport can only be elucidated if the signalling pathway underlying this process is understood. Furthermore, insulin-sensitizing drugs, TZDs, have been reported to cause side effects of fluid retention leading to complications including oedema and heart failure. Abnormal stimulation of ENaC in the collecting duct has been proposed to be responsible yet conflicting data leaves the subject unresolved (Guan *et al.*, 2005, Nofziger *et al.*, 2005).

Previous studies examining the roles of PI3-kinase and SGK1 in hormonal stimulation of Na^+ transport have utilised oocyte expression systems and the A6 amphibian kidney cell line (Chen *et al.*, 1999, Blazer-Yost *et al.*, 2003). Whilst these studies have provided valuable information, how well they relate to mammalian systems is not clear. The creation of novel small molecule inhibitors has allowed a method by which to target specific proposed mediators of these signalling pathways (Feldman *et al.*, 2009, Thoreen *et al.*, 2009, Barnett *et al.*, 2005, Sherk *et al.*, 2008, Folkes *et al.*, 2008). Furthermore with the development of mammalian collecting duct cell lines these inhibitors can be tested in a native system (Bens *et al.*, 1999). The main focus of this thesis is to determine the importance of PI3-kinase, mTORC2, SGK1 and Akt in mediating both spontaneous Na^+ transport and the stimulation of this transport brought about by insulin. This has been carried in a murine collecting duct cell line using novel small molecule inhibitors. The role that two TZDs, pioglitazone and rosiglitazone, play in altering both basal and insulin-stimulated Na^+ transport as well as SGK1 activity was also investigated. The responses to two other hormonal regulators of Na^+ transport were also examined: the glucocorticoid dexamethasone and the

peptide hormone arginine vasopressin. By using novel small molecule inhibitors, the pathways underlying these responses were investigated allowing a comparison of signalling pathways by three different hormones in a mammalian system.

Chapter 2 - Materials and Methods

2.1 Cell culture

To study the signalling pathways allowing hormonal regulation of ENaC-mediated Na^+ transport in the collecting duct, a murine collecting duct cell line mpkCCDcl4 was used. This cell line was chosen as it represented a mammalian system in which the expression of native transporters including ENaC and Na^+ / K^+ ATPase were retained following immortalization (Bens *et al.*, 1999, Summa *et al.*, 2001). These cells were also reported to respond to the hormones aldosterone, insulin and vasopressin (Bens *et al.*, 1999, Shane *et al.*, 2006). During the course of the present study however, it became clear that the mpkCCDcl4 cells required supraphysiological doses (5 μM) of aldosterone to stimulate ENaC-mediated Na^+ transport and this highlights a limitation of using this cell line. Whilst this finding allowed us to investigate the signalling pathway allowing GR-mediated Na^+ transport it did not allow us to target the more physiological MR-mediated Na^+ transport. This finding highlights an inherent problem when utilising cell lines from the distal nephron and it is of note that there a large number of studies investigating the effects of aldosterone using this hormone at very high concentrations (≥ 1 μM) (Fakitsas *et al.*, 2007, Summa *et al.*, 2001, Robert-Nicoud *et al.*, 2001, Stockand *et al.*, 1999, Helman *et al.*, 1998). These cells did however form highly-resistive monolayers and generated spontaneous ENaC-mediated Na^+ absorption that responded to both insulin and vasopressin. Thus the mpkCCDcl4 cell line provided a useful model to investigate ENaC-mediated Na^+ transport so long as its limitations were noted and understood.

2.1.1 Routine culture

mpkCCDc14 cells were routinely cultured in Dulbecco's Modified Eagle Medium (DMEM) / F12 Ham's media 1:1 mix (Invitrogen, UK) supplemented with hormones, growth factors and serum (Table 2.1) as specified by Bens *et al.* (1999). Fully supplemented media, hereafter called complete media, was used to culture the cells which were seeded and grown in 75cm^2 filter capped culture flasks (Greiner Bio-one, Frickenhausen, Germany). Cells were incubated at 37°C in a humidified atmosphere of 13% O_2, 5% CO_2 and 82 % N_2 and were used at a passage no greater than 45. Cells were passaged twice weekly at ~95% confluence using a Trypsin / EDTA solution (Sigma Aldrich, Poole, UK) to lift cells from the flask. Complete media was used to inactivate the trypsin / EDTA solution and cells were spun at 1200 rpm for two minutes before resuspension in complete media and counted using plastic haemocytometers (ISL "Fast Read", Paignton, UK). Cells were then seeded into fresh flasks at a known density with media being replaced every two days.

2.1.2 Cell culture for experimental use

For experiments, cells were seeded onto permeable filters with 0.4 µM pore size (Corning Costar, NY, USA). Cell were seeded at either at 0.5 x 10^6 cells on 12 mm Snapwell membranes for Ussing chamber recordings or at 1 x 10^6 cells on 24 mm Transwell membranes for protein lysates. These cells were maintained in complete media for 6 days with media changes every two days. The media was then replaced with basal media supplemented only with charcoal stripped serum

and antibiotics, (Table 2.1) for 24 hours. This was then replaced with basal media completely free from serum (Table 2.1) for a further 18-24 hours prior to use in experiments.

Table 2.1 Media compositions for mpkCCDc14 cell culture

Supplement	Complete	Charcoal-stripped	Serum-free
Fetal Bovine Serum (FBS) *	2%	-	-
Charcoal Stripped FBS *	-	2%	-
Sodium selenite *	5ng / ml	-	-
Insulin *	5µg / ml	-	-
Transferrin *	5µg / ml	-	-
Triiodothryonine (T_3) *	1nM	-	-
Dexamethasone*		-	-
Epidermal Growth Factor (EGF) †	10ng / ml	-	-
Glutamine *	2mM	-	-
Penicillin *	100 units /ml	100 units / ml	100 units / ml
Streptomycin *	100µg / ml	100µg / ml	100µg / ml

* Sigma Aldrich (Poole, UK) † Invitrogen (Paisley, UK)

2.2 Ussing chamber recordings

2.2.1 Ussing Chamber setup

Ussing chambers were used to record either short circuit current (I_{SC}) or transepithelial voltage (V_t), across a monolayer of mpkCCDcl4 cells grown on snapwells as described above. Cells that displayed a R_t of < 1kΩ were not used as this demonstrated that the cells had not formed a tight epithelia typical of the collecting duct. The filter membranes were secured within the chamber creating completely separate apical and basolateral baths. Each side of the chamber was filled with 15ml KREBS buffer (Table 2.2) which was gassed continuously with 95% O_2 and 5% CO_2 (BOC, UK). The temperature of the buffer was maintained at 37°C by water jackets that surrounded the chambers, connected to a water bath (GRANT instruments, Cambridge, UK). Voltage and current Ag / AgCl electrodes were held in a 3% Agar / 3M KCl gel and attached to the apical and basolateral sides of the chamber, respectively. The tips of the electrodes were attached to crocodile clips connected to the pre-amplifier. BNC cables then connected the pre-amplifier (WPI model DVC-3, Herts, UK) to the amplifier (WPI DVC 1000, Herts, UK) which was in turn, connected to a Powerlab (AD instruments, Oxfordshire, UK) which converted the analogue voltage signal to a digital one. This was then connected to a PC via a USB cable which allowed recording using the Chart 5 software package (AD instruments, Oxfordshire, UK). A schematic diagram of the Ussing chamber setup can be seen in Figure 2.1.

Prior to recording under experimental conditions, empty snapwells were mounted in Ussing chambers and 15 ml KREBs buffer was added to both baths. Any offsets to the liquid junction potential brought about by the empty setup were compensated. Buffer was aspirated, blank snapwells removed and snapwells containing monolayers of cells were mounted in the chambers with fresh KREBs buffer and V_t was recorded under open circuit conditions. Once V_t had stablilised recordings of either I_{SC} or V_t were made as described below.

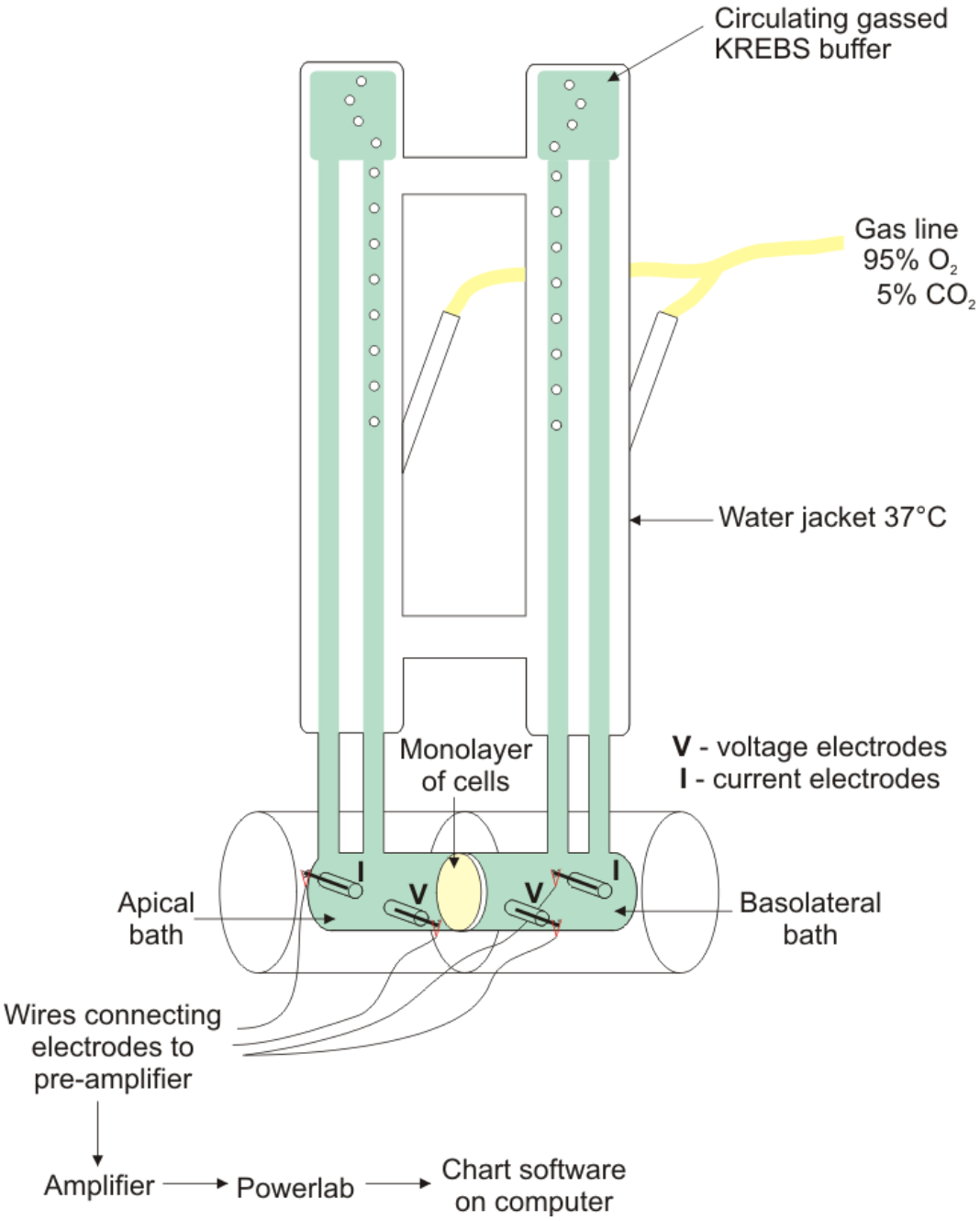

Figure 2.1 Schematic diagram of a modified Ussing chamber.

Monolayers of cells were mounted in the central chamber which separated the apical and basolateral baths. KREBS buffer bathed the cells, kept at 37°C by the surrounding water jacket and gassed with 95 % O_2 and 5 % CO_2. Voltage and current electrodes were attached to both sides of the chamber and were connected to a pre-amplifier connected to an amplifier. This was then connected to a Powerlab and finally a computer.

Table 2.2 Composition of KREBS buffer used in all Ussing experiments.

Chemical	**Concentration (mM)**
KCl	4.7
$CaCl_2$	2.5
$MgSO_4$	1.2
KH_2PO_4	1.2
NaCl	112.0
$NaHCO_3$	25.0
Glucose	11.6

The pH of the KREBS solution was maintained at pH 7.4 in the Ussing chambers by constantly gassing the solution with 5 % CO_2. All chemicals were from Sigma Aldrich (Poole, UK).

2.2.2 Short circuit current recording

Experiments examining the effects of PPARγ agonists were carried out in collaboration with Dr. Sarah Inglis where V_t was clamped to 0 mV allowing a direct measurement of the short circuit current (I_{SC}). I_{SC} is defined as the current that must be passed in order to maintain V_t at 0 mV and gives a measure of the net ion transport across the monolayer. As these cells generated a large V_t clamping this to 0 mV imposed an altered electrochemical gradient than that which existed under the more physiological open circuit conditions. It was therefore decided that all further experiments would be carried out under open circuit conditions where

V_t would be recorded using a pulse protocol and the equivalent short circuit current I_{eq} could be calculated.

2.2.3 Transepithelial voltage recording

In the present study V_t was measured using a reference electrode in the basolateral bath and a recording electrode in the apical bath. Using this configuration, movement of cations e.g. Na^+ from the apical to basolateral baths would give rise to a negative V_t. Once V_t had stabilised, a current clamp protocol was employed: the current was clamped to -10 µA for 20 sec then returned to 0 µA (open circuit conditions) for 40 sec with continuous recording of the V_t at 4 Hz. This was maintained throughout the experiment and allowed an indirect method of measuring the current passing across the monolayer, which could be calculated using Ohm's Law. Having measured V_t at 0 current clamp and then clamped at -10 µA, ΔV_t can be calculated. The transepithelial resistance can therefore be calculated according to Ohm's law:

$$R_t = \frac{\Delta V_t}{\Delta I}$$

where ΔI = -10 µA.

The equivalent short circuit current, I_{eq}, can be therefore be calculated using V_t recorded under open circuit conditions and R_t:

$$I_{eq} = \frac{V_t}{R_t}$$

Since baseline V_t is negative by convention with a basolateral earth, baseline I_{eq} will therefore be negative. Using this definition, an increase in the movement of cations e.g. Na^+ moving from the apical to basolateral bath or anions e.g. Cl^-

moving from the basolateral to apical bath would produce a more negative current indicated by a downward deflection on a trace. Likewise, I_{eq} would become more positive if these ionic movements were reversed.

2.3 Western blotting

2.3.1 Preparation of Samples

Cells were seeded onto Transwells (Section 2.1.2.) and on the 8th day of culture when cells had been exposed to serum-free media for 18-24 h, the media was replaced with serum-free media containing the vehicle/drug of interest and returned to the incubator for the experimental time period. Cells were then removed, placed onto ice and washed three times with ice-cold phosphate buffered saline (PBS). 175 µl of lysis buffer (Table 2.3) was added to each well and cells were resuspended by scraping. Lysis buffer contained both protease and phosphatase inhibitors to prevent sample degradation. The lysate was then sonicated for ~10 s (Soniprep150, London, UK) and spun down at 4°C at 14000 rpm for 10 min to remove cell debris. The mass of protein in the raw lysate was then determined using the Bradford method (2.3.2). After determining the mass of protein in the lysate, samples were made up to a specific concentration by adding 2 x sample buffer (Table 2.4) and then bringing each sample to a defined final volume with deionised H_2O . Samples were heated to 100°C for five minutes to denature the protein and then either ran in a gel straight away or frozen for later use.

Table 2.3 Composition of Lysis Buffer.

Chemical Name	Concentration
Tris HCl pH7.5	50.0 mM
EDTA	1.0 mM
EGTA	1.0 mM
Sodium Ortho Vanadate	1.0 mM
Glycerol Phosphate	10.0 mM
Sodium Fluoride	50.0 mM
Sodium Pyrophosphate	5.0 mM
Sucrose	270.0 mM
Triton x100	1.0 % (v/v)

All chemicals were from Sigma Aldrich (Poole, UK).

One complete mini protease inhibitor (Roche, Mannheim, Germany) + 10 µl β-mercaptoethanol (Sigma Aldrich, Poole, UK) was added to 10 ml of lysis buffer stock and then frozen and used as required.

Table 2.4 Composition of Sample Buffer

Chemical Name	Concentration
Tris HCl pH 6.8	66.0 mM
Glycerol	26.3 % (v/v)
SDS	2.1 % (v/v)
Bromophenol Blue	0.01 % (v/v)

2.3.2 Bradford Assay

The protein lysate was diluted 1:10 with deionised water and 5 µl added in duplicate to a 96 well plate. Protein standards made up with bovine serum albumin at concentrations: 0.05; 0.1; 0.2; 0.3; 0.4; 0.5; 0.7; and 1.0 µg / µl in deionised water as well as a water control were added in triplicate to the plate to allow construction of a standard curve. 100 µl of Protein Assay Dye Reagent (BIORAD, Hertfordshire, UK) (diluted 1:4 with deionised water and filtered through Whatman no.1 filter paper) was added to the protein samples and incubated for 5 min at room temperature. The absorbance of the samples at 595nm was read using a microplate reader (MRX, Guernsey, UK). These values were then entered into an Excel worksheet and the protein mass of the samples were calculated.

2.3.3 Gel Casting

A 10 % resolving gel (Table 2.5) was poured into glass plates (BIORAD, Hertfordshire, UK) with 1 mm spacers and allowed to set with 500 µl of butanol added to the surface to ensure removal of air bubbles. Once set, the butanol was poured off and the gel washed thoroughly with deionised water. A 5 % stacking gel (Table 2.6) was then poured on top of the resolving gel and the comb carefully inserted making sure of no air bubbles. This was left to set and the gel was then used for electrophoresis or wrapped up in damp tissue paper and kept in the fridge overnight for use the next day.

Table 2.5 Composition of 10% Resolving Gel

	Concentration
Bis / acrylamide	10.0 % (v/v)
Tris HCl pH8.5	380.0 mM
SDS	0.1 %
Ammonium persulfate	0.1 %
TEMED	0.4 µl / ml

Table 2.6 Composition of 5% Stacking Gel

	Concentration
Bis / acrylamide	5.0 %
Tris pH 8.5	750.0 mM
SDS	1.0 %
Ammonium persulfate	1.0 %
TEMED	1.0 µl / ml

2.3.4 SDS-Gel Electrophoresis

Gels were clipped into place in gel tanks (Novex mini cell XCell II, Invitrogen, Paisley, UK) with running buffer (Table 2.7) added so that it was just above the level of the wells. The specified mass of protein was added to each well with a visible rainbow marker and a biotinylated marker added to allow visualization of protein movement. The tanks were sealed and set at 200 V to run for 50 min.

Table 2.7 Composition of Running Buffer.

Running Buffer	Concentration (mM)
Trizma Base	24.8
Glycine	191.8
SDS	3.5

2.3.5 Western Blotting

Gels were removed from the tank and rinsed with deionised water. Pieces of Hybond-P PVDF membrane (8 x 7 cm, GE Healthcare, Buckinghamshire, UK) were prepared by soaking in methanol for 15 s, submerging in transfer buffer (Table 2.8) for 5 minutes to allow equilibration and then carefully placed onto the surface of the gel. An 8 x 8 cm piece of blotting paper, briefly wetted in transfer buffer, was then placed on top of the PVDF. The gel was then flipped over and another piece of blotting paper (GE Healthcare, Buckinhamshire, UK) placed gently on the surface of the gel, creating a "sandwich". Care was taken to remove any visible air bubbles. Sponges presoaked in transfer buffer were then placed into a transfer cassette (XCell II blot module, Invitrogen, Paisley, UK) with the "blot sandwich" in the middle. If two gels were being transferred, a sponge was placed between them. The cassette was placed into the gel tank and the sealed inner chamber was filled with transfer buffer. The outer chamber surrounding the cassette was filled with deionised water ~1 cm from the top of the tank. Gels were transferred at 30 V for 2 h.

Table 2.8 Composition of Transfer Buffer.

	Concentration
Trizma Base	19.8 mM
Glycine	150.5 mM
Methanol	20.0 % (v/v)

2.3.6 Blocking and antibody treatment

Once transfer was complete the membrane was quickly moved to a small container and submerged in ~15 ml of blocking solution (5% dried skimmed milk, Tesco, UK) in tris-buffered saline with Tween (TBS-T, see Table 2.9). This was placed on a rocker (Bibby Stuart, UK) for 1 h to allow the milk protein to block non-specific binding sites on the membrane. The primary antibody was then made up in 5% milk / TBS-T unless otherwise stated at the appropriate concentration in a 50 ml falcon tube. The membrane was removed from the blocking solution and placed protein side up in the 50 ml tube with primary antibody and placed on a rotating roller (Bibby Scientific, UK) overnight at 4°C. The following day, the blot was removed from the primary antibody and washed for 3 x 10 min in TBS-T on a rocker at room temperature. The primary antibody was then frozen and would be re-used for a specified number of repeats. The secondary antibody was then made fresh on the day in 5% milk / TBS-T and was added after the wash steps for 1 hour. The blot was then washed for 3 x 10 min in TBS-T to remove the secondary antibody.

Table 2.9 Composition of TBS-T.

	Concentration
Trizma Base	19.8 mM
NaCl	136.9 mM
Tween 20	0.1 % (v/v)

The solution was brought to pH 7.6 with concentrated HCl.

2.3.7 ECL and exposure

The blot was then dabbed dry on tissue paper and 3 ml of the pre-mixed ECL solution (Table 2.10) was pipetted carefully on top of the membrane. This was given ~1 min to react and then the excess was dabbed off the membrane which was then placed into a plastic bag with excess solution being pressed out. The membrane was then taken to the dark room where it was placed into a cassette (Amersham Biosciences, UK) and a piece of film (Konica Minolta Medical Film AX, Japan) laid on top for an appropriate period of time. The film was then developed in the x-ograph machine (Compact X4, Wiltshire, UK).

Table 2.10 Composition of ECL

Solution I	Concentration	Solution II	Concentration
Luminol	2.5 mM	H_2O_2	0.02 % (v/v)
p-coumaric acid	0.4 mM	Tris HCl pH 8.5	1000.0 mM
Tris HCl pH 8.5	1000.0 mM		

2.3.8 Densitometry and Analysis

The exposed film was captured using GeneGenius CCD camera system (Syngene, Cambridge) using the GeneSnap acquisition software. Densitometric readings were carried out using the associated analysis software GeneTools. These values were entered into an Excel worksheet for analysis.

2.3.9 Antibodies

Throughout this thesis the following antibodies were used. Phosphorylation of NDRG1 (n-myc downstream regulated gene 1) at $Thr^{346/356/366}$ was used to monitor SGK1 activity. These specific residues have been shown to be phosphorylated by SGK1 and not other closely related kinases (Murray *et al.*, 2004). Phospho-PRAS40-Ser^{246} was used to monitor Akt activity as this kinase has been shown to be a specific substrate for Akt (Kovacina *et al.*, 2003). The abundance of the respective total protein for NDRG1 and PRAS40 was also monitored. These antibodies were produced in the Medical Research Centre Protein Phosphoylation Unit, Dundee and were a kind gift from Sir Professor Phillip Cohen.

Phospho-Akt-Ser^{473} was used to monitor PI3-kinase downstream signalling. This site is specifically phosphorylated by the mammalian target of rapamycin complex 2, mTORC2, and could therefore be used to monitor its activity. Phospho-P70-S6K-Thr^{389} was used to monitor mTORC1 activity as it has been previously shown to be a substrate for this kinase (Proud, 2007). The abundance of total Akt

and P70-S6K was also monitored. These antibodies were from Cell Signalling Technology – New England Biolabs, Herts, UK.

2.4 Pharmacological agents

Throughout this research project a number of small molecule inhibitors and hormones were used in both Ussing chamber experiments and western analysis of protein phosphorylation. Details of these drugs and hormones are found below in Table 2.11 and Table 2.12 respectively.

Table 2.11 Small molecule inhibitors used in experiments

Compound	Function	Vehicle	Conc. (µM)	Reference
Wortmannin *	PI3-kinase inhibitor	DMSO	0.1	(Wymann *et al.*, 1996)
PI103 *	PI3-kinase inhibitor	DMSO	1.0	(Fan *et al.*, 2006)
GDC-0941 †	PI3-kinase inhibitor	DMSO	1.0	(Garcia-Echeverria and Sellers, 2008)
Rapamycin *	mTORC1 inhibitor	DMSO	0.1	(Proud, 2007)
Akti-1/2 *	Akt 1 / 2 inhibitor	DMSO	1.0-10.0	(Barnett *et al.*, 2005)
GSK650394A †	SGK1 inhibitor	DMSO	1.0-10.0	(Sherk *et al.*, 2008)
TORIN1 **	mTOR inhibitor	DMSO	1.0-10.0	(Thoreen *et al.*, 2009)
PP242 †	mTOR inhibitor	DMSO	1.0	(Feldman *et al.*, 2009)
Amiloride *	ENaC inhibitor	H_2O	10.0	(Canessa *et al.*, 1994)

Table 2.12 Hormones used in experiments

Hormone	Vehicle	Conc. (nM)	Reference
Insulin ***	H_2O	20.0	(Record *et al.*, 1998)
Dexamethasone ***	Basal Media	200.0	(Chen *et al.*, 1999)
Arginine vasopressin (AVP) ***	H_2O	10.0	(Bugaj *et al.*, 2009)

Pharmacological agents from:

* Merck, Beeston, UK

† GDC-0941, GSK650394A and PP242 were generous gifts from Professor D.R. Alessi, MRC Protein Phosphorylation Unit, University of Dundee, UK

** TORIN1 was a generous gift from Professor D.M. Sabatini, Whitehead Institute for Biomedical Research, Cambridge, MA, USA

*** Sigma Aldrich, Poole, UK

2.5 Statistical Analyses

Data recorded from Ussing chambers in the Chart 5 software were copied into Microsoft Excel worksheets and experiments were time-matched to allow comparison of data. Densitometry data collected from western analysis were also entered into Microsoft Excel worksheets where data could be compiled for mean results. All data are presented as mean ± S.E.M. and values of *n* refer to the number of times an experiment was repeated using a different passage of cells. The statistical significance between mean values was assessed using Student's unpaired *t*-test or using a one- or two-way ANOVA where appropriate using GraphPad Prism. For calculation of statistical significance of the pooled densitometric analysis of western blots, raw values were compared.

Chapter 3 - Basal Na^+ transport in mpkCCDcl4 cells, the response to insulin and the effects of PPARγ agonists

3.1 Introduction

3.1.1 mpkCCDc14 cells

A difficulty faced when trying to investigate the hormonal regulation of ion transport in epithelia *in vitro* is finding a cellular system that has retained the ion transport properties and regulation typical of the native system. Na^+ transport across the late distal tubule of the nephron and the collecting duct is governed by the hormones aldosterone and arginine vasopressin as well as insulin (Kellenberger and Schild, 2002). It has been suggested that these hormones alter the rate of Na^+ absorption by increasing the number of ENaCs in the apical membrane (Blazer-Yost *et al.*, 1998, Snyder, 2000); and that aldosterone can also increase protein synthesis of ENaC subunits (Alvarez De La Rosa *et al.*, 2002). The first models used for investigating Na^+ transport were the frog skin (Herrera *et al.*, 1963) and the toad urinary bladder (Herrera, 1965). Both of these tissues exhibit high epithelial resistance, generate a spontaneous Na^+ current and are regulated by hormones such as aldosterone and insulin. These tissues provided a wealth of information regarding the nature of transepithelial Na^+ transport and its modulation by various hormones. However, although these tissues exhibited Na^+ transport across tight epithelia, they were not related specifically to Na^+ transport in the distal nephron. Therefore the emergence of cultured kidney cells provided models related to specific parts of the nephron allowing more detailed experimental studies of ion transport in the nephron.

The A6 toad kidney cell line has been used extensively to model the distal tubule of the nephron (Fidelman *et al.*, 1982, Handler *et al.*, 1981a, Kemendy *et al.*, 1992). The use of cultured cells offers certain advantages, for instance, cells for one entire study can be derived from the same precursor cells, therefore reducing genetic variability. Factors such as the environment in which the epithelia grow can be tightly regulated and cell culture can allow genetic manipulation i.e. transfecting in (Faletti *et al.*, 2002) or silencing genes of interest (Lee *et al.*, 2007). However the limitations of many immortalised cell lines are that they have lost certain features of the native tissue such as high transepithelial resistance or regulation of Na^+ transport by various hormones (Chen *et al.*, 1998). Stable and transient transfection of cell lines, including COS-7, HEK-293 and Fisher rat thyroid cells, with ENaC and related proteins have also been studied (Lee *et al.*, 2007, Lu *et al.*, 2010). Therefore although transfected cell cultures and amphibian cells lines can provide invaluable information regarding interactions within these systems, they might not provide as accurate a comparison as mammalian models could. For example in expression studies where an interaction between ENaC and overexpressed protein are observed, it is difficult to determine whether this would happen in the native system where the protein of interest may be expressed at a very low level (Alvarez De La Rosa and Canessa, 2003).

The murine M1 cell line was the first example of an immortalised mammalian cortical collecting duct cell line that retained well-differentiated epithelia and exhibited high transepithelial resistance as well as expressing ENaC and CFTR channels (Stoos *et al.*, 1991, Helms *et al.*, 2003). However, despite these qualities,

this cell line lacked a mineralocorticoid receptor (MR)-mediated response to aldosterone which led another research group to stably express MR in these cells, M1-MR$^+$ (Náray-Fejes-Tóth *et al.*, 2004b), allowing the control of Na^+ transport by aldosterone. The mpkCCDcl4 murine cell line was derived from collecting duct principal cells through targeted oncogenesis in transgenic mice (Bens et al., 1999). This strategy allowed differentiated epithelia, which importantly retained many of the key features of collecting duct cells, including high transepithelial resistance and amiloride-sensitive electrogenic Na^+ transport that could be hormonally regulated by aldosterone, vasopressin and insulin. This cell line was therefore chosen to investigate the role of insulin in the regulation of Na^+ transport in collecting duct principal cells.

3.1.2 Previous studies on the effect of insulin on Na^+ transport

The first observation that insulin was involved in Na^+ transport was in 1933 when Atchley *et al.* observed that halting insulin treatment in type II diabetic patients significantly increased the level of sodium excreted in the urine (Atchley *et al.*, 1933). The reintroduction of insulin treatment reversed this effect. Miller and Brogdonoff in 1954 showed that treating normal subjects, undergoing either a solute (glucose) diuresis or water diuresis, with insulin reduced the levels of sodium excreted in the urine (Miller and Bogdonoff, 1954). The addition of insulin to isolated perfused dog kidneys also produced a decrease in sodium excretion in the urine (Nizet *et al.*, 1971). Whilst these studies clearly demonstrated the role of insulin in stimulating sodium reabsorption, they did not define the mechanism by which it was being mediated.

The groundbreaking work of Ussing and Koefoed-Johnsen in 1958, allowed a technique, Ussing chamber recording, by which sodium transport across a membrane could be recorded. Hererra *et al*. (1963) applied similar techniques in experiments using frog skin and showed that application of insulin increased short circuit current. Similar results were obtained using toad urinary bladder (Herrera, 1965). A further study identified that insulin only exerted natriferic effects when applied to the serosal side of the bladder (Cox and Singer, 1977), consistent with finding that the majority of insulin receptors are found on the serosal / basolateral membrane (Blazer-Yost *et al.,* 1992). Experiments carried out in A6 cells demonstrated that these cultured cells generated a spontaneous Na^+ current which could be stimulated by insulin (Handler *et al.,* 1981b, Fidelman *et al.,* 1982). More recent studies utitlising mammalian cell lines including the M1 cell line (Nofziger et al., 2005) and the mpkCCDc14 cell line (Shane et al., 2006, Nofziger et al., 2005) also confirm the natriferic effect of insulin. These extensive studies clearly demonstrate that insulin can stimulate Na^+ transport, particularly in the collecting duct of the nephron. Patch clamp analysis of A6 cells concluded that insulin was increasing the open probability of the amiloride-sensitive sodium channel, ENaC, without affecting single-channel current or conductance (Marunaka *et al.,* 1992). However, a study using blocker-induced noise analysis demonstrated that insulin mainly acts to increase the number of ENaCs in the membrane, more so than alterations to P_o (Blazer-Yost *et al.,* 1998). Whilst the final effects on ENaC were not certain, the mechanism by which insulin could alter ENaC activity also remained unclear.

3.1.3 PPARγ agonists

During the late 1990s, a new class of drugs were made available for the treatment of type-II diabetes called thiazolidinediones (TZDs) or glitazones (Lehmann *et al.*, 1995). These drugs are agonists of the peroxisome proliferator-activated receptor γ (PPARγ) and act to sensitize cells to insulin thereby increasing glucose uptake in insulin-sensitive tissues (Stumvoll and Häring, 2002). PPARγ is a nuclear receptor that is highly expressed in adipose tissue but is also found in the vasculature as well as the kidney (Vallon *et al.*, 2009). PPARs form heterodimers with retinoid X receptors (RXRs) and together act to regulate transcription of a number of genes (Stumvoll and Häring, 2002). These include genes encoding proteins that are involved in both lipid and glucose metabolism as well as proteins that are involved in molecular cascades including inflammation (Buckingham and Hanna, 2008). Whilst these drugs have been shown to lower blood glucose effectively, these anti-diabetic drugs have also been found to produce side effects including fluid retention leading to complications such as oedema and congestive heart failure (Tang and Maroo, 2007). For these reasons, TZD treatment has been withdrawn in 10-15% of cases (Buckingham and Hanna, 2008).

The physiological basis of this fluid retention remains unclear but it has been proposed that abnormal stimulation of ENaC in the distal nephron leads to increased Na^+ absorption and therefore water absorption (Zhang *et al.*, 2005, Guan *et al.*, 2005, Hong *et al.*, 2003). PPARγ were found to be expressed along the nephron from human kidney samples but most abundantly in the collecting duct (Hong *et al.*, 2003). Mice treated with either pioglitazone or rosiglitazone

increased in body weight within four days and this was associated with an increase in total body water volume (Guan *et al.*, 2005, Zhang *et al.*, 2005). Furthermore, these studies revealed that selective knockout of PPARγ in the collecting duct of mice prevented increases in body weight with TZD treatment. These data suggest that a collecting duct specific mechanism was involved in the fluid retention associated with TZD treatment. It was postulated that altered ENaC-mediated Na^+ absorption could be responsible since there is high expression of this channel in the collecting duct (Hong *et al.*, 2003). Consistent with this, Hong and colleagues demonstrated that treating a human collecting duct cell line with TZDs for four hours increased the membrane abundance of α-ENaC (Hong *et al.*, 2003). 24 h treatment with these drugs resulted in an increased expression of α-ENaC mRNA and the authors concluded that PPARγ-agonists were mediating Na^+ absorption in a similar manner to aldosterone (Hong *et al.*, 2003). Consistent with this data, two other studies revealed that treatment of primary cultures of collecting duct cells from mice with TZDs stimulated amiloride-sensitive Na^+ transport (Guan *et al.*, 2005, Zhang *et al.*, 2005). Furthermore, cultured cells from PPAR$\gamma^{-/-}$ mice did not show this increase in Na^+ transport. SGK1 activity and mRNA expression in a human collecting duct cell line was also shown to be upregulated in response to TZD treatment (Hong *et al.*, 2003). Further evidence for a role of SGK1 was demonstrated in SGK1$^{-/-}$ mice who did not gain weight with pioglitazone treatment (Artunc *et al.*, 2008). It was therefore postulated that PPARγ agonists were signalling via SGK1 to upregulate Na^+ absorption in a manner analogous to insulin / aldosterone regulation of ENaC.

Whilst these studies provided a great deal of evidence for PPARγ-agonist-mediated fluid retention being the result of increased ENaC activity in the collecting duct, a number of further studies were not in agreement with this hypothesis (Nofziger *et al.*, 2005, Song *et al.*, 2004, Vallon *et al.*, 2009). Song *et al.* showed that rats treated with rosiglitazone stimulated Na^+ and water reabsorption but found increased mRNA expression of other transporters including Na^+ / K^+ ATPase, NKCC2 and NHE_3 but not of ENaC (Song *et al.*, 2004). Interestingly this study showed that rosiglitazone-treatment actually lowered mean arterial blood pressure which seems at odds with increased Na^+ and water absorption. In three different kidney cell lines: A6, M1 and mpkCCDcl4, Nofziger and colleagues demonstrated that two TZDs did not alter ENaC-mediated Na^+ transport under basal or insulin-stimulated conditions (Nofziger *et al.*, 2005). Very strong evidence for a lack of ENaC in mediating fluid retention in response to PPARγ-agonists came from a study that showed rosiglitazone could still stimulate fluid retention in mice with a selective knockout of α-ENaC in the collecting duct (Vallon *et al.*, 2009). Furthermore this study demonstrated that in patch clamp recordings from split-open tubules from the collecting duct, TZD treatment did not alter ENaC activity (Vallon *et al.*, 2009). Collectively these studies reveal that the mechanism underpinning TZD-induced fluid retention is not fully understood and the role that ENaC as well as SGK1 play in this response is inconclusive, clearly warranting further study.

The aim of the first experiments in this thesis were to confirm that mpkCCDcl4 cells could generate spontaneous Na^+ transport as described previously (Bens et

al., 1999) and to further characterize some basic pharmacological properties of this transport. Furthermore, the responsiveness of these cells to insulin was tested and the electrophysiological effects that this hormone brought about were examined. The phosphorylation of endogenous proteins in the presence of insulin was also studied in an attempt to identify the signalling pathway involved. To explore the hypothesis that PPARγ agonists could alter Na^+ absorption in the mpkCCDcl4 cell line, the effects of two of these drugs: pioglitazone and rosiglitazone; on basal and insulin-stimulated Na^+ transport were examined. The activity of SGK1 was also monitored by measuring the phosphorylation of a downstream substrate NDRG1.

3.2 Results

3.2.1 Bioelectric properties of mpkCCDc14 cells

Initial experiments were undertaken to investigate the bioelectric properties of mpkCCDc14 cells as they had not been previously characterised in our laboratory. The cells were seeded on snapwells and mounted in Ussing chambers to record V_t. Baseline V_t in hormone-deprived cells was -47.8 ± 0.8 mV (n = 302). When the current clamp pulse protocol was applied (Chapter 2), as can be seen in Figure 3.1, V_t hyperpolarised. R_t was calculated to be 2.5 ± 0.1 kΩ cm^2 (n = 302) and I_{eq} was -20.4 ± 0.5 µA cm^{-2} (n = 302). These data demonstrate that mpkCCDc14 cells generate a large transepithelial voltage as well as a high resistance indicating these cells form a tight epithelial monolayer which give rise to a spontaneous current.

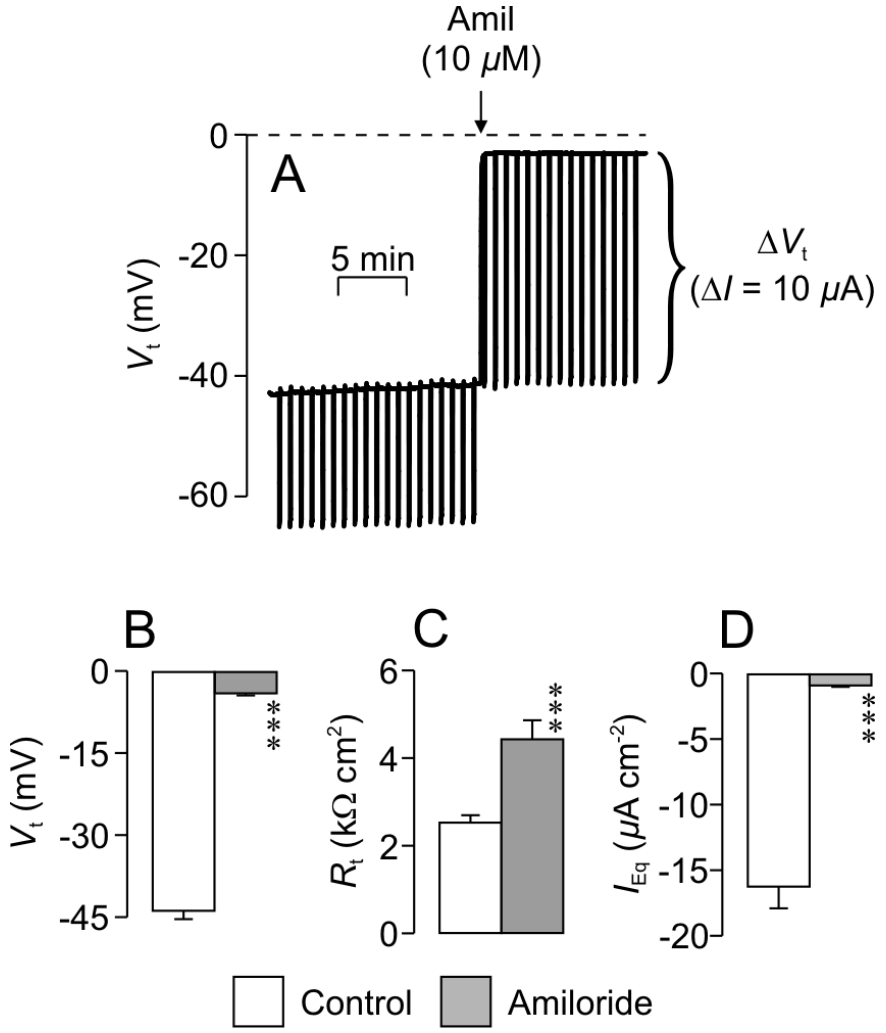

Figure 3.1 Bioelectric properties of mpkCCDc14 cells.

(A) Example of continuous recording of V_t in mpkCCDc14 cells. The pulse protocol elicits baseline V_t and a -10 µA pulse produces a hyperpolarisation seen as a downward deflection. Addition of 10 µM amiloride to the apical bath is denoted by the arrow, Amil. (B-D) Pooled data (n = 8) showing control and amiloride treated V_t, R_t and I_{eq}. Data is shown as mean ± S.E.M. with asterisks denoting statistical significance (Student's unpaired t-test), *** $p < 0.001$.

Amiloride, a potent inhibitor of the epithelial sodium channel (ENaC), was applied to the apical bath, arrow notes addition in Figure 3.1A. The effects of this ENaC inhibitor on V_t, R_t and I_{eq} can be seen in Figure 3.1B-D. This drug significantly depolarised V_t from -43.8 ± 1.5 mV to -3.9 ± 0.4 mV (Figure 3.1B, *n*

= 8, $p < 0.001$).This was associated with a significant increase in R_t from 2.5 ± 0.2 kΩ cm^2 to 4.4 ± 0.4 kΩ cm^2 (Figure 3.1B, n = 8, $p < 0.001$). Finally, I_{eq} was significantly reduced from -16.2 ± 1.7 µA cm^{-2} to -0.9 ± 0.1 µA cm^{-2} (Figure 3.1D, n = 8, $p < 0.001$). Amiloride clearly inhibits the transepithelial voltage and the current that remains following the addition of the drug is negligible. These data clearly demonstrate that the majority of I_{eq} is carried by Na^+ ions moving via ENaC.

To further characterize ENaC-mediated I_{eq} in these cells, experiments were carried out to define the dose-response relationship of amiloride as well as two other well-known inhibitors of ENaC: benzamil and 5-(N-Ethyl-N-isopropyl) amiloride (EIPA). Amiloride was added to the apical bath in increasing doses in a cumulative manner. Changes in V_t were recorded which allowed calculation of both R_t and I_{eq} (Figure 3.2, see Chapter 2). Increasing concentrations of amiloride were associated with a depolarisation of V_t, with the maximal dose (300µM) leaving a transepithelial voltage of -1.8 ± 0.4 mV (Figure 3.2A, n = 9). R_t increased in response to increasing concentrations of amiloride, peaking at 4.1 ± 0.5 kΩ cm^2 at a dose of 10 µM, then began to gradually fall over the final three doses, but remaining above that of control (Figure 3.2B, n = 9). I_{eq} was inhibited with increasing concentrations of amiloride with the maximum dose (300 µM). At this concentration I_{eq} was negligible, -0.6 ± 0.1 µA cm^{-2} (Figure 3.2C, n = 9). The concentration of amiloride need for half-maximal inhibition of I_{eq} (IC_{50}) was calculated to be 0.77 ± 0.07 µM.

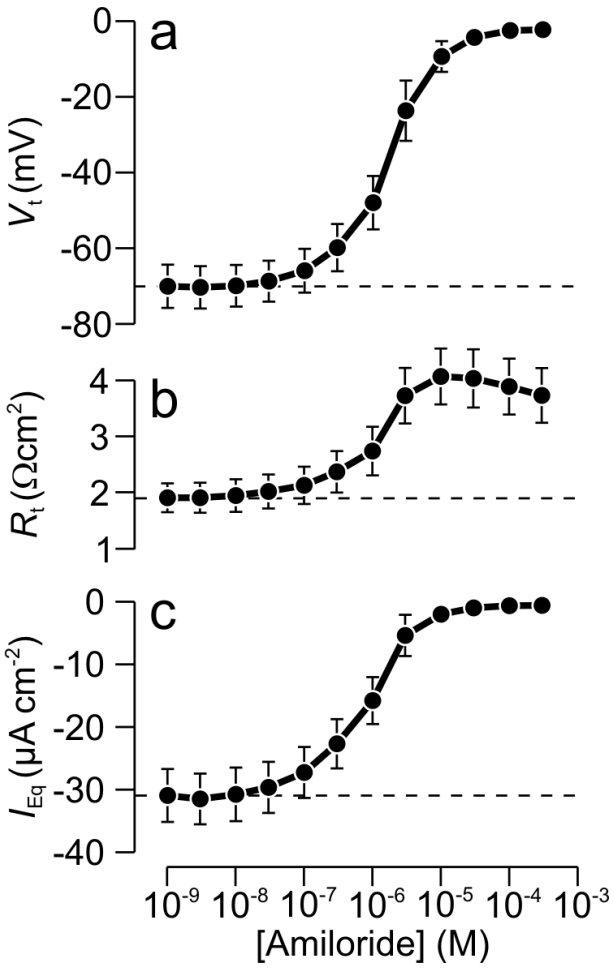

Figure 3.2 Dose response of amiloride - a potent ENaC inhibitor.

The electrometric response to increasing concentrations of amiloride added to the apical bath in a cumulative manner: (a) V_t , (b) R_t and (c) I_{eq} . Data is shown as mean ± S.E.M. (n = 9).

Identical experiments were carried out to determine the dose-response relationships of two other known inhibitors of ENaC: benzamil and EIPA; I_{eq} was calculated for each drug (Figure 3.3 Dose response of benzamil, amiloride and EIPA. Sigmoid curves were fitted to the data using least squares regression (GraFit 5, Erithacus Software Limited) and the IC_{50} was calculated to determine the concentration of the drug that caused 50 % inhibition of I_{eq}. The IC_{50} of benzamil was calculated to be 22.6 ± 1.0 nM and this drug was therefore more

potent than amiloride. EIPA was the least potent and although the IC_{50} was calculated to be 90.0 ± 20.0 µM, the highest concentration tested (300 µM) caused only ~75% inhibition of I_{eq} making it difficult to accurately calculate the IC_{50}. The rank order potencies amongst these compounds are therefore benzamil > amiloride > EIPA. These data confirm that mpkCCDcl4 cells spontaneously absorb Na^+ from the apical bath via an ENaC-dependent mechanism (Bens *et al.*, 1999).

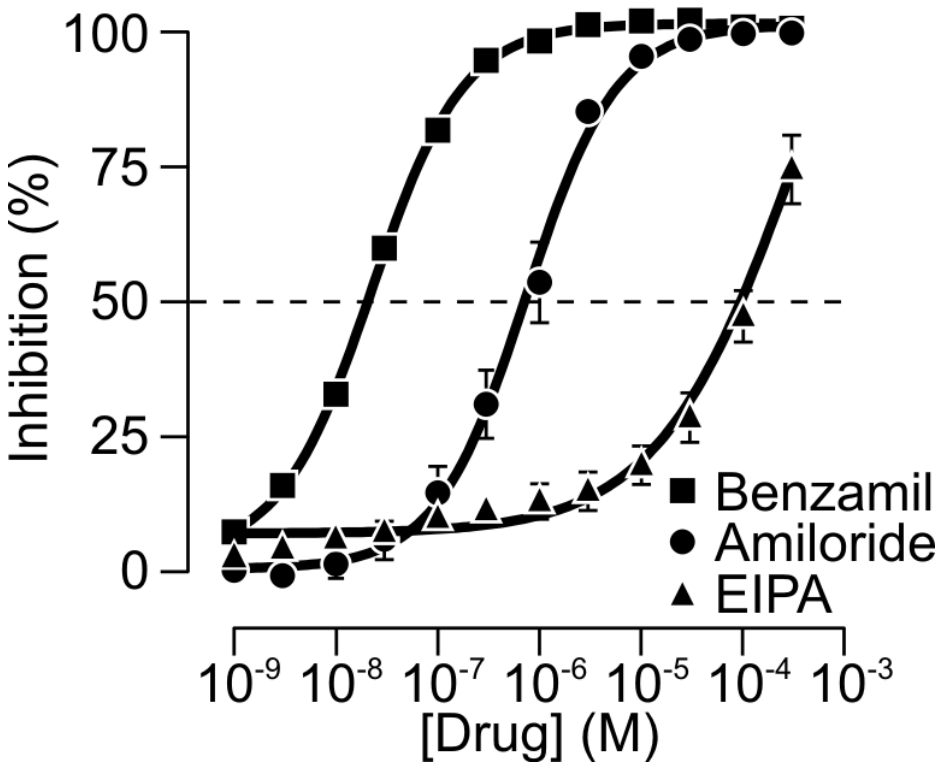

Figure 3.3 Dose response of benzamil, amiloride and EIPA.

The effects of increasing concentrations of three inhibitors of ENaC on basal I_{eq}. Data is shown as mean percentage inhibition of I_{eq} ± S.E.M. (benzamil, n = 8, amiloride, n = 9, EIPA, n = 7). The sigmoid curves were fitted to these data by least squares regression (GraFit 5, Erithacus Software Limited).

3.2.2 The electrometric response to insulin

To explore the effects of the hormone insulin on the basal current in the collecting duct cells, the electrical parameters of control and insulin-treated cells were compared. 20 nM insulin was chosen as a dose as this concentration had previously been shown to stimulate ENaC-mediated Na^+ transport in the A6 cell line (Blazer-Yost *et al.,* 1998). Other studies have found half-maximal concentrations of insulin required to stimulate Na^+ transport in the low nM region (Blazer-Yost *et al.*, 1989, Marunaka *et al.*, 1992). Similarly, a more recent study demonstrated that in three cell lines: A6, M1 and mpkCCDcl4, the half-maximal dose required for stimulation of Na^+ transport was 1-3 nM (Nofziger *et al.*, 2005). Nofziger *et al.* showed that the concentration of insulin required to maximally stimulate Na^+ transport in the mpkCCDcl4 cell line was 30 nM, therefore in the experiments carried out in the present study, 20 nM would be stimulating near-maximal Na^+ transport (Nofziger *et al.*, 2005).

Solvent vehicle or insulin (20 nM) were added to the basolateral bath after a 10 min baseline recording. After a latency period of 5 min, the effects of this hormone became visible and after 60 min treatment V_t had become significantly hyperpolarised (Figure 3.4, $n = 8$, $p < 0.001$). This response was not seen in control cells which instead depolarized slightly over time (Figure 3.4, $n = 8$, $p < 0.01$). This depolarization was observed in all Ussing chamber recordings in the present study and appears to be a slight run-down over time. In the presence of insulin, R_t significantly decreased (Figure 3.4, $n = 8$, $p < 0.01$) whereas control cells showed no change. With a hyperpolarisation of V_t and a decrease in R_t, a

significant increase in I_{eq} was observed (Figure 3.4, $n = 8$, $p < 0.001$). Under control conditions I_{eq} slightly decreased (Figure 3.4, $n = 8$, $p < 0.001$), which is consistent with a slight depolarisation of V_t and no change in R_t. The application of amiloride (10 μM) to the apical bath caused an inhibition of I_{eq} due to a depolarisation of V_t and an increase in R_t (Figure 3.4) as seen previously (Figure 3.1). Therefore, acute addition of insulin stimulates an increase in ENaC-mediated Na^+ absorption in this cell line. Interestingly in the presence of insulin following application of amiloride, R_t was significantly increased compared with control values (Figure 3.4, $n = 8$, $p < 0.01$) indicating that this hormone must be having another effect such as increasing paracellular resistance; these effects were not investigated further. Mean values for the electrical parameters measured at all compared time-points under control and insulin-stimulated conditions can be found in Table 3.1.

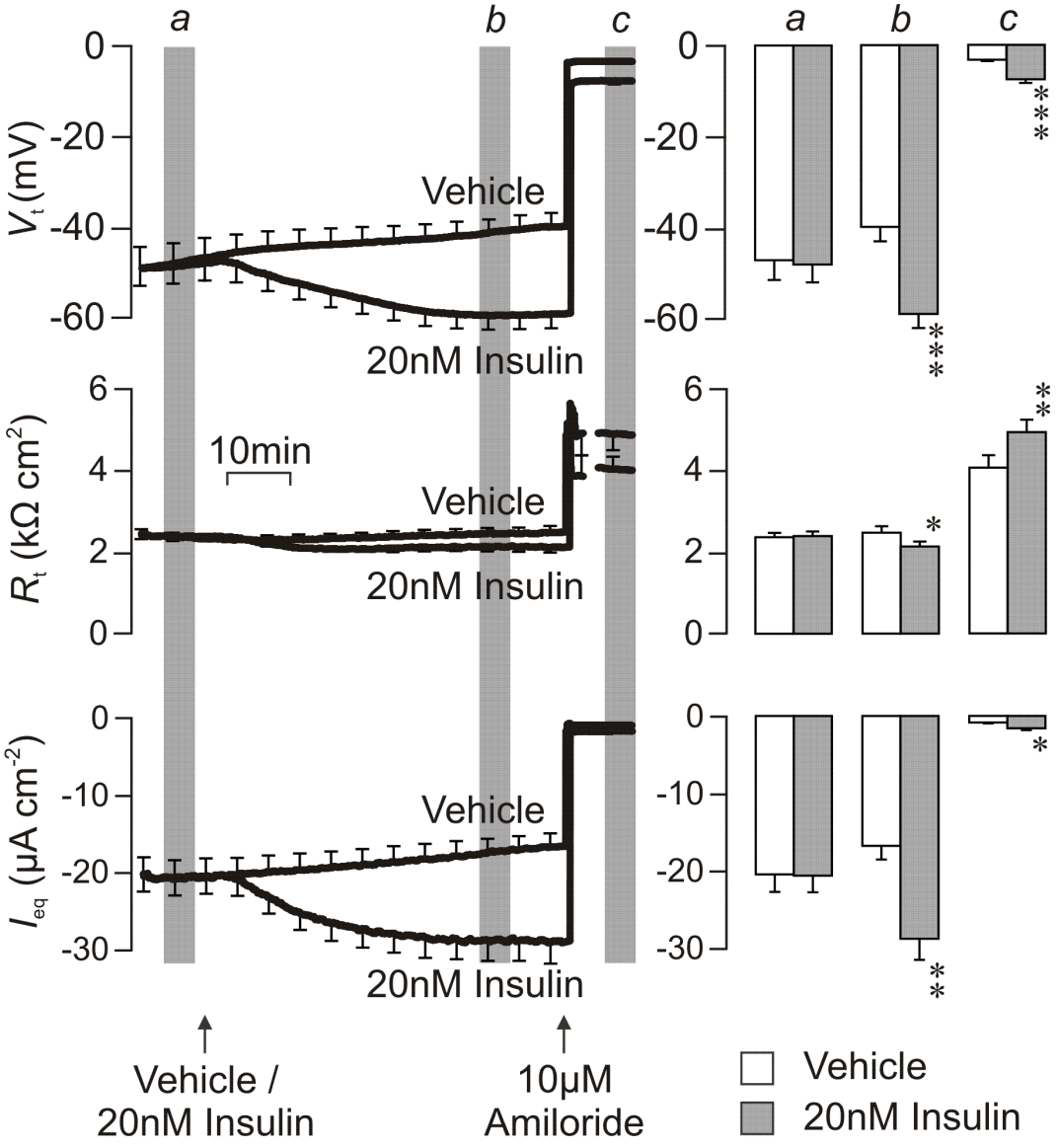

Figure 3.4 The electrometric response to acute application of insulin.

Transepithelial voltage V_t recorded (top left trace) under control conditions or with addition of insulin (20nM), allowing calculation of R_t and I_{eq} (middle and bottom left traces). Mean values from time points throughout the experiment were taken (a) prior to addition of vehicle / drug, (b) once the response to insulin was established and (c) after application of amiloride (10μM), shaded areas denote the sampling periods. Right hand panels show mean values for V_t (top), R_t (middle) and I_{eq} (bottom). Data is shown as mean ± S.E.M. (n = 8) and statistical significance (Student's unpaired t-test) denoted by asterisks (* $p < 0.05$, ** $p < 0.01$, *** $p < 0.001$).

Table 3.1 Electrical parameters of control and insulin-treated cells.

Mean data ± S.E.M. (n = 8) for V_t, R_t and I_{eq} recorded from vehicle- or insulin-treated cells. Time points are taken from a baseline recording, 60 min after vehicle / insulin and following 10 min exposure to amiloride. Asterisks denote statistically significant effects of insulin on V_t, R_t and I_{eq} compared to control cells (Student's unpaired t-test), *, $p < 0.05$, **, $p < 0.01$, *** $p < 0.001$.

	Vehicle-treated			Insulin (20 nM)		
	Pre-exposure	60 min exposure	Post-amiloride	Pre-exposure	60 min exposure	Post-amiloride
V_t (mV)	-47.0 ± 4.3	-39.8 ± 3.2	-3.0 ± 0.3	-47.9 ± 3.9	-58.8 ± 3.1***	-7.5 ± 0.8***
R_t (kΩ cm^2)	2.4 ± 0.1	2.5 ± 0.2	4.1 ± 0.3	2.4 ± 0.1	2.1 ± 0.1*	4.9 ± 0.4**
I_{eq} (μA cm^{-2})	-20.4 ± 2.3	-16.7 ± 1.8	-1.6 ± 0.2	-20.5 ± 2.1	-28.6 ± 2.7**	-0.9 ± 0.1*

3.2.3 The effect of insulin on phosphorylation of endogenous proteins

To investigate the signalling pathway underlying the insulin-mediated increase in amiloride-sensitive Na^+ transport, the phosphorylation of endogenous proteins in response to insulin was monitored. Cells grown on transwells were maintained in serum-free media for 18-24 h, as described previously (Chapter 2), and cells were lysed (see Methods, 2.3.1) after 0-6 h exposure to insulin. This allowed construction of a time course showing the effects of insulin on the abundance of phosphorylated NDRG1-Thr$^{346/356/366}$ and total protein. Within 15 min of application of insulin, the abundance of P-NDRG1-Thr$^{346/356/366}$ was three-fold that of control (Figure 3.5B). This increased response peaked over the first hour of exposure to insulin, then fell slightly but remained elevated above that of control

for the following 5 hours (Figure 3.5B). These changes in abundance of phosphorlyated NDRG1-Thr$^{346/356/366}$ occurred with no alteration to the abundance of total NDRG1 protein.

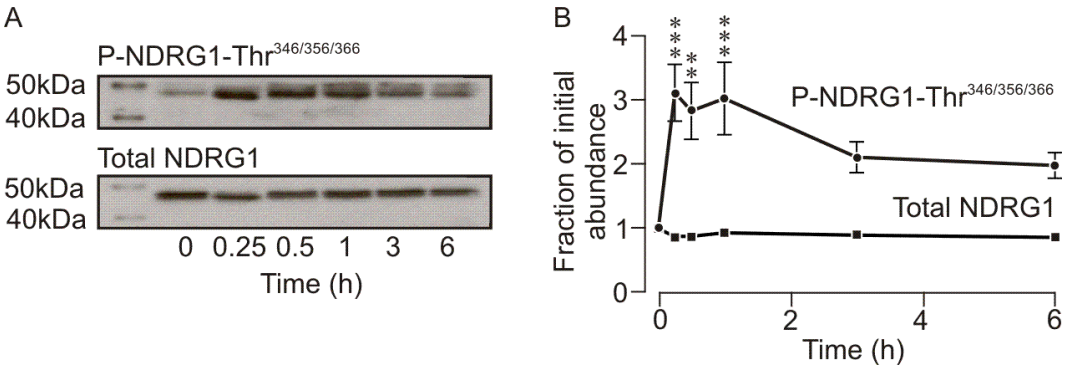

Figure 3.5 Insulin-evoked phosphorylation of NDRG1-Thr$^{346/356/366}$.

Insulin (20nM) was applied to cells over a time course (0-6h), cells were then lysed and Western analysis was carried out. (A) Typical blot showing abundance of phospho-NDRG1-Thr$^{346/356/366}$ (top panel) and total NDRG1 (bottom panel). (B) Densitometric analysis showing levels of phospho-NDRG1-Thr$^{346/356/366}$ and total NDRG1. Data is shown as a mean fraction of initial abundance ± S.E.M (n = 5). Statistical significance of insulin stimulation versus untreated cells is denoted by asterisks, ** p < 0.01, *** p < 0.001, calculated by one-way ANOVA with Bonferroni's multiple comparison post test.

Parallel experiments monitoring the abundance of phosphorylated Akt-Ser^{473} and total protein in response to a time course of insulin (20 nM, 0-6 h) were undertaken. Figure 3.6 shows the results of experiments that used this protocol to explore the effects of insulin upon the phosphorylation of Akt-Ser^{473}. A four-fold increase in the abundance of P-Akt-Ser^{473} was observed within 15 min and this response peaked within the first hour (Figure 3.6B). Similar to the phosphorylation of NDRG1, the abundance of P-Akt-Ser^{473} declined over the next 5 h but remained significantly stimulated over control (Figure 3.6B). Although

phosphorylation of Akt-Ser^{473} provides information about the status of this residue, phosphorylation of another residue, Thr^{308}, is required for full activation of Akt. Since mTORC2 acts downstream of PI3-kinase to phosphorylate Akt at Ser^{473}, this phosphorylation provides an excellent marker of PI3-kinase activity. Therefore these data show that exposing this cell line to insulin increases PI3-kinase activity. To investigate the activity of Akt itself, the phosphorylation of a substrate of this kinase, PRAS40, was therefore monitored.

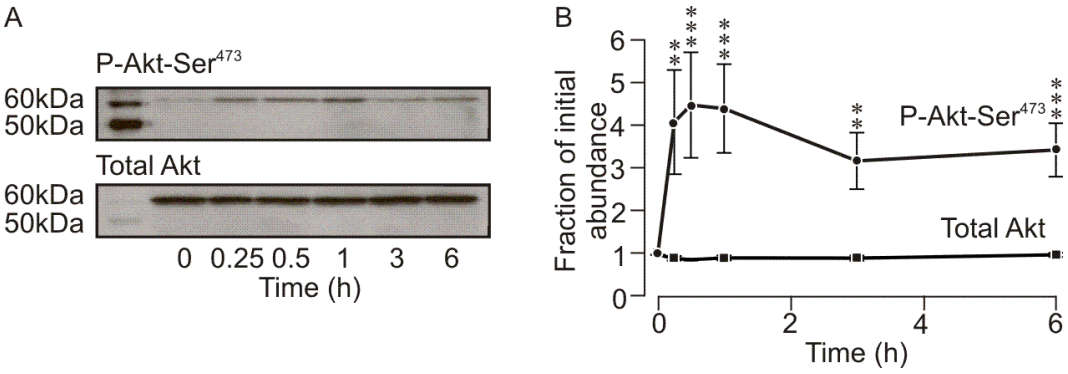

Figure 3.6 Insulin evoked phosphorylation of Akt-Ser^{473}.

Insulin (20 nM) was applied to cells over a time course (0-6 h), cells were then lysed and Western analysis was carried out. (A) Typical blot showing abundance of phospho-Akt-Ser^{473} (top panel) and total Akt (bottom panel). (B) Densitometric analysis showing levels of phospho-Akt-Ser^{473} and total Akt. Data is shown as mean fraction of initial abundance ± S.E.M (n = 5). Statistical significance of insulin stimulation versus untreated cells is denoted by asterisks, ** $p < 0.01$, *** $p < 0.001$, calculated by one-way ANOVA with Bonferroni's multiple comparison post test.

The abundance of phosphorylated PRAS40-Ser^{246} and total PRAS40 were measured under control and insulin stimulated conditions (20 nM, 30 min) to examine the effects of insulin upon Akt activity. After 30 min treatment with insulin, the level of phosphorylated PRAS40-Ser^{246} was double that of control (Figure 3.7B). However, a slight yet significant decrease in the abundance of total

protein was also observed (Figure 3.7B). Due to this change, the level of the phosphorylated form of PRAS40 may be underestimated so the abundance of phosphorylated-PRAS40-Ser^{246} was normalised to the overall abundance of PRAS40. Using this analysis, insulin induces nearly a 3-fold increase in phosphorylated PRAS40-Ser^{246} (Figure 3.7C). This format of calculating the level of phosphorylated PRAS40 has been employed in all subsequent studies of this protein. These data clearly show that 30 min exposure to insulin increases Akt activity in this cell line.

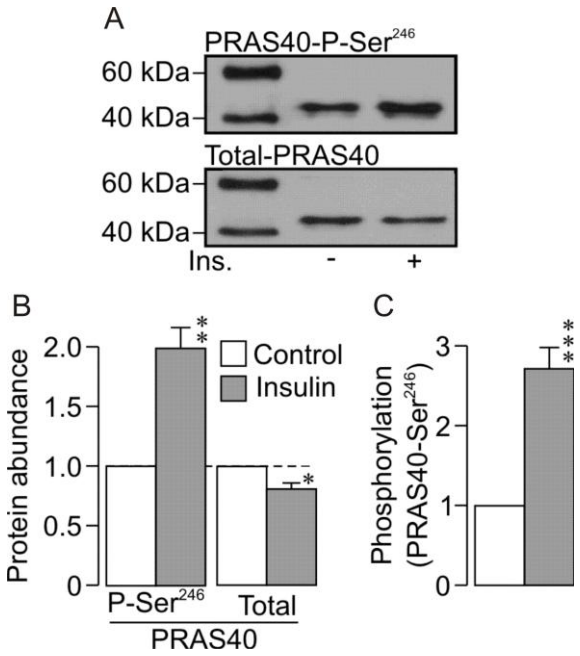

Figure 3.7 Insulin evoked phosphorylation of PRAS40-Ser^{246}.

(A) Typical western blot showing the effects of insulin (20 nM) on the abundance of phosphorylated-PRAS40-Ser^{246} (upper panel) and total PRAS40 (lower panel). (B) Densitometric analysis showing levels of phospho-PRAS40-Ser^{246} and total PRAS40. (C) Further analysis of these data where the abundance of phosphorylated-PRAS40-Ser^{246} was normalised to the total abundance of this protein. Pooled data is shown as mean fraction of initial abundance ± S.E.M (n = 28), asterisks denote statistical significance (*, $p < 0.05$, **, $p < 0.01$, ***, $p < 0.001$) determined by Student's unpaired t-test.

3.2.4 The effect of PPARγ agonists on insulin-stimulated Na^+ transport and SGK1 activity

To investigate the role that PPARγ agonists play in basal and insulin-stimulated Na^+ transport, two of these drugs: pioglitazone and rosiglitazone were used to examine the effect they exerted on both basal and insulin-stimulated I_{SC} in mpkCCDc14 cells as well as their effect on SGK1 activity. Ussing chamber experiments were carried out in collaboration with Dr. Sarah Inglis, a postdoctoral research fellow in our laboratory.

Under control conditions, insulin (20 nM) stimulated I_{SC} (Figure 3.1) in a similar manner to recordings made under open circuit conditions (3.2.3). This response became apparent after 5 min and was inhibited with application of amiloride (10 μM). Preincubating cells with either pioglitazone (10 μM) or rosiglitazone (2 μM) for four hours did not alter the basal I_{SC}, see Table 3.2. Furthermore, preincubation with either PPARγ agonist did not significantly alter the natriferic response to insulin (Figure 3.8). Thus neither pioglitazone or rosiglitazone alter ENaC activity in this murine collecting duct cell line.

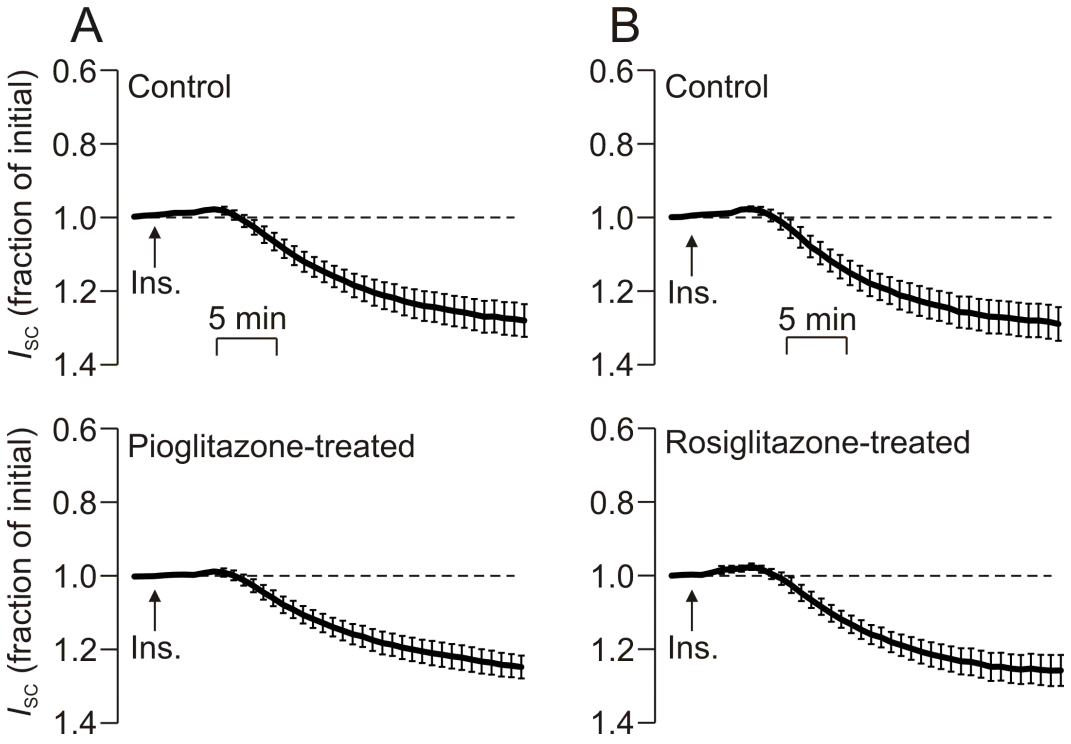

Figure 3.8 The effects of PPARγ agonists on insulin-stimulated I_{eq}.

PPARγ agonist-treated cells were preincubated (4hr) with either (A) pioglitazone (10μM) or (B) rosiglitazone (2μM), whilst control cells were preincubated with solvent vehicle alone. Insulin (20nM) was added basolaterally to the bath as indicated by the arrow and the short circuit current, I_{SC}, recorded under each condition (mean ± S.E.M.) is shown as a fraction of the initial current recorded under unstimulated conditions at the onset of the experiment.

Table 3.2 The effects of PPARγ agonists on basal I_{SC}.

Basal I_{SC} recorded from either pioglitazone-treated cells (10μM, 4 h) or rosiglitazone-treated cells (2μM, 4 h) with their respective controls. Data is shown as mean ± S.E.M. (n = 9 for both pairs).

	Basal I_{SC} (μA cm^{-2})	
	Control	PPARγ agonist treated
Rosiglitazone (2 μM, 4 h)	10.3 ± 1.3	10.6 ± 1.3
Pioglitazone (10 μM, 4 h)	9.8 ± 1.3	10.0 ± 1.2

Since SGK1 activity has previously been reported to be stimulated with exposure to PPARγ-agonists, the effects that pioglitazone and rosiglitazone had on SGK1 activity, by monitoring NDRG1-Thr$^{346/356/366}$ phosphorylation, was investigated. Under control conditions, insulin (20 nM, 30 min) stimulated phosphorylation of NDRG1-Thr$^{346/356/366}$ above basal levels (Figure 3.9). This is consistent with the results of the time course monitoring insulin stimulation of NDRG1-Thr$^{346/356/366}$ phosphorylation (Figure 3.5). Preincubation with pioglitazone (10 μM, 4 h) caused an inhibition of basal NDRG1-Thr$^{346/356/366}$ phosphorylation (Figure 3.9A) and this was statistically significant. The addition of insulin increased phosphorylation of NDRG1-Thr$^{346/356/366}$ to a level similar to control conditions (Figure 3.9A). Preincubation with rosiglitazone (2 μM, 4 h) did not alter either basal or insulin-stimulated NDRG1-Thr$^{346/356/366}$ phosphorylation (Figure 3.9B). These changes in phosphorylation of NDRG1-Thr$^{346/356/366}$ occurred without any alteration in the abundance of total NDRG1 (Figure 3.9). These data demonstrate that these drugs do not stimulate basal SGK1 activity in these cells and in the case of pioglitazone, actually suppress it. Furthermore, these PPARγ-agonists also do not alter insulin-stimulated SGK1 activity.

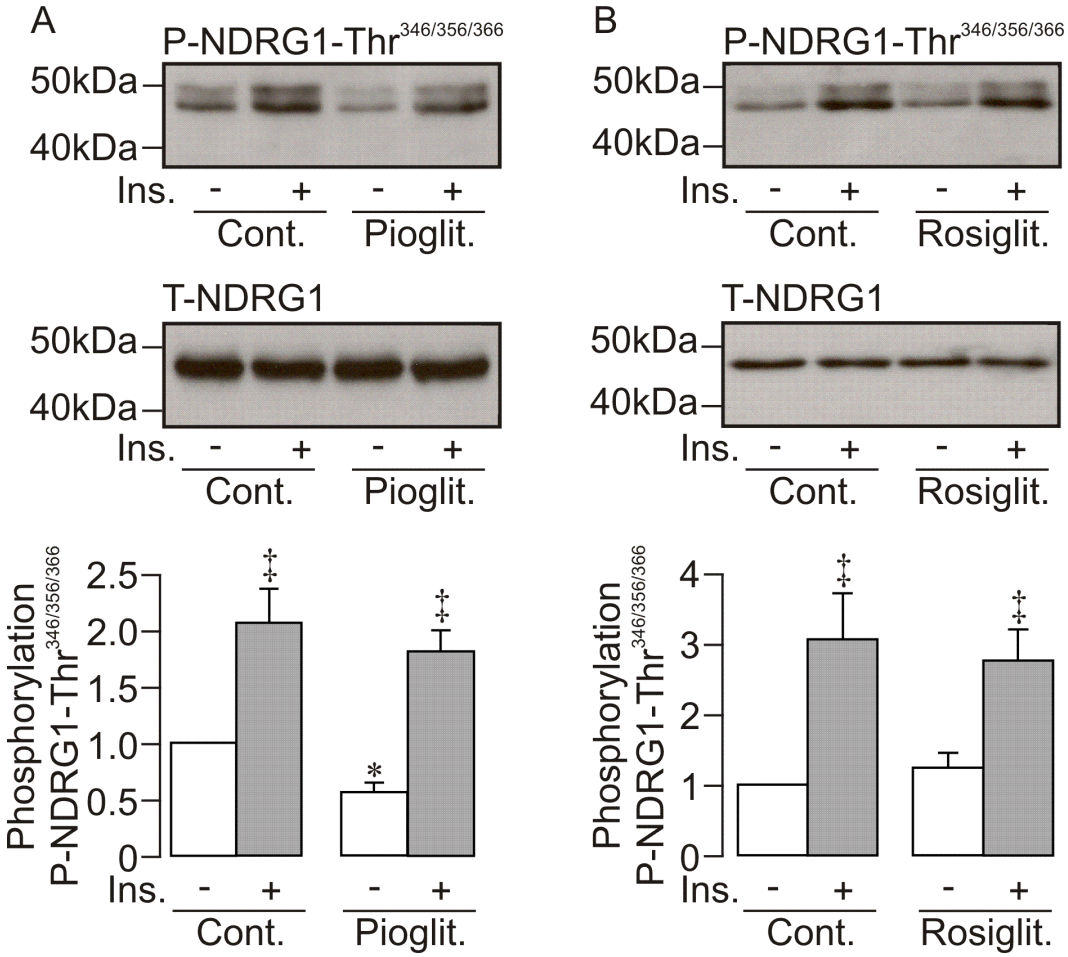

Figure 3.9 The effects of PPARγ agonists on SGK1 activity.

Top panels: typical western blots showing the phosphorylation of NDRG1-Thr$^{346/356/366}$ under unstimulated or insulin-stimulated (20nM, 30 min) conditions in cells pretreated (4 hr) with either PPARγ agonists, (A) pioglitazone (10μM) or (B) rosiglitazone (2μM) or in control cells pretreated with solvent vehicle alone. Middle panels show the respective total protein blots for NDRG1. Lower panels show pooled data of phosphorylation of NDRG1-Thr$^{346/356/366}$ (n = 6) and data is shown as mean ± S.E.M. Daggers denote statistical significance between unstimulated and insulin-treated cells: ‡, $p < 0.01$. Asterisks denote statistically significant effects (One-way ANOVA Bonferroni post hoc test) of pioglitazone on basal phosphorylation of NDRG1-Thr$^{346/356/366}$, *, $p < 0.05$.

3.3 Discussion

3.3.1 Bioelectric and pharmacological properties of unstimulated mpkCCDc14 cells

Under hormone-deprived conditions mpkCCDcl4 cells display a spontaneous voltage with high resistance giving rise to a spontaneous current across the monolayer of -20.4 ± 0.5 µA cm^{-2} (*n* = 302). This finding accords well with other groups who have studied the electrical properties of these cells and found basal currents of 11.1 ± 0.1 µA / cm^2 (Bens *et al.*, 1999) and 10-15 µA / cm^2 (Shane *et al.*, 2006). It is important to note that these research groups used a convention in which I_{SC} was described with positive values, the product of defining the movement of cations across a monolayer of cells as a positive movement of charge. The spontaneous current observed in this study occurs in the absence of any hormones which is unlike a bronchiolar cell line previously used in this laboratory that required the glucocorticoid dexamethasone to produce resistive monolayers with spontaneous currents (Ramminger *et al.*, 2004).

I_{eq} can be inhibited in a dose-dependent manner by amiloride, benzamil and EIPA, with the first two compounds known to be potent blockers of ENaC. The present data shows that the rank order potency of these drugs is benzamil > amiloride > EIPA. The EC_{50} values of amiloride and benzamil are similar to the values found by Bens *et al.* of 500 nM and 30 nM respectively (Bens *et al.*, 1999). The basal current therefore can be attributed to the movement of Na^+ ions passing through ENaCs in the apical membranes of these cells.

3.3.2 Bioelectric and pharmacological properties of insulin-stimulated cells

The addition of insulin (20nM) to the basolateral bath resulted in a significant hyperpolarisation of V_t and fall in R_t resulting in a significant increase in I_{eq}. Insulin produced a change in I_{eq}, $\Delta I_{eq,}$ of -8.1 ± 0.6 μA cm^{-2}. This finding accords well with those of Nofziger *et al.* who demonstrated that insulin (30nM) induced a change in short circuit current (ΔI_{SC}) of ~ 6 μA cm^{-2} in mpkCCDcl4 cells (Nofziger *et al.*, 2005). Although the insulin response presented in this study has already been documented, the current clamp protocol employed here allows the quantification of V_t, R_t and I_{eq}. Furthermore, these data demonstrate that this method gives comparable results to direct short circuit measurements. The present data demonstrates a clear and significant natriferic response to insulin providing a model that allows exploration of the signalling pathway underpinning this response.

A time course investigating the effect of treating cells with insulin (20 nM) revealed that within 15 min phosphorylation of both NDRG1-$Thr^{346/356/366}$ and Akt-Ser^{473} had peaked to 3-fold or 4-fold that of control respectively. The peak response to insulin occurred within one hour and allowed identification of a time point (30 min) that produced a maximal response. This time point was therefore used in all subsequent experiments. As described previously (Chapter 2), NDRG1-$Thr^{346/356/366}$ is a specific substrate of SGK1 but not of other closely related kinases such as Akt and therefore provides a method for monitoring SGK1 activity. From these experiments it is clear that acute treatment with insulin

stimulates SGK1 activity as well as PI3-kinase activity. This finding is consistent with other studies that have reported an increase in phosphorylation of SGK1 in response to insulin in mpkCCDcl4 cells (Wang *et al.*, 2008). Phosphorylation of PRAS40-Ser^{246} also increased with 30 min exposure to insulin indicating that Akt activity is also stimulated in response to insulin, this effect has also previously been demonstrated (Alessi *et al.*, 1996).

3.3.3 The effects of PPARγ agonists on I_{SC} and SGK1 activity

Preincubating cells with the PPARγ agonists pioglitazone or rosiglitazone did not alter basal or insulin-stimulated I_{SC} indicating these drugs do not change ENaC activity in this cell line (Wilson *et al.*, 2010). This finding is in accordance with a number of studies that have shown volume retention by PPARγ agonist treatment does not correlate with increased ENaC activity. Nofziger *et al*. demonstrated that in three different kidney-derived cells lines: A6, M1 and mpkCCDcl4; pioglitazone and GW7845, both PPARγ agonists did not enhance basal or insulin-stimulated ENaC activity (Nofziger *et al.*, 2005). Our laboratory has also demonstrated that both pioglitazone and rosiglitazone do not alter insulin-induced Na^+ transport in another Na^+ absorbing cell line, H441, derived from airway epithelia (Wilson *et al.*, 2010). Vallon and colleages demonstrated that ENaC expression remained unaltered with rosiglitazone treatment and that this drug caused fluid retention in α-ENaC$^{-/-}$ mice. Furthermore, the authors demonstrated that in patch clamp studies of split-open cortical collecting ducts from wild-type mice neither rosiglitazone nor pioglitazone altered the open probability or the number of ENaC channels per patch (Vallon *et al.*, 2009). Further evidence for

that lack of ENaC involvement came from a study that showed addition of amiloride did not prevent the increase in plasma volume brought about by farglitazar (Chen *et al.*, 2005). Together with the present study, these findings do not support the theory that increased fluid retention due to PPARγ agonist treatment is brought about by alterations to ENaC activity in the distal nephron.

These studies contrast with earlier work where it was demonstrated that fluid retention in mice brought about by treatment with either pioglitazone (Guan *et al.*, 2005) or rosiglitazone (Zhang *et al.*, 2005) could be prevented by deletion of PPARγ in the collecting duct. Both of these studies also showed that TZDs could increase amiloride-sensitive Na^+ transport, as shown by measuring transepithelial radiolabelled Na^+ flux, in cultured collecting duct cells (Guan *et al.*, 2005, Zhang *et al.*, 2005). It is of note that the study carried out by Guan *et al*. showed an increase in Na^{22} flux but in the supplementary information give details of the electrical parameters recorded showing pioglitazone caused a depolarisation of V_t and a fall in R_t. Using Ohm's law the transepithelial current can be calculated before and after pioglitazone treatment and there is no change in current; this is not consistent with an increase in ENaC-mediated Na^+ absorption (Guan *et al.*, 2005). More recently, Pavlov *et al.* demonstrated that whilst PPARγ agonists did not alter short circuit current in mpkCCDcl4 cells, two PPARγ antagonists significantly decreased short circuit current. This study also showed that co-expression of PPARγ with α-, β- and γ-ENaC in Chinese hamster ovary (CHO) cells could increase ENaC activity (Pavlov *et al.*, 2009). Whilst Hong *et al.* demonstrated that TZD treatment increased expression of α-ENaC (Hong *et al.*,

2003) other studies found no alteration to any subunits of ENaC but rather saw increased expression of the Na^+ / K^+ ATPase in mice treated with farglitazar (Chen *et al.*, 2005) as well as rosiglitazone (Song *et al.*, 2004). Furthermore, the abundance of the water channel aquaporin 2 (AQP2) mRNA was found to be increased in mice treated with farglitazar (Chen *et al.*, 2005). These studies provide alternative mechanisms for fluid retention that do not involve direct increases in ENaC activity. It is also interesting to note that Vallon *et al.* discuss the possibility that TZD treatment can lead to activation of a non-selective cation channel in mouse inner medullary collecting duct (IMCD) cells. This channel is sensitive to amiloride at concentrations used in the study by Guan *et al.* and could account for the amiloride-sensitive current they measured in primary collecting duct cells (Guan *et al.*, 2005, Vallon *et al.*, 2009).

The present study demonstrated that whilst pioglitazone decreased basal SGK1 activity, insulin stimulated activity similar to control conditions. Rosiglitazone had no apparent effect on basal or insulin-stimulated SGK1 activity. These data do not indicate a role for SGK1 in response to PPARγ activation. This is in contrast with studies that have found exposing human CCD cells (Hong *et al.*, 2003) or proximal tubule cells (Saad *et al.*, 2009) to PPARγ agonists increased both SGK1 mRNA and protein expression. It is important to note that the study carried out by Hong *et al*. immunoprecipitated SGK1 out of human CCD cells and then used a generic peptide sequence as a substrate to measure SGK1 activity (Hong *et al.*, 2003). This peptide can be recognised by various AGC kinases and therefore the results absolutely depend on the accurate immunoprecipitation of

SGK1, as any other similar kinases could equally phosphorylate the substrate. Artunc and colleagues studied $SGK1^{-/-}$ mice and discovered that $SGK1^{-/-}$ mice still retained fluid in response to pioglitazone, albeit to a lesser extent than in wild-type mice (Artunc *et al.*, 2008). This finding indicates that SGK1 contributes in mediating PPARγ-induced fluid retention, but it does not fully account for it. The findings of the present study do not support a role for increased SGK1 activity in response to PPARγ agonist treatment in mpkCCDcl4 cells and this is consistent with Nofziger *et al.* who did not observe any alteration to SGK1 expression in response to PPARγ agonist exposure (Nofziger *et al.*, 2005).

Together our findings conclude that the PPARγ agonists pioglitazone and rosiglitazone do not alter basal or insulin-stimulated ENaC activity in the mpkCCDcl4 cell line and do not stimulate SGK1 activity. The present data also confirm that mpkCCDcl4 cells generate spontaneous Na^+ absorption mediated via ENaC. Insulin can stimulate this response and also increase activity of PI3-kinase, Akt and SGK1. To further investigate the role that these kinases play in mediating the natriferic effect of insulin in the collecting duct, specific small molecule inhibitors were used. The first of these inhibitor experiments investigated the role of PI3-kinase in mediating basal and insulin-stimulated Na^+ transport.

Chapter 4 - The role of PI3-kinase in basal and insulin-stimulated Na^+ transport

4.1 Introduction

Having identified a model of insulin-stimulated Na^+ transport in the collecting duct (see Chapter 3), the next aim in this thesis was to investigate the signalling pathway involved in this stimulation.

When insulin binds its receptor in the basolateral membrane of epithelial cells the receptor undergoes autophosphorylation at several tyrosine residues (White *et al.*, 1985). These phosphorylated residues are recognised by phosphotyrosine-binding (PTB) domains of insulin receptor substrates (IRS) which are recruited to the plasma membrane (Sun *et al.*, 1991). The phosphorylated insulin receptor subsequently phosphorylates the IRS at various residues, some of which are recognised by the p85 regulatory subunit of PI3-kinase, in turn recruiting it to the plasma membrane. The catalytic subunit of PI3-kinase, p110, phosphorylates phosphatidylinositol (4,5) bisphosphate (PIP_2) to produce phosphatidylinositol (3,4,5) triphosphate (PIP_3). PIP_3 binds to pleckstrin homology (PH) domains on effector proteins including 3-phosphoinositide-dependent protein kinase 1 (PDK1) which is thought to play a role in insulin signalling by phosphorylating the activation loop of AGC kinases including Akt, SGK1 and S6K (Park *et al.*, 1999). PDK1 has been shown to be PI3-kinase-dependent as studies where, in the presence of excess PIP_3, phosphorylation of Akt-Thr^{308} was greatly increased (Komander *et al.*, 2004). Inhibition of PI3-kinase in mammary tumour cells with wortmannin (100nM) or LY294002 (50μM) resulted in a novel dephosphorylation

of SGK1 (Park *et al.*, 1999). Taken together these studies suggest that PDK1 acts downstream of PI3-kinase in the insulin signalling pathway.

PI3-kinase also activates the mammalian target of rapamycin complex 2, mTORC2, by an unknown mechanism. mTORC2 is also thought to play a role in insulin signalling by phosphorylating the hydrophobic motif of AGC kinases including Akt-Ser^{473} and SGK1-Ser^{422}. Studies where PI3-kinase was inhibited with PI103 (1μM, 30 min) resulted in dephosphorylation of both Akt-Ser^{473} and SGK1-Ser^{422} (García-Martínez and Alessi, 2008) indicating mTORC2 lies downstream of PI3-kinase.

Furthermore, insulin-stimulated Na^+ transport has also been shown to be dependent on PI3-kinase. Treatment of the A6 kidney cell line with an insulin tyrosine receptor kinase inhibitor, HNMPA, inhibited the insulin-stimulated short circuit current by ~50% (Record et al., 1998). Two PI3-kinase inhibitors: wortmannin and LY294002 also inhibited the insulin-stimulated short circuit current. These findings demonstrate that the natriferic effect of insulin is dependent on PI3-kinase. A study involving the mpkCCDcl4 cell line showed that an analogous stimulation of Na^+ absorption using insulin-like growth factor (IGF) could be inhibited using LY294002 (Staruschenko *et al.*, 2007). Furthermore, another study using this cell line where the p110α subunit of PI3-kinase was inhibited using compounds that specifically target this subunit: PI103 and PIK90, revealed that p110α was required for the stimulation of Na^+ transport by insulin (Wang *et al.*, 2008). Both of these studies show that insulin stimulates Na^+

transport in mpkCCDcl4 cells and that PI3-kinase activity is critical for this response. Interestingly in the H441 airway epithelial cell line, application of insulin alone cannot evoke an ENaC-mediated Na^+ current (Brown *et al.*, 2008). Similarly expression of constitutively active PI3-kinase mimics this effect, also with no stimulation of ENaC-mediated transport. Therefore activation of PI3-kinase does not always equate to an increase in ENaC activity in absorptive epithelia. Wang *et al*. also showed that inhibition of the Na^+ current in mpkCCDcl4 cells with PI103 and PIK90 is accompanied by inhibition of the phosphorylation of downstream kinases including SGK1 and Akt. This further suggests that these proteins are involved in the signalling pathway linking insulin binding its receptor to increased Na^+ reabsorption.

The majority of these studies have demonstrated an involvement of PI3-kinase in the insulin signalling pathway. To confirm a role of PI3-kinase in our model of insulin signalling, we investigated the effects of three PI3-kinase inhibitors: wortmannin, PI103 and the more novel GDC0941. The effects of these compounds on basal and insulin-stimulated Na^+ transport were examined in addition to measuring the activity of the endogenous proteins PI3-kinase, SGK1 and Akt. Both PI103 (Raynaud *et al.*, 2007) and wortmannin (Brunn *et al.*, 1996) have previously been shown to inhibit the mammalian target of rapamycin complex 1 (mTORC1) in addition to inhibiting PI3-kinase. Therefore the effects of a specific inhibitor of mTORC1, rapamycin, on unstimulated and insulin-stimulated current as well as the phosphorylation of endogenous proteins were also investigated.

4.2 Results

4.2.1 The effects of PI3-kinase inhibtors on I_{eq}

Wortmannin (100 nM) or solvent vehicle were added bilaterally to Ussing chambers for 30 min followed with basolateral application of insulin (20 nM) for a further 60 min. Figure 4.1 shows that wortmannin rapidly and significantly inhibited the basal current by 48.8 ± 2.4% (n = 5, p < 0.01). This decrease in I_{eq} occurred with a concomitant decrease in V_t and little effect on R_t, full details of the effects on electrical parameters can be found in Table 4.1. Control cells showed a slight decrease in I_{eq} over the same 30 min period but this was not statistically significant. Therefore wortmannin is inhibiting basal Na^+ absorption and suggests PI3-kinase plays an important role in this transport.

The addition of insulin (20nM) to the basolateral bath in control cells produced a stimulation of I_{eq}, (Figure 4.1) however due to the baseline drift in V_t this stimulation is difficult to quantify. In the presence of wortmannin however, the addition of insulin does not stimulate I_{eq}, instead it decreases slightly over 60 min (Figure 4.1). This decrease in I_{eq} is accompanied by a statistically significant fall in R_t over the 60 min period (Table 4.1, n = 5, p < 0.001). The resistance in control cells remained unchanged with the addition of insulin as seen previously. Wortmannin is preventing stimulation of Na^+ transport indicating a role for PI3-kinase in this signalling pathway. However, the alteration to R_t suggests that this drug is affecting epithelial integrity therefore further investigation into the role of PI3-kinase was studied using two other inhibitors.

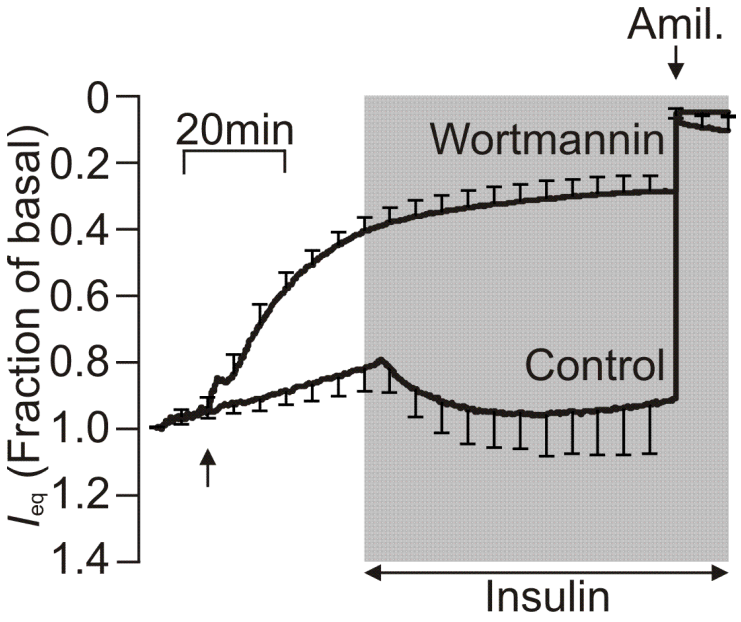

Figure 4.1 Effects of wortmannin on insulin-stimulated I_{eq}.

I_{eq} of control and wortmannin (100 nM) treated cells. Vehicle / drug were added bilaterally for 30min, arrow indicates addition. Insulin (20nM) was added basolaterally for 60 min, grey shading indicates treatment. Amiloride (10μM) was added for 10min at the end of the experiment, arrow and Amil. indicates addition. Mean data is shown as fraction of the initial current ± S.E.M. (n = 5).

Table 4.1 Electrical parameters of control and wortmannin-treated cells.

Mean data ± S.E.M. (n = 5) for V_t, R_t and I_{eq} from vehicle- or wortmannin-treated cells. Values are from baseline, 30 min exposure to vehicle / drug and 60 min after exposure to insulin. Asterisks denote statistically significant effects of vehicle / wortmannin on V_t, R_t and I_{eq} calculated using a Student's unpaired t-test, *, $p < 0.05$, **, $p < 0.01$, *** $p < 0.001$.

	Vehicle-treated			Wortmannin (100 nM)		
	Baseline	30 min vehicle	60 min insulin	Baseline	30 min wort.	60 min insulin
V_t (mV)	-57.0 ± 3.4	-50.2 ± 2.1	-54.4 ± 5.3	-52.6 ± 4.9	-21.8 ± 2.4***	-3.6 ± 1.9***
R_t (kΩ cm^2)	2.1 ± 0.2	2.2 ± 0.2	2.2 ± 0.1	2.2 ± 0.2	2.0 ± 0.2	0.5± 0.2***
I_{eq} (μA cm^{-2})	-27.5 ± 2.7	-23.1 ± 1.1	-24.9 ± 1.9	-25.4 ± 3.6	-9.0 ± 2.0**	-7.3 ± 0.7*

The role of PI3-kinase in mediating both basal and insulin-stimulated Na^+ absorption was further investigated using PI103. Experiments identical to that used to explore the effects of wortmannin were carried out. Figure 4.2 and Table 4.2 show that PI103 (1 µM, 30 min) caused no significant alteration to basal I_{eq}. Control values also showed a decay in I_{eq} over 30 min treatment with solvent vehicle. Both changes in I_{eq} in control and PI103 treated cells were accompanied by a depolarisation of V_t but no change in R_t, all mean values of electrical parameters for this experiment can be found in Table 4.2. The addition of 20nM insulin to the basolateral bath in control cells produced a significant increase in I_{eq} (Figure 4.2, $n = 6$, $p < 0.01$). In PI103-treated cells, the response to insulin was almost completely abolished. Therefore similar to wortmannin, PI103 is preventing the natriferic effect of insulin but unlike wortmannin, PI103 is not inhibiting the basal current.

Table 4.2 Electrical parameters of control and PI103-treated cells.

Mean data ± S.E.M. ($n = 6$) for V_t, R_t and I_{eq} recorded from vehicle-treated or PI103-treated cells. Values are from baseline, 30 min exposure to vehicle / PI103 and then 60 min after exposure to insulin. Asterisks denote statistically significant changes in V_t, R_t and I_{eq} in vehicle- and PI103-treated cells calculated using a Student's unpaired t-test, **, $p < 0.01$.

	Vehicle-treated			PI103 (1µM)		
	Baseline	30 min vehicle	60 min insulin	Baseline	30 min PI103	60 min insulin
V_t (mV)	-50.7 ± 6.2	-46.8 ± 5.3	-57.0 ± 7.0*	-53.1 ± 7.2	-45.7 ± 6.4	-43.6 ± 5.3
R_t (kΩ cm^2)	2.1 ± 0.2	2.1 ± 0.2	2.0 ± 0.1	2.1 ± 0.4	2.1 ± 0.4	2.3 ± 0.4
I_{eq} (µA cm^{-2})	-26.1 ± 5.0	-24.0 ± 4.2	-29.1 ± 3.6**	-30.0 ± 6.5	-22.4 ± 6.1	-23.5 ± 5.0

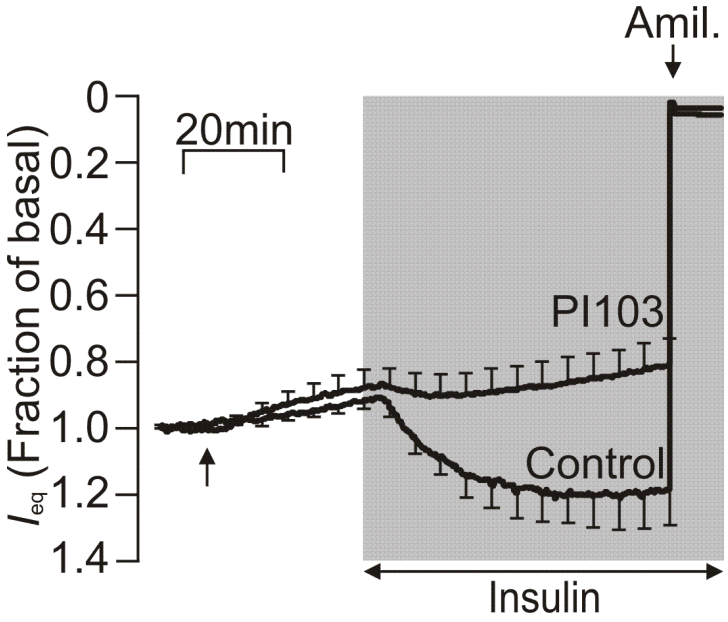

Figure 4.2 Effects of PI103 on insulin-stimulated I_{eq}.

I_{eq} of cells treated with either solvent vehicle or PI103 (1µM) for 30 min, arrow indicates the addition of solvent / drug. Insulin (20nM) was added basolaterally for 60 min, followed by the addition of amiloride (10µM, 10 min) indicated by the arrow, Amil. Mean data is represented as a fraction of the basal current at the beginning of the experiment ± S.E.M (n = 6).

The final PI3-kinase inhibitor tested was a relatively new compound, GDC0941 (Folkes *et al.*, 2008). The effects of this compound were tested in a slightly different manner; the duration of insulin stimulation was reduced to 30 min. This was due to parallel studies monitoring phosphorylation of endogenous proteins with exposure to insulin which revealed maximal stimulation occurred within 30 min (3.2.3). Figure 4.3 shows that bilateral application of 1µM GDC0941 did not significantly alter basal I_{eq}, V_t or R_t (Table 4.3). Similarly there was no change to control cells (Figure 4.3). GDC0941 is having no effect on the basal current and this suggests that PI3-kinase activity is not required for the maintenance of spontaneous Na^+ absorption in this cell line.

Figure 4.3 shows that the addition of insulin normally produced an increase in I_{eq} and this effect was significant (Table 4.3). This change in I_{eq} was accompanied by a hyperpolarisaton of V_t and a small decrease in R_t (Table 4.3). The application of insulin to GDC0941-treated cells produced only a small stimulation of I_{eq}. This change in I_{eq} occurred with no significant change in either V_t or R_t (Table 4.3). Therefore similar to both wortmannin and PI103, GDC0941 almost completely abolishes the insulin-stimulated I_{eq}, providing further evidence that this response is dependent on PI3-kinase activity.

Table 4.3 Electrical parameters of control and GDC0941-treated cells.

Mean data ± S.E.M. (n = 5) for V_t, R_t and I_{eq} from vehicle- or GDC0941-treated cells. Values are from baseline, 30 min exposure to vehicle / GDC0941 and then 30 min after exposure to insulin. Asterisks denote statistically significant changes in V_t, R_t and I_{eq} in vehicle- and GDC0941-treated cells calculated using a Student's unpaired t-test, *, $p < 0.05$.

	Vehicle-treated			GDC0941 (1 µM)		
	Baseline	30 min vehicle	30 min insulin	Baseline	30 min GDC0941	30 min insulin
V_t (mV)	-46.5 ± 6.8	-46.3 ± 6.5	-55.8 ± 5.0	53.7 ± 3.6	-43.0 ± 5.6	-39.2 ± 4.9
R_t (kΩ cm^2)	2.2 ± 0.2	2.3 ± 0.2	2.2 ± 0.2	2.7 ± 0.2	2.4 ± 0.2	2.1 ± 0.2
I_{eq} (µA cm^{-2})	-20.7 ± 1.3	-19.5 ± 1.3	-25.5 ± 1.4*	-20.9 ± 3.3	-18.9 ± 4.1	-19.5 ± 4.4

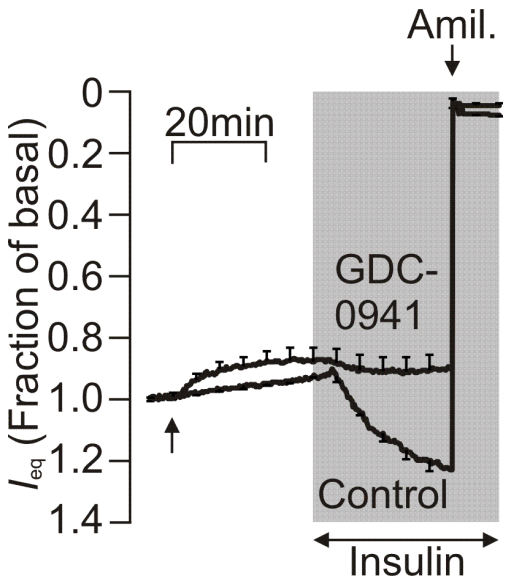

Figure 4.3 Effects of GDC0941 on insulin-stimulated I_{eq}.

I_{eq} of cells treated with either solvent vehicle or GDC0941 (1μM) for 30 min, arrow indicates the addition of solvent / drug. Insulin (20nM) was added basolaterally for 30 min, followed by the addition of amiloride (10μM, 10 min) indicated by the arrow, Amil. Mean data is represented as a fraction of the basal current at the beginning of the experiment ± S.E.M (n = 5).

Wortmannin and PI103 are also known to inhibit the mammalian target of rapamycin complex 1, mTORC1 (Fan *et al.*, 2006, Bain *et al.*, 2007). To investigate the role that this protein complex plays in insulin-stimulated Na^+ transport in the collecting duct, a highly selective inhibitor of this complex, rapamycin (Bain *et al.*, 2007), was studied. An identical experimental approach to the PI3-kinase inhibitors was employed. Figure 4.4 shows that rapamycin had no effect upon the current recorded from unstimulated cells and also failed to modify the electrometric response to insulin. These data suggest that mTORC1 does not contribute to the mechanism allowing spontaneous Na^+ absorption or the signalling pathway by which insulin stimulates Na^+ transport. All mean values of the electrical parameters recorded can be found in Table 4.4.

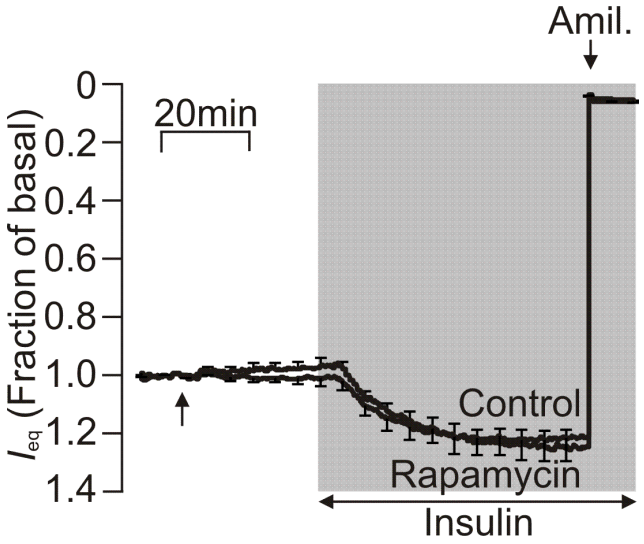

Figure 4.4 Effects of rapamycin on insulin-stimulated I_{eq}.

I_{eq} of cells treated with either solvent vehicle or rapamycin (100nM) for 30 min, arrow indicates the addition of solvent / drug. Insulin (20nM) was added basolaterally for 60 min, followed by the addition of amiloride (10µM, 10 min) indicated by the arrow, Amil. Mean data is represented as a fraction of the basal current at the beginning of the experiment ± S.E.M (n = 5).

Table 4.4 Electrical parameters of control and rapamycin-treated cells.

Mean data ± S.E.M. (n = 5) for V_t, R_t and I_{eq} from vehicle- or rapamycin-treated cells. Values are from baseline, 30 min exposure to vehicle / rapamycin and then 60 min after exposure to insulin. Asterisks denote statistically significant changes in V_t, R_t and I_{eq} in vehicle- and rapamycin-treated cells calculated using a Student's unpaired t-test, *, $p < 0.05$.

	Vehicle-treated			Rapamycin (100nM)		
	Baseline	30 min vehicle	60 min insulin	Baseline	30 min rapamycin	60 min insulin
V_t (mV)	-63.0 ± 2.3	-59.9 ± 2.8	-65.9 ± 1.5*	-49.3 ± 9.7	-47.9 ± 9.2	-54.0 ± 8.0
R_t (kΩ cm^2)	2.4 ± 0.2	2.3 ± 0.2	2.0 ± 0.2	2.1 ± 0.3	2.1 ± 0.3	2.0 ± 0.4
I_{eq} (µA cm^{-2})	-27.8 ± 3.4	-27.3 ± 3.7	-34.2 ± 3.0*	-23.3 ± 4.1	-23.8 ± 4.5	-28.7 ± 5.3*

4.2.2 The effects of PI3-kinase inhibitors on phosphorylation of endogenous proteins

The effects that three PI3-kinase inhibitors exerted on the activity of PI3 kinase, SGK1 and Akt were investigated by measuring the phosphorylation of their respective substrates: Akt-Ser^{473}, NDRG-Thr$^{346/356/366}$ and PRAS40-Ser^{246} (see Chapter 3). Under control conditions, insulin (20 nM, 30 min) normally increased phosphorylation of Akt-Ser^{473} (Figure 4.5A), NDRG-Thr$^{346/356/366}$ (Figure 4.5B) and PRAS40-Ser^{246} (Figure 4.5C), above basal levels confirming previous findings. Wortmannin (100nM, 30 min) caused a complete loss of phosphorylated-Akt-Ser^{473} (Figure 4.5A) and NDRG-Thr$^{346/356/366}$ (Figure 4.5B) under control and insulin-stimulated conditions. Phosphorylation of PRAS40-Ser^{246} in wortmannin-treated cells was also greatly reduced under control and insulin-stimulated conditions (Figure 4.5C). The changes in phosphorylation of Akt and NDRG1 occured without any change to the abundance of their respective total protein. As described previously, the abundance of total PRAS40 does appear to alter slightly in the presence of insulin therefore the pooled data of P-PRAS40-Ser^{246} has been adjusted to accommodate these changes. These data indicate that wortmannin is inhibiting PI3-kinase activity, as shown by a loss of phosphorylation of mTORC2. Furthermore these data demonstrate that both SGK1 and Akt lie downstream of PI3-kinase as phosphorylation of their respective substrates has been abolished or greatly reduced.

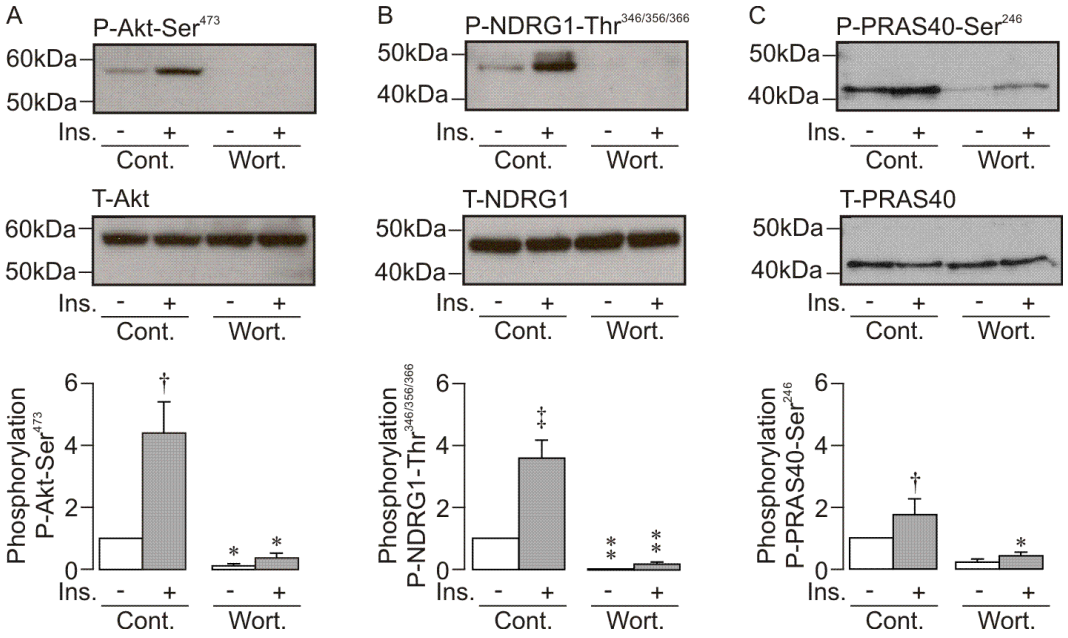

Figure 4.5 Effects of wortmannin on the phosphorylation of endogenous proteins.

Top panels: typical western blots showing the phosphorylation of (A) Akt-Ser^{473}, (B) NDRG1-Thr$^{346/356/366}$ and (C) PRAS40-Ser^{246} under unstimulated or insulin-treated (20nM, 30 min) conditions in vehicle treated, left hand pair, or wortmannin treated (100nM, 30 min) cells, right hand pair. Middle panels show the respective total protein blots for (A) Akt, (B) NDRG1 and (C) PRAS40. Lower panels: pooled data of phosphorylation of (A) Akt-Ser^{473}, n = 5, (B) NDRG1-Thr$^{346/356/366}$, n = 7, and (C) PRAS40-Ser^{246}, n = 4. Data is shown as mean ± S.E.M. and asterisks denote statistical significance (One-way ANOVA Bonferroni post hoc test) between control and wortmannin-treated cells: *, $p < 0.05$, **, $p < 0.01$, whilst daggers denote statistical significance between basal and insulin-treated cells under control conditions: †, $p < 0.05$, ‡, $p < 0.01$.

The control data in Figure 4.6 confirm that insulin normally evokes increased phosphorylation of Akt-Ser^{473} (Figure 4.6A), NDRG-Thr$^{346/356/366}$ (Figure 4.6B) and PRAS40-Ser^{246} (Figure 4.6C). PI103 (1 µM, 30 min) abolished mTORC2 activity, as shown by a complete loss of phosphorylated Akt-Ser^{473}, under both control and insulin-stimulated conditions (Figure 4.6A). SGK1 activity was inhibited in the presence of PI103, as seen by a complete loss of NDRG1-

Thr$^{346/356/366}$ phosphorylation (Figure 4.6B). Similarly Akt activity was inhibited as seen by reduced phosphorylation of PRAS40-Ser^{246} (Figure 4.6C). These data show that PI103 can inhibit PI3-kinase activity as seen with a loss of downstream phosphorylation and these findings are consistent with those examining the effects of wortmannin.

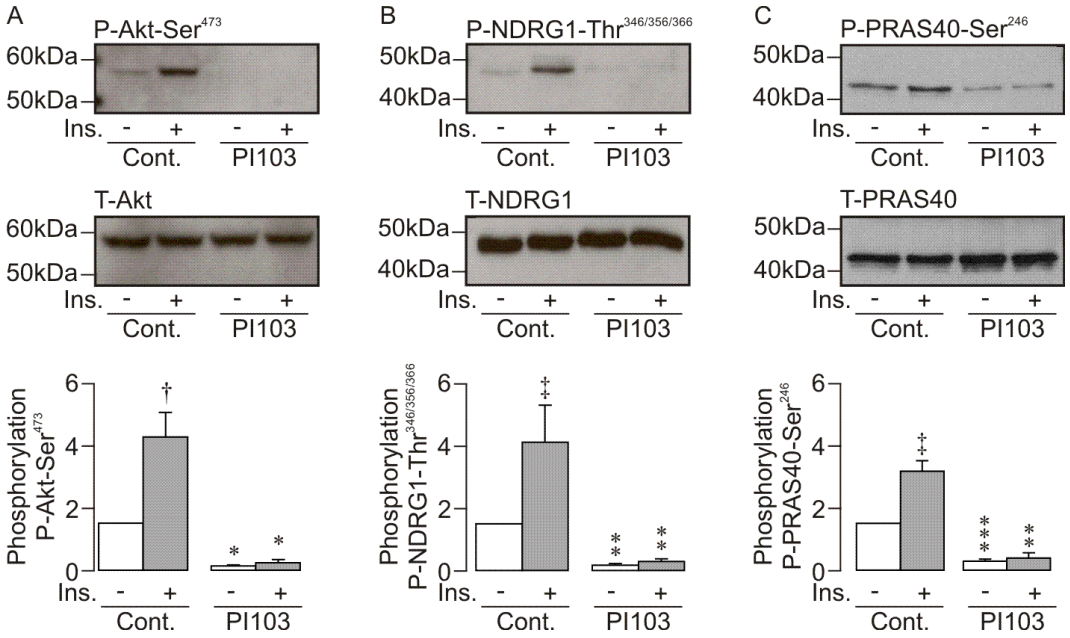

Figure 4.6 Effects of PI103 on the phosphorylation of endogenous proteins.

Top panels: typical western blots showing the phosphorylation of (A) Akt-Ser^{473}, (B) NDRG1-Thr$^{346/356/366}$ and (C) PRAS40-Ser^{246} under unstimulated or insulin-treated (20nM, 30 min) conditions in vehicle treated, left hand pair, or PI103 treated (1μM, 30 min) cells, right hand pair. Middle panels show the respective total protein blots for (A) Akt, (B) NDRG1 and (C) PRAS40. Lower panels show pooled data of phosphorylation of (A) Akt-Ser^{473}, n = 5, (B) NDRG1-Thr$^{346/356/366}$, n = 6, and (C) PRAS40-Ser^{246}, n = 5. Data is shown as mean ± S.E.M. and asterisks denote statistical significance (One-way ANOVA Bonferroni post hoc test) between control and PI103-treated cells: *, $p < 0.05$, **, $p < 0.01$, *** $P < 0.001$, whilst daggers denote statistical significance between basal and insulin-treated cells under control conditions: †, $p < 0.05$, ‡, $p < 0.01$.

Figure 4.7 shows again that insulin greatly increases phosphorylation of Akt-Ser^{473} (Figure 4.7A), NDRG1-Thr$^{346/356/366}$ (Figure 4.7B) and PRAS40-Ser^{246} (Figure 4.7C). GDC0941 (1 µM, 30 min) completely abolished Akt-Ser^{473} and NDRG1-Thr$^{346/356/366}$ phosphorylation under control and insulin-stimulated conditions (Figure 4.7A, B). Phosphorylation of PRAS40-Ser^{246} was also markedly reduced (Figure 4.7C). These data indicate that GDC0941 inhibits PI3-kinase as shown by loss of phosphorylation of downstream substrates.

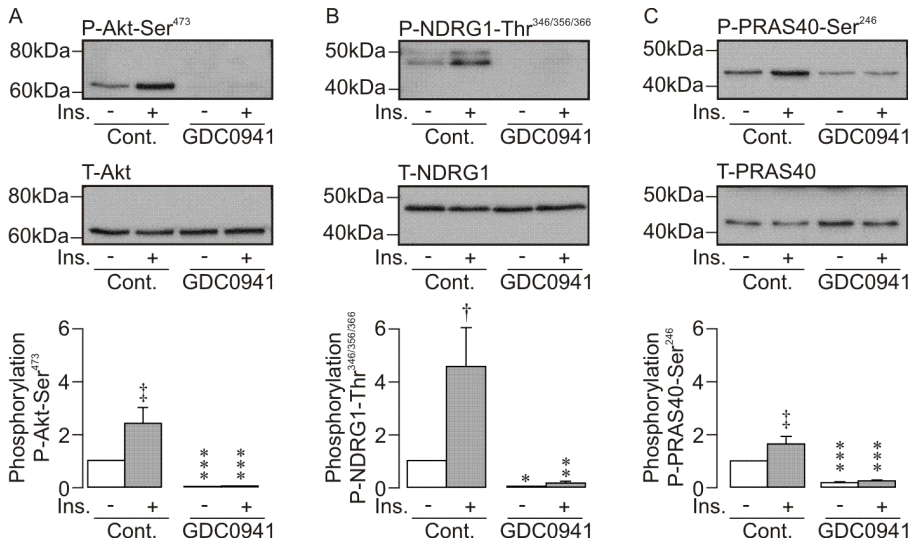

Figure 4.7 Effects of GDC0941 on the phosphorylation of endogenous proteins.

Top panels: typical western blots showing phosphorylation of (A) Akt-Ser^{473}, (B) NDRG1-Thr$^{346/356/366}$ and (C) PRAS40-Ser^{246} under unstimulated or insulin-treated (20nM, 30 min) conditions in vehicle treated, left hand pair, or GDC0941 treated (1µM, 30 min) cells, right hand pair. Middle panels: respective total protein blots for (A) Akt, (B) NDRG1 and (C) PRAS40. Lower panels: pooled data of phosphorylation of (A) Akt-Ser^{473}, n = 6, (B) NDRG1-Thr$^{346/356/366}$, n = 6, and (C) PRAS40-Ser^{246}, n = 6. Data is shown as mean ± S.E.M. and asterisks denote statistical significance (One-way ANOVA Bonferroni post hoc test) between control and GDC0941-treated cells: *, $p < 0.05$, **, $p < 0.01$, *** $p < 0.001$, whilst daggers denote statistical significance between basal and insulin-treated cells under control conditions: †, $p < 0.05$, ‡, $p < 0.01$.

The effects rapamycin exerted on the phosphorylation of endogenous proteins was examined to investigate the role of mTORC1. Figure 4.8 shows under control conditions acute addition of insulin increased phosphorylation of Akt-Ser^{-473} (Figure 4.8A), NDRG1-Thr$^{346/356/366}$ (Figure 4.8B) and PRAS40-Ser^{246} (Figure 4.8C). Rapamycin (100 nM, 30 min) did not alter phosphorylation of any of the three substrates examined, under both unstimulated and insulin-stimulated conditions (Figure 4.8). These data indicate that mTORC1 is not involved in basal or insulin-stimulated mTORC2, SGK1 or Akt activity.

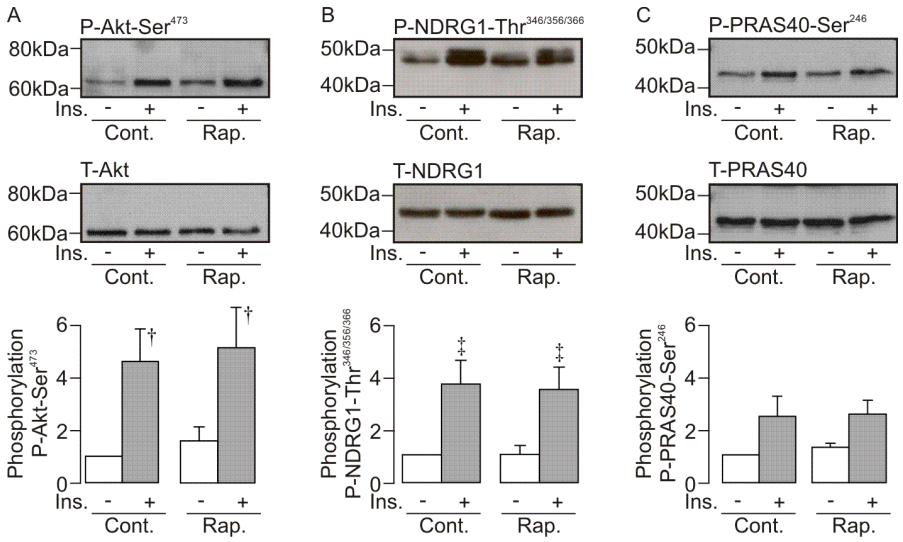

Figure 4.8 Effects of rapamycin on the phosphorylation of endogenous proteins.

Top panels: typical western blots showing the phosphorylation of (A) Akt-Ser^{473}, (B) NDRG1-Thr$^{346/356/366}$ and (C) PRAS40-Ser^{246} under unstimulated or insulin-treated (20nM, 30 min) conditions in vehicle treated, left hand pair, or rapamycin treated (100nM, 30 min) cells, right hand pair. Middle panels show the respective total protein blots for (A) Akt, (B) NDRG1 and (C) PRAS40. Lower panels show pooled data of phosphorylation of (A) Akt-Ser^{473}, n = 5, (B) NDRG1-Thr$^{346/356/366}$, n = 7, and (C) PRAS40-Ser^{246}, n = 5. Data is shown as mean ± S.E.M. and daggers denote statistical significance (One-way ANOVA Bonferroni post hoc test) between basal and insulin-treated cells under control conditions: †, $p < 0.05$, ‡, $p < 0.01$.

To confirm that rapamycin inhibited mTORC1, the same lysates were subject to western analysis using antibodies against a physiological substrate of mTORC1: the 70kDa ribosomal S6 kinase (P70-S6K) by measuring phosphorylation of the Thr^{389} residue as well as the abundance of total S6K. Under control conditions insulin increased phosphorylation of P70-S6K-Thr^{389} (Figure 4.9, $n = 4$, $p < 0.01$). Rapamycin (100nM, 30 min) completely abolished phosphorylation of P70-S6K-Thr^{389}. This finding demonstrates that insulin can stimulate mTORC1 activity and that rapamycin specifically inhibits mTORC1 in these cells.

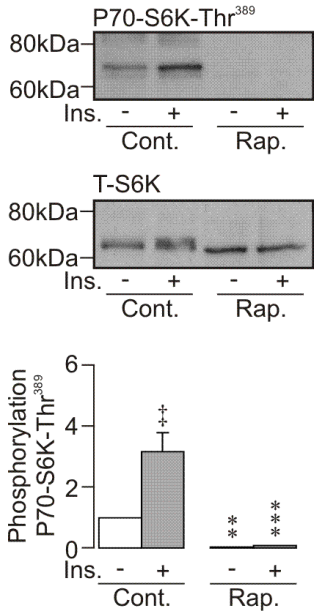

Figure 4.9 Effects of rapamycin on the phosphorylation of P70-S6kinase-Thr^{389}.

Top panel: typical western blots showing the phosphorylation of P70-S6K-Thr^{389} under unstimulated or insulin-treated (20nM, 30 min) conditions in vehicle treated, left hand pair, or rapamycin treated (100nM, 30 min) cells, right hand pair. Middle panel shows the respective total protein blots for S6K. Lower panel shows the pooled data of phosphorylation of P70-S6K-Thr^{389} $n = 4$. Data is shown as mean ± S.E.M. and asterisks denote statistical significance (One-way ANOVA Bonferroni post hoc test) between control and rapamycin-treated cells: **, $p < 0.01$, ***, $p < 0.001$, whilst daggers denote statistical significance between basal and insulin-treated cells under control conditions: ‡, $p < 0.01$.

4.3 Discussion

4.3.1 The role of PI3-kinase in basal and insulin-stimulated Na^+ transport

Bilateral addition of wortmannin to cells mounted in Ussing chambers produced a rapid inhibition of basal I_{eq} suggesting that spontaneous transport of Na^+ across these epithelial cells is dependent on PI3-kinase. Wortmannin is a well-used inhibitor of PI3-kinase and inhibits signalling by covalently binding a lysine residue within the catalytic p110α subunit (Wymann et al., 1996). The present finding is in accordance with a study showing inhibition of basal sodium current in A6 cells (Record et al., 1998) by treatment with wortmannin (100 nM). Further studies demonstrating the importance of PI3-kinase in maintaining the basal current have come from using the inhibitor LY-294002 in A6 cells (Păunescu *et al.*, 2000, Record *et al.*, 1998, Wang *et al.*, 2001) and mpkCCDcl4 cells (Staruschenko *et al.*, 2007). However, two other compounds used in the present study: PI103 and GDC0941; had only modest effects on the basal current. Both PI103 and GDC0941 are relatively recent additions to the growing number of PI3-kinase inhibitors and GDC0941 in particular has been reported to be highly selective (Garcia-Echeverria and Sellers, 2008). All three compounds tested in the present study caused complete loss of mTORC2 activity and since this kinase lies downstream of PI3-kinase indicates these drugs abolish PI3-kinase activity. It therefore seems likely that wortmannin is producing its effects on the basal current through inhibition of other targets. Wortmannin has been reported to inhibit both polo-like kinase (PLK) and smooth-muscle myosin light-chain kinase

(SmMLCK) (Bain et al., 2007). These kinases have not previously been reported to play a role in Na^+ transport but could explain why this compound, but not the other two, had significant effects on the basal current. It is also interesting to note that LY-294002 has been reported to have several off-target effects including mTORC1, PLK1 (polo like kinase 1), PIMK1 (provirus integration site for Moloney murine leukaemia virus kinase 1), HIPK (homeodomain-interacting protein kinase), GSK3 (glycogen synthase kinase 3) and CK2 (casein kinase 2) (Davies *et al.*, 2000, Bain *et al.*, 2007). It is of note that CK2 is inhibited by LY294002 since this kinase has been linked to modulation of ENaC activity (Bachhuber *et al.*, 2008). Therefore both wortmannin and LY-294002 do not inhibit PI3-kinase selectively and it seems prudent that the use of either of these compounds to study ENaC-mediated Na^+ transport is discontinued and replaced with more novel selective inhibitors. The present data provide novel evidence that spontaneous Na^+ absorption can occur in the complete absence of PI3-kinase activity.

Furthermore, since both PI103 and GDC0941 caused a complete loss of phosphorylated NDRG1-$Thr^{346/356/366}$ under basal conditions yet exerted only modest effects on the basal current, this suggests that spontaneous Na^+ absorption can also occur in the absence of SGK1 activity. This is in sharp contrast to previous studies where overexpression of a kinase-dead form of SGK1 in A6 and M1 cells completely abolished amiloride-sensitive currents (Faletti *et al.*, 2002, Helms *et al.*, 2003, Náray-Fejes-Tóth *et al.*, 2004a). Similar findings were also observed in a study where isolated rabbit cortical collecting duct cells transfected

with antisense nucleotides targeting SGK1 displayed minimal amiloride-sensitive currents (Náray-Fejes-Tóth *et al.*, 2004a). Whilst these studies clearly indicate that SGK1 is required for basal Na^+ absorption the results from the present study are not consistent with this. Whilst the above data have been obtained from overexpression studies which may not reflect physiological conditions, our work has been carried out in a mammalian collecting duct cell line under physiological conditions. This highlights the benefits of using these novel small molecule inhibitors in a native cell line. The present study also demonstrates that both PI103 and GDC0941 significantly reduced Akt activity and also suggests that Akt does not play a major role in the maintenance of the basal current.

Insulin-stimulated I_{eq} was significantly inhibited by all three compounds tested and this finding is consistent with several other studies that have shown inhibitors of PI3-kinase: LY-294002 and wortmannin (Record et al., 1998) and PI103 (Wang et al., 2008) abolish the natriferic response to insulin. Under insulin-stimulated conditions all three PI3-kinase inhibitors tested in the present study abolished the activity of mTORC2 indicating inhibition of PI3-kinase. This is consistent with a study that showed inhibition of insulin-induced phosphorylation of Akt-Ser^{473} using PI103 in the same cell line (Wang *et al.*, 2008). Furthermore all three inhibitors used in the present study caused a complete loss of phosphorylated NDRG1-$Thr^{346/356/366}$ indicating insulin can stimulate SGK1 activity downstream of PI3-kinase. This result accords well with a study that showed that both LY294002 and wortmannin inhibited serum-induced phosphorylation of SGK1 in mammary tumour cells (Park et al., 1999). Another

study carried out in the mpkCCDcl4 cell line also revealed both LY294002 and PI103 prevented the insulin-induced phosphorylation of SGK1 by insulin (100 nM, 1hr) (Wang et al., 2008). Similarly the insulin-stimulated phosphorylation of the Akt substrate PRAS40-Ser^{246} was significantly reduced in the presence of all three compounds tested. This demonstrates that like SGK1, Akt activity is largely dependent on PI3-kinase. This finding is in accordance with a study that showed that the phosphorylation of two residues on Akt is required for full activity: Ser^{473} and Thr^{308}; and activity was abolished by the inhibitors LY294002 and PI103 (Wang et al., 2008). Together these data provide novel evidence that PI3-kinase as well as mTORC2 and SGK1 are not required for spontaneous Na^+ absorption in the collecting duct. PI3-kinase however, appears to be absolutely crucial for insulin-stimulated Na^+ transport.

4.3.2 The role of mTORC1 in basal and insulin-stimulated Na^+ transport

The present data confirmed rapamycin is a specific inhibitor of mTORC1 (Proud, 2007) as shown with loss of phosphorylation of a downstream substrate but with no effects on downstream substrates of mTORC2, SGK1 or Akt. This confirms that the PI3-kinase inhibitors employed in this study were not exerting additional effects on Na^+ transport via off-target inhibition of mTORC1 as previously reported (Fan *et al.*, 2006, Bain *et al.*, 2007). Furthermore with the lack of effect on SGK1 activity, the present data provide evidence that mTORC1 does not phosphorylate and activate SGK1. This is in sharp contrast to a recent paper that

reported mTORC1 was the elusive "PDK2" due to the finding that rapamycin could inhibit SGK1-Ser^{422} phosphorylation (Hong *et al.*, 2008). Another study however demonstrated rapamycin did not alter SGK1-Ser^{422} in three different cell lines expressing full length SGK1 (García-Martínez and Alessi, 2008). The authors concluded that the results seen by Hong *et al*. were due to a commercial SGK1 antibody recognising phosphorylated bands of S6K since these two kinases share similar hydrophobic motifs (García-Martínez and Alessi, 2008). Therefore the present data is in accordance with García-Martínez and Alessi and indicates that mTORC1 does not lie upstream of SGK1.

Rapamycin did not alter either basal or insulin-stimulated I_{eq} indicating that this complex is not involved in either maintaining basal Na^+ transport or mediating the natriferic response to insulin. This data is in contrast to a study examining the effects of rapamycin in the A6 cell line (Rokaw *et al.*, 1996a). The authors reported that acute addition of rapamycin stimulated amiloride-sensitive Na^+ transport and this response was additive to insulin-stimulated Na^+ transport. This suggests that mTORC1 can modulate ENaC-mediated Na^+ transport and the authors attribute this effect to the inhibition of protein kinase C (Rokaw *et al.*, 1996a). Interestingly, in complete contrast, a study from fetal airway cells reported rapamycin as having an inhibitory effect on basal amiloride-sensitive currents (Otulakowski *et al.*, 2007). The authors concluded that this was due to an inhibition of α-ENaC translation. The results from the present study in a mammalian collecting duct cell line do not report either an inhibitory or stimulatory effect of rapamycin, indicating a lack of a role of mTORC1 in basal or

insulin-stimulated Na^+ transport. These contrasting data could be due to the different cell lines utilised. However ongoing research in our laboratory has found that rapamycin also does not alter amiloride-sensitive Na^+ currents recorded from groups of H441 airway epithelial cells (unpublished data), providing further evidence that mTORC1 is not involved in basal Na^+ transport in absorptive epithelia.

The experiments in this chapter provide novel evidence that the mpkCCDcl4 cell line can spontaneously absorb Na^+ via ENaC in the absence of PI3-kinase activity. In contrast, these data highlight that PI3-kinase activity is absolutely crucial in mediating the stimulation of Na^+ absorption by insulin. Furthermore, these findings also indicate that mTORC1 plays no role in either the basal or insulin-stimulated current.

Chapter 5 – The role of Akt and SGK1 in basal and insulin-stimulated Na^+ transport

5.1 Introduction

The serum and glucocorticoid regulated kinase (SGK1), a downstream target of PI3-kinase, has previously been implicated in mediating ENaC activity (Chen *et al.*, 1999, Náray-Fejes-Tóth *et al.*, 1999, Debonneville *et al.*, 2001). SGK1 was discovered in a rat mammary tumour cell line by Webster and colleagues and was the first example of protein kinase transcription being regulated by glucocorticoids (Webster *et al.*, 1993b). This study observed that both serum and the glucocorticoid dexamethasone could induce SGK1 mRNA expression within 30 min, with the latter having greater effect. SGK1 was found to contain a glucocorticoid response element (GRE) in its promoter region that allowed dexamethasone to bind and mediate transcription (Webster *et al.*, 1993b, Itani *et al.*, 2002). This increase in SGK1 mRNA levels in response to dexamethasone was subsequently found to be induced by aldosterone as well and this was demonstrated in the amphibian A6 kidney cell line (Chen *et al.*, 1999), in primary cortical collecting duct cells from rabbit (Náray-Fejes-Tóth *et al.*, 1999) and also in rat colon (Shigaev *et al.*, 2000). Oocyte expression studies revealed that co-expression of α-, β- and γ- ENaC subunits with SGK1 increased amiloride-sensitive currents (Chen *et al.*, 1999, Shigaev *et al.*, 2000), indicating that SGK1 could enhance ENaC activity. However, the mechanism by which it did so remained unclear.

These studies revealed SGK1 involvement in mineralocorticoid / glucocorticoid stimulation of Na^+ transport. SGK1 was subsequently shown to play a role in

insulin-stimulated Na^+ transport (Faletti *et al.*, 2002). As discussed previously (Chapter 3), insulin has been shown to increase ENaC activity in the kidney (Handler *et al.*, 1981a, Fidelman *et al.*, 1982). A6 cells overexpressing full-length wild-type SGK1 have been shown to display increased ENaC activity (Faletti *et al.*, 2002). This increased activity could not be potentiated further by stimulation with insulin but matched the response of untransfected parent cells to insulin. Overexpression of a kinase dead SGK1 mutant in this cell line not only prevented the natriferic response to insulin but also inhibited basal levels of Na^+ transport (Faletti *et al.*, 2002). Another study using a tetracycline-inducible system in A6 cells showed that expression of a constitutively active SGK1 increased basal Na^+ transport but addition of insulin could not stimulate the short circuit current further as seen in control cells (Alvarez De La Rosa and Canessa, 2003). These data together indicate a role for SGK1 in insulin-mediated stimulation of ENaC.

Insulin is thought to act via a signalling cascade dependent on PI3-kinase resulting in an increase in SGK1 activity (Park *et al.*, 1999, Kobayashi and Cohen, 1999) rather than increasing the expression of this kinase like corticosteroids. SGK1 activity requires phosphorylation at two residues: Thr^{256} in the activation loop and Ser^{422} in the catalytic domain. PDK1 was shown to be the kinase responsible for phosphorylation of Thr^{256} *in vitro* (Kobayashi and Cohen, 1999) and *in vivo* (Park *et al.*, 1999). More recently, the elusive kinase that phosphorylates the Ser^{422} residue, previously termed PDK2, was found to be the mammalian target of rapamycin complex 2 (mTORC2) (García-Martínez and Alessi, 2008). Without phosphorylation at the hydrophobic motif by mTORC2, SGK1 cannot be

phosphorylated by PDK1 on the activation loop, therefore phosphorylation of Ser^{422} is critical for SGK1 activity (García-Martínez and Alessi, 2008).

It has been proposed that active SGK1 mediates its effects on Na^+ transport by phosphorylating the ubiquitin ligase Nedd4-2. Phosphorylation of Nedd4-2 prevents it from interacting with PY motifs on ENaC, normally tagging the channel for degradation. Therefore with less internalisation and more Na^+ channels in the membrane there would be an increase in Na^+ transport (Snyder *et al.*, 2002). SGK1 has also been shown to directly interact with ENaC itself (Diakov and Korbmacher, 2004) although whether this happens under physiological conditions remains unclear.

The role of SGK1 in mediating hormone-stimulated Na^+ transport in the kidney has been well-documented (for review see Pearce and Kleyman, 2007), therefore it came as a surprise that SGK1 knockout mice displayed no overt phenotype (Wulff *et al.*, 2002). Only when mice were fed a low-sodium diet did they show an impaired ability to upregulate Na^+ reabsorption. Another study demonstrated that Na^+ absorption in the colon, which can be regulated in a similar manner to the collecting duct with corticosteroids, was actually enhanced in $SGK1^{-/-}$ mice (Rexhepaj *et al.*, 2006). Work carried out in our laboratory has shown that in H441 airway epithelial cells, expression of a constitutively active SGK1 can increase amiloride-sensitive Na^+ currents (Brown *et al.*, 2008) but the expression of an inactive SGK1 mutant did not suppress glucocorticoid-induced currents (Inglis *et al.*, 2007). These findings suggest that mediators other than SGK1 can

regulate Na^+ absorption, possibly other isoforms of SGK including SGK2 and SGK3 or other protein kinases that share a similar homology to SGK1 such as protein kinase B (Akt).

The role of Akt in mediating hormonal stimulation of ENaC activity was investigated in a study that used a tetracycline inducible system expressing either constitutively active or inactive Akt in A6 cells (Arteaga and Canessa, 2005). This study demonstrated that expression of constitutively active or inactive Akt did not alter levels of ENaC activity measured as amiloride sensitive short circuit current. The application of insulin produced a stimulation of ENaC activity but this was not different to control cells indicating that expression of active or inactive Akt did not alter the insulin-mediated increase in Na^+ transport. In sharp contrast, a study carried out by Lee *et al.* (2007) observed that overexpression of Akt or SGK1 in fisher rat thyroid cells expressing ENaC greatly increased amiloride-sensitive short circuit currents. Inhibition of both Akt and SGK1 expression using siRNA reduced ENaC activity below basal levels and also prevented the increase in current in response to insulin treatment. Furthermore in M1 cells, silencing expression of Akt prevented insulin stimulation of ENaC activity (Lee *et al.*, 2008). This study suggests that both Akt and SGK1 are involved in mediating increases in Na^+ transport via ENaC in response to insulin. Clearly the role that Akt plays in mediating either basal or homone-stimulated Na^+ absorption remains unclear and both of the above studies utilised expression systems which do not always depict physiological conditions.

The creation of novel small molecule inhibitors of Akt and SGK1, Akti-1/2 (Barnett *et al.*, 2005) and GSK650394A (Sherk *et al.*, 2008) respectively, allowed a method by which to inhibit either kinase and examine their effects in a native system. The following experiments investigated the effects these drugs exerted on both basal and insulin-stimulated Na^+ transport in the mpkCCDc14 collecting duct cell line. By monitoring the phosphorylation of endogenous proteins we could also confirm that the inhibitors were selective and identify the doses required for effective inhibition of kinase activity.

Due to the difficulty that a drifting baseline in Ussing chamber experiments caused when trying to draw comparisons from data collected, identified in the PI3-kinase inhibitor studies, the experimental design was subsequently improved. Double paired experiments were setup where four cultures of cells from identical passage were grown on snapwells, mounted in Ussing chambers and recorded from. The first pair allowed recording of a control response to insulin with unstimulated and insulin-stimulated conditions. The second pair allowed recording of the effects of a test substance under unstimulated and insulin-stimulated conditions. This allowed accurate measurement of the effects a drug exerted on unstimulated current and allowed calculation of the change in current, $\Delta I_{eq.}$

5.2 Results

5.2.1 Effects of Akti-1/2 on basal and insulin-stimulated Na^+ transport

The effects that three doses of Akti-1/2 (1, 3, 10 µM) had on basal levels of Na^+ transport were examined. Figure 5.1 and Table 5.1 show that bilateral addition of both 1 µM and 3 µM Akti-1/2 for 30 min did not alter the basal current significantly. At 10µM Akti-1/2 the basal current was significantly inhibited by 17.8 ± 7.0% (Table 5.1). Despite this inhibition, more than 80 % of the spontaneous current remained suggesting that Akti-1/2 is not inhibiting the mechanism allowing spontaneous Na^+ absorption. All mean values of I_{eq} are presented in Table 5.1.

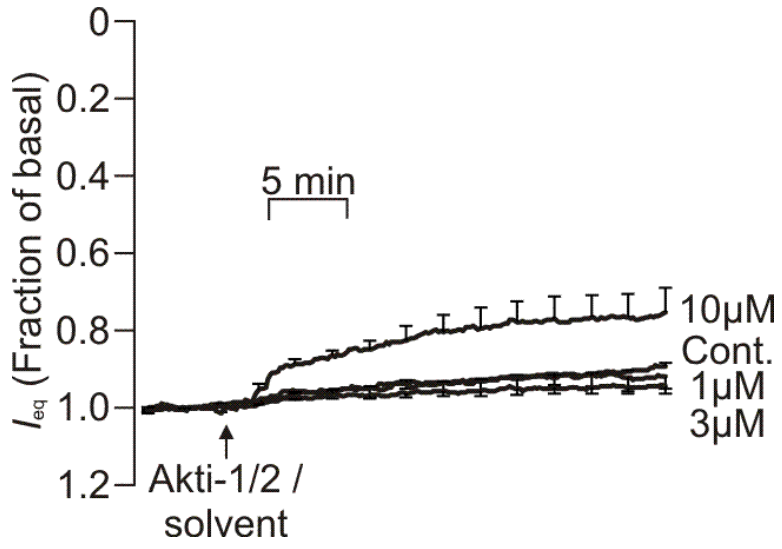

Figure 5.1 Effects of Akti-1/2 on basal I_{eq}.

I_{eq} of cells treated with solvent vehicle or Akti-1/2 (1-10 µM) for 30 min, arrow indicates addition. Data is shown as mean current, calculated as a fraction of the initial current, ± S.E.M. (n = 5).

Table 5.1 I_{eq} of control and Akti-1/2-treated cells.

Mean data ± S.E.M. (n = 5) for I_{eq} recorded from cells treated with vehicle or Akti-1/2 (1-10 µM). Values are from baseline and after 30 min exposure to vehicle / Akti-1/2. Statistical significance was calculated using unpaired Student's t-test, * $p < 0.05$.

Treatment		I_{eq} (µA cm^{-2})	
		Baseline	30 min exposure
1µM Akti-1/2	Control	-24.2 ± 2.0	-23.6 ± 2.1
	Experimental	-20.3 ± 2.4	-18.7 ± 2.4
3µM Akti-1/2	Control	-14.5 ± 1.3	-13.6 ± 1.1
	Experimental	-15.8 ± 1.0	-14.5 ± 0.9
10µM Akti-1/2	Control	-14.9 ± 3.2	-14.0 ± 3.1
	Experimental	-15.1 ± 2.7	-11.1 ± 1.2*

The effects of Akti-1/2 on insulin-stimulated Na^+ transport were subsequently investigated and for each dose tested, a separate control response to insulin was measured. Due to the nature of the double-paired experiments the change in I_{eq}, ΔI_{eq}, brought about by insulin stimulation could be calculated. Figure 5.2A-C shows that in control experiments, insulin (20 nM, 30 min) consistently produced a significant increase in ΔI_{eq}: 1µM control: -7.1 ± 1.8 µA cm^{-2} (n = 5, $p < 0.01$); 3µM control: -5.4 ± 0.7 µA cm^{-2} (n = 5, $p < 0.001$); 10µM control: -5.2 ± 0.8 µA cm^{-2} (n = 5, $p < 0.001$). Statistical significance was calculated by comparing the mean ΔI_{eq} after 30 min in both control and Akti-1/2-treated cells using an unpaired Student's t-test. These insulin-induced increases in I_{eq} were associated with a hyperpolarisation of V_t and a slight fall in R_t; all mean values of electrical parameters measured can be found in the appendix (Chapter 9).

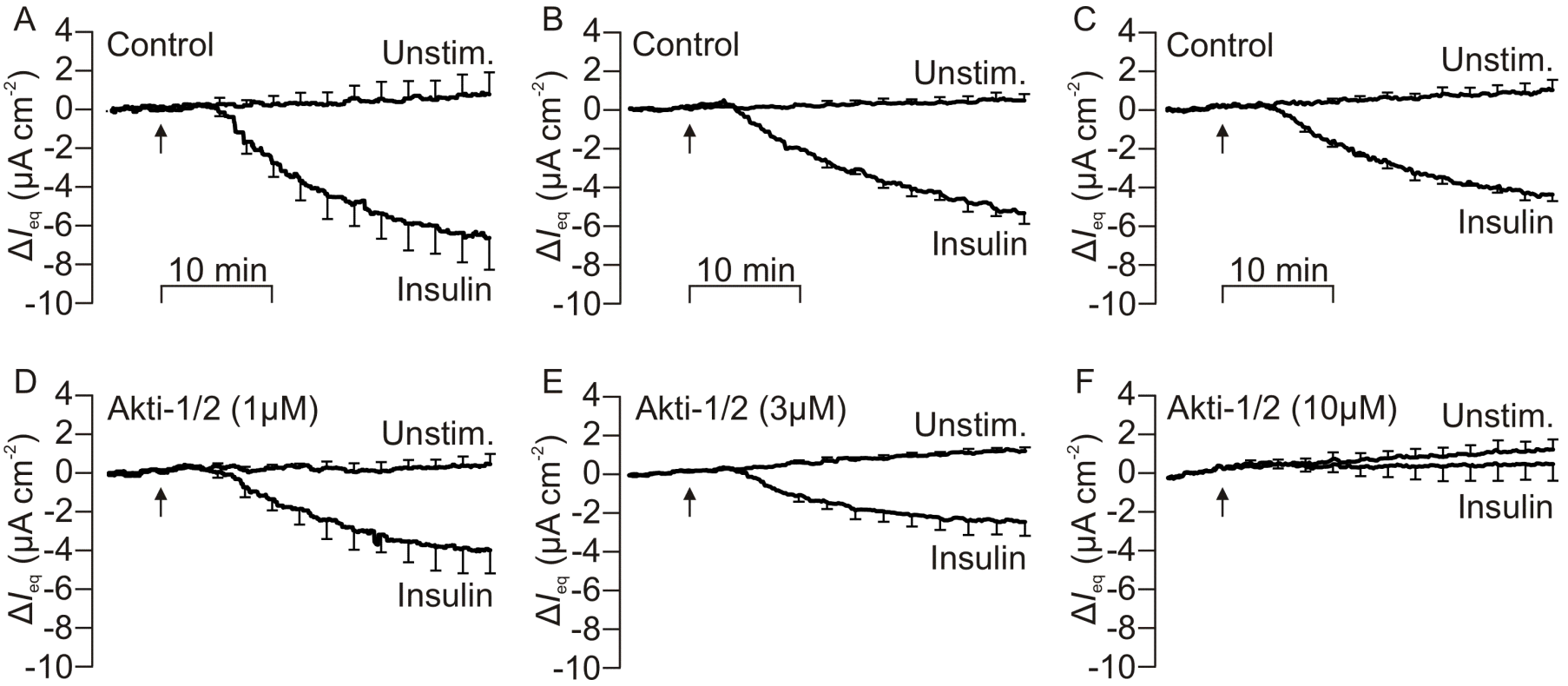

Figure 5.2. Effects of Akti-1/2 on the insulin-evoked current.

I_{eq} of cells pre-treated for 30 min with either solvent vehicle (A-C) or increasing doses of Akti-1/2 (D-F) then exposed to either unstimulated or insulin-stimulated (20nM) conditions for a further 30 min, arrow indicates addition of vehicle / insulin. Data is presented as mean ΔI_{eq}, calculated as a fraction of the current 5 min before insulin was added, ± S.E.M (n = 5).

Figure 5.2D-F show increasing concentrations of Akti-1/2 caused a dose-dependent inhibition of the insulin-stimulated I_{eq}. 1µM Akti-1/2 inhibited the response to insulin by 43.4 ± 4.6% with a ΔI_{eq} of -3.5 ± 1.6 µA cm^{-2} (n = 5, p < 0.05). 3µM Akti-1/2 inhibited the insulin-evoked I_{eq} by 31.3 ± 12.5% with a ΔI_{eq} of -3.6 ± 0.8 µA cm^{-2} (n = 5, p < 0.05). Finally 10µM Akti-1/2 inhibited the response to insulin by 80.8 ± 7.3% with a ΔI_{eq} of 0.8 ± 0.3µA cm^{-2} (n = 5, p < 0.01). Together these results indicate that Akti-1/2 is inhibiting the natriferic response to insulin.

5.2.2 Effects of Akti-1/2 on phosphorylation of endogenous proteins

As previously observed (see Chapter 3), insulin (20 nM) normally increased the phosphorylation of Akt-Ser^{473} indicating an increase in mTORC2 activity, this can be seen in Figure 5.3. At all concentrations tested, Akti-1/2 significantly reduced both basal and insulin-stimulated phosphorylation of Akt-Ser^{473}. This data indicates that Akti-1/2 is preventing the mTORC2-mediated phosphorylation of Akt-Ser^{473}. Figure 5.4 shows that under unstimulated conditions, the addition of insulin (20 nM) also significantly increased the phosphorylation of PRAS40-Ser^{246}, indicating an increase in Akt activity. Akti-1/2 significantly reduced basal phosphorylation of PRAS40-Ser^{246} at 3µM and 10µM and inhibited insulin-stimulated phosphorylation of PRAS40-Ser^{246} at all concentrations (Figure 5.4). These data demonstrate that in this cell line Akti-1/2 is inhibiting Akt activity.

The data in Figure 5.5 show that control cells show a significant increase in the phosphorylation of NDRG-Thr$^{346/356/366}$ with the addition of insulin, demonstrating again that insulin stimulates SGK1 activity. A surprising find was that at all doses of Akti-1/2, phosphorylated NDRG-Thr$^{346/356/366}$ was significantly inhibited under unstimulated and insulin-stimulated conditions.

These data provide evidence that whilst Akti-1/2 inhibits Akt activity, this drug is also inhibiting SGK1 activity and is therefore not selective. Akti-1/2 inhibits Akt by direct interactions with the PH domain (Barnett *et al.*, 2005) so it is surprising that it inhibits SGK1 which does not have a PH domain. The inhibition of mTORC2 phosphorylation of Akt-Ser^{473} provides a common pathway for inhibition of SGK1 since SGK1 absolutely requires mTORC2 activity, so perhaps Akti-1/2 is inhibiting this kinase off-target. The data from the Ussing chamber experiments can therefore not be attributed to specifically targeting Akt and these results highlight the importance of checking specificity of inhibitors within particular cell lines.

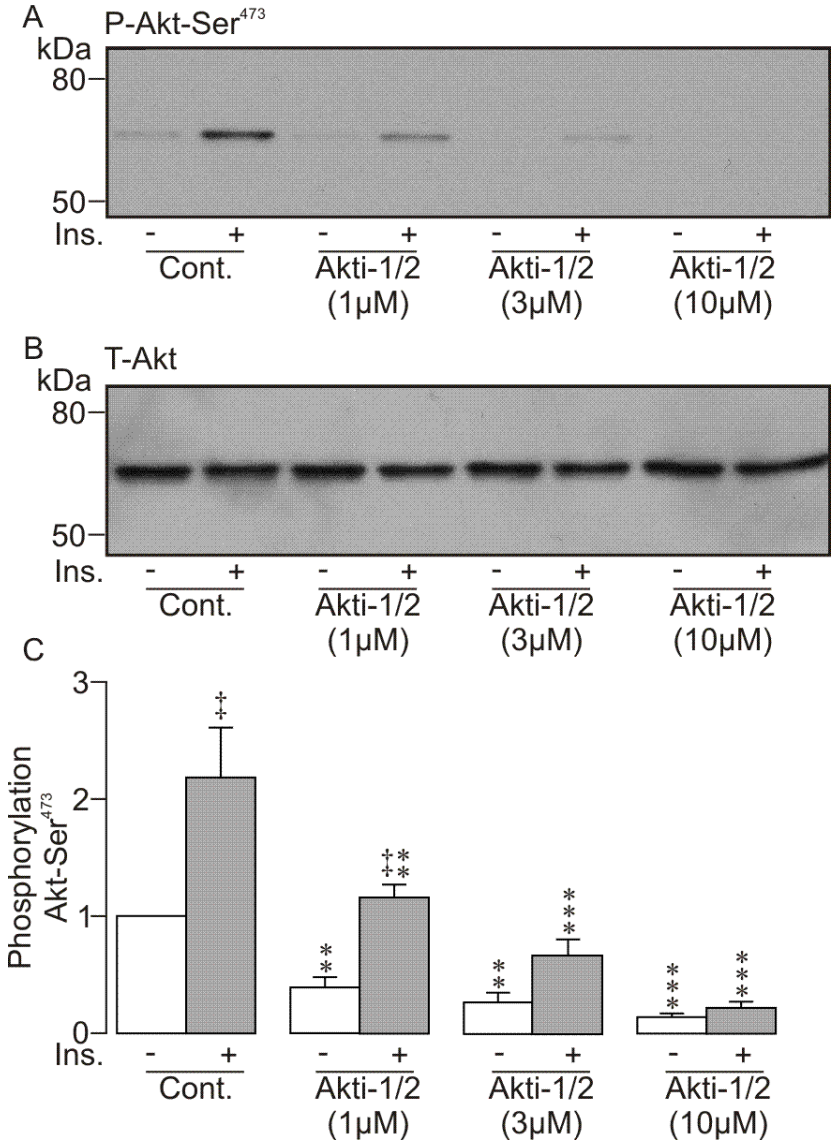

Figure 5.3 Effects of Akti-1/2 on the phosphorylation of Akt-Ser^{473}.

Cells were exposed to solvent vehicle (Cont.) or to Akti-1/2 (1, 3 or 10μM, 30 min preincubation) and then maintained under hormone-free conditions (Ins. -) or exposed to 20nM insulin (Ins. +) for a further 30 min before being lysed. (A) Typical western blot showing phosphorylation of Akt-Ser^{473}. (B) Typical western blot showing total Akt protein. (C) Pooled data from phospho-Akt-Ser^{473} blots, n = 6, data is presented at mean ± S.E.M. Daggers denote statistically significant effects of insulin on the phosphorylation of Akt-Ser^{473}: †, $p < 0.05$, ‡, $p < 0.01$. Asterisks denote statistically significant effects (Two-way ANOVA Bonferroni post hoc test) of Akti-1/2 on either basal or insulin-stimulated phosphorylation of Akt-Ser^{473}: *, $p < 0.05$, **, $p < 0.01$, $p < 0.001$.

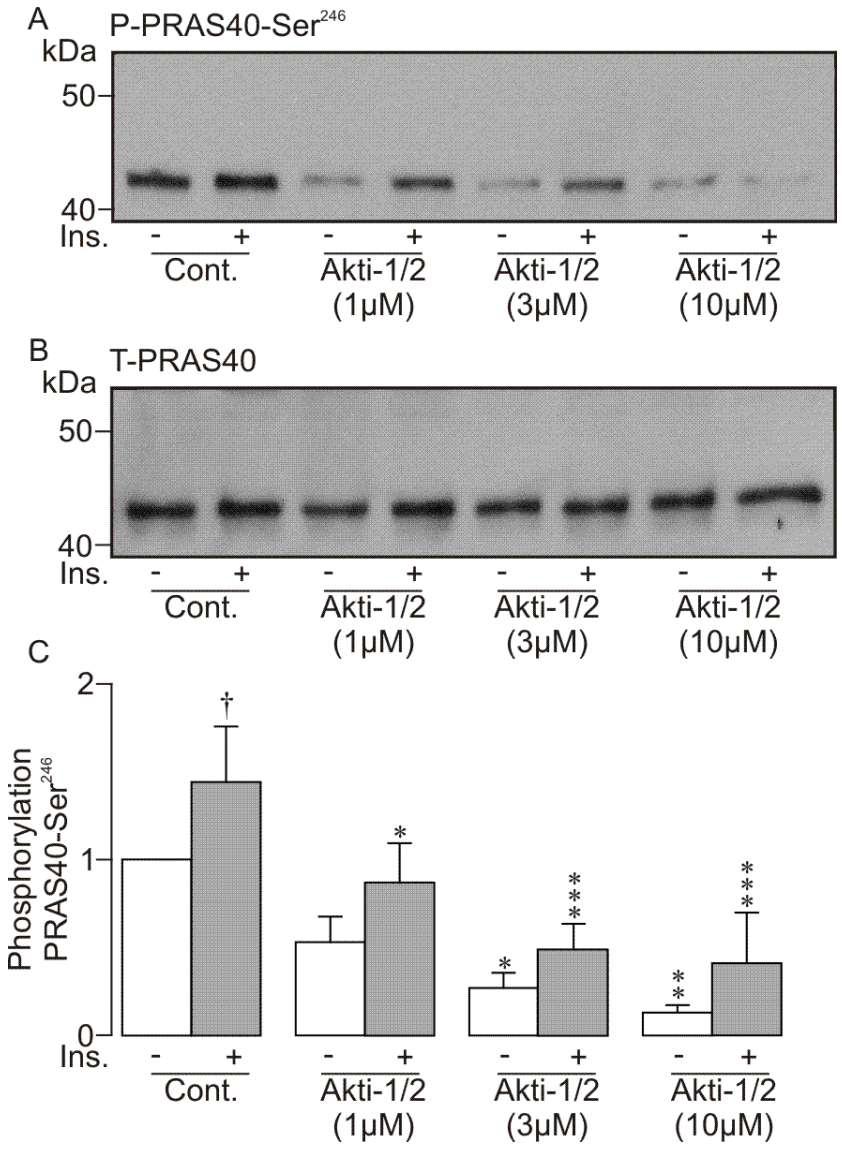

Figure 5.4 Effects of Akti-1/2 on the phosphorylation of PRAS40-Ser^{246}.

Cells were exposed to solvent vehicle (Cont.) or to Akti-1/2 (1, 3 or 10μM, 30 min preincubation) and then maintained under hormone-free conditions (Ins. -) or exposed to 20nM insulin (Ins. +) for a further 30 min before being lysed. (A) Typical western blot showing phosphorylation of PRAS40-Ser^{246}. (B) Typical western blot showing total PRAS40 protein. (C) Pooled data from phospho-PRAS40-Ser^{246} blots, n = 5, data is presented at mean ± S.E.M. Daggers denote statistically significant effects of insulin on the phosphorylation of PRAS40-Ser^{246}: †, $p < 0.05$, ‡, $p < 0.01$. Asterisks denote statistically significant effects (Two-way ANOVA Bonferroni post hoc test) of Akti-1/2 on either basal or insulin-stimulated phosphorylation of PRAS40-Ser^{246}: *, $p < 0.05$, **, $p < 0.01$, $p < 0.001$.

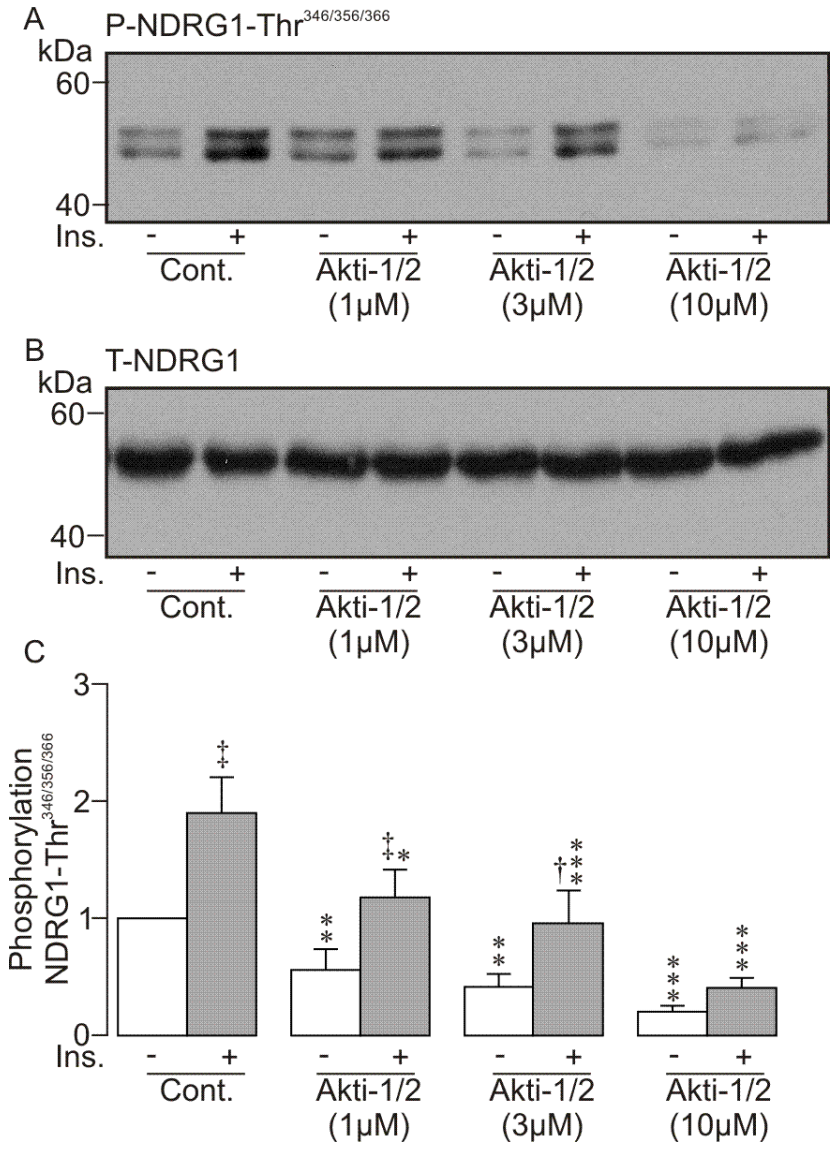

Figure 5.5 Effects of Akti-1/2 on the phosphorylation of NDRG1-Thr$^{346/356/366}$.

Cells were exposed to solvent vehicle (Cont.) or to Akti-1/2 (1, 3 or 10μM, 30 min preincubation) and then maintained under hormone-free conditions (Ins. -) or exposed to 20nM insulin (Ins. +) for a further 30 min before being lysed. (A) Typical western blot showing phosphorylation of NDRG1-Thr$^{346/356/366}$. (B) Typical western blot showing total NDRG1 protein. (C) Pooled data from phospho-NDRG1-Thr$^{346/356/366}$ blots, n = 6, data is presented at mean ± S.E.M. Daggers denote statistically significant effects of insulin on the phosphorylation of NDRG-Thr$^{346/356/366}$: †, $p < 0.05$, ‡, $p < 0.01$. Asterisks denote statistically significant effects (Two-way ANOVA Bonferroni post hoc test) of Akti-1/2 on either basal or insulin-stimulated phosphorylation of NDRG1-Thr$^{346/356/366}$: *, $p < 0.05$, **, $p < 0.01$, $p < 0.001$.

5.2.3 Effects of GSK650394A on basal and insulin-stimulated Na^+ transport

Identical experiments to those carried out with Akti-1/2 were used to investigate the effects of three doses of the SGK1 inhibitor, GSK650394A (1, 3, 10μM) on basal I_{eq}. Figure 5.6 shows that similar to Akti-1/2, lower doses of GSK650394A do not alter basal I_{eq} significantly. 10μM GSK650394A significantly inhibited the basal current by 21.4 ± 10.6% (Table 5.2). Again, similar to the results with Akti-1/2, ~ 80 % of the current remains, therefore GSK650394A cannot be inhibiting the major mechanism allowing spontaneous Na^+ absorption. All basal values of I_{eq} before and after treatment with vehicle / drug can be found in Table 5.2.

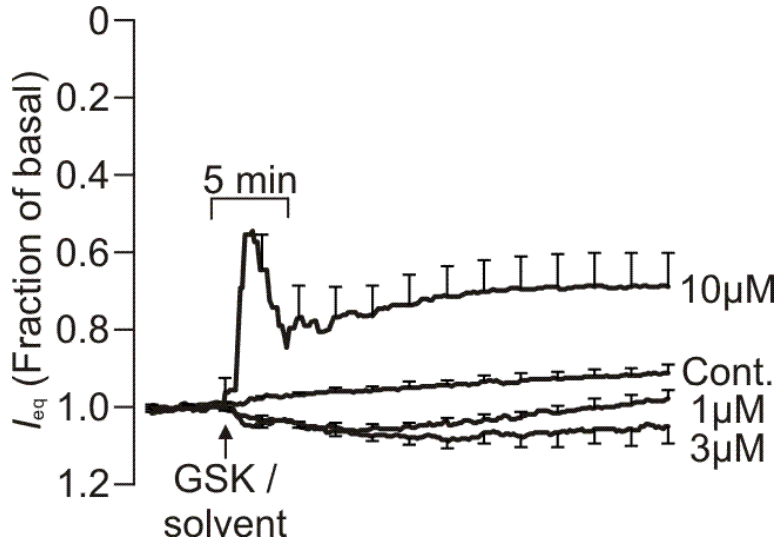

Figure 5.6 Effects of GSK650394A on basal I_{eq}.

I_{eq} of cells treated with solvent vehicle or GSK650394A (1-10μM) for 30 min, arrow indicates addition. Data is shown as mean I_{eq}, calculated as a fraction of the initial current, ± S.E.M. (n = 5).

Table 5.2 I_{eq} of control and GSK650394A-treated cells.

Mean data ± S.E.M. (n = 5) for I_{eq} recorded from cells treated with vehicle or GSK650394A (1-10 µM). Values are from baseline and after 30 min exposure to vehicle / GSK650394A. Statistical significance was calculated using an unpaired Student's t-test, * $p < 0.05$.

Treatment		I_{eq} (µA cm^{-2})	
		Baseline	30 min exposure
1µM GSK650394A	Control	-12.8 ± 2.2	-12.0 ± 2.1
	Experimental	-12.6 ± 2.1	-13.0 ± 2.6
3µM GSK650394A	Control	-17.6 ± 2.5	-16.5 ± 2.8
	Experimental	-20.0 ± 3.4	-20.9 ±3.9
10µM GSK650394A	Control	-18.7 ± 4.0	-16.4 ± 3.1
	Experimental	-21.9 ± 3.9	-15.4 ± 3.9*

The effects of GSK650394A on insulin-stimulated Na^+ transport were subsequently examined. Similar to the experiments carried out with Akti-1/2, a separate control response to insulin was carried out for each dose of GSK650394A tested. Figure 5.7A-C shows the control experiments where insulin (20 nM, 30 min) consistently produced a significant increase in ΔI_{eq}: 1µM control: -5.8 ± 0.5 µA cm^{-2} (n = 5, $p < 0.001$); 3µM control: -5.8 ± 0.2 µA cm^{-2} (n = 5, $p <$ 0.001); 10µM control: -8.3 ± 2.2 µA cm^{-2} (n = 5, $p < 0.01$). Statistical significance was determined by comparing the mean ΔI_{eq} after 30 min in both control and GSK650394A-treated cells using an unpaired Student's t-test. Again, insulin-induced changes in I_{eq} were associated with a depolarisation of V_t and small fall in R_t and these values can be found in the appendix. The effects of increasing doses of GSK650394A on insulin-induced I_{eq} can be seen in Figure 5.7D-F.

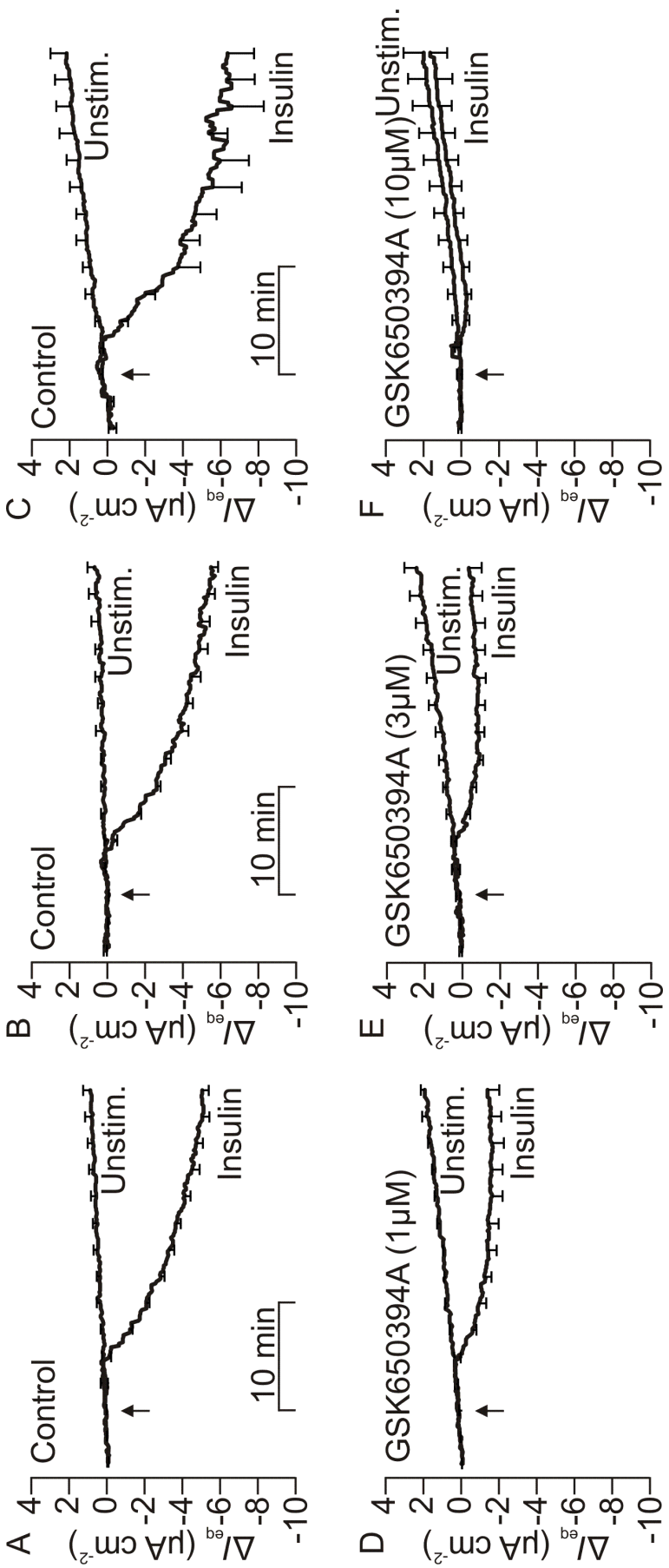

Figure 5.7 Effects of GSK650394A on the insulin-evoked current.

I_{eq} of cells pre-treated for 30 min with either solvent vehicle (A-C) or increasing doses of GSK650394A (D-F) then exposed to either unstimulated or insulin-stimulated (20nM) conditions for a further 30 min, arrow indicates addition of vehicle / insulin. Data is presented as mean ΔI_{eq}, calculated as a fraction of the current 5 min before insulin was added, ± S.E.M (n = 5).

This compound causes a dose-dependent inhibition of insulin-stimulated I_{eq}. 1μM GSK650394A inhibited the response to insulin by 44.5 ± 7.6% with a ΔI_{eq} of -3.3 ± 0.6 μA cm^{-2} (n = 5, p < 0.05). 3μM GSK650394A inhibited the insulin-evoked I_{eq} by 54.8 ± 1.5% with a ΔI_{eq} of -2.6 ± 0.1 μA cm^{-2} (n = 5, p < 0.001). Finally 10μM GSK650394A essentially abolished the response to insulin with an inhibition of 96.9 ± 5.6% and a ΔI_{eq} of 0.5 ± 0.4μA cm^{-2} (n = 5, p < 0.01). This data clearly demonstrates that GSK650394A can effectively block the natriferic response to insulin. The phosphorylation of endogenous proteins was subsequently examined to determine the specificity of this inhibitor.

5.2.4 Effects of GSK650394A on phosphorylation of endogenous proteins

Insulin (20 nM) increased SGK1 activity under control conditions as shown by significantly increased phosphorylation of NDRG1-Thr$^{346/356/366}$ (Figure 5.8). The addition of GSK650394A to cells significantly reduced basal phosphorylation of NDRG1-Thr$^{346/356/366}$ at 3μM and 10μM. Insulin-stimulated phosphorylation of NDRG1-Thr$^{346/356/366}$ was significantly reduced by all concentrations of GSK650394A (Figure 5.8). These data are consistent with GSK650394A inhibiting SGK1 activity.

Figure 5.9 again shows that the addition of insulin significantly increased the phosphorylation of Akt-Ser^{473} indicating an increase in mTORC2 activity. The addition of GSK650394A did not significantly alter basal phosphorylation of Akt-

Ser^{473} at any of the concentrations tested. Insulin-stimulated phosphorylation of Akt-Ser^{473} remained unaltered at 1µM GSK650394A, however at increased concentrations of the drug, insulin-stimulated phosphorylation of Akt-Ser^{473} was significantly reduced (Figure 5.9). These findings suggest that at higher doses of GSK650394A, mTORC2 activity or PI3-kinase activity become inhibited.

The effects of this drug on Akt activity were subsequently examined. Under control conditions, insulin significantly increased the phosphorylation of PRAS40-Ser^{246}, see Figure 5.10. The addition of GSK650394A did not significantly alter basal phosphorylation of PRAS40-Ser^{246} at any of the concentrations tested and similarly, insulin-stimulated phosphorylation of PRAS40-Ser^{246} also remained unaltered at all concentrations of GSK650394A tested (Figure 5.10). These data indicate that Akt activity remains unaltered in the presence of this compound. The inhibition of insulin-stimulated I_{eq} does appear to occur with an inhibition of SGK1 activity and not Akt activity but this compound may be inhibiting further upstream of SGK1 as well as shown by a decrease in mTORC2 activity.

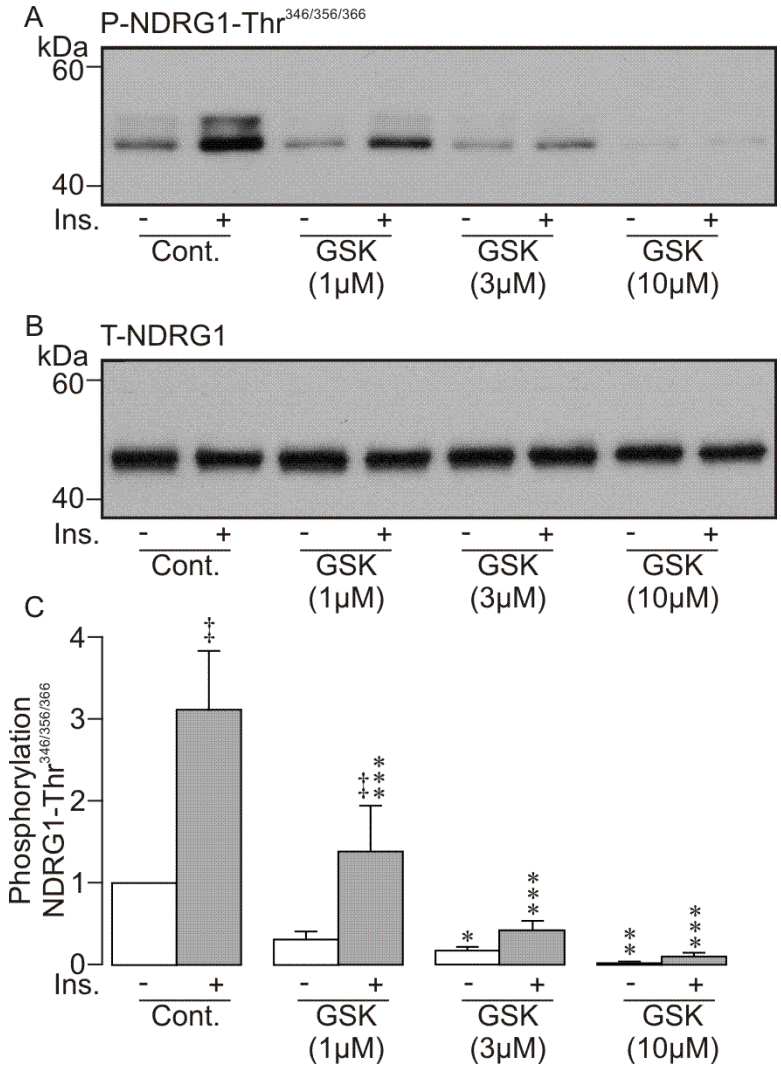

Figure 5.8 Effects of GSK650394A on the phosphorylation of NDRG1-Thr$^{346/356/366}$.

Cells were exposed to solvent vehicle (Cont.) or to GSK650394A (1-10μM, 30 min preincubation) and then maintained under hormone-free conditions (Ins. -) or exposed to 20nM insulin (Ins. +) for a further 30 min before being lysed. (A) Typical western blot showing phosphorylation of NDRG1-Thr$^{346/356/366}$. (B) Typical western blot showing total NDRG1 protein. (C) Pooled data from P-NDRG1-Thr$^{346/356/366}$ blots, n = 6, data is presented as mean ± S.E.M. Daggers denote statistically significant effects of insulin on the phosphorylation of NDRG-Thr$^{346/356/366}$: ‡, p < 0.01. Asterisks denote statistically significant effects (Two-way ANOVA Bonferroni post hoc test) of GSK650394A on either basal or insulin-stimulated phosphorylation of NDRG1-Thr$^{346/356/366}$: *, p < 0.05, **, p < 0.01, ***, p < 0.001.

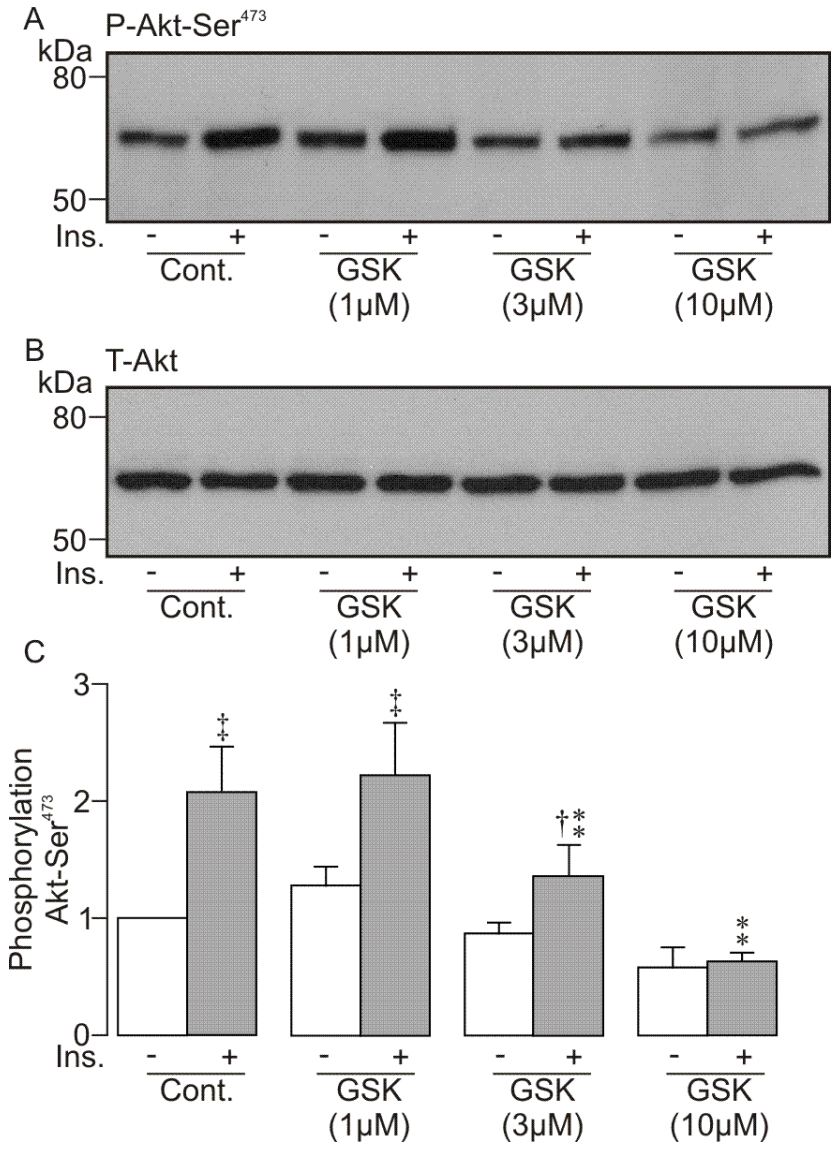

Figure 5.9 Effects of GSK650394A on the phosphorylation of Akt-Ser^{473}.

Cells were exposed to solvent vehicle (Cont.) or to GSK650394A (1, 3 or 10μM, 30 min preincubation) and then maintained under hormone-free conditions (Ins. -) or exposed to 20nM insulin (Ins. +) for a further 30 min before being lysed. (A) Typical western blot showing phosphorylation of Akt-Ser^{473}. (B) Typical western blot showing total Akt protein. (C) Pooled data from phospho-Akt-Ser^{473} blots, n = 6, data is presented as mean ± S.E.M. Daggers denote statistically significant effects of insulin on the phosphorylation of Akt-Ser^{473}: †, $p < 0.05$, ‡, $p < 0.01$. Asterisks denote statistically significant effects (Two-way ANOVA Bonferroni post hoc test) of GSK650394A on either basal or insulin-stimulated phosphorylation of Akt-Ser^{473}: **, $p < 0.01$.

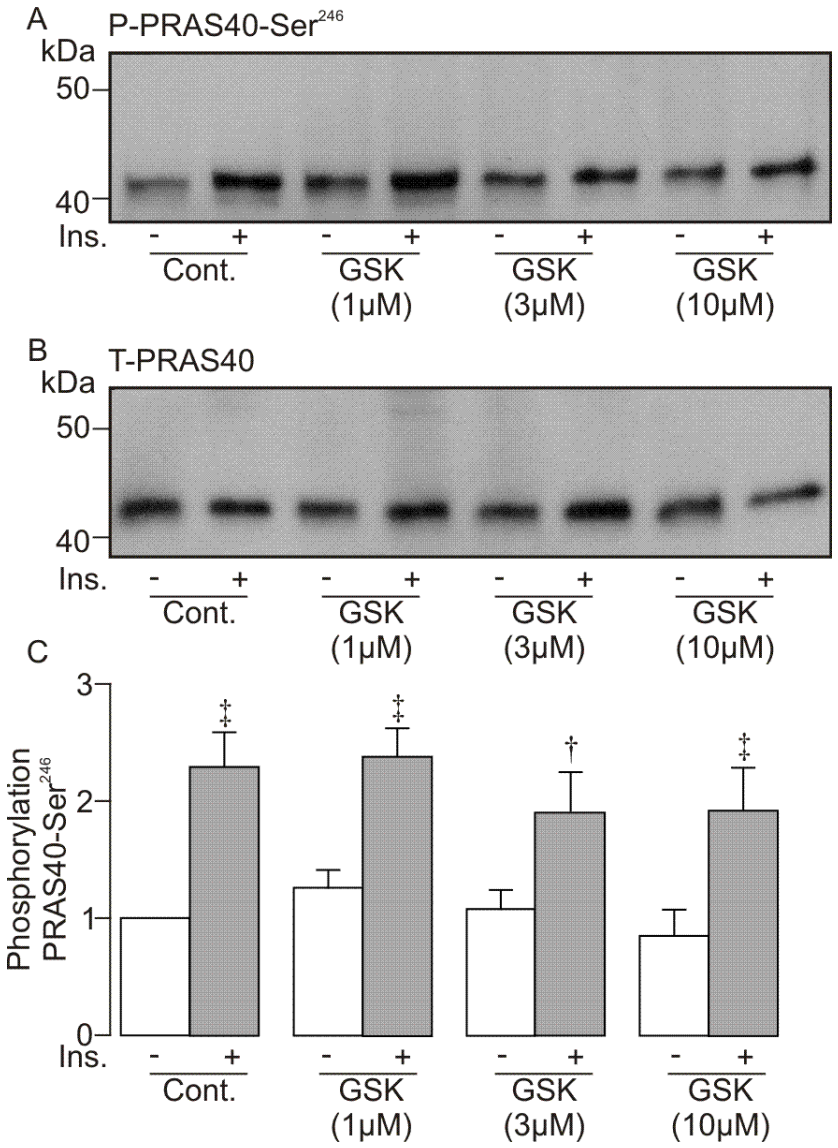

Figure 5.10 Effects of GSK650394A on the phosphorylation of PRAS40-Ser^{246}.

Cells were exposed to solvent vehicle (Cont.) or to GSK650394A (1-10μM, 30 min preincubation) and then maintained under hormone-free conditions (Ins. -) or exposed to 20nM insulin (Ins. +) for a further 30 min before being lysed. (A) Typical western blot showing phosphorylation of PRAS40-Ser^{246}. (B) Typical western blot showing total PRAS40 protein. (C) Pooled data from phospho-PRAS40-Ser^{246} blots, n = 6, data is presented as mean ± S.E.M. Daggers denote statistically significant effects (Two-way ANOVA Bonferroni post hoc test) of insulin on the phosphorylation of PRAS40-Ser^{246}: †, $p < 0.05$, ‡, $p < 0.01$.

5.3 Discussion

5.3.1 Effects of Akti-1/2 on basal and insulin-stimulated Na^+ transport

Initial experiments carried out investigated the effects of Akti-1/2 on the basal I_{eq}. Of the three concentrations tested only 10 µM Akti-1/2 caused a significant inhibition of the basal current. However, this effect was modest with ~ 80% of the current remaining implying that this compound does not inhibit the major mechanism allowing the apparently spontaneous absorption of Na^+. The effect that Akti-1/2 exerted on the insulin-induced I_{eq} was subsequently tested. As seen previously (Chapter 2), insulin evoked an increase in I_{eq} in all control recordings with a hyperpolarisation of V_t and reduction in R_t. At increasing doses, Akti-1/2 inhibited the insulin-induced Na^+ current, with the response essentially abolished at 10µM.

To determine the effectiveness of Akti-1/2 and examine the specificity of this compound, phosphorylation of endogenous proteins were monitored. Akti-1/2 inhibited the phosphorylation of both Akt-Ser^{473} and PRAS40-Ser^{246} in a dose-dependent manner. This data confirms that the inhibitor is significantly reducing Akt activity. The original study that characterized the effects of Akti-1/2 found that this compound had an IC_{50} of 4.6 µM and 21.0 µM for Akt1 and Akt2 respectively (Barnett *et al.*, 2005). In the present study 10 µM Akti-1/2 was required to fully inhibit Akt activity shown with loss of PRAS40-Ser^{246} phosphorylation. Another study investigating the effects of Akti-1/2 on Akt

activity in the presence of insulin in liver cells revealed that 1μM Akti-1/2 inhibited insulin-stimulated Akt1 and Akt2 activity (Logie *et al.*, 2007). The authors found that insulin (10 nM) increased the activity of PKBα by over 10-fold and that treatment with Akti-1/2 (0.1-10 μM) significantly reduced this activity. Phosphorylation of Akt-Ser^{473} and Akt-Thr^{308} were both abolished at 0.5 μM and PRAS40-Ser^{246} phosphorylation was greatly reduced. In the present study, much higher doses of Akti-1/2 were required to abolish Akt-Ser^{473} phosphorylation (10 μM) and this could be due to differing levels of PKB activity in the kidney versus the liver (Logie *et al.*, 2007).

To establish the selectivity of Akti1/2 for Akt / SGK1, the activity of the closely related kinase SGK1 was monitored. Interestingly, at all doses tested, both basal and insulin-stimulated levels of phosphorylation of NDRG-Thr$^{346/356/366}$ were significantly reduced and at 10μM Akti-1/2, SGK1 activity was essentially abolished. In vitro kinase assays of Akti-1/2 assayed against other protein kinases revealed that at low doses of Akti-1/2 (0.1μM, 1μM), SGK1 activity was modestly reduced but at 10 μM SGK1 activity was only 15% of the control value (Logie *et al.*, 2007), which is in accordance with the present data. In mpkCCDcl4 cells, 10μM Akti-1/2 was required to fully inhibit the insulin-induced increase in I_{eq}. However, at this concentration, the activity of both Akt and SGK1 has been abolished as demonstrated by loss of phosphorylated-NDRG1-Thr$^{346/356/366}$ and Akt-Ser^{473}, as well as a significant reduction in PRAS40-Ser^{246} phosphorylation. These findings therefore demonstrate that inhibition of the insulin-induced I_{eq} cannot solely be attributed to inhibition of Akt alone since SGK1 activity is

abolished as well. This highlights the difference in effective doses between cell lines and that using larger doses can result in loss of specificity. Thus, the role that Akt plays in both basal and insulin-mediated Na^+ transport across the collecting duct cannot be excluded and clearly warrants further investigation.

5.3.2 Effects of GSK650394A on basal and insulin-stimulated Na^+ transport

Experiments examining the effect of the SGK1 inhibitor GSK650394A on the basal I_{eq} revealed that, similar to Akti-1/2, at low concentrations there were no significant alterations to the current but at 10 µM the current was inhibited by ~ 20%. The effects of GSK650394A on the insulin-induced increase in Na^+ transport were also investigated. All three doses of this drug tested significantly inhibited the insulin-evoked I_{eq} but at 10 µM the response was essentially abolished. SGK1 activity, as monitored by phosphorylation of NDRG1-$Thr^{346/356/366}$, was dose-dependently inhibited by GSK650394A and was absent at 10 µM. These data accord well with the group that first described this drug who showed a dose-dependent inhibition of SGK1 activity, as monitored using an *in vitro* activity-based scintillation proximity assay, by GSK650394A and observed an IC_{50} for SGK1 of 62 nmol / L (Sherk *et al.*, 2008). This concentration is a lot lower than the doses tested in the present study and suggests larger basal activity in the collecting duct compared to the level found in the prostate cancer cell line utilised by Sherk *et al.* in their study. It seems unusual that 3 µM GSK650394A results in ~ 55% inhibition of insulin-stimulated I_{eq} but the activity of SGK1 as

monitored by NDRG1-Thr$^{346/356/366}$ phosphorylation was almost abolished. This could suggest that low levels of SGK1 have enough capacity to mediate the insulin-stimulated response but when SGK1 activity is completely abolished at 10 µM there is no natriferic effect of insulin.

In the present study, GSK650394A did not alter phosphorylation of the Akt substrate PRAS40-Ser^{246} at any of the concentrations tested which suggests that Akt activity remains unaltered. This finding is in agreement with *in vitro* kinase assay studies that showed GSK650394A had > 30 fold selectivity for SGK1 over Akt 1, 2 and 3 (Sherk *et al.*, 2008). However, in the present study it was also observed that insulin-stimulated phosphorylation of Akt-Ser^{473} was inhibited by 3µM and 10µM GSK650394A. This could suggest that at high concentrations GSK650394A can inhibit mTORC2 since this kinase specifically phosphorylates Akt-Ser^{473} although no other studies have reported this. Equally this compound could be inhibiting PI3-kinase which would decrease both PDK1 and mTORC2 activity which would be expected to lower Akt activity. The present data show no alteration to the phosphorylation of an Akt substrate indicating Akt activity is unaffected. However phosphorylation of downstream subtrates of Akt have been shown to persist at low levels of Akt activity (Logie *et al.*, 2007) therefore the effects of GSK650394A on mTORC2 or PI3-kinase remain uncertain.

These findings suggest that GSK650394A is inhibiting SGK1 but may be acting upstream at mTORC2 or PI3-kinase, further work could investigate off-target inhibition. Despite this, Akt activity remains unaltered and therefore the inhibition

of the current by GSK650394A can be attributed to inhibition of the SGK1 signalling pathway. These results firstly indicate that SGK1 is not involved in mediating basal I_{eq} since ~ 80% of the current remains and this is consistent with the data found in the previous chapter (Chapter 4). These findings are modest compared with those seen in a study where Fisher rat thyroid cells expressing α, β and γ ENaC subunits were co-transfected with siRNA against SGK1 and the activity of ENaC measured as amiloride-sensitive short circuit current was reduced by 50 % compared to control cells (Lee *et al.*, 2007). Furthermore a dominant negative form of SGK1 expressed in A6 cells inhibited all natriferic activity which would suggest that SGK1 plays an essential role in mediating basal Na^+ transport (Faletti *et al.*, 2002). However, expression of an inactive form of SGK1 in A6 cells in which Ser^{422} was mutated to an alanine, caused no significant alteration to the short circuit current compared to either a parental cell line or cells expressing an empty vector (Faletti *et al.*, 2002). In agreement with the present study, this would suggest that SGK1 does not play a vital role in maintaining basal levels of Na^+ transport.

The present data also indicate that SGK1 is a key mediator of the natriferic effect of insulin in the collecting duct since the response is fully abolished at 10 μM GSK650394A. This finding supports previous studies who showed that either stable expression of wild-type SGK1 (Faletti *et al.*, 2002) or tetracycline-induced expression of constitutively active SGK1 (Alvarez De La Rosa and Canessa, 2003, Arteaga and Canessa, 2005) in A6 cells induced an increase in ENaC activity that could not be potentiated any further with insulin stimulation,

indicating insulin acts via SGK1. Futhermore, silencing the expression of SGK1 in fisher rat thyroid cells that express α, β and γ ENaC subunits prevents increases in amiloride-sensitive current by application of insulin (Lee *et al.*, 2007). Our laboratory has also demonstrated that insulin can stimulate glucocorticoid-induced currents in H441 airway epithelial cells and this occurs with an increase in SGK1 activity, suggesting a role for SGK1 in hormone-regulated Na^+ transport (Inglis *et al.*, 2009). Thus, the findings of the present study and previous work indicate a crucial role for SGK1 in the insulin-mediated increase in Na^+ transport.

Altogether the findings in this chapter demonstrate that in this cell line Akti-1/2 inhibits SGK1 activity and therefore highlights the importance of verifying the effects of an inhibitor in a specific cell line. The role that Akt plays in mediating Na^+ transport consequently remains unresolved. The present results also indicate GSK650394A can inhibit SGK1 activity without affecting Akt activity but at higher concentrations impinges on mTORC2 activity suggesting that this compound may begin to target either mTORC2 or PI3-kinase at greater doses. However, SGK1 signalling appears to be blocked without altering Akt activity and these findings demonstrate that the majority of the basal I_{eq} in these cells is independent of SGK1 activity but conversely insulin-stimulated I_{eq} is absolutely dependent on it.

Chapter 6 - The role of mTORC2 in hormonal stimulation of Na^+ transport

6.1 Introduction

mTOR can form two complexes; mTORC1 and mTORC2, both of which lie downstream of PI3-kinase and can phosphorylate various AGC kinases including Akt, S6 kinase and SGK1. mTORC2 comprises six subunits: mTOR, rictor (rapamycin-insensitive companion of mTOR), mSin1, mLST8, PROTOR and DEPTOR (Guertin and Sabatini, 2007) and phosphorylates the Ser^{422} residue of SGK1 (García-Martínez and Alessi, 2008). This event allows PDK1 to phosphorylate the Thr^{256} residue and activate SGK1 (5.1). mTORC2 therefore forms a link between PI3-kinase and SGK1 in the insulin signalling pathway. Previous studies have demonstrated the involvement of PI3-kinase (Record *et al.*, 1998), SGK1 (Faletti *et al.*, 2002) and Nedd4-2 (Kamynina and Staub, 2002) in the stimulation of Na^+ transport by insulin but the role of mTORC2 is unknown. Having identified a role for both PI3-kinase and SGK1 in mediating the natriferic effect of insulin in the mpkCCDcl4 collecting duct cell line we sought to determine the role of mTORC2 in this pathway. The recent creation of two novel small molecule inhibitors of mTOR: PP242 (Feldman *et al.*, 2009) and TORIN1 (Thoreen *et al.*, 2009) allowed a method of targeting mTORC2 by using them in conjunction with the selective inhibitor of mTORC1, rapamycin. The present study has demonstrated that mTORC1 plays no role in mediating the stimulation of Na^+ transport by insulin (4.2.2) so any effect of TORIN1 and PP242 can be attributed to an inhibition of mTORC2 activity. This methodology allows a novel means by which to test the role of mTORC2 in mediating a physiological response in a collecting duct cell line.

As well as insulin mediating ENaC activity in the collecting duct, other hormones can stimulate Na^+ transport via this channel including aldosterone (Lee *et al.*, 2008) and vasopressin (Bugaj *et al.*, 2009). We therefore used our novel approach of targeting mTORC2 activity in a native system to determine the role this kinase plays in mediating the actions of aldosterone and vasopressin. The mineralocorticoid aldosterone is a steroid hormone secreted by the adrenal gland and stimulates Na^+ absorption, K^+ secretion and H_2O absorption in the aldosterone-sensitive distal nephron (ASDN), which includes the connecting tubule, cortical and medullary collecting ducts. This hormone, similar to the glucocorticoid dexamethasone, is thought to increase Na^+ absorption firstly by increasing expression of SGK1 followed by expression of ENaC and Na^+ / K^+ ATPase subunits (Loffing and Korbmacher, 2009). Whilst aldosterone has been shown to increase transcription of SGK1, it has also been implicated in activating a PI3-kinase signalling pathway that would activate SGK1 (Blazer-Yost *et al.*, 1999, Faletti *et al.*, 2002, Tong *et al.*, 2004b, Păunescu *et al.*, 2000). This activation would require mTORC2 activity, therefore to investigate this hypothesis, two mTOR inhibitors TORIN1 and PP242, as well as the mTORC1 inhibitor rapamycin were utilised and their effects on Na^+ transport examined.

Abnormal glucocorticoid or mineralocorcticoid receptor activation can similarly stimulate ENaC-mediated Na^+ transport and this is seen in certain forms of hypertension (Ulick *et al.*, 1979). These clinical conditions can be due to abnormal aldosterone secretion or lack of 11-β-hydroxysteroid dehydrogenase activity metabolizing cortisol to cortisone (Lifton *et al.*, 2001). In the case of

apparent mineralocorticoid syndrome, the MR is abnormally activated by cortisol which cannot be converted to the inactive cortisone due to the lack of 11-βHSD2 activity (Mune *et al.*, 1995). It would also lead to increased GR activation due to increased concentrations of glucocorticoids. Together this would give rise to an abnormal stimulation of ENaC and a resulting hypertensive condition (New *et al.*, 1977). It has been proposed that the effects of excess glucocorticoids occurs due to increased transcription of SGK1 (Wang *et al.*, 2001) in an analogous manner to aldosterone.

Vasopressin (AVP), also known as anti-diuretic hormone (ADH) is a peptide hormone released from the hypothalamus and alters water and salt reabsorption in the kidney. AVP exerts its effects by binding V_2 receptors in the basolateral membrane of epithelia lining the ASDN, activating adenylate cyclase which produces the second messenger cAMP (Morel, 1981). Membrane permeable analogues of cAMP as well as activators of the downstream protein kinase A (PKA) have previously been shown to activate Na^+ transport via ENaC in M1 cells (Nakhoul *et al.*, 1998), perfused rat cortical collecting duct cells (Schafer and Troutman, 1990) as well as mpkCCDcl4 cells (Butterworth *et al.*, 2005). cAMP is thought to act via protein kinase A (PKA) to increase ENaC-mediated Na^+ transport by increasing insertion of ENaCs into the membrane from a recycling channel pool (Morris and Schafer, 2002, Butterworth *et al.*, 2005). As well as increasing the number of ENaCs in the apical membrane, cAMP is also thought to increase the basolateral surface expression of the Na^+ / K^+ ATPase pumps (Gonin *et al.*, 2001). SGK1 has been implicated in mediating the effects of AVP

downstream of cAMP as Perrotti and colleagues showed that SGK1 activity was increased with the addition of cAMP in COS-7 cells expressing SGK1 (Perrotti *et al.*, 2001). Furthermore, mTORC2 was implicated as a mutated Ser^{422} on SGK1 prevented cAMP stimulation of activity. The authors concluded that SGK1 contains PKA phosphorylation site and that PKA could phosphorylate SGK1 and stimulate ENaC-mediated Na^+ transport (Perrotti *et al.*, 2001). cAMP has been shown to stimulate benzamil-sensitive I_{SC} in H441 airway epithelial cells (Thomas *et al.*, 2004). SGK1 phoshorylation was also stimulated with cAMP but this occurred after the increase in I_{SC}. Similarly in a submandibular gland cell line cAMP was found to stimulate amiloride-sensitive I_{SC} and this was attributed to an increase in SGK1 and α-ENaC expression (Vasquez *et al.*, 2008). To investigate the role of mTOR and SGK1 in the signalling pathway linking vasopressin with increased ENaC-mediated Na^+ transport in the mpkCCDcl4 cell line, the inhibitors TORIN1 and PP242 were used.

6.2 Results

6.2.1 The effects of TORIN1 on basal and insulin-stimulated Na^+ transport

As TORIN1 had not been used in this laboratory or in this cell line before, a dose-response study was carried out to determine an effective dose of this drug that would inhibit mTORC2 activity. The phosphorylation of Akt-Ser^{473} and NDRG1-$Thr^{346/356/366}$ were therefore monitored as markers of mTORC2 activity and SGK1 activity; Akt activity was also monitored. Increasing concentrations of TORIN1 (0.01 µM-1 µM) were added to cells for 30 min and exposed to either unstimulated or insulin-stimulated conditions (20 nM) for a further 30 min. Cells were then lysed and western analysis carried out probing for phosphorylation of Akt-Ser^{473}, NDRG1-$Thr^{346/356/366}$ or PRAS40-Ser^{246} as well as the respective total protein.

Figure 6.1 shows that under control conditions, insulin significantly stimulated phosphorylation of Akt-Ser^{473}. All concentrations tested of TORIN1 significantly reduced both basal and stimulated phosphorylation of Akt-Ser^{473} but at concentrations at 100 nM or greater there was a complete loss of phosphorlyation. Therefore this drug appears to be very effective at inhibiting mTORC2 activity. Figure 6.2 shows that insulin also significantly stimulated phosphorylation of NDRG1-$Thr^{346/356/366}$ indicating increased SGK1 activity. Increasing concentrations of TORIN1 reduced basal phosphorylation of NDRG1-$Thr^{346/356/366}$. All concentrations of TORIN1 tested significantly reduced the

insulin-stimulated phosphorylation of NDRG1-Thr$^{346/356/366}$ (Figure 6.2). This data is consistent with SGK1 activity being dependent on mTORC2. Akt activity was significantly stimulated by application of insulin to cells as seen with increased phosphorylation of PRAS40-Ser^{246} in Figure 6.3. Whilst increasing doses did not inhibit basal phosphorylation significantly there was a clear trend showing a reduction in the phosphorylation of this kinase. At all concentrations of TORIN1 tested, insulin-stimulated phosphorylation of PRAS40-Ser^{246} was significantly reduced (Figure 6.3) indicating an inhibition of Akt activity. From these finding a dose of 100 nM was chosen as mTORC2 and SGK1 activity were abolished.

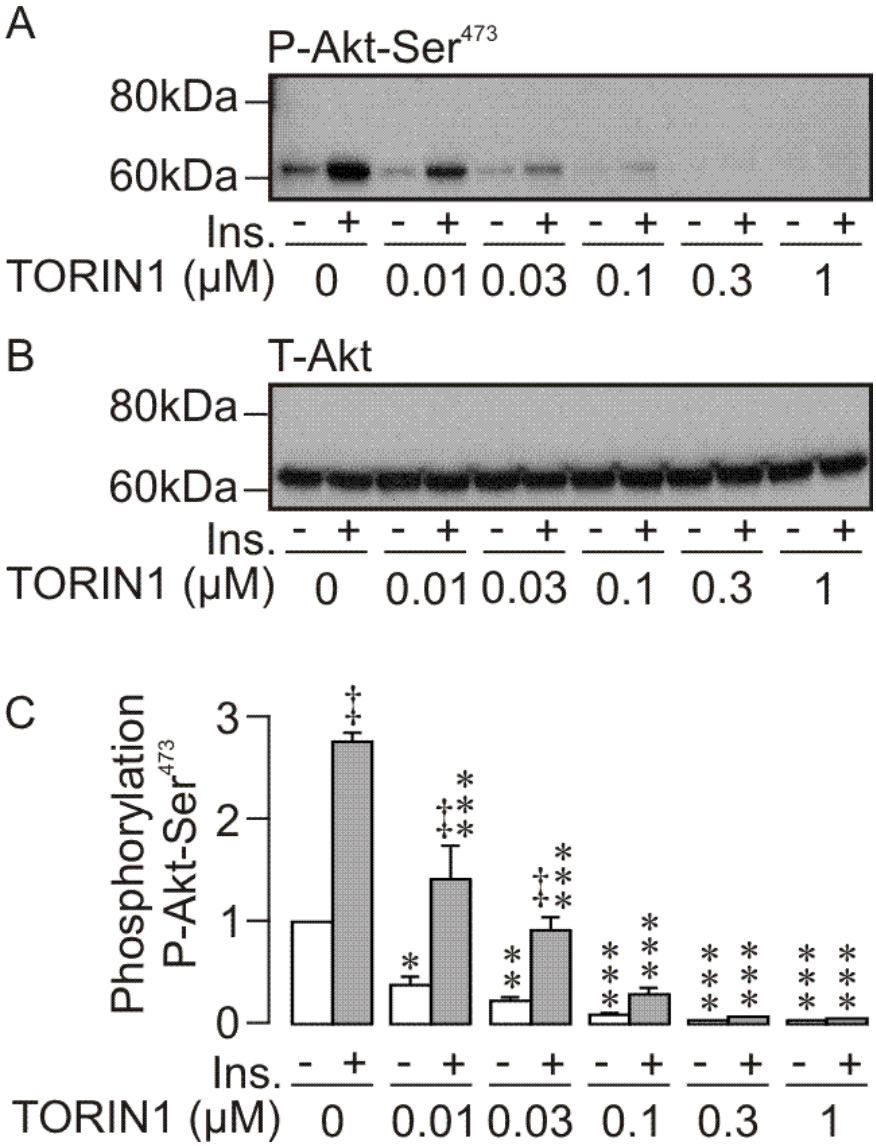

Figure 6.1 The effects of TORIN1 on the phosphorylation of Akt-Ser^{473}.

(A) Typical western blot showing phosphorylated Akt-Ser^{473} under unstimulated or insulin-stimulated (20 nM, 30 min) conditions and exposed to increasing concentrations of TORIN1 (30 min). (B) Typical western blot showing total Akt protein. (C) Pooled data of Akt-Ser^{473} phosphorylation (n = 5). Data is shown as mean ± S.E.M. and daggers denote statistical significance between basal and insulin-treated cells under control conditions: †, $p < 0.05$, ‡, $p < 0.01$. Asterisks denote statistically significant effects (Two-way ANOVA Bonferroni post hoc test) of TORIN1 on either basal or insulin-stimulated phosphorylation of Akt-Ser^{473}: *, $p < 0.05$, **, $p < 0.01$, ***, $p < 0.001$.

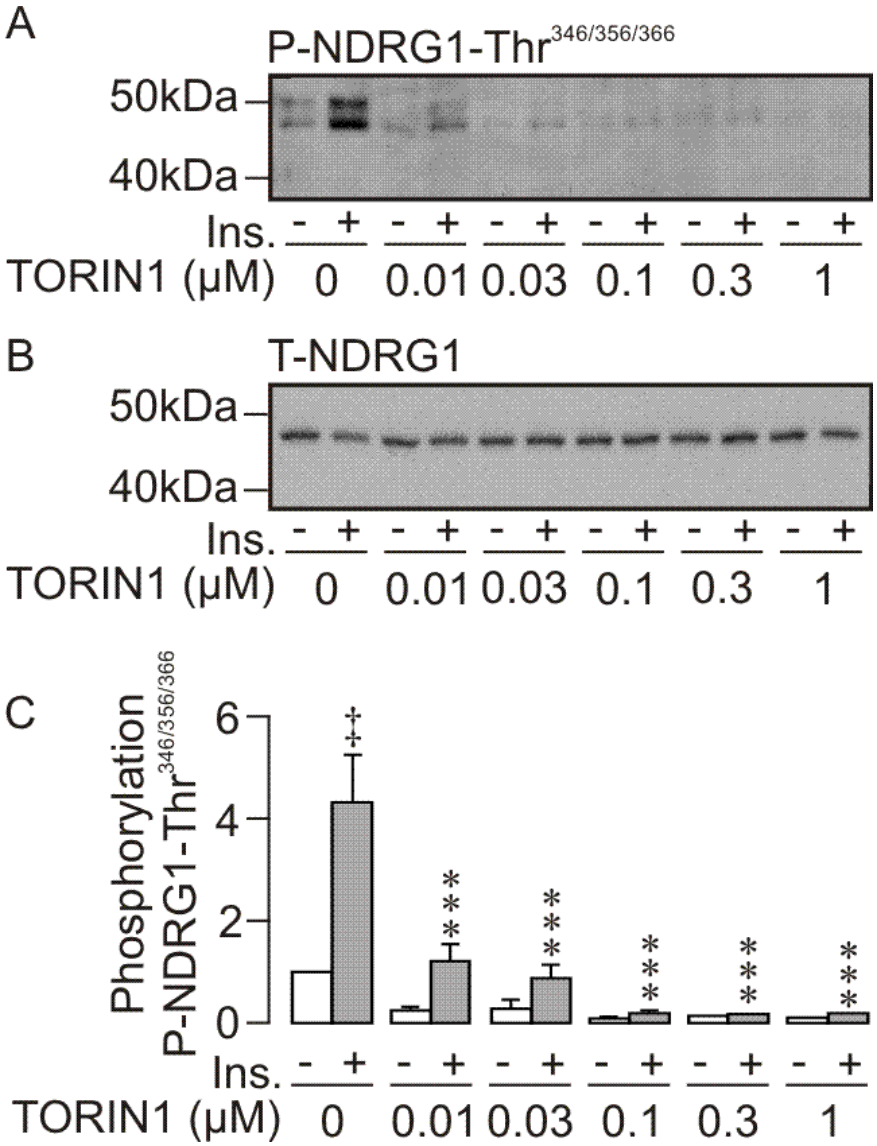

Figure 6.2 The effects of TORIN1 on the phosphorylation of NDRG1-Thr$^{346/356/366}$.

(A) Typical western blot showing phosphorylation NDRG1-Thr$^{346/356/366}$ under unstimulated or insulin-stimulated (20 nM, 30 min) conditions and exposed to increasing concentrations of TORIN1 (30 min). (B) Typical western blot showing total NDRG1 protein. (C) Pooled data of NDRG1-Thr$^{346/356/366}$ phosphorylation (n = 5). Data is shown as mean ± S.E.M. and daggers denote statistical significance between basal and insulin-treated cells under control conditions: †, $p < 0.05$, ‡, $p < 0.01$. Asterisks denote statistically significant effects (Two-way ANOVA Bonferroni post hoc test) of TORIN1 on either basal or insulin-stimulated phosphorylation of NDRG1-Thr$^{346/356/366}$: ***, $p < 0.001$.

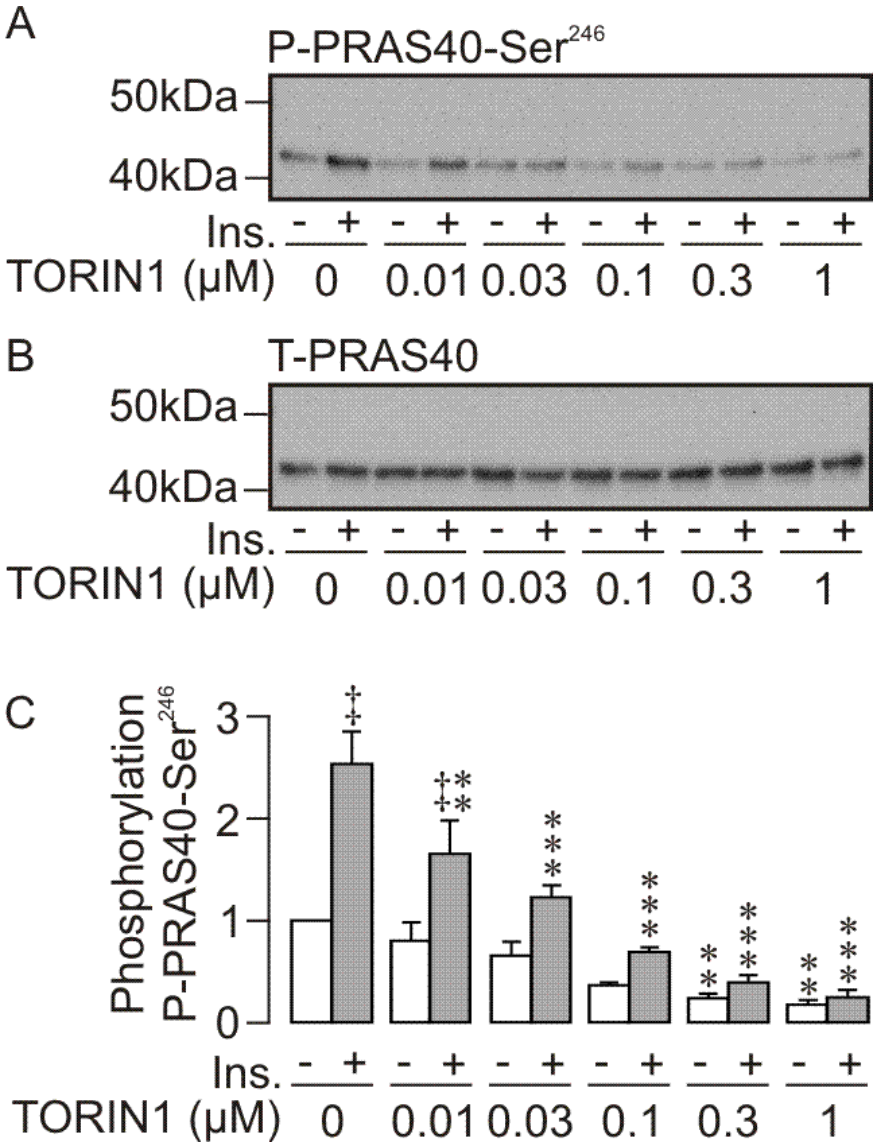

Figure 6.3 The effects of TORIN1 on the phosphorylation of PRAS40-Ser^{246}.

(A) Typical western blot showing phosphorylation PRAS40-Ser^{246} under unstimulated or insulin-stimulated (20 nM, 30 min) conditions and exposed to increasing concentrations of TORIN1 (30 min). (B) Typical western blot showing total PRAS40 protein. (C) Pooled data of PRAS40-Ser^{246} phosphorylation (n = 5). Data is shown as mean ± S.E.M. and daggers denote statistical significance between basal and insulin-treated cells under control conditions: †, $p < 0.05$, ‡, $p < 0.01$. Asterisks denote statistically significant effects (Two-way ANOVA Bonferroni post hoc test) of TORIN1 on either basal or insulin-stimulated phosphorylation of PRAS40-Ser^{246}: **, $p < 0.01$, ***, $p < 0.001$

With an effective dose of TORIN1 established the effects that this compound exerted on basal I_{eq} were investigated. Figure 6.4 shows that TORIN1 (100 nM, 60 min) modestly but significantly inhibited basal I_{eq} by 10.8 ± 3.1% (n = 14, p < 0.05). Table 6.1 shows the mean values of I_{eq} recorded and values of V_t and R_t can be found in the appendix (Chapter 9).

Figure 6.5A shows that insulin (20 nM, 30 min) significantly stimulated I_{eq} with a ΔI_{eq} of -6.2 ± 0.9 μA cm^{-2} (n = 5, p < 0.001). Statistical significance was calculated by comparing the mean ΔI_{eq} after 30 min in both control and TORIN1-treated cells using an unpaired Student's t-test. TORIN1 significantly inhibited the insulin-stimulated increase in I_{eq} by 73.3 ± 3.6% (Figure 6.5C, n = 5, p < 0.01). The addition of insulin in the presence of TORIN1 produced a small but significant increase in I_{eq} of -1.6 ± 0.4 μA cm^{-2}, (Figure 6.5B, n = 5, p < 0.05). All values of V_t and R_t can be found in the appendix. These results clearly demonstrate that TORIN1 is inhibiting insulin-stimulated Na^+ transport indicating that mTORC2 must play an important role in this action.

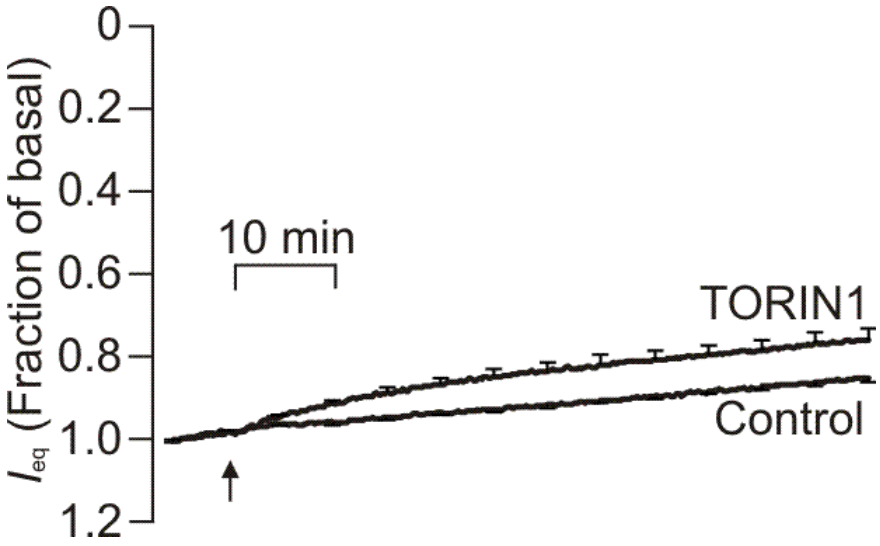

Figure 6.4 The effects of TORIN1 on basal I_{eq}.

I_{eq} of cells treated with solvent vehicle or TORIN1 (100nM) for 60 min, arrow indicates addition. Data is shown as mean current, presented as a fraction of the initial current, ± S.E.M. (n = 14).

Table 6.1 I_{eq} of control and TORIN1-treated cells.

Mean data ± S.E.M. (n = 14) for I_{eq} recorded from cells treated with vehicle or TORIN1 (100 nM, 60 min). Values are from baseline and after 60 min exposure to vehicle / TORIN1. Statistical significance was calculated using an unpaired Student's t-test, * $p < 0.05$.

Treatment	I_{eq} (µA cm^{-2})	
	Baseline	60 min exposure
Vehicle	-18.3 ± 1.3	-15.8 ± 1.1
100 nM TORIN1	-16.8 ± 1.1	-12.9 ± 0.8*

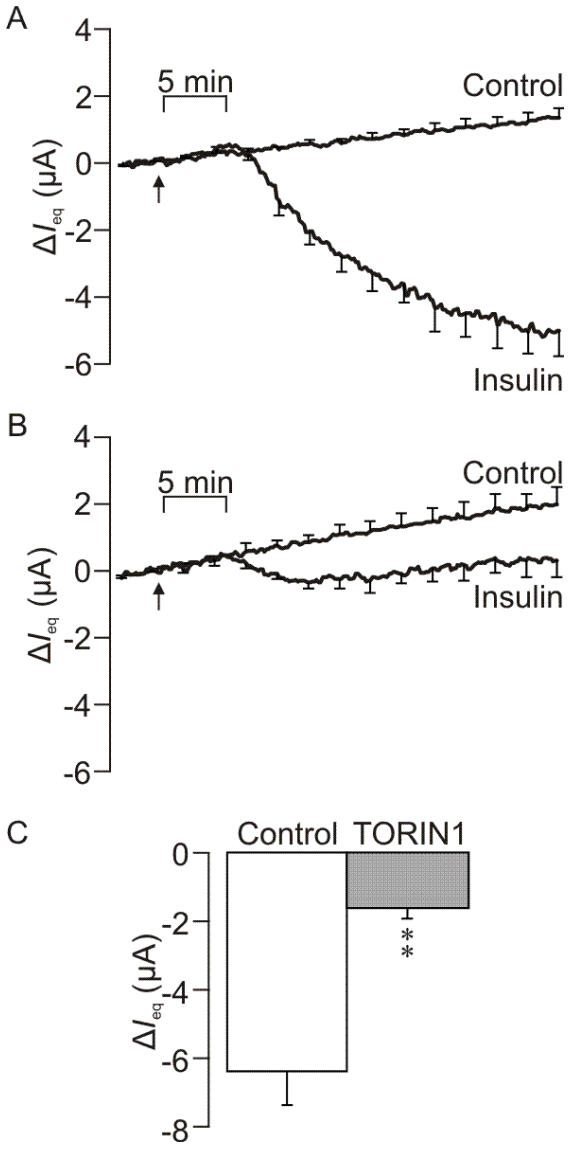

Figure 6.5 The effects of TORIN1 on insulin-stimulated I_{eq}.

I_{eq} of cells pre-treated for 30 min with either (A) solvent vehicle or (B) TORIN (100nM) then exposed to either unstimulated or insulin-stimulated (20nM) conditions for a further 30 min, arrow indicates addition of vehicle / insulin. Data is presented as mean ΔI_{eq}, calculated as a fraction of the current 5 min before insulin was added, ± S.E.M (n = 5). (C) Pooled data from the peak response, ΔI_{eq}, to insulin under control and TORIN1 treated cells. Data is presented as mean ± S.E.M. (n = 5) and statistical significance (Student's unpaired t-test) is denoted by asterisks, **, $p < 0.01$.

6.2.2 The effects of PP242 on basal and insulin-stimulated Na^+ transport

The role of mTORC2 was further investigated using another mTOR inhibitor PP242. The effect that this compound had on phosphorylation of endogenous proteins was again confirmed first. Figure 6.6 shows that under control conditions insulin significantly increased the phosphorylation of Akt-Ser^{473}, NDRG-$Thr^{346/356/366}$ and PRAS40-Ser^{246} again demonstrating that this hormone stimulates mTORC2, SGK1 and Akt activity respectively.

PP242 caused a complete loss of phosphorylated-Akt-Ser^{473} under control and insulin-stimulated conditions indicating mTORC2 activity was abolished, see Figure 6.6A. Similarly, SGK1 activity was inhibited by PP242 as seen by a loss of NDRG-$Thr^{346/356/366}$ phosphorylation (Figure 6.6B). The activity of Akt was significantly inhibited in response to PP242 as phosphorylation of PRAS40-Ser^{246} in PP242-treated cells was greatly reduced (Figure 6.6C). The changes in phosphorylation of Akt and NDRG1 occurred without any change to the abundance of total protein. These findings demonstrate that PP242 at 1 μM abolishes mTORC2 activity which inhibits SGK1 activity and reduces Akt activity.

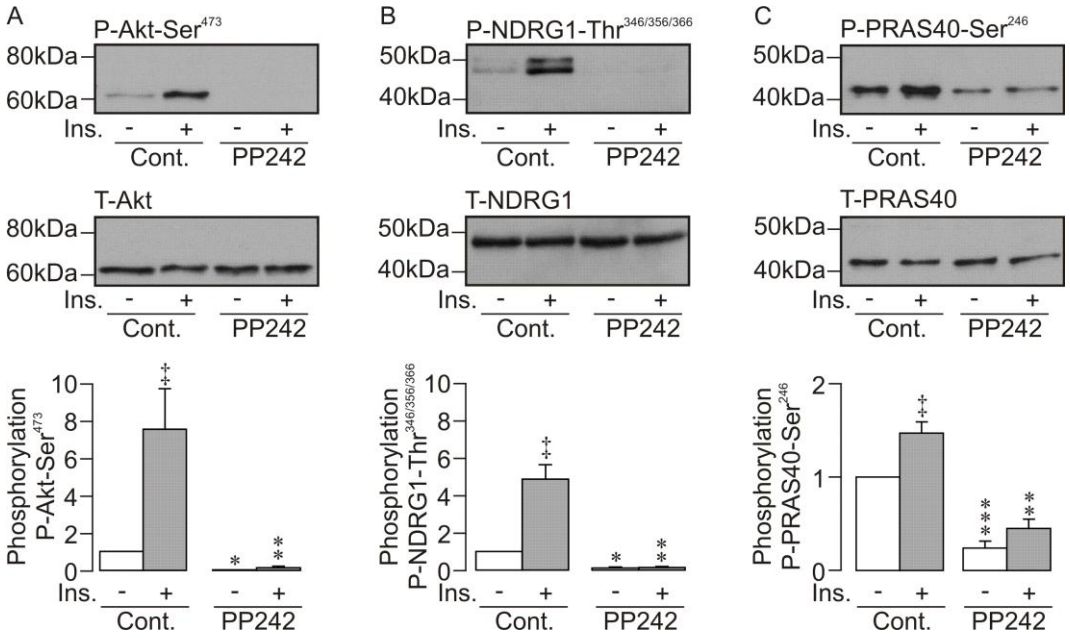

Figure 6.6 The effects of PP242 on the phosphorylation of endogenous proteins.

Top panels: typical western blots showing the phosphorylation of (A) Akt-Ser^{473}, (B) NDRG1-Thr$^{346/356/366}$ and (C) PRAS40-Ser^{246} under unstimulated or insulin-stimulated (20nM, 30 min) conditions in vehicle treated, left hand pair, or PP242 treated (1μM, 30 min) cells, right hand pair. Middle panels show the respective total protein blots for (A) Akt, (B) NDRG1 and (C) PRAS40. Lower panels show pooled data of phosphorylation of (A) Akt-Ser^{473}, n = 5, (B) NDRG1-Thr$^{346/356/366}$, n =5, and (C) PRAS40-Ser^{246}, n = 5. Data is shown as mean ± S.E.M. and daggers denote statistical significance between basal and insulin-treated cells under control conditions: †, $p < 0.05$, ‡, $p < 0.01$. Asterisks denote statistically significant effects (One-way ANOVA Bonferroni post hoc test) of TORIN1 on either basal or insulin-stimulated phosphorylation of NDRG1-Thr$^{346/356/366}$, Akt-Ser^{473} or PRAS40-Ser^{246}: *, $p < 0.05$, **, $p < 0.01$, ***, $p < 0.001$.

Since PP242 was shown to clearly inhibit mTORC2, the effects this compound exerted upon basal I_{eq} were subsequently investigated. Figure 6.7 shows that PP242 (1 µM, 60 min) inhibited basal I_{eq} by 24.3 ± 2.1%, a statistically significant effect (Table 6.2). All values of I_{eq} from control and PP242-treated cells before and after treatment can be seen in Table 6.2, values of V_t and R_t can be found in the appendix. This data suggests that mTORC2 is not playing the dominant role in the mechanism allowing spontaneous Na^+ absorption in this cell line. This is consistent with the data found with TORIN1 and also SGK1 (Chapter 5) and PI3-kinase inhibition (Chapter 4).

Figure 6.8A shows that insulin (20 nM, 30 min) stimulated I_{eq} by -6.7 ± 0.5 µA cm^{-2} (n = 5, p < 0.001). This increase in current under control conditions occurred with a significant hyperpolarisation of V_t and a decrease in R_t (see appendix for values). PP242 significantly inhibited the natriferic response by 83.7 ± 6.7% (Figure 6.8C, n = 5, p < 0.001). The addition of insulin produced a small increase in I_{eq} of -1.1 ± 0.4 µA cm^{-2} and this response was significant (Figure 6.8B, n = 5, p < 0.05). Therefore, similar to TORIN1, PP242 is inhibiting insulin-stimulated Na^+ transport indicating that mTORC2 plays an important role in this response. These findings provide further evidence for insulin signalling via a PI3-kinase / mTORC2 / SGK1 pathway to stimulate ENaC activity.

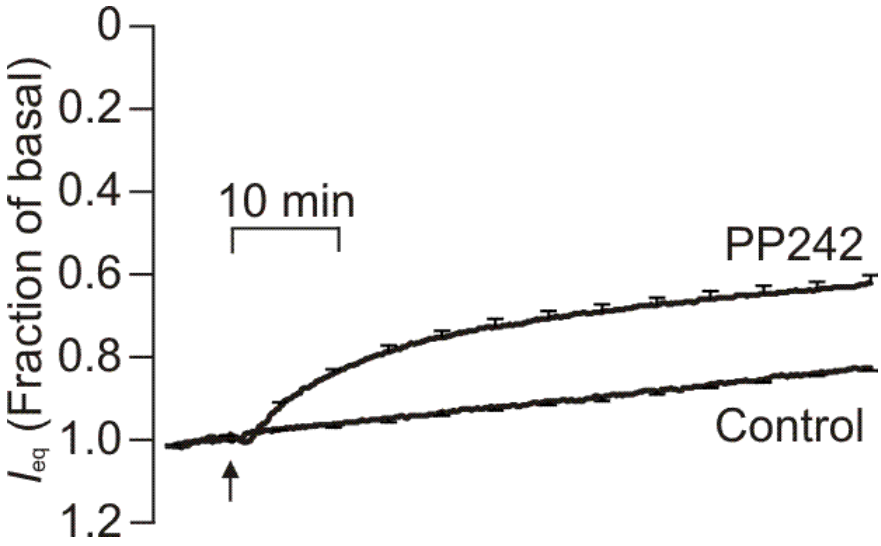

Figure 6.7 The effects of PP242 on basal I_{eq}.

I_{eq} of cells treated with solvent vehicle or PP242 (1µM) for 60 min, arrow indicates addition. Data is shown as mean current, calculated as a fraction of the initial current, ± S.E.M. (n = 15).

Table 6.2 I_{eq} of control and PP242-treated cells.

Mean data ± S.E.M. (n = 15) for I_{eq} recorded from cells treated with vehicle or PP242 (1 µM, 60 min). Values are from baseline and after 60 min exposure to vehicle / PP242. Statistical significance was calculated using an unpaired Student's t-test, ** $p < 0.01$.

Treatment	I_{eq} (µA cm^{-2})	
	Baseline	60 min exposure
Vehicle	-24.0 ± 1.6	-19.9 ± 1.3
1 µM PP242	-23.4 ± 2.0	-14.3 ± 1.0**

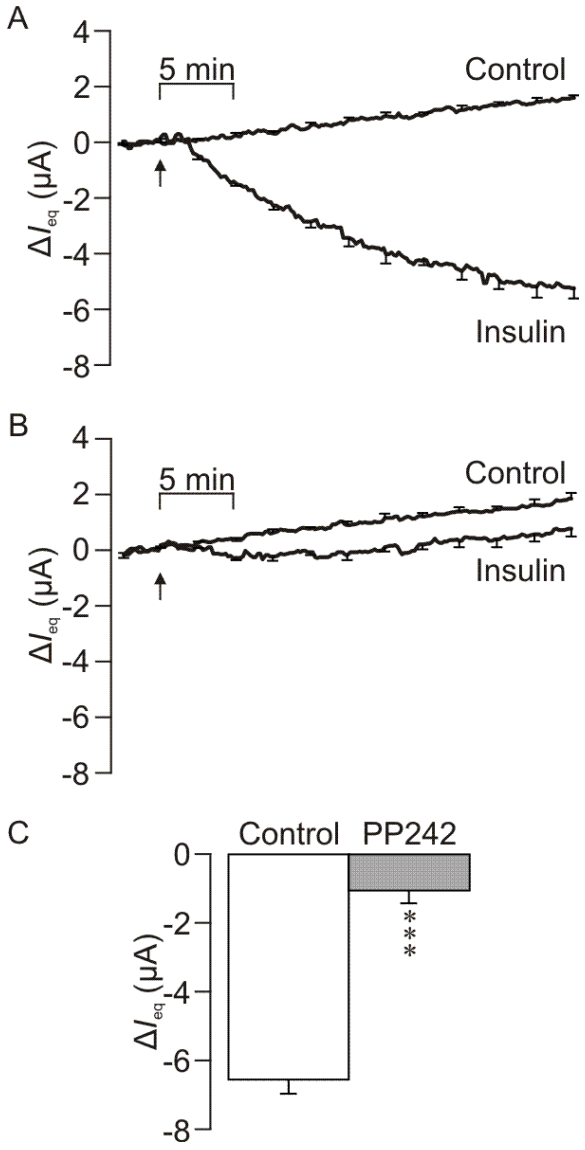

Figure 6.8 The effects of PP242 on insulin-stimulated I_{eq}.

I_{eq} of cells pre-treated for 30 min with either (A) solvent vehicle or (B) PP242 (1μM) then exposed to either unstimulated or insulin-stimulated (20nM) conditions for a further 30 min, arrow indicates addition of vehicle / insulin. Data is presented as mean ΔI_{eq}, calculated as a fraction of the current 5 min before insulin was added, ± S.E.M (n = 5). (C) Pooled data from the peak response, ΔI_{eq}, to insulin under control and PP242 treated cells. Data is presented as mean ± S.E.M. (n = 5) and statistical significance (Student's unpaired t-test) is denoted by asterisks, ***, $p < 0.001$.

6.2.3 The role of mTORC2 in aldosterone-mediated stimulation of Na^+ transport

Preliminary experiments of the present study examined the stimulatory effects of aldosterone on I_{eq} at two different concentrations (500 nM, 5 µM). Each recording had a separate control and Table 6.3 shows that in unstimulated cells, I_{eq} runs down over 3 h. With the addition of 500 nM aldosterone, there was no stimulation above initial baseline I_{eq} but this hormone prevented the run-down seen in control cells. Only at 5 µM did aldosterone produce a significant stimulation of I_{eq} (Table 6.3). However at this supraphysiological dose of aldosterone it is likely that these effects are being mediated by GR-activation rather than MR-activation and is not representative of the physiological action of aldosterone (Gaeggeler *et al.*, 2005).

Table 6.3 I_{eq} of control and aldosterone-treated cells.

Mean data ± S.E.M. (n = 7) for I_{eq} recorded from paired experiments looking at two concentrations of aldosterone (500 nM, 5 µM) added bilaterally. Each experiment has its own control recording. Values are from baseline and after 3 h exposure to vehicle / aldosterone. Statistical significance was calculated using an unpaired Student's t-test, * $p < 0.05$.

Treatment	I_{eq} (µA cm^{-2})	
	Baseline	3 h exposure
Vehicle	-18.8 ± 2.1	-13.3 ± 2.0
500 nM aldosterone	-19.1 ± 2.4	-17.7 ± 3.2
Vehicle	-23.7 ± 1.3	-17.7 ± 2.0
5 µM aldosterone	-20.7 ± 1.3	-26.7 ± 1.7*

6.2.4 The role of mTORC2 in dexamethasone-mediated stimulation of Na^+ transport

Since the mpkCCDc14 cell line appeared to display GR-mediated Na^+ transport the effects of a synthetic GR agonist, dexamethasone, on Na^+ transport were investigated. Furthermore, the role that mTORC2 / SGK1 played in this response was investigated using TORIN1 and PP242.

The electrometric response to dexamethasone was examined in a similar manner to insulin. Dexamethasone was added bilaterally to the Ussing chambers at a physiological dose (200 nM) after a 10 min baseline recording. The recording time was increased to 2.5 h since this hormone is thought to exert it effects by increasing transcription of the downstream effector SGK1 (Wang *et al.*, 2001). Similar to the experiments studying the electrometric response to insulin, time points were taken from: the initial baseline recording; the peak response to the drug; and following treatment with amiloride; allowing a comparison with the responses seen in control and dexamethasone-treated cells (Figure 6.9, shaded areas A, B and C). Figure 6.9 shows that after 2.5 h dexamethasone had produced a significant stimulation of Na^+ transport with a ΔI_{eq} of -15.1 ± 1.3 μA cm^{-2}. This increase in current occurred with a concomittant hyperpolarisation of V_t and a small but significant decrease in R_t (Figure 6.9). This is in contrast with control cells where I_{eq} decreased over time, V_t depolarized slightly and there was a small but significant increase in R_t (Figure 6.9). All mean values of the electrical parameters recorded can be seen in Table 6.4.

The apical addition of amiloride (10 μM) caused nearly complete inhibition of I_{eq} in control cells. In dexamethasone-treated cells I_{eq} was also inhibited but the current remaining was significantly greater than control (Figure 6.9). Amiloride depolarised V_t in both control and hormone-treated cells but V_t in control cells was significantly smaller than dexamethasone-treated cells. R_t increased following treatment with amiloride in both control and dexamethasone-treated cells, but in control cells R_t was significantly larger than in hormone-treated cells (Figure 6.9). These data demonstrate that dexamethasone is stimulating ENaC-mediated Na^+ transport.

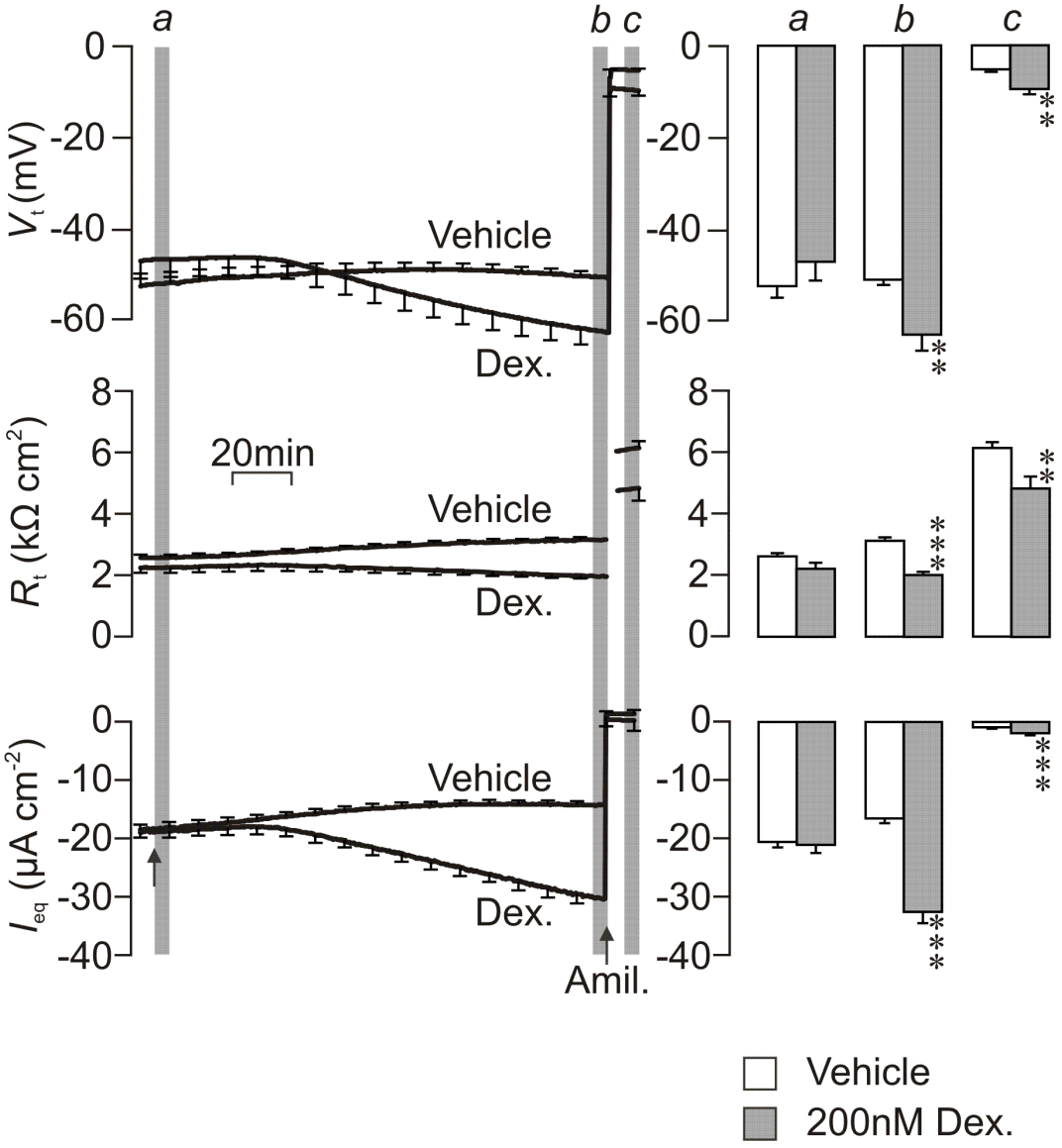

Figure 6.9 The electrometric response to acute application of dexamethasone.

Transepithelial voltage V_t was recorded (top left trace) under control conditions or with application of dexamethasone (200 nM), allowing calculation of R_t and I_{eq} (middle and bottom left traces). Mean values from different time points throughout the experiment were taken (a) prior to addition of vehicle / drug, (b) once the response to dexamethasone was established and (c) after application of amiloride (10 μM), shaded areas denote the sampling periods. The right hand panels show the mean values for V_t (top), R_t (middle) and I_{eq} (bottom). Data is shown as mean ± S.E.M. (n = 13) and statistical significance (Student's unpaired t-test) is denoted by asterisks (**, $p < 0.01$, ***, $p < 0.001$).

Table 6.4 Electrical parameters of control and dexamethasone-treated cells.

Mean data ± S.E.M. (n = 13) for V_t, R_t and I_{eq} recorded from vehicle-treated or dexamethasone-treated cells. Time points are taken from a baseline recording, 2.5 h after vehicle / dexamethasone and following 10 min exposure to amiloride. Asterisks denote statistically significant effects of dexamethasone on V_t, R_t and I_{eq} compared to control cells calculated using a Student's unpaired t-test, **, $p < 0.01$, ***, $p < 0.001$.

	Vehicle-treated			Dexamethasone (200 nM)		
	Pre-exposure	2.5 h exposure	Post-amiloride	Pre-exposure	2.5 h exposure	Post-amiloride
V_t (mV)	-52.2 ± 2.5	-50.8 ± 1.1	-5.2 ± 0.4	-46.9 ± 4.0	-62.8 ± 3.6**	-9.5 ± 1.1**
R_t (kΩ cm^2)	2.6 ± 0.1	3.1 ± 0.1	6.1 ± 0.2	2.2 ± 0.2	2.0 ± 0.1***	4.8 ± 0.4**
I_{eq} (μA cm^{-2})	-20.4 ± 0.8	-16.4 ± 0.7	-0.9 ± 0.1	-20.9 ± 1.2	-32.2 ± 1.9***	-1.9 ± 0.2***

6.2.4.1 The effects of TORIN1 on dexamethasone-stimulated Na^+ transport

Experiments similar to those carried out looking at the effects of TORIN1 on the insulin-induced current were carried out using dexamethasone. Figure 6.10 shows that under control conditions dexamethasone (200 nM, 2.5 h) produced a significant stimulation of I_{eq} with a ΔI_{eq} of -13.8 ± 3.1 μA cm^{-2} (n = 5, $p < 0.001$). This was accompanied by a hyperpolarisation of V_t and decrease in R_t (see Appendix). Following pre-treatment with TORIN1 (100 nM, 30 min), the response to dexamethasone was significantly inhibited by 87.3 ± 3.7 % (Figure 6.10C, n = 5, $p < 0.01$) with a ΔI_{eq} of -1.7 ± 0.5 μA cm^{-2} which was not a significant response. TORIN1 is inhibiting dexamethasone-stimulated I_{eq} indicating a role for mTORC1/2.

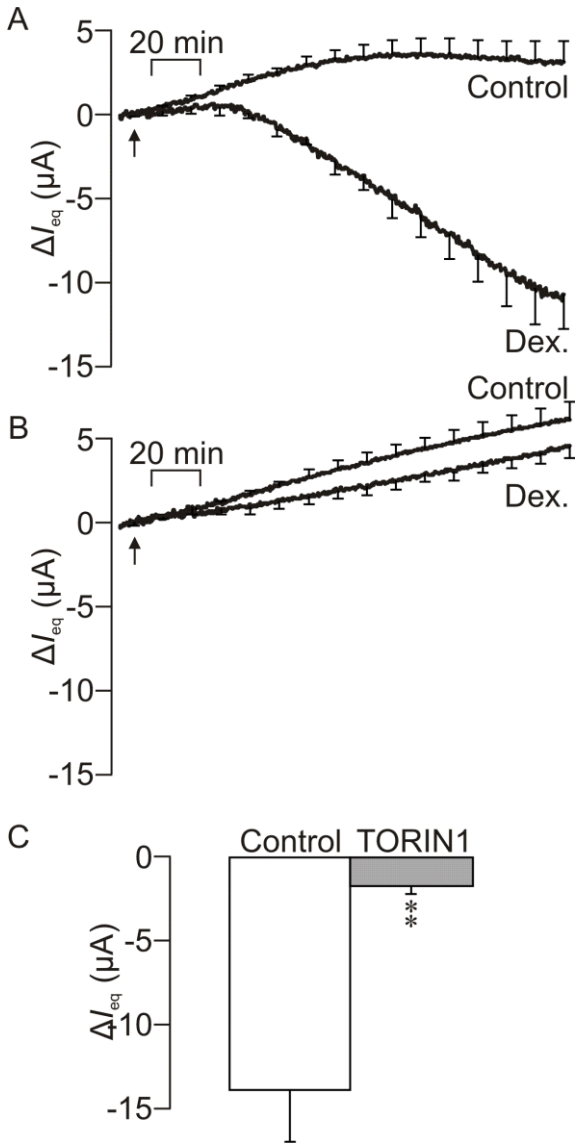

Figure 6.10 The effects of TORIN1 on dexamethasone-stimulated I_{eq}.

I_{eq} of cells pre-treated for 30 min with either (A) solvent vehicle or (B) TORIN1 (100nM) then exposed to either unstimulated or dexamethosone-stimulated (200nM) conditions for a further 2.5 h, arrow indicates addition of vehicle / dexamethasone. Data is presented as mean ΔI_{eq}, calculated as a fraction of the current 5 min before dexamethasone was added, ± S.E.M (n = 5). (C) Pooled data from the peak response, ΔI_{eq}, to dexamethasone under control and TORIN1 treated cells. Data is presented as mean ± S.E.M. (n = 5) and statistical significance (Student's unpaired t-test) is denoted by asterisks, ** $p < 0.01$.

The effects of dexamethasone on both mTORC2 and SGK1 activity were subsequently examined by monitoring the phosphorylation of endogenous proteins. The effects of TORIN1 on the activity of these kinases were also investigated. Figure 6.11 shows that as seen previously under control conditions, basal levels of phosphorylation of both Akt-Ser^{473} and NDRG1-Thr$^{346/356/366}$ persist under control conditions. Exposure of cells to dexamethasone (200 nM) for 2.5 h did not alter the level of phosphorylation of Akt-Ser^{473} (Figure 6.11A). However, there was a substantial increase in the phosphorylation of NDRG1-Thr$^{346/356/366}$, nearly a 10-fold increase above basal levels, (Figure 6.11B). These data indicate that SGK1 activity but not mTORC2 activity is stimulated with exposure to dexamethasone.

In cells pre-treated with TORIN1, phosphorylation of Akt-Ser^{473} was essentially abolished under both unstimulated and dexamethasone-stimulated conditions (Figure 6.11A). Similarly, the phosphorylation of NDRG1-Thr$^{346/356/366}$ was abolished under hormone-free conditions and was significantly reduced in dexamethasone-treated cells (Figure 6.11B), however some phosphorylation remained. This is consistent with TORIN1 inhibiting the already active mTORC2, preventing SGK1 activation and therefore phosphorylation of downstream NDRG1-Thr$^{346/356/366}$. Changes in Akt-Ser^{473} phosphorylation occurred without alteration to the overall expression of Akt. It is interesting to note that under control conditions with dexamethasone-treatment (2nd lane), expression of total NDRG1 was reduced, as well as the appearance of a second, slower migrating band (Figure 6.11B).

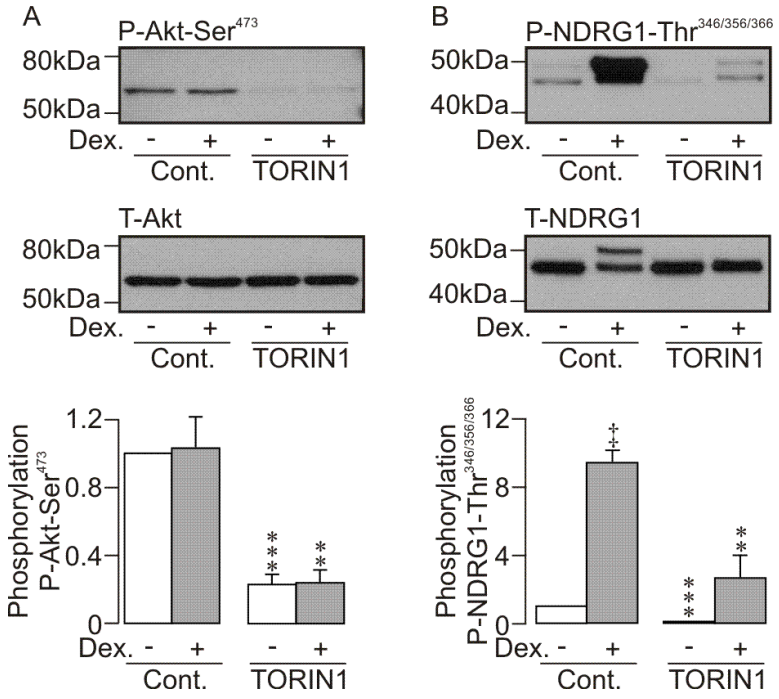

Figure 6.11 The effects of TORIN1 on the phosphorylation of endogenous proteins in response to treatment with dexamethasone.

Top panels: typical western blots showing the phosphorylation of (A) Akt-Ser^{473} and (B) NDRG1-Thr$^{346/356/366}$ under unstimulated or dexamethasone-stimulated (200nM, 2.5 hr) conditions in vehicle treated, left hand pair, or TORIN1 treated (100nM, 30 min) cells, right hand pair. Middle panels show the respective total protein blots for (A) Akt and (B) NDRG1. Lower panels show pooled data of phosphorylation of (A) Akt-Ser^{473}, $n = 6$, and (B) NDRG1-Thr$^{346/356/366}$, $n = 6$. Data is shown as mean ± S.E.M. and daggers denote statistical significance between basal and dexamethasone-treated cells under control conditions: ‡, $p < 0.01$. Asterisks denote statistically significant effects (One-way ANOVA Bonferroni post hoc test) of TORIN1 on either basal or dexamethasone-stimulated phosphorylation of Akt-Ser^{473} or NDRG1-Thr$^{346/356/366}$: **, $p < 0.01$, ***, $p < 0.001$.

6.2.4.2 The effects of PP242 on dexamethasone-stimulated Na^+ transport

Identical experiments to those carried out looking at the effects of TORIN1 were carried out to investigate the effects of PP242 on the dexamethasone stimulation of Na^+ transport. Figure 6.12A shows that under control conditions dexamethasone produced a significant stimulation of ΔI_{eq} of -16.0 ± 1.4 μA cm^{-2} (n = 5, p < 0.001). This increase in amiloride-sensitive I_{eq} was accompanied by a significant hyperpolarisation of V_t and decrease in R_t (see Appendix for values). Pre-treating cells with 1 μM PP242 significantly inhibited the response to dexamethasone by 92.1 ± 3.9 % (Figure 6.12B), with a ΔI_{eq} of -1.7 ± 0.5 μA cm^{-2} which was significantly smaller than the control response (Figure 6.12C, n = 5, p < 0.001). PP242 is therefore also clearly inhibiting dexamethasone-stimulated Na^+ transport, similar to TORIN1 and this indicates that mTORC1/2 is involved in this action.

The effects that PP242 exerted on the phosphorylation of endogenous proteins under unstimulated and dexamethasone-stimulated conditions were subsequently investigated. Figure 6.13 shows that under hormone-free conditions, cells exhibit basal levels of phosphorylation of both Akt-Ser^{473} (Figure 6.13A) and NDRG1-$Thr^{346/356/366}$ (Figure 6.13B). Exposing cells to dexamethasone did not alter Akt-Ser^{473} phosphorylation as seen in the TORIN1 experiments (Figure 6.13A), but again NDRG1-$Thr^{346/356/366}$ was significantly increased, nearly 10-fold that

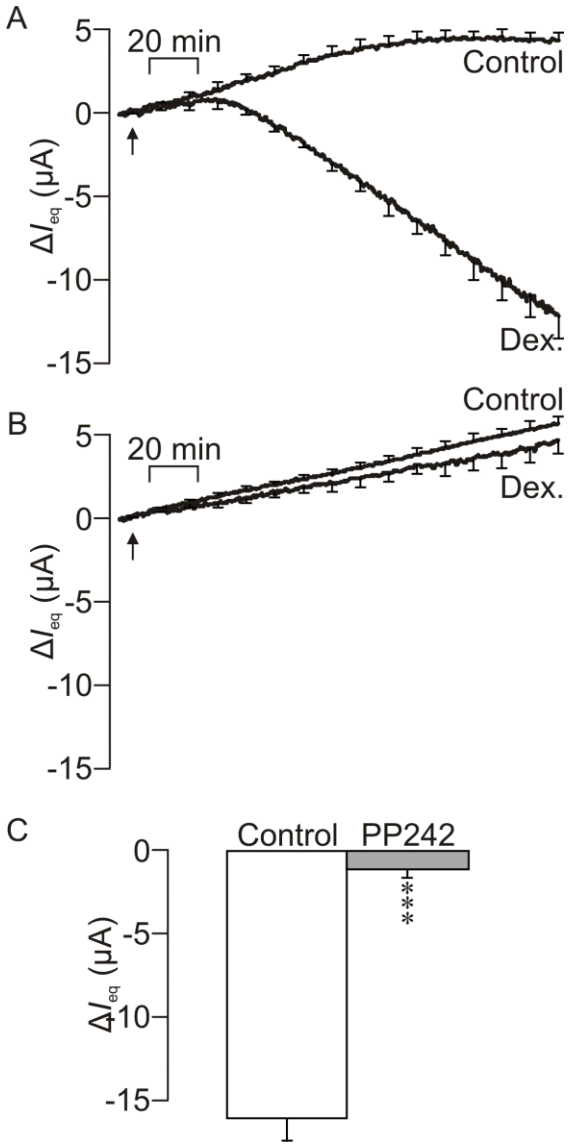

Figure 6.12 The effects of PP242 on dexamethasone-stimulated I_{eq}.

I_{eq} of cells pre-treated for 30 min with either (A) solvent vehicle or (B) PP242 (1μM) then exposed to either unstimulated or dexamethosone-stimulated (200nM) conditions for a further 2.5 h, arrow indicates addition of vehicle / dexamethasone. Data is presented as mean ΔI_{eq}, calculated as a fraction of the current 5 min before dexamethasone was added, ± S.E.M (n = 5). (C) Pooled data from the peak response, ΔI_{eq}, to dexamethasone under control and PP242 treated cells. Data is presented as mean ± S.E.M. (n = 5) and statistical significance (Student's unpaired t-test) is denoted by asterisks, *** $p < 0.001$.

above basal levels (Figure 6.13) This again indicates that dexamethasone is increasing SGK1 but not mTORC2 activity.

Application of PP242 significantly reduced phosphorylation of Akt-Ser^{473} under both unstimulated and dexamethasone-treated conditions (Figure 6.13A). Similarly, PP242 essentially abolished phosphorylated NDRG1-Thr$^{346/356/366}$ under hormone-free and dexamethasone-stimulated conditions (Figure 6.13B). This confirms that PP242 is inhibiting basal mTORC2 activity and that SGK1 activity is clearly dependent on mTORC2 activity. Changes to Akt-Ser^{473} phosphorylation occurred without any alteration to total Akt expression, but again total NDRG1 was reduced under control conditions in the presence of dexamethasone (Figure 6.13B, 2nd lane) and a faint band shift was also observed. These findings suggest that the inhibition of I_{eq} with PP242 can be attributed to an inhibition of mTORC2 resulting in SGK1 not being activated shown as with abolished phosphorylation of NDRG1-Thr$^{346/356/366}$. Furthermore these data are consistent with the results examining the effects of TORIN1.

6.2.4.3 The effects of rapamycin on dexamethasone-stimulated Na^+ transport

Since TORIN1 and PP242 inhibit both mTORC1 and mTORC2, a selective inhibitor of mTORC1, rapamycin, was used to investigate the role of mTORC1 in the dexamethasone-mediated stimulation of Na^+ transport. Experiments identical to those carried out examining the effects of TORIN1 and PP242 were carried out

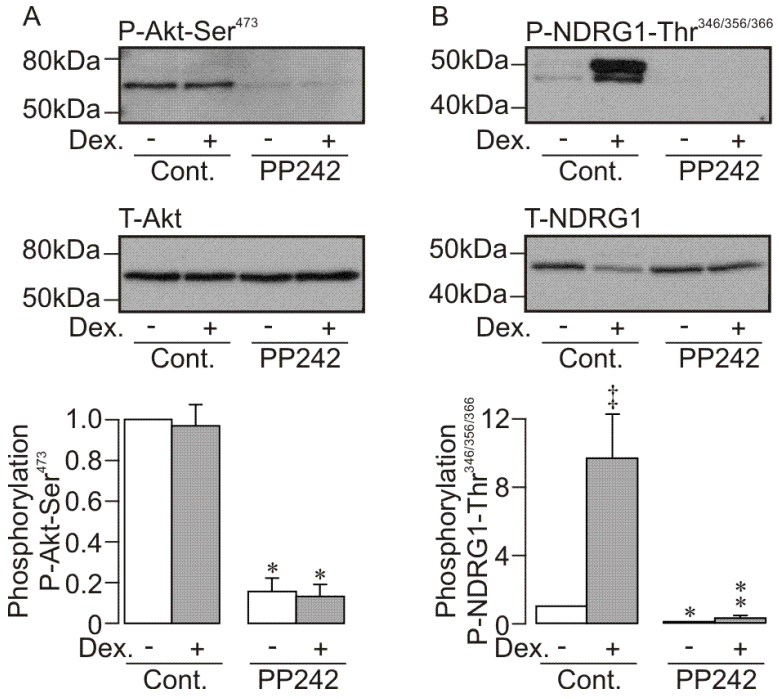

Figure 6.13 The effects of PP242 on the phosphorylation of endogenous proteins in response to treatment with dexamethasone.

Top panels: typical western blots showing the phosphorylation of (A) Akt-Ser^{473} and (B) NDRG1-Thr$^{346/356/366}$ under unstimulated or dexamethasone-stimulated (200nM, 2.5 hr) conditions in vehicle treated, left hand pair, or PP242 treated (1µM, 30 min) cells, right hand pair. Middle panels show the respective total protein blots for (A) Akt and (B) NDRG1. Lower panels show pooled data of phosphorylation of (A) Akt-Ser^{473}, n = 4, and (B) NDRG1-Thr$^{346/356/366}$, n = 4. Data is shown as mean ± S.E.M. and daggers denote statistical significance between basal and dexamethasone-treated cells under control conditions: ‡, $p < 0.01$. Asterisks denote statistically significant effects (One-way ANOVA Bonferroni post hoc test) of PP242 on either basal or dexamethasone-stimulated phosphorylation of Akt-Ser^{473} or NDRG1-Thr$^{346/356/366}$: *, $p < 0.05$, **, $p < 0.01$.

to investigate the effects of rapamycin on I_{eq}. Figure 6.9 shows that dexamethasone stimulated sodium transport under control conditions with a ΔI_{eq} of -15.8 ± 2.0 µA cm^{-2} (n = 3, $p < 0.01$). This increase in I_{eq} occurred with a

concomitant hyperpolarisation of V_t and a slight decrease in R_t (for values see Appendix).

Rapamycin had no effect on basal current, as seen previously in Chapter 4. However, unlike in the insulin-stimulated cells, rapamycin caused an 84.2 ± 3.4 % inhibition of the response to dexamethasone (Figure 6.14B, $n = 3$, $p < 0.01$). In the presence of rapamycin, ΔI_{eq} was reduced to -2.6 ± 0.9 μA cm^{-2} and this was significantly smaller than the control response (Figure 6.14C). This data indicates that mTORC1 is playing an important role in mediating the dexamethasone stimulation of Na^+ transport.

The effects that rapamycin had on phosphorylation of endogenous protein was examined. Cells were lysed and western analysis carried out examining phosphorylation of Akt-Ser^{473}, NDRG1-Thr$^{346/356/366}$ as well as for the mTORC1 substrate P70-S6K-Thr^{389}. Figure 6.15 shows basal levels of phosphorylation were observed for Akt-Ser^{473} (Figure 6.15A), NDRG-Thr$^{346/356/366}$ (Figure 6.15B) and P70-S6K-Thr^{389} (Figure 6.15C). Application of dexamethasone did not alter levels of phosphorylation compared to control conditions in either Akt-Ser^{473} (Figure 6.15A) or P70-S6K-Thr^{389} (Figure 6.15C). As previously seen (Figure 6.13),

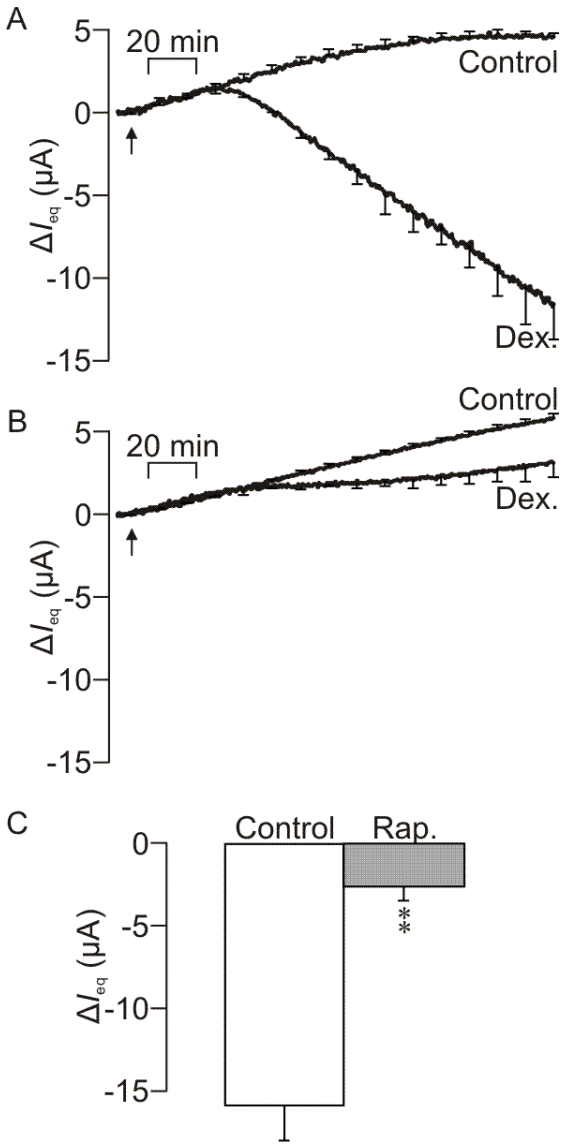

Figure 6.14 The effects of rapamycin on dexamethasone-stimulated I_{eq}.

I_{eq} of cells pre-treated for 30 min with either (A) solvent vehicle or (B) rapamycin (100nM) then exposed to either unstimulated or dexamethosone-stimulated (200nM) conditions for a further 2.5 h, arrow indicates addition of vehicle / dexamethasone. Data is presented as mean ΔI_{eq}, calculated as a fraction of the current 5 min before dexamethasone was added, ± S.E.M (n = 5). (C) Pooled data from the peak response, ΔI_{eq}, to dexamethasone under control and rapamycin treated cells. Data is presented as mean ± S.E.M. (n = 5) and statistical significance (Student's unpaired t-test) is denoted by asterisks, **, $p < 0.01$.

exposure of cells to dexamethasone produced a considerable increase in phosphorylation of NDRG1-Thr$^{346/356/366}$ (Figure 6.15B) again indicating that this hormone is stimulating SGK1 activity but not mTORC1 or mTORC2 activity.

In the presence of rapamycin, phosphorylation of Akt-Ser^{473} remained unaltered in control conditions under hormone-free and hormone-treated cells (Figure 6.15A). Similarly, phosphorylation of NDRG1-Thr$^{346/356/366}$ was unaffected by rapamycin with basal levels of phosphorylation and a very large increase in phosphorylation following 2.5 h exposure to dexamethasone (Figure 6.15B). However, phosphorylation of P70-S6K-Thr^{389} was essentially abolished in the presence of rapamycin under both unstimulated and dexamethasone-stimulated conditions (Figure 6.15C). Changes in phosphorylation of Akt-Ser^{473} occurred without any alteration to overall expression of Akt. As seen previously (Figure 6.13), expression of total NDRG1 was altered with a lighter band and a darker band that migrated more slowly (Figure 6.15B). In the presence of rapamycin, total S6K was slightly reduced under both unstimulated and dexamethasone-treated conditions (Figure 6.15C) and also appeared to migrate slightly quicker than in control conditions. These data indicate that whilst rapamycin inhibits mTORC1 activity it exerts no effect on either SGK1 or mTORC2 activity.

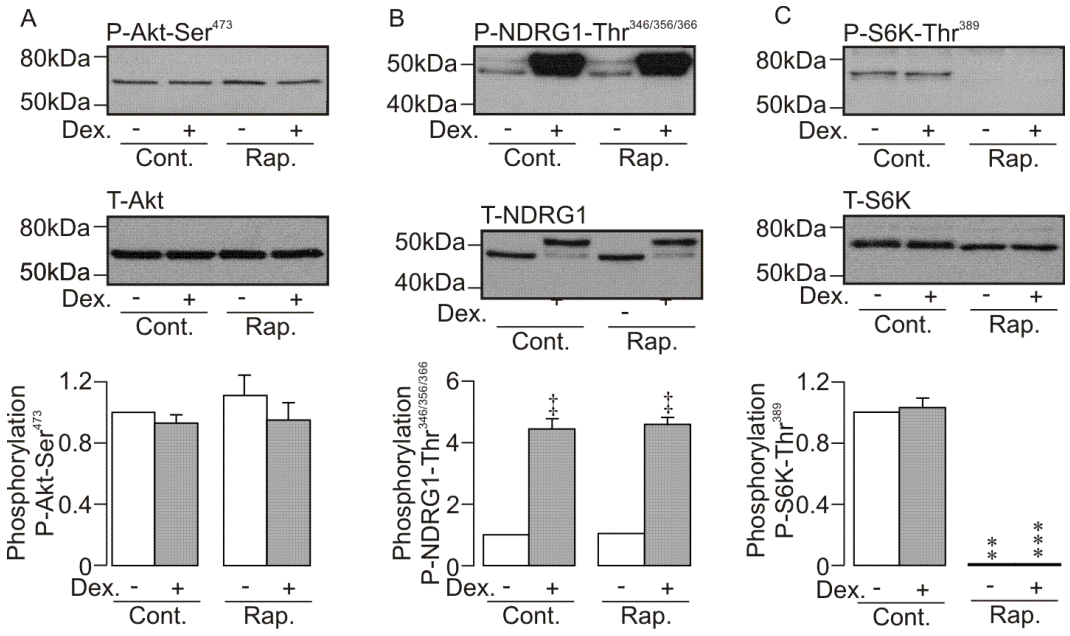

Figure 6.15 The effects of rapamycin on the phosphorylation of endogenous proteins in response to treatment with dexamethasone.

Top panels: typical western blots showing the phosphorylation of (A) Akt-Ser^{473}, (B) NDRG1-Thr$^{346/356/366}$ and (C) P70-S6K-Thr^{389} under unstimulated or dexamethasone-stimulated (200nM, 2.5 hr) conditions in vehicle treated, left hand pair, or rapamycin treated (100nM, 30 min) cells, right hand pair. Middle panels show the respective total protein blots for (A) Akt , (B) NDRG1 and (C) S6K. Lower panels show pooled data of phosphorylation of (A) Akt-Ser^{473}, n = 4, (B) NDRG1-Thr$^{346/356/366}$, n = 4, and (C) P70-S6K-Thr^{389}, n = 4. Data is shown as mean ± S.E.M. and daggers denote statistical significance between basal and dexamethasone-treated cells under control conditions: ‡, $p < 0.01$. Asterisks denote statistically significant effects (One-way ANOVA Bonferroni post hoc test) of rapamycin on either basal or dexamethasone-stimulated phosphorylation of Akt-Ser^{473}, NDRG1-Thr$^{346/356/366}$ or P70-S6K-Thr^{389}: **, $p < 0.01$, *** $p < 0.001$.

6.2.5 The role of mTORC2 in AVP-mediated stimulation of Na^+ transport

The effect that the peptide hormone arginine vasopressin (AVP) exerted on the biophysical properties of the collecting duct cells was investigated in a similar manner to insulin and dexamethasone. Figure 6.16 shows that basolateral addition of AVP (10 nM, 30 min) produced a rapid and significant stimulation of Na^+ transport with a ΔI_{eq} of -16.3 ± 1.7 μA cm^{-2}. This stimulation of I_{eq} occurred with a depolarisation of V_t and a marked decrease in R_t (Figure 6.18). This response is in sharp contrast to both insulin and dexamethasone that stimulated I_{eq} by hyperpolarising V_t and causing only a slight fall in R_t. All values of electrical parameters recorded can be found in Table 6.5.

The addition of amiloride (10 μM, 10 min) in both control and AVP-treated cells significantly inhibited I_{eq} (Figure 6.16). V_t was also significantly reduced in both untreated and AVP-treated cells and the V_t remaining following amiloride-treatment in AVP-treated cells was consistently and significantly smaller than that found in control cells (Figure 6.18). Under control conditions the addition of amiloride caused a significant increase in R_t but in AVP-treated cells however, R_t did not alter with the addition of amiloride (Figure 6.18). This is an unusual finding since amiloride has consistenly increased R_t in control experiments.

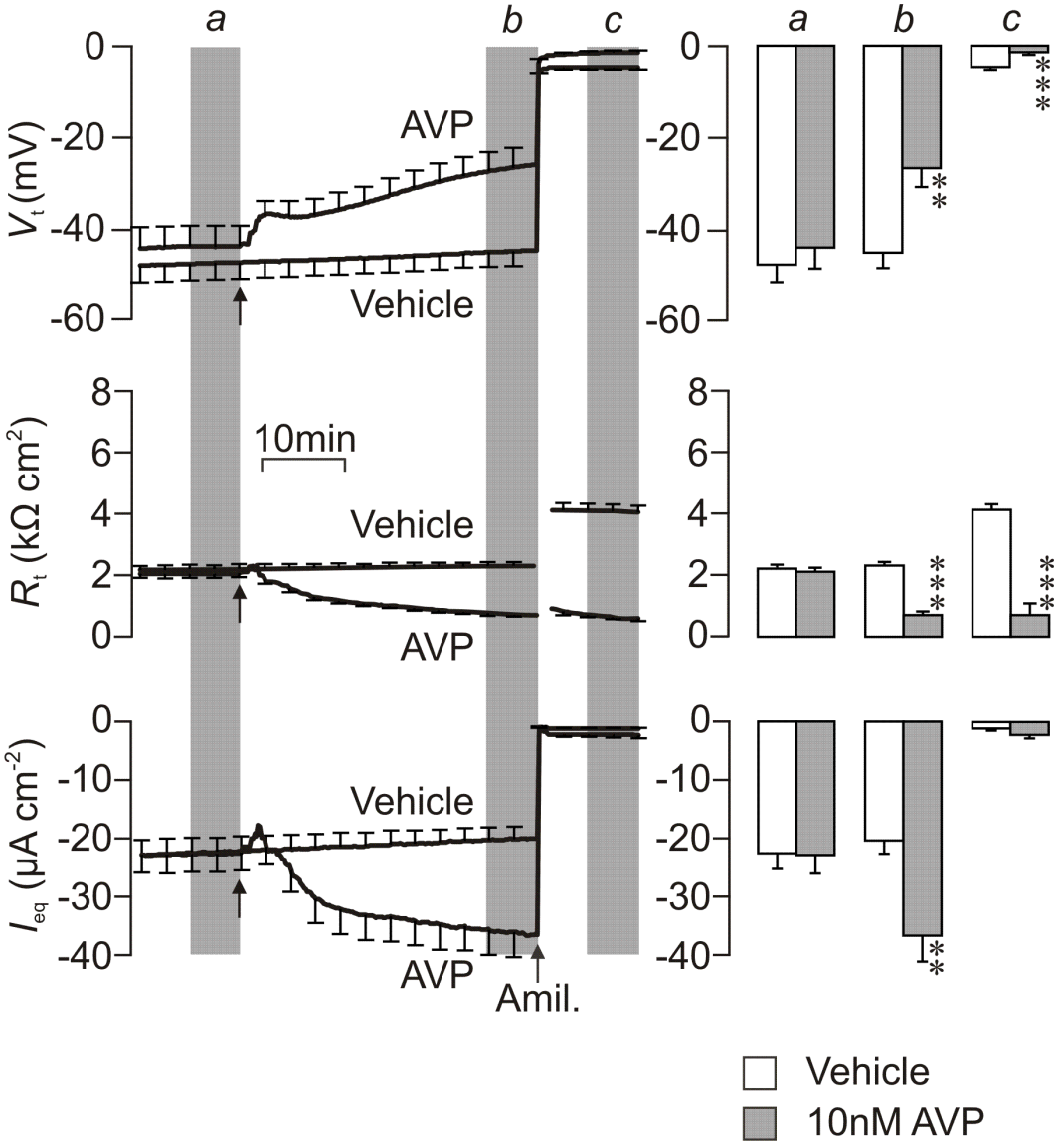

Figure 6.16 The electrometric response to acute application of vasopressin.

Transepithelial voltage V_t was recorded (top left trace) under control conditions or with application of arginine vasopressin (AVP, 10nM), allowing calculation of R_t and I_{eq} (middle and bottom left traces). Mean values from different time points throughout the experiment were taken (a) prior to addition of vehicle / drug, (b) once the response to AVP was established and (c) after application of amiloride (10μM), shaded areas denote the sampling periods. The right hand panels show the mean values for V_t (top), R_t (middle) and I_{eq} (bottom). Data is shown as mean ± S.E.M. (n = 9) and statistical significance (Student's unpaired t-test) is denoted by asterisks (**, $p < 0.01$, ***, $p < 0.001$).

Table 6.5 Electrical parameters of control and AVP-treated cells.

Mean data ± S.E.M. (n = 9) for V_t, R_t and I_{eq} recorded from vehicle-treated or AVP-treated cells. Time points are taken from a baseline recording, 30 min after vehicle / dexamethasone and following 10 min exposure to amiloride. Asterisks denote statistically significant effects of AVP on V_t, R_t and I_{eq} compared to control cells calculated using a Student's unpaired t-test, *** $p < 0.001$.

	Vehicle-treated			AVP (10 nM)		
	Pre-exposure	30 min exposure	Post-amiloride	Pre-exposure	30 min exposure	Post-amiloride
V_t (mV)	-47.5 ± 3.6	-44.9 ± 3.9	-4.6 ± 0.5	-43.8 ± 4.5	-26.6 ± 4.2**	-1.4 ± 0.4***
R_t (kΩ cm^2)	2.2 ± 0.1	2.3 ± 0.1	4.1 ± 0.2	2.1 ± 0.1	0.7 ± 0.1***	0.7 ± 0.1***
I_{eq} (μA cm^{-2})	-22.4 ± 2.6	-20.2 ± 2.1	-1.1 ± 0.1	-22.7 ± 3.1	-36.4 ± 4.3**	-2.2 ± 0.5

Vasopressin is known to mediate its effects via a cAMP- and PKA-dependent pathway. To confirm this in our cell line the phosphorylation of CREB-Ser^{133}, a substrate of PKA, was monitored. Figure 6.17 shows that AVP evoked a significant increase in the abundance of phosphorylated-CREB-Ser^{133} without altering overall expression of this protein, therefore AVP is activating a cAMP / PKA-dependent pathway.

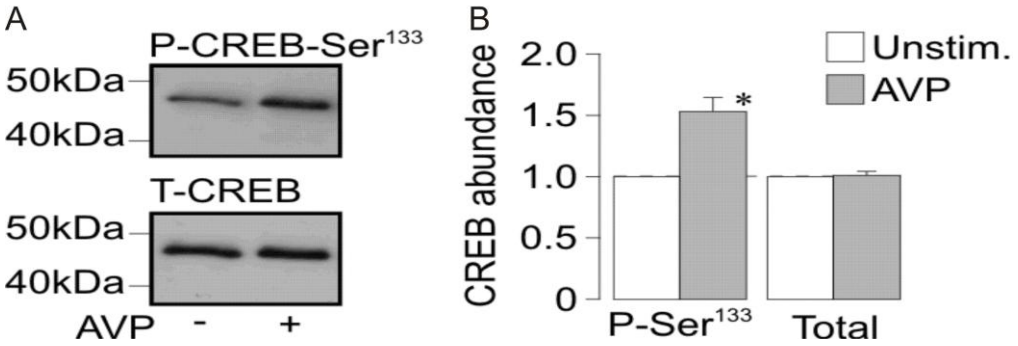

Figure 6.17 The effects of AVP on the phosphorylation of CREB-Ser^{133}.

(A) Typical western blots showing phosphorylated-CREB-Ser^{133} (upper) or total CREB (lower) under unstimulated or AVP-stimulated (10 nM, 30 min) conditions. (B) Pooled data of phosphorylated-CREB-Ser^{133} or total CREB (n = 14). Data is shown as mean ± S.E.M. and asterisks denote statistical significance (Student's unpaired t-test) between basal and AVP-treated cells: *, $p < 0.05$.

6.2.5.1 The effects of TORIN1 on AVP-stimulated Na+ transport

The effects of TORIN1 on the AVP-induced Na^+ current were investigated employing experiments identical to those examining the effects of this compound on the insulin-induced Na^+ current. Figure 6.18A shows that acute addition of AVP produced a marked stimulation of I_{eq} with a ΔI_{eq} of -11.9 ± 1.1 μA cm^{-2}. This was accompanied by a significant depolarisation of V_t as well as a significant decrease in R_t (see Appendix). In the presence of TORIN1, AVP produced a significant stimulation of I_{eq} with a ΔI_{eq} of -10.7 ± 1.3 μA cm^{-2} in a similar manner to control cells (Figure 6.18B) and this was not significantly different from the response seen in vehicle-treated cells (Figure 6.18C). These findings demonstrate that TORIN1 is not inhibiting AVP-stimulated Na^+ transport and therefore neither mTORC1/2 appear to be involved in this response.

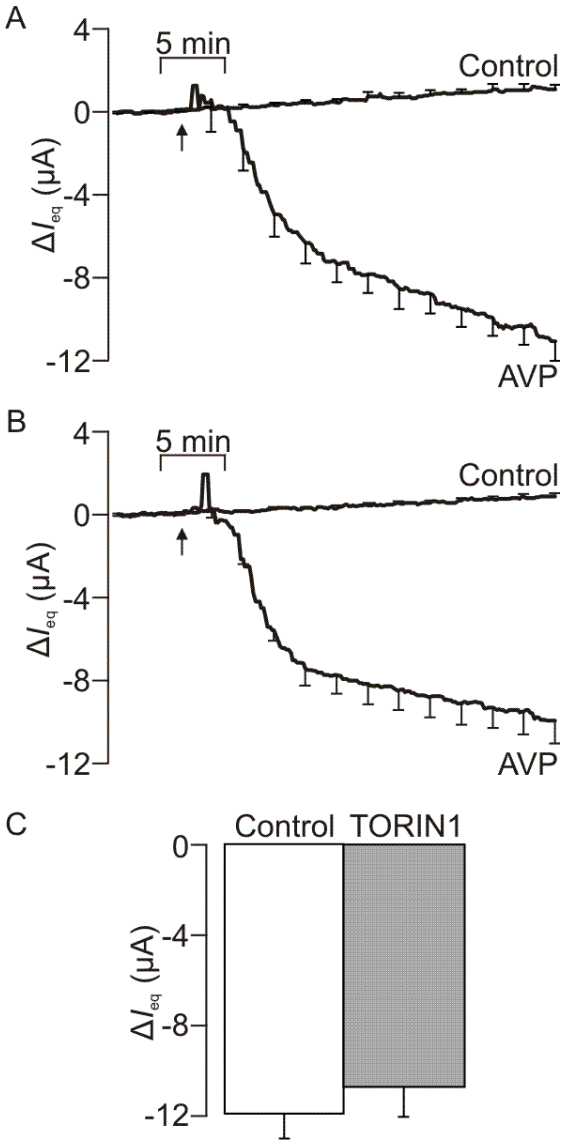

Figure 6.18 The effects of TORIN1 on AVP-stimulated I_{eq}.

I_{eq} of cells pre-treated for 30 min with either (A) solvent vehicle or (B) TORIN1 (100nM) then exposed to either unstimulated or AVP-stimulated (10nM) conditions for a further 30 min, arrow indicates addition of vehicle / AVP. Data is presented as mean ΔI_{eq}, calculated as a fraction of the current 5 min before AVP was added, ± S.E.M (n = 5). (C) Pooled data from the peak response, ΔI_{eq}, to AVP under control and TORIN1 treated cells. Data is presented as mean ± S.E.M. (n = 5).

The phosphorylation of NDRG1-Thr$^{346/356/366}$ in response to AVP and in the presence of TORIN1 was monitored to investigate the role of SGK1 in the AVP response. Under control conditions, basal levels of phosphorylation were observed for NDRG1-Thr$^{346/356/366}$ (Figure 6.19B). Application of AVP significantly suppressed phosphorylation of NDRG1-Thr$^{346/356/366}$ (Figure 6.19B). This data indicates that AVP is inhibiting SGK1 activity.

Phosphorylation of NDRG1-Thr$^{346/356/366}$ in the presence of TORIN1 was essentially abolished under both unstimulated and AVP-stimulated conditions (Figure 6.19B). This is consistent with SGK1 lying downstream of mTORC2. Changes in phosphorylation of NDRG1-Thr$^{346/356/366}$ occurred without any alteration to the overall expression of the total protein (Figure 6.19).

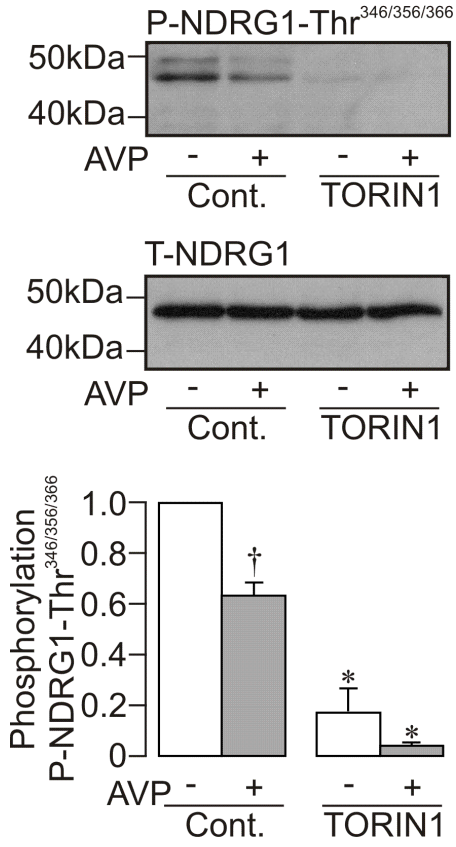

Figure 6.19 The effects of TORIN1 on the phosphorylation of NDRG1-Thr$^{346/356/366}$ under control and AVP-stimulated conditions.

Top panel: typical western blots showing the phosphorylation of NDRG1-Thr$^{346/356/366}$ under unstimulated or AVP-stimulated (10 nM, 30 min) conditions in vehicle treated, left hand pair, or TORIN1 treated (100nM, 30 min) cells, right hand pair. Middle panel shows the respective total protein blot for NDRG1. Lower panel shows pooled data of phosphorylated-NDRG1-Thr$^{346/356/366}$, n = 4. Data is shown as mean ± S.E.M. and daggers denote statistical significance between basal and AVP-treated cells under control conditions: †, $p < 0.05$. Asterisks denote statistically significant effects (One-way ANOVA Bonferroni post hoc test) of TORIN1 on basal or AVP-stimulated phosphorylation of NDRG1-Thr$^{346/356/366}$: *, $p < 0.05$.

6.2.5.2 The effects of PP242 on AVP-stimulated Na^+ transport

Identical experiments to those looking at the effects of TORIN1 on AVP-stimulated I_{eq} were carried out investigating the effects of PP242. Acute addition of AVP produced a marked stimulation of I_{eq} with a ΔI_{eq} of -19.8 ± 1.8 μA cm^{-2} (Figure 6.20A). This increase in current occurred with a concomitant depolarisation of V_t as well as a significant decrease in R_t (for values see Appendix). Again AVP is clearly stimulating ENaC-mediated Na^+ transport. In PP242-treated cells, AVP also produced a significant stimulation of I_{eq} with a ΔI_{eq} of -21.2 ± 3.3 μA cm^{-2} (Figure 6.20B) and this response was not significantly different to that seen in vehicle-treated cells (Figure 6.20C). This increase in I_{eq} occurred in an identical manner to the control cell with a depolarisation of V_t and large fall in R_t. These findings indicate that similar to TORIN1, PP242 is exerting no effect on AVP-stimulated Na^+ transport and therefore mTORC1/2 is not involved in this response.

Under control conditions, basal levels of phosphorylation were observed for NDRG1-$Thr^{346/356/366}$ (Figure 6.21B) indicating SGK1 is active under control conditions. Phosphorylation of NDRG1-$Thr^{346/356/366}$ in the presence of AVP was significantly suppressed (Figure 6.21B). This data again suggests that AVP is inhibiting SGK1 activity. In the presence of PP242, phosphorylation of NDRG1-$Thr^{346/356/366}$ was essentially abolished under both unstimulated and AVP-stimulated conditions (Figure 6.21B). These data indicate that PP242 inhibits SGK1 activity.

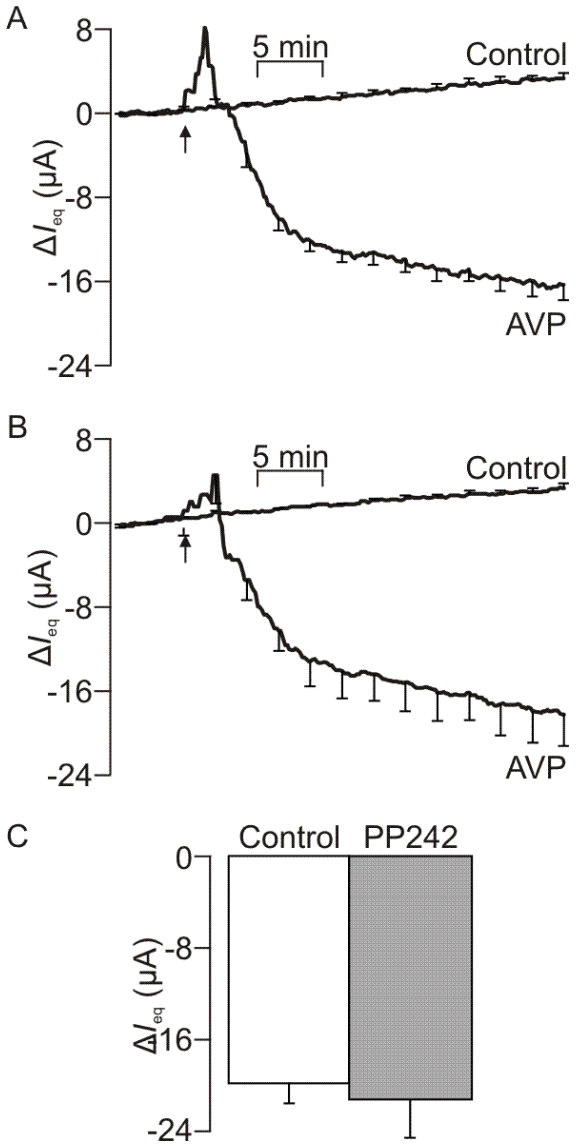

Figure 6.20 The effects of PP242 on AVP-stimulated I_{eq}.

I_{eq} of cells pre-treated for 30 min with either (A) solvent vehicle or (B) PP242 (1μM) then exposed to either unstimulated or AVP-stimulated (10nM) conditions for a further 30 min, arrow indicates addition of vehicle / AVP. Data is presented as mean ΔI_{eq}, calculated as a fraction of the current 5 min before AVP was added, ± S.E.M (n = 5). (C) Pooled data from the peak response, ΔI_{eq}, to AVP under control and PP242 treated cells. Data is presented as mean ± S.E.M. (n = 5).

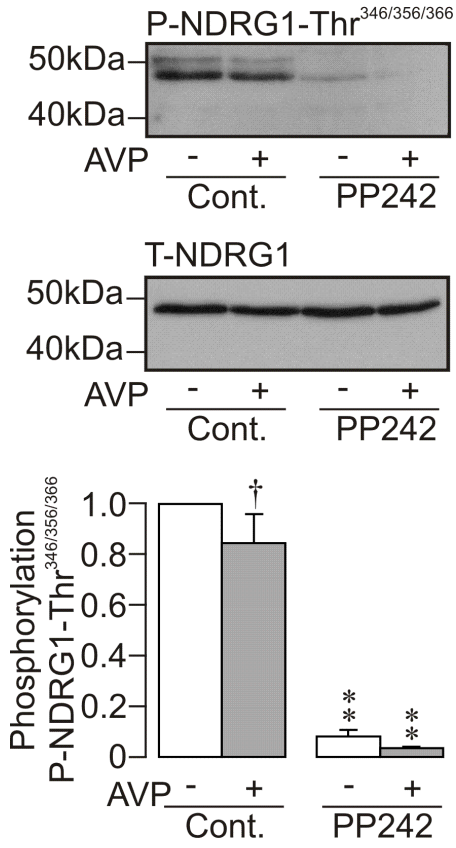

Figure 6.21 The effects of PP242 on the phosphorylation of NDRG1-Thr$^{346/356/366}$ under control and AVP-stimulated conditions.

Top panels: typical western blot showing the phosphorylation of NDRG1-Thr$^{346/356/366}$ under unstimulated or AVP-stimulated (10 nM, 30 min) conditions in vehicle treated, left hand pair, or PP242 treated (100nM, 30 min) cells, right hand pair. Middle panel shows the respective total protein blots for NDRG1. Lower panel shows the pooled data of phosphorylated-NDRG1-Thr$^{346/356/366}$, n = 6. Data is shown as mean ± S.E.M. and daggers denote statistical significance between basal and AVP-treated cells under control conditions: ‡, $p < 0.01$. Asterisks denote statistically significant effects (One-way ANOVA Bonferroni post hoc test) of TORIN1 on either basal or AVP-stimulated phosphorylation of NDRG1-Thr$^{346/356/366}$: **, $p < 0.01$.

6.3 Discussion

6.3.1 The role of mTORC2 in basal and insulin-stimulated Na^+ transport

Since the selective blocker of mTORC1 rapamycin did not alter basal Na^+ transport, any effects with the mTOR inhibitors PP242 and TORIN1 could be attributed to inhibition of mTORC2. Both PP242 and TORIN1 modestly inhibited the basal I_{eq} with PP242 showing a greater inhibition of the current than TORIN1. Since mTORC2 acts downstream of PI3-kinase, these modest effects on basal current are in accordance with our findings that inhibition of PI3-kinase with both PI103 and GDC0941 did not greatly inhibit basal I_{eq}. It is interesting to note however, that whilst PI103 and GDC0941 did not significantly alter basal I_{eq}, both TORIN1 and PP242 did so. With mTORC2 acting downstream of PI3-kinase this suggests that another factor may play a role in mTORC2 activation and elucidation of the mechanism of mTORC2 activation would be of great interest in this regard. These findings provide further evidence that the mechanism maintaining spontaneous Na^+ absorption in this cell line is largely independent of PI3-kinase, mTORC2 and SGK1 contrary to previous findings (Record *et al.*, 1998, Wang *et al.*, 2001, Faletti *et al.*, 2002). The difference with the findings from the present study compared to previous investigations could be due to the use of more selective inhibitors rather than using less specific inhibitors (Păunescu *et al.*, 2000) or overexpression systems (Alvarez De La Rosa and Canessa, 2003) to target the signalling pathway. The present study have also utilised novel drugs to target mTORC2 and examine the effect on basal Na^+

absorption which has not been studied previously. The use of these drugs is a novel method of preventing activation of SGK1, shown by the loss of downstream signalling, and provides convincing evidence that neither mTORC2 nor SGK1 play a dominant role in the maintenance of spontaneous ENaC-mediated Na^+ absorption.

The effects of both PP242 and TORIN1 on the insulin-induced I_{eq} were examined. As seen previously (Chapter 2), insulin evokes a stimulation of I_{eq} that reflects a hyperpolarisation of V_t and fall in R_t. Both inhibitors significantly reduced the insulin-induced current but they did not abolish it fully, a small response to insulin could still be seen. Therefore mTORC2 appears to play a major role in mediating the natriferic response to insulin, although other factors must play a minor role in this response. The residual response that has been seen with PI3-kinase, mTORC2 and SGK1 inhibition could be due to the effects of phospholipids. PIP_2 and PIP_3 are present at low levels under unstimulated conditions and it has been proposed that these lipids themselves can modulate ENaC activity (Blazer-Yost and Nofziger, 2005). ENaC has been shown to contain a PIP_2 binding site and mutation of this domain lowers basal ENaC activity (Kunzelmann *et al.*, 2005). PIP_2 has been proposed to alter both open probability and number of channels in the membrane (Pochynyuk *et al.*, 2006). PIP_3 appears to play a more regulatory role as levels of this phosphoinositol are dependent on PI3-kinase activity (Blazer-Yost and Nofziger, 2005). It has been proposed that PIP_2 however could maintain basal levels of ENaC and therefore be responsible or at least play a role in maintaining spontaneous Na^+ absorption (Pochynyuk *et al.*, 2008).

To identify the role of mTORC2 in the insulin signalling cascade leading to increased Na^+ absorption, the phosphorylation of endogenous proteins was monitored. mTORC2 has been shown to directly phosphorylate Akt at Ser^{473} on its hydrophobic motif (Sarbassov *et al.*, 2005) therefore the phosphorylation of this residue was monitored as a marker of mTORC2 activity. The activity of two downstream targets of mTORC2: SGK1 (García-Martínez and Alessi, 2008) and Akt (Sarbassov *et al.*, 2005) were also examined by measuring the phosphorylation of their substrates NDRG1-$Thr^{346/356/366}$ and PRAS40-Ser^{246} respectively. The phosphorylation of all three of these proteins was significantly increased by treatment with insulin, as seen previously (Chapter 3). TORIN1 inhibited the phosphorylation of Akt-Ser^{473} at 100nM under unstimulated and insulin-stimulated conditions and this phosphorylation was completely abolished at higher concentrations. PP242 completely abolished basal and insulin-stimulated phosphorylation of Akt-Ser^{473} at 1µM. SGK1 activity was abolished at 100nM TORIN1 and 1µM PP242 and Akt activity was reduced with both compounds but not completely abolished. This data is in accordance with studies that show mTORC2 is required for activation of SGK1 by phosphorylating the hydrophobic domain Ser^{422} which allows PDK1 to bind and phosphorylate the Thr^{256} residue (Biondi *et al.*, 2001), activating the kinase. In contrast, Akt activation does not require phosphorylation at its hydrophobic motif by mTORC2, therefore Akt can still be active without phosphorylation at Akt-Ser^{473} (Alessi *et al.*, 1996) which would explain PRAS40-Ser^{246} phosphorylation.

These results highlight the role of mTORC2 in mediating insulin-induced Na^+ transport. However, there is a high degree of homology in the catalytic domains of PI3-kinase, mTORC1 and mTORC2 (Bain *et al.*, 2007) which raises the possibility that these inhibitors could be acting on PI3-kinase. This kinase is a critical effector in the signalling pathway, inhibition of it abolishes the natriferic response to insulin as seen previously (Chapter 4). This issue was addressed in the study in which TORIN1 was first described (Thoreen *et al.*, 2009). The authors used cells in which a key component of both TOR complexes, mLST8, had been deleted rendering Akt-Ser^{473} constitutively dephosphorylated. They then monitored the phosphorylation of Akt-Thr^{308}, a process that requires two key steps: recruitment to the plasma membrane by PIP_3 and phosphorylation by the 3-phosphoinositide-dependent protein kinase-1 PDK1, both of which are downstream of PI3-kinase. This process can be modified in response to phosphorylation of the hydrophobic motif Akt-Ser^{473} (Frödin *et al.*, 2002) but since this was constitutively dephosphorylated, any phosphorylation of Akt-Thr^{308} would reflect PI3-kinase activity. The phosphorylation of this residue was only reduced by TORIN1 at high concentrations, > 1 μM (Thoreen *et al.*, 2009). Therefore, our results with TORIN1 can be attributed to an inhibition of mTOR and not PI3-kinase. Similarly, parallel studies in our laboratory using H441 airway epithelial cells have revealed that TORIN1 exerts only a small effect on Akt-Thr^{308} phosphorylation whilst abolishing Akt-Ser^{473} phosphorylation (unpublished data), providing further evidence that TORIN1 is not affecting PI3-kinase activity.

Although similar experiments were not carried out in the study that first described PP242 (Feldman *et al.*, 2009), the authors showed that only at high doses of this drug (2.5 μM) was there a loss of Akt-Thr^{308} phosphorylation. Moreover this loss of phosphorylation was removed in cells that were transfected with an inactive mutant Akt-Ser^{473} and treated with increasing doses of PP242. This suggests that a loss of interaction of Akt-Ser^{473} with Akt-Thr^{308} rather than a loss of PI3-kinase activity was responsible for the decrease in Akt-Thr^{308} phosphorylation (Feldman *et al.*, 2009). Therefore PP242 appears to be a selective inhibitor of mTOR rather than PI3-kinase, similar to TORIN1. Therefore the results found with both TORIN1 and PP242 can be attributed to inhibition of mTOR and not PI3-kinase. Since rapamycin does not alter basal or insulin-induced Na^+ transport excluding a role for mTORC1, these effects can also be attributed to inhibition of mTORC2.

6.3.2 The role of mTORC2 in dexamethasone-stimulated Na^+ transport

With supraphysiological doses of aldosterone required to elicit a response in this cell line it is clear that GR-activation rather than MR-activation of Na^+ transport is occurring. It is interesting to note that the original paper that described these cells use concentrations of 0.5 μM aldosterone in the bulk of the experiments and conclude that the responses seen are likewise mediated via GR-activation (Bens *et al.*, 1999). Whilst this cell line cannot be used to study the physiological response of aldosterone, since GR-mediated Na^+ transport was clearly present we studied

the effects of a synthetic GR agonist dexamethasone. This stimulation of Na^+ transport is of physiological relevance since certain forms of hypertension are caused either by increased concentrations of aldosterone or cortisol abnormally stimulating Na^+ transport by activating both the MR and GR. This is true in apparent mineralocorticoid excess (AME) syndrome where excess aldosterone is produced or in cases where 11-βHSDH activity is lost and cortisol cannot be metabolized into cortisone thereby activating MR as well as GR (Lifton *et al.*, 2001).

Dexamethasone stimulated Na^+ transport in the mpkCCDcl4 cell line by hyperpolarising V_t and reducing R_t, a similar electrometric response to insulin (Chapter 3), albeit at a slower rate. I_{eq} was abolished with application of the ENaC inhibitor amiloride, confirming that the current observed is carried by Na^+ ions via ENaC. The changes in electrical properties across the monolayer are comparable to those observed in A6 cells where treatment with 100 nM dexamethasone produced a hyperpolarisation of V_t and a decrease in R_t therefore giving an increase in I_{eq} (Wang *et al.*, 2001). This study revealed that the dexamethasone-induced increase in Na^+ transport was maximal at 8 hours and fell slightly after 24 hours, indicating that this glucocorticoid induces a substantial and long-lasting increase in ENaC-mediated Na^+ transport. This stimulation of Na^+ reabsorption occurs much later than that seen with insulin and this is consistent with the theory that whilst insulin stimulates a signalling pathway that activates SGK1, dexamethasone increases expression of SGK1 followed by increasing expression of ENaC subunits (Wang *et al.*, 2001). Here the increase in Na^+ transport after

2.5 h exposure to dexamethasone was greater than that observed with a 30 min exposure to insulin, with ΔI_{eq} of -15.1 ± 1.3 μA cm^{-2} and -11.7 ± 1.4 μA cm^{-2} respectively. These data demonstrate that dexamethasone also stimulates ENaC-mediated Na^+ transport in mpkCCDc14 cells.

The role of mTOR in the stimulation of Na^+ transport by dexamethasone was examined using inhibitors of mTOR: PP242 and TORIN1; and mTORC1 with rapamycin. The dexamethasone-induced stimulation of Na^+ transport was essentially abolished in the presence of both TORIN1 and PP242. To determine whether this result was solely due to mTORC2 activity the effects of rapamycin on the natriferic effect of dexamethasone were examined. Interestingly, rapamycin substantially inhibited the dexamethasone-induced I_{eq} although not as fully as with TORIN1 and PP242. These data suggest that mTORC1 plays a major role in mediating this response with perhaps a small role for mTORC2 to account for the difference in inhibition. This is in sharp contrast with the insulin-induced I_{eq} where mTORC1 played no role. This finding is consistent with a previous study that has demonstrated that aldosterone-stimulated amiloride-sensitive currents in A6 cells can be inhibited by rapamycin (Rokaw *et al.*, 1996b). The mechanism by which this occurred was investigated in a later study, using dexamethasone in this case, and the authors concluded that rapamycin inhibited translocation of the activated-GR into the nucleus (Edinger *et al.*, 2002). This finding provides a mechanism by which rapamycin inhibits I_{eq}, however this effect was only seen in cells pretreated for 8 h with rapamycin. The results from the present study were drawn from experiments where rapamycin was added acutely and this prevented

the onset of dexamethasone-stimulated Na^+ transport. Interestingly a very recent study shows that Na^+ transport in mpkCCDcl4 cells pre-stimulated with insulin and aldosterone was not inhibited with acute treatment of rapamycin indicating a lack of a role of mTORC1 in this natriferic response (Lu *et al.*, 2010). Clearly further work into the role of mTORC1 in corticosteroid-mediated Na^+ absorption is warranted.

To elucidate the signalling mechanism involved in the dexamethasone-induced increase in Na^+ transport, phosphorylation of endogenous proteins in the presence of these inhibitors were examined. Under control conditions dexamethasone produced a hyperphosphorylation of NDRG1-$Thr^{346/356/366}$ indicating a large increase in SGK1 activity. This is in agreement with previous studies that observed a substantial increase in SGK1 phosphorylation in response to dexamethasone treatment (Chen *et al.*, 1999, Wang *et al.*, 2001). In contrast, Akt-Ser^{473} phosphorylation remained unaltered in response to dexamethasone. The lack of alteration to Akt-Ser^{473} phosphorylation indicates that mTORC2 activity is unchanged since this kinase specifically phosphorylates this site (Sarbassov *et al.*, 2005). It is therefore unusual that SGK1 activity is so greatly increased, as SGK1 activity relies on mTORC2 phosphorylation (García-Martínez and Alessi, 2008). One possible explanation for this is that instead of dexamethasone increasing SGK1 activity but instead increasing the abundance of this kinase, basal levels of PI3-kinase activity and therefore mTORC2 and PDK1 activity could be activating the increased number of SGK1 molecules. This could explain why SGK1 activity increases without an increase in mTORC2 activity. Further experiments

measuring expression of SGK1 at the mRNA and protein level would confirm this. These findings indicate that dexamethasone instead of stimulating a PI3-kinase and mTORC2 signalling pathway, increases the abundance of SGK1 that can feed into an already active pathway. This is at odds with previous studies that have proposed that aldosterone / dexamethasone stimulate the PI3-kinase / SGK1 signalling cascade that increase SGK1 activity and therefore ENaC activity (Blazer-Yost *et al.*, 1999, Faletti *et al.*, 2002, Păunescu *et al.*, 2000, Wang *et al.*, 2001, Tong *et al.*, 2004a). In A6 cells, levels of PIP_3 were increased following exposure to aldosterone indicating an increase in PI3-kinase activity (Blazer-Yost *et al.*, 1999). Several groups have shown that inhibiting PI3-kinase with LY-294002 prevent aldosterone / dexamethasone induced ENaC-mediated Na^+ transport in A6 cells (Wang *et al.*, 2001, Păunescu *et al.*, 2000). Similarly A6 cells expressing a mutant SGK1 which cannot be activated abolishes the stimulation of current seen in A6 cells expressing wild-type SGK1, highlighting the importance of active SGK1 in mediating increased Na^+ transport (Faletti *et al.*, 2002). However, whilst these latter studies highlight the importance of PI3-kinase and SGK1 activity in mediating hormonal transport they do not directly demonstrate increased activation of these kinases in response to mineralocorticoids. The present data do not support dexamethasone stimulating PI3-kinase activity and this suggests that an already active pathway can mediate an increase in Na^+ transport.

PP242 and TORIN1 substantially reduce Akt-Ser^{473} and NDRG1-$Thr^{346/356/366}$ phosphorylation under control and dexamethasone-treated conditions, indicating

inhibition of mTORC2 and SGK1 activity respectively. However, in the presence of rapamycin, the phosphorylation of Akt-Ser^{473} and NDRG1-Thr$^{346/356/366}$ remain unaltered under control and dexamethasone-treated conditions. These data suggest that mTORC1 does not phosphorylate Akt-Ser^{473} and this is in accordance with a study that showed that mTORC2 and not mTORC1 phosphorylates this residue (Sarbassov *et al.*, 2005). Furthermore, mTORC1 is not involved in SGK1 activity as NDRG1-Thr$^{346/356/366}$ remains hyperphosphorylated in response to dexamethasone. This is in contrast with a study that showed that rapamycin could inhibit SGK1-Ser^{422} phosphorylation and that this complex was the elusive "PDK2" (Hong *et al.*, 2008). However a more recent study has demonstrated that rapamycin had no effect on SGK1-Ser^{422} phosphorylation (García-Martínez and Alessi, 2008). Furthermore these authors conclude that the results from Hong *et al*. were due to a commerical SGK1 antibody recognising phosphorylated bands of S6K since these two kinases share similar hydrophobic motifs (García-Martínez and Alessi, 2008, Lu *et al.*, 2010). Therefore the data from the present study demonstrate that rapamycin does not inhibit SGK1 activity and mTORC1 is not the kinase responsible for hydrophobic domain phosphorylation in SGK1, confirming the work of García-Martínez and Alessi. Rapamycin did however inhibit mTORC1 activity as shown by complete loss of phosphorylated P70-S6K-Thr^{389}, a downstream substrate of mTORC1 and this is consistent with previous findings that rapamycin is a selective inhibitor of this complex (García-Martínez and Alessi, 2008, Lu *et al.*, 2010).

Altogether, these data provide a somewhat confusing result. Whilst the natriferic response to insulin is dependent on mTORC2 and not mTORC1, the natriferc response to dexamethasone appears to be dependent on mTORC1, since mTOR and mTORC1 inhibition substantially reduces dexamethasone-induced I_{eq}. A role for mTORC2 cannot be completely ruled out and perhaps both complexes are required for the full response to dexamethasone. Since mTORC2 activity does not appear to be increased in response to dexamethasone, with no alteration seen in Akt-Ser^{473} phosphorylation, it does not seem likely that this kinase is involved in a pathway leading to increased Na^+ transport. With perhaps an increase in the abundance of SGK1 explaining the increase in SGK1 activity, the dexamethasone-mediated stimulation of Na^+ transport appears to be occurring outwith the signalling model used to explain the natriferic effect of insulin. Furthermore, the inhibition of the current with rapamycin suggests a role for S6 kinase in mediating this response although this kinase has not previously been linked with ENaC activity. Edinger and colleagues demonstrated that rapamycin prevented the activated-GR translocating into the nucleus (Edinger *et al.*, 2002). Studies of fetal distal lung epithelial FDLE cells revealed that basal amiloride-sensitive currents were sensitive to rapamycin (Otulakowski *et al.*, 2007). The authors postulated that the decreased currents were due to an inhibition of mTOR-dependent pathways leading to protein synthesis of transport proteins. These studies indicate that mTORC1-dependent protein synthesis is important in hormonally regulated Na^+ transport. Investigation into other signalling molecules upregulated by corticosteroids such as GILZ or KiRas2A which have been linked to ENaC activity would be of great interest to examine this hypothesis further.

6.3.3 The role of mTORC2 in AVP-stimulated Na^+ transport

The basolateral addition of AVP rapidly depolarised V_t but also significantly reduced R_t. Therefore an overall increase in I_{eq} was observed and this response was quite different to that elicited by either insulin (3.2.3) or dexamethasone (6.2.4). The addition of amiloride abolished V_t but had no significant effect on R_t giving an overall inhibition of I_{eq}. Since amiloride inhibits I_{eq} at the end of the experiment this suggests that there is a stimulation of ENaC-mediated Na^+ transport. The initial fall in R_t which is associated with depolarisation of V_t could suggest that there is an increase in Cl^- absorption but since there is no current left in the presence of amiloride and R_t remains unaltered, this seems unlikely. Previous studies have found in contrast with our findings, that AVP hyperpolarises V_t in isolated perfused rat cortical collecting ducts (Schafer and Troutman, 1990) and in the M1 collecting duct cell line (Nakhoul *et al.*, 1998) which is consistent with an increase in Na^+ absorption. In A6 cells application of vasotocin, analogous to mammalian vasopressin, produced a hyperpolarisation of V_t (Verrey, 1994). However when cells were pre-treated with aldosterone which produced a larger baseline V_t, the addition of vasotocin depolarised V_t with a concomitant increase in conductance indicating a fall in R_t and an overall increase in I_{eq}. This is similar to what was observed in the present study and it is of note that the average baseline V_t in these cells is ~ -45 mV is even larger than the than V_t recorded across the aldosterone-treated A6 cells.

Furthermore the study by Verrey highlights the differences in recording under short-circuit and open-circuit conditions. Under short-circuit conditions vasotocin

stimulated net Na^+ absorption and Cl^- secretion, however under open-circuit conditions this hormone stimulated net Na^+ and Cl^- absorption (Verrey, 1994). By short-circuiting V_t, the electrochemical gradient across the apical membrane will be altered and favour Cl^- secretion. Indeed several studies recording short circuit current from A6 cells and transimmortalized collecting duct cell lines have reported an increase in Cl^- secretion in response to AVP (Chalfant *et al.*, 1993, Duong Van Huyen *et al.*, 1998, Shane *et al.*, 2006). However, open-circuit conditions represents V_t under physiological conditions and it has been demonstrated that under these conditions AVP can increase net Cl^- absorption (Nagy *et al.*, 1994, Verrey, 1994, Duong Van Huyen *et al.*, 2001). Therefore further work would need to be carried to determine the role of Cl^- in the AVP response seen in mpkCCDcl4 cells.

The abolition of V_t by amiloride application suggests that AVP is stimulating Na^+ absorption which confirms findings in many previous studies (Nakhoul *et al.*, 1998, Butterworth *et al.*, 2005, Shane *et al.*, 2006). It is interesting however that R_t does not increase following addition of amiloride which is seen in control cells as well as in insulin- (3.2.4) and dexamethasone-treated cells (6.2.4). AVP also potently stimulates incorporation of aquaporins in collecting duct epithelia (Nielsen *et al.*, 2002), so perhaps insertion of these water channels could explain the low resistance and mask the effect of amiloride on ENaC. Another possible explanation is that AVP is altering the epithelial integrity by increasing tight junction permeability. Overall, AVP clearly stimulates I_{eq} in the mpkCCDc14 cell

line and since this is sensitive to amiloride it is associated with increased ENaC-mediated Na^+ absorption.

It is well-known that AVP acts via a cAMP / PKA pathway (Loffing and Korbmacher, 2009), however it was recently proposed that SGK1 is phosphorylated downstream of PKA which could then mediate effects on ENaC (Perrotti *et al.*, 2001, Thomas *et al.*, 2004, Vasquez *et al.*, 2008, Inglis *et al.*, 2009). To test the hypothesis that AVP could stimulate ENaC activity in an SGK1-dependent manner the mTOR inhibitors PP242 and TORIN1 were used as these drugs completely abolished SGK1 activity in previous experiments (6.2.1, 6.2.3). Neither inhibitor attenuated the response to AVP and this result clearly indicates that mTOR (including mTORC1 and mTORC2) and therefore SGK1 play no role in mediating a stimulation of I_{eq} by AVP. The present findings are in contrast with a study that linked AVP stimulation of ENaC with SGK1 signalling (Alvarez De La Rosa and Canessa, 2003). This study showed that inducing constitutively active SGK1 expression in A6 cells prevented any further potentiation of amiloride-sensitive current with the addition of AVP (Alvarez De La Rosa and Canessa, 2003). This suggested that AVP signalled via the same SGK1-dependent pathway to stimulate ENaC, however that lack of effect of AVP could due to maximal stimulation of ENaC. The same study showed that inducing expression of a kinase dead form of SGK1 did not prevent AVP from stimulating ENaC-mediated Na^+ transport thereby demonstrating this kinase was not necessary for the response (Alvarez De La Rosa and Canessa, 2003). Studies of H441 airway epithelial cells (Inglis *et al.*, 2009, Thomas *et al.*, 2004) and

submandibular gland cells (Vasquez *et al.*, 2008) have also shown that cAMP can stimulate ENaC activity and this is associated with an increase in SGK1 phosphorylation. However, it is important to note that the increase in current in all of these studies occured before the increase in SGK1 phosphorylation was observed. This suggests that SGK1 is not mediating the increase in ENaC-mediated Na^+ transport. Furthermore, the present data in a collecting duct cell line show that SGK1 activity is actually suppressed in response to AVP.

This finding is in sharp contrast with a study that showed that application of cAMP to COS-7 cells expressing recombinant SGK1 activated this kinase, measured using *in vitro* kinase assays (Perrotti *et al.*, 2001), suggesting that PKA can act upstream of SGK1. cAMP has been found to stimulate ENaC-mediated Na^+ transport in the H441 bronchiolar epithelial cell line in a PI3-kinase-, PKA- and MAPK-dependent manner as shown by using inhibitors of each kinase (Thomas *et al.*, 2004). Whilst this study found increased phosphorylation of SGK1, the increase in cAMP-mediated Na^+ transport preceded it indicating that cAMP does not signal via SGK1 to stimulate Na^+ transport in these cells (Thomas *et al.*, 2004). Another study has demonstrated that neither SGK1 activity nor expression is altered by cAMP (Shelly and Herrera, 2002). The present study suggests cAMP actually suppresses SGK1 activity. These inconsistent findings regarding SGK1 phosphorylation in response to cAMP could be due to different cell lines utilised. In the present study the addition of AVP stimulated PKA as demonstrated by an increase in the phosphorylation of CREB-Ser^{133}. This

confirms that AVP is signalling via cAMP and PKA and accords well with previous studies (Shelly and Herrera, 2002).

The findings from the present study indicate a lack of a role of SGK1, and it has been demonstrated that AVP exerts its effects on ENaC by binding V_2 receptors in the basolateral membrane and signalling via a cAMP-dependent pathway (Morris and Schafer, 2002, Butterworth *et al.*, 2005). Indeed it has been shown that the effects of vasopressin in the collecting duct can be mimicked using membrane permeable cAMP analogues including DBcAMP, phosphodiesterase inhibitors including IBMX as well as adenylate cyclase activators such as forskolin (Schafer and Troutman, 1990, Verrey, 1994). These contrasting results can be explained by a further study which revealed that similar to SGK1, PKA can phosphorylate residues on Nedd4-2 and therefore regulate ENaC-mediated Na^+ transport (Snyder *et al.*, 2004a). Therefore if AVP signals via cAMP and PKA to phosphorylate Nedd4-2, a constitutively active form of SGK1 could saturate Nedd4-2 phosphorylation and AVP would not be able to further potentiate the response. Similarly AVP could still evoke a response with expression of kinase dead SGK1 by phosphorylating Nedd4-2 and thereby decreasing ENaC ubiquitilation and internalisation. Nedd4-2 therefore marks a converging pathway between SGK1 and PKA and their regulation of ENaC.

Chapter 7 – Conclusions and Future Work

7.1 Conclusions

Treatment of type II diabetes with the insulin-sensitizing drugs thiazolidinediones (TZDs) has been the subject of recent studies due to reports of side effects of fluid retention leading to oedema and congestive heart failure. These complications have resulted in treatment being withdrawn in patients, particularly those at risk of heart failure. Initial studies proposed that fluid retention was caused by abnormal stimulation of ENaC in the collecting duct (Guan *et al.*, 2005, Hong *et al.*, 2003). The experiments carried out in the present study, using a murine collecting duct cell line, found no alteration to either basal or insulin-stimulated Na^+ transport in the presence of either the TZDs pioglitazone or rosiglitazone. These data therefore do not support the hypothesis that TZDs alter ENaC activity in the collecting duct and this is consistent with a study examining the effects of these drugs on ENaC-mediated transport in three kidney cell lines (Nofziger *et al.*, 2005). The present data furthermore unequivocally demonstrate that SGK1 activity is not increased in response to TZD-treatment, previously reported as a signalling molecule involved in increasing ENaC activity (Hong *et al.*, 2003).

One of the most interesting results to come from the work involved in this thesis was the evidence that spontaneous Na^+ absorption in this cell line occurred in a PI3-kinase-, mTORC2- and SGK1-independent manner. Selectively inhibiting each kinase left ~80 % of the basal I_{eq} intact and this data is in sharp contrast to previous studies. Inhibition of PI3-kinase using LY294002 and wortmannin was shown to inhibit basal currents in A6 cells (Păunescu *et al.*, 2000, Record *et al.*, 1998, Wang *et al.*, 2001) and mpkCCDcl4 cells (Staruschenko *et al.*, 2007). The

data from the present study utilised three different inhibitors of PI3-kinase and whilst each fully inhibited downstream kinase activity it was clear wortmannin had a substantial effect on basal I_{eq} that the others did not. These findings strongly suggest that wortmannin is inhibiting basal currents due to off-target inhibition consistent with previous findings with wortmannin as well as LY-294002 as discussed earlier (4.3.1).

The proposed role of SGK1 in maintaining spontaneous Na^+ absorption came from studies in A6 and M1 cells overexpressing a kinase-dead mutant of SGK1 which completely abolished basal Na^+ transport (Faletti *et al.*, 2002, Helms *et al.*, 2003). In the present study, cells exposed to a novel inhibitor of SGK1, GSK650394A, showed only a modest decrease in basal I_{eq}. This inhibitor however completely abolished phosphorylation of a downstream substrate indicating that these cells could spontaneously absorb Na^+ without SGK1 activity. The results in this thesis also provide evidence for the first time that mTORC2 does not play a major role in the maintenance of the basal current. This is consistent with mTORC2 lying downstream of PI3-kinase and upstream of SGK1, both of which were demonstrated to not be major contributors of the basal current. The use of the mTOR inhibitors PP242 and TORIN1 in conjunction with rapamycin, the specific inhibitor of mTORC1, allowed a novel means to target mTORC2 in a native system.

Unlike the spontaneous Na^+ absorption recorded from this cell line, insulin-stimulated Na^+ transport was found to be PI3-kinase-, mTORC2- and SGK1-

dependent. Inhibiting PI3-kinase completely abolished the response and this is consistent with previous studies that also used chemical agents to block this pathway (Blazer-Yost *et al.*, 2003, Record *et al.*, 1998, Staruschenko *et al.*, 2007). Similar to previous work was the finding that SGK1 was required for the natriferic effect of insulin. Studies where A6 cells expressed wild-type or constitutively active SGK1 showed increased rates of Na^+ transport that could not further be potentiated with exposure to insulin, indicating a similar pathway (Faletti *et al.*, 2002, Alvarez De La Rosa and Canessa, 2003, Arteaga and Canessa, 2005). Similarly in studies where SGK1 expression was silenced insulin could not stimulate ENaC-mediated Na^+ transport (Lee *et al.*, 2007). The data from the experiments carried out in this project confirm these findings using a novel drug to inhibit SGK1 in a mammalian collecting duct cell line. The role that Akt plays in mediating insulin-stimulated Na^+ transport from cannot be excluded and remains uncertain. The present study shows that Akt remains active when cells are exposed to GSK650394A and therefore establishes that Akt is not sufficient to maintain the response to insulin. It can be concluded that Akti-1/2 is not a selective inhibitor of Akt as it inhibits SGK1 activity as monitored by phosphorylation of NDRG1. This highlights the importance of confirming the specificity of inhibitors employed in experiments, particularly in a native cell line. A novel finding from the work carried out during this thesis was the demonstration that insulin-stimulated Na^+ transport is mTORC2-dependent. Whilst SGK1 has been shown to play an important role in this response and mTORC2 has recently been shown to be crucial for SGK1 activity (García-Martínez and Alessi, 2008), the importance of mTORC2 in Na^+ transport had not

previously been demonstrated. The data presented in this thesis shows that mTORC2 plays a vital role in mediating insulin-stimulated Na^+ absorption. Whilst a paper that has just been published investigates the role of mTORC2 in mediating hormonally-stimulated Na^+ transport, this study looks at the additive effect of insulin and aldosterone (Lu *et al.*, 2010). Whilst this newly-published study shows that aldosterone and insulin require mTORC2 activity, it does not separate these responses and our data clearly show that mTORC2 is required for the natiferic effect of insulin. Since insulin and aldosterone display an additive effect on Na^+ transport, this suggests that they are using different mechanisms to do so; therefore more than one signalling pathway may be involved.

Dexamethasone stimulated Na^+ absorption in these cells in a similar manner to insulin but over a longer time period; the response was apparent after an hour. This finding is consistent with other studies that found that dexamethasone stimulated Na^+ transport (Wang *et al.*, 2001). This response could be blocked by the novel mTOR inhibitors PP242 and TORIN1 but interestingly also with rapamycin, a specific inhibitor of mTORC1. These results were unexpected as dexamethasone has previously been shown to increase the abundance of SGK1 in a similar manner to aldosterone (Wang *et al.*, 2001, Robert-Nicoud *et al.*, 2001). Therefore it was anticipated that mTORC2, a crucial component of the SGK1 pathway, would play an important role in this response. The results from the present study indicate that the natriferic response to dexamethasone is in fact largely mTORC1-dependent. This has previously been reported in A6 cells but was dependent on much longer exposure to rapamycin (Rokaw *et al.*, 1996b).

Another study has shown that rapamycin can inhibit basal amiloride-sensitive currents in fetal airway epithelial cells (Otulakowski *et al.*, 2007). However in the present study, rapamycin has no effect on the basal current, therefore the acute mTORC1-dependence of the dexamethasone-stimulated current appears to be a novel finding. Of even greater interest is that whilst rapamycin can inhibit this natriferic response, SGK1 activity remains unaltered suggesting that activation of SGK1 does not provide a sufficient stimulus to explain the response. Our data indicate that SGK1 activity is increased in response to dexamethasone, but since mTORC2 activity is not increased it seems that instead of stimulating the PI3-kinase / mTORC2 / SGK1 pathway, the increased abundance of SGK1 is feeding into an already active pathway. Since the current can be blocked with full SGK1 activity, this suggests SGK1 is not a key component of this response.

Vasopressin stimulated I_{eq} in these cells in a different manner to both insulin and dexamethasone by causing a large fall in R_t and an associated depolarisation of V_t. This response is unusual as an increase in Na^+ absorption would give rise to a hyperpolarisation of V_t and the opposite is observed. The fall in R_t suggests that the paracellular pathway may be increased due to increased tight junction permeability. However, I_{eq} can still be blocked with amiloride consistent with an increase in ENaC-mediated Na^+ absorption. The stimulated I_{eq} was unaffected by both PP242 and TORIN, a novel finding, indicating that this response is independent of both mTORC1 and mTORC2. Vasopressin stimulates PKA as demonstrated by an increase in phosphorylation of a downstream substrate and this is consistent with a number of studies (Shelly and Herrera, 2002, Hallows *et*

al., 2009). Another interesting finding from the present study is that vasopressin suppresses SGK1 activity and this is in sharp contrast to a study that showed SGK1 phosphorylation was increased in response to this hormone (Perrotti *et al.*, 2001). Furthermore, since SGK1 activity is abolished in the presence of both PP242 and TORIN1, SGK1 must play no role in the vasopressin-stimulated I_{eq} and that this hormone stimulates a completely different signalling pathway to increase ENaC activity.

7.2 Future work

Whilst the work carried out for this thesis has identified crucial steps in the insulin signalling pathway: PI3-kinase, mTORC2 and SGK1; the final effector that mediates changes in ENaC activity was not studied. Many groups have focussed their work on the ubiquitin ligase Nedd4-2 and have provided convincing data that phosphorylation by SGK1 prevents Nedd4-2 interacting with ENaC (Debonneville *et al.*, 2001). With less ENaCs being targeted for internalisation and degradation there will be an associated increase in Na^+ transport. This has been demonstrated in oocyte expression studies as well as renal cell lines where overexpression of Nedd4-2 reduces ENaC-mediated currents and silencing expression increases them (Goulet *et al.*, 1998, Lee *et al.*, 2007, Kamynina *et al.*, 2001a). Studying the role of Nedd4-2 in the murine collecting duct cell line utilized in the present study would provide conclusions to the signalling pathway investigated thus far. There are no specific inhibitors of this ubiquitin ligase

therefore a knockdown of Nedd4-2 would provide an insight into its role in hormonally regulated ENaC activity.

Due to the lack of selectivity exerted by Akti-1/2 the question of the role that Akt plays in mediating insulin-stimulated Na^+ transport remains unanswered. The simplest action would be to identify another Akt inhibitor, confirm specificity and then look at effects on insulin-stimulated Na^+ transport. Alternatively, silencing Akt would provide a means to investigate the relative importance of this kinase in a mammalian collecting duct cell line. Another interesting interpretation of the data described here is that rather than Akti-1/2 being non-specific, there could be a direct interaction between Akt and SGK1. Immunoprecipitation studies could reveal whether Akt can physically bind SGK1.

The interesting results from dexamethasone-stimulated cells opened up many questions. Firstly, how much of a role does SGK1 play in mediating dexamethasone-stimulated Na^+ transport in the collecting duct? It seems unusual that this hormone would stimulate increased expression of SGK1 but the natriferic response can be inhibited without altering activity of this kinase. It would be prudent to confirm that SGK1 abundance is in fact increased in this cell line by measuring SGK1 transcripts. Experiments examining the effects of GSK650394A on dexamethasone-stimulated Na^+ transport should also give answers to the importance of SGK1 in this response. Perhaps SGK1 is exerting effects on other transport proteins such as the Na^+ / K^+ ATPase, inhibitor studies could confirm this. It would also be interesting to verify the role of PI3-kinase in this response

using the more novel and specific inhibitor GDC0941. Another important question from the dexamethasone studies is whether this relates to aldosterone signalling. Whilst the present study provides information on GR-mediated Na^+ absorption, which is relevant in hypertensive conditions such as Apparent Mineralocorticoid Excess syndrome, it cannot give information regarding the action of aldosterone. Since this mineralocorticoid plays a vital role in mediating Na^+ transport in the distal nephron it would seem prudent to repeat these experiments in an aldosterone-sensitive collecting duct cell line. It would be of great interest whether aldosterone-stimulated Na^+ transport is mTORC1-dependent as this is largely an unexplored area of ENaC signalling. Could it be that by blocking mTORC1 and the downstream S6kinase, synthesis of protein molecules other than SGK1 are being blocked which make a much larger contribution to ENaC-mediated transport? In this respect further work into the roles of GILZ would be of interest as this protein inhibits the ERK pathway (Soundararajan *et al.*, 2005) which could account for a non-PI3-kinase-dependent action.

Finally, the unusual response to AVP prompted many questions. The odd fall in R_t and depolarisation of V_t seemed at odds with a stimulation of ENaC-mediated Na^+ transport. It would be interesting to look at the response in the presence of amiloride or Cl^- channel blockers such as NPBB. Furthermore it would certainly be of interest to investigate the response of AVP under short circuit conditions and compare with recordings under open circuit conditions. The V_t generated by these cells is very large, -45mV, therefore clamping the voltage to 0mV would

alter the electrochemical gradients. Any differences noted between the two recording conditions would certainly be useful for planning future experiments. The scope of the short-term experiments carried out in this thesis was to investigate the effects of PP242 and TORIN1. Indeed it could be concluded that AVP does not signal via an mTORC1/2 pathway and that SGK1 is not involved. Further confirmation for the lack of SGK1 involvement could be obtained by using GSK650394A but the present data appears unequivocal. Since PKA has been reported to also phosphorylate Nedd4-2 in a similar manner to SGK1, it would be interesting to target the ubiquitin ligase with respect to AVP.

7.3 Concluding remarks

The data presented in this thesis provides evidence that spontaneous Na^+ absorption in a renal collecting duct cell line is largely a PI3-kinase-, mTORC2-, and SGK1-independent response. Insulin-stimulated Na^+ transport conversely occurs in a manner absolutely dependent on these signalling molecules. Both pioglitazone and rosiglitazone do not alter basal or insulin-stimulated Na^+ transport nor SGK1 activity and the side effects brought about by these drugs cannot be attributed to alterations to ENaC activity. Dexamethasone-stimulated Na^+ transport was mTORC1-dependent but SGK1-independent. Vasopressin-stimulated Na^+ transport was mTORC1-, mTORC2- and therefore SGK1-independent. This hormone did stimulate PKA which could therefore interact with Nedd4-2. All results from the work carried out in this thesis have stimulated further questions needing answered. The methods utilised in these studies where

the effects of novel inhibitors on both biophysical properties and protein phosphorylation in a mammalian collecting duct cell line were examined are of great potential in future studies.

Chapter 8 - Appendix

Table 8.1 Electrical parameters from control and Akti-1/2-treated cells.

Mean values ± S.E.M. of I_{eq}, V_t and R_t recorded from control and Akti-1/2-treated cells. Each treatment has its own unstimulated and insulin-stimulated response. Values are calculated as a mean of 3 min: before vehicle / insulin was added and after 30 min exposure to vehicle / insulin.

		I_{eq}(μA cm^{-2})		V_t (mV)		R_t (kΩ cm^2)	
		Pre-vehicle / insulin	Post-vehicle / insulin	Pre-vehicle / insulin	Post-vehicle / insulin	Pre-vehicle / insulin	Post-vehicle / insulin
Control	Vehicle	-23.6 ± 2.1	-22.1 ± 2.4	-57.1 ± 2.7	-54.5 ± 3.7	2.5 ± 0.2	2.5 ± 0.2
	Insulin	-23.6 ± 2.1	-30.1 ± 3.0	-54.3 ± 2.7	-63.0 ± 1.4	2.4 ± 0.2	2.2 ± 0.2
1μM Akti-1/2	Vehicle	-18.9 ± 2.1	-17.8 ± 2.3	-47.0 ± 5.0	-46.8 ± 5.1	2.6 ± 0.3	2.7 ± 0.3
	Insulin	-19.0 ± 2.0	-23.3 ± 3.9	-51.1 ± 5.2	-55.6 ± 4.4	2.9 ± 0.2	2.8 ± 0.3
Control	Vehicle	-13.7 ± 1.1	-13.2 ± 1.1	-26.1 ± 2.4	-25.6 ± 2.2	1.9 ± 0.2	2.0 ± 0.2
	Insulin	-14.2 ± 1.4	-19.6 ± 1.8	-34.4 ± 3.1	-43.8 ± 3.8	2.5 ± 0.2	2.3 ± 0.2
3μM Akti-1/2	Vehicle	-14.6 ± 0.9	-13.5 ± 0.8	-37.7 ± 2.3	-36.6 ± 2.0	2.6 ± 0.1	2.7 ± 0.1
	Insulin	-13.1 ± 0.8	-15.6 ± 1.2	-33.5 ± 1.2	-39.0 ± 1.5	2.6 ± 0.2	2.5 ± 0.2
Control	Vehicle	-14.1 ± 3.2	-13.3 ± 2.8	-39.8 ± 5.9	-37.7 ± 5.2	3.1 ± 0.3	3.0 ± 0.3
	Insulin	-14.4 ± 3.8	-18.9 ± 4.1	-42.8 ± 7.0	-48.7 ± 6.3	3.2 ± 0.3	2.8 ± 0.3
10μM Akti-1/2	Vehicle	-11.3 ± 1.4	-10.3 ± 1.0	-37.8 ± 4.0	-32.4 ± 2.3	3.4 ± 0.2	3.2 ± 0.1
	Insulin	-10.6 ± 2.0	-10.4 ± 1.6	-32.9 ± 5.3	-31.9 ± 3.6	3.3 ± 0.4	3.3 ± 0.4

Table 8.2 Electrical parameters from control and GSK650394A-treated cells.

Mean values ± S.E.M. of I_{eq}, V_t and R_t recorded from control and GSK650394A-treated cells. Each treatment has its own unstimulated and insulin-stimulated response. Values are calculated as a mean of 3 min: before vehicle / insulin was added and after 30 min exposure to vehicle / insulin.

		I_{eq}(μA cm^{-2})		V_t (mV)		R_t (kΩ cm^2)	
		Pre-vehicle / insulin	Post-vehicle / insulin	Pre-vehicle / insulin	Post-vehicle / insulin	Pre-vehicle / insulin	Post-vehicle / insulin
Control	Vehicle	-12.0 ± 2.1	-11.3 ± 1.9	-38.7 ± 5.5	-37.7 ± 5.0	3.3 ± 0.2	3.4 ± 0.2
	Insulin	-13.7 ± 1.9	-18.8 ± 2.2	-34.7 ± 6.2	-44.6 ± 5.4	2.5 ± 0.2	2.4 ± 0.1
1μM GSK650394A	Vehicle	-12.6 ± 2.1	-10.9 ±2.2	-33.6 ± 3.8	-32.1 ± 3.5	2.9 ± 0.4	3.2 ± 0.5
	Insulin	-11.6 ± 2.7	-13.2 ± 2.9	-32.0 ± 5.8	-30.9 ± 4.4	3.0 ± 0.4	2.7 ± 0.6
Control	Vehicle	-16.5 ± 2.8	-16.0 ± 2.5	-41.9 ± 3.9	-41.2 ± 4.9	2.7 ± 0.3	2.7 ± 0.2
	Insulin	-16.4 ± 3.6	-21.9 ± 3.4	-38.8 ± 4.6	-49.4 ± 3.7	2.6 ± 0.3	2.3 ± 0.2
3μM GSK650394A	Vehicle	-20.9 ± 3.3	-18.9 ± 2.9	-35.7 ± 5.1	-33.7 ± 5.1	1.8 ± 0.2	1.9 ± 0.3
	Insulin	-17.4 ± 2.8	-18.0 ± 2.3	-31.1 ± 3.5	-24.7 ± 7.1	2.0 ± 0.4	1.5 ± 0.5
Control	Vehicle	-16.4 ± 3.1	-14.4 ± 2.5	-33.8 ± 4.4	-31.4 ± 4.4	2.2 ± 0.3	2.3 ± 0.2
	Insulin	-17.7 ± 2.7	-24.3 ± 4.0	-43.7 ± 3.8	-50.3 ± 4.4	2.6 ± 0.3	2.2 ± 0.3
10μM GSK650394A	Vehicle	-15.4 ± 3.9	-13.6 ± 3.1	-17.6 ± 4.4	-18.5 ± 4.3	1.2 ± 0.2	1.4 ± 0.2
	Insulin	-13.9 ± 3.5	-12.5 ± 2.9	-17.8 ± 4.9	-18.1 ± 4.9	1.4 ± 0.3	1.5 ± 0.3

Table 8.3 Electrical parameters from unstimulated control and TORIN1-treated cells.

Mean values ± S.E.M. of I_{eq}, V_t and R_t recorded from control and TORIN1-treated cells. Values are calculated as a mean of 3 min: before vehicle / TORIN1 was added and after 60 min exposure to vehicle / TORIN1.

Treatment	I_{eq}(μA cm^{-2})		V_t (mV)		R_t (kΩ cm^2)	
	Baseline	60 min exposure	Baseline	60 min exposure	Baseline	60 min exposure
Vehicle	-18.3 ± 1.3	-15.8 ± 1.1	-47.8 ± 3.0	-41.1 ± 2.7	2.4 ± 0.1	2.5 ± 0.1
TORIN1	-16.8 ± 1.1	-12.9 ± 0.8	-39.8 ± 3.2	-32.1 ± 2.5	2.2 ± 0.2	2.5 ± 0.1
Vehicle	-24.0 ± 1.6	-19.9 ± 1.3	-57.2 ± 2.5	-49.2 ± 1.5	2.3 ± 0.1	2.4 ± 0.1
PP242	-23.4 ± 2.0	-14.3 ± 1.0	-53.8 ± 2.3	-37.6 ± 1.4	2.5 ± 0.2	2.8 ± 0.3

Table 8.4 Electrical parameters from insulin-stimulated TORIN1- and PP242-treated cells

Mean values ± S.E.M. of I_{eq}, V_t and R_t recorded from control and inhibitor-treated cells (n = 5 for each compound). Each treatment has its own unstimulated and insulin-stimulated response. Values are calculated as a mean of 3 min: before vehicle / insulin was added and after 30 min exposure to vehicle / insulin.

		I_{eq}(μA cm^{-2})		V_t (mV)		R_t (kΩ cm^2)	
		Pre-vehicle / insulin	Post-vehicle / insulin	Pre-vehicle / insulin	Post-vehicle / insulin	Pre-vehicle / insulin	Post-vehicle / insulin
Control	Vehicle	-14.4 ± 1.9	-13.1 ± 1.7	-45.9 ± 2.2	-35.6 ± 3.1	2.8 ± 0.1	2.9 ± 0.1
	Insulin	-17.0 ± 2.0	-22.6 ± 2.6	-39.9 ± 5.7	-43.6 ± 7.0	2.5 ± 0.2	2.5 ± 0.2
100nM TORIN1	Vehicle	-13.6 ± 1.2	-11.8 ± 1.2	-38.4 ± 6.3	-29.1 ± 4.7	2.3 ± 0.3	2.4 ± 0.3
	Insulin	-14.6 ± 1.4	-14.4 ± 1.6	-39.4 ± 5.4	-40.8 ± 5.5	2.7 ± 0.2	2.8 ± 0.2
Control	Vehicle	-17.5 ± 1.0	-15.8 ± 0.9	-50.2 ± 2.2	-47.2 ± 2.1	2.9 ± 0.1	3.0 ± 0.1
	Insulin	-20.1 ± 1.6	-25.2 ± 1.8	-50.5 ± 4.5	-55.9 ± 3.9	2.5 ± 0.1	2.2 ± 0.1
1μM PP242	Vehicle	-13.9 ± 1.1	-11.9 ± 1.0	-41.4 ± 1.6	-36.4 ± 1.9	3.1 ± 0.1	3.1 ± 0.3
	Insulin	-15.7 ± 1.3	-14.9 ± 1.3	-48.0 ± 2.4	-46.6 ± 2.7	3.1 ± 0.1	3.2 ± 0.1

Table 8.5 Electrical parameters from dexamethasone-stimulated TORIN1-, PP242- and rapamycin-treated cells

Mean values ± S.E.M. of I_{eq}, V_t and R_t recorded from control and inhibitor-treated cells. Each treatment has its own unstimulated and dexamethasone -stimulated response. Values are calculated as a mean of 3 min: before vehicle / dexamethasone was added and after 2.5 h exposure to vehicle / dexamethasone.

		I_{eq}(μA cm^{-2})		V_t (mV)		R_t (kΩ cm^2)	
		Pre-vehicle / dexamethasone	Post-vehicle / dexamethasone	Pre-vehicle / dexamethasone	Post-vehicle / dexamethasone	Pre-vehicle / dexamethasone	Post-vehicle / dexamethasone
Control (n = 5)	Vehicle	-20.7 ± 1.7	-17.6 ± 1.2	-51.7 ± 5.0	-51.9 ± 1.9	2.5 ± 0.2	3.0 ± 0.2
	Dexamethasone	-22.0 ± 2.8	-32.8 ± 4.1	-47.2 ± 7.3	-60.9 ± 6.9	2.2 ± 0.3	1.9 ± 0.2
100 nM TORIN1	Vehicle	-15.9 ± 1.8	-9.7 ± 0.8	-40.9 ± 3.1	-36.0 ± 2.9	2.6 ± 0.2	3.7 ± 0.2
	Dexamethasone	-18.9 ± 2.2	-14.3 ± 1.8	-43.2 ± 6.3	-44.4 ± 6.6	2.3 ± 0.1	3.1 ± 0.2
Control (n = 5)	Vehicle	-20.8 ± 1.0	-16.6 ± 0.9	-51.2 ± 4.5	-49.8 ± 2.1	2.4 ± 0.1	3.0 ± 0.1
	Dexamethasone	-20.8 ± 1.5	-32.9 ± 2.2	-50.1 ± 5.7	-66.3 ± 4.4	2.4 ± 0.2	2.0 ± 0.1
1 μM PP242	Vehicle	-14.0 ± 1.0	-8.4 ±0.7	-40.6 ± 1.0	-32.8 ± 1.7	3.0 ± 0.2	4.0 ± 0.4
	Dexamethasone	-14.7 ± 1.4	-10.1 ± 1.2	-37.6 ± 6.1	-36.2 ± 5.2	2.5 ± 0.3	3.6 ± 0.3
Control (n = 3)	Vehicle	-18.7 ± 0.2	-14.1 ± 0.1	-54.5 ± 1.5	-50.9 ± 0.6	2.9 ± 0.1	3.6 ± 0.1
	Dexamethasone	-19.2 ± 1.7	-30.8 ± 4.1	-41.1 ± 9.8	-60.9 ± 9.9	2.1 ± 0.5	2.0 ± 0.2
100 nM rapamycin	Vehicle	-14.9 ± 1.0	-9.1 ± 0.8	-37.9 ± 5.4	-34.3 ± 3.4	2.6 ± 0.5	3.9 ± 0.7
	Dexamethasone	-15.4 ± 1.9	-12.3 ± 2.2	-44.9 ± 3.4	-47.1 ± 4.5	3.0 ± 0.2	4.0 ± 0.4

Table 8.6 Electrical parameters from AVP-stimulated TORIN1- and PP242-treated cells

Mean values ± S.E.M. of I_{eq}, V_t and R_t recorded from control and inhibitor-treated cells. Each treatment has its own unstimulated and AVP-stimulated response. Values are calculated as a mean of 3 min: before vehicle / AVP was added and after 30 min exposure to vehicle / AVP.

		I_{eq}(μA cm^{-2})		V_t (mV)		R_t (kΩ cm^2)	
		Pre-vehicle / AVP	Post-vehicle / AVP	Pre-vehicle / AVP	Post-vehicle / AVP	Pre-vehicle / AVP	Post-vehicle / AVP
Control (n = 5)	Vehicle	-15.8 ± 0.6	-14.7 ± 0.5	-38.1 ± 4.2	-36.9 ± 3.7	2.4 ± 0.2	2.5 ± 0.2
	AVP	-13.1 ± 1.0	-23.9 ± 1.7	-30.9 ± 2.8	-17.1 ± 3.0	2.4 ± 0.1	0.7 ± 0.1
100 nM TORIN1	Vehicle	-12.8 ± 1.5	-12.0 ± 1.4	-28.4 ± 4.3	-27.1 ± 3.7	2.2 ±0.3	2.3 ± 0.3
	AVP	-13.3 ± 2.0	-23.2 ± 1.9	-29.5 ± 3.6	-12.5 ± 2.1	2.3 ± 0.2	0.6 ± 0.1
Control (n = 4)	Vehicle	-27.5 ± 2.5	-24.4 ± 2.5	-54.9 ± 2.1	-51.2 ± 2.1	2.1 ± 0.2	2.2 ± 0.1
	AVP	-30.3 ± 1.4	-46.9 ± 2.7	-54.2 ± 3.0	-33.4 ± 5.6	1.8 ± 0.2	0.7 ± 0.1
1 μM PP242	Vehicle	-20.8 ± 1.8	-18.1 ± 1.6	-44.0 ± 3.1	-37.6 ± 3.6	2.2 ± 0.2	2.1 ± 0.2
	AVP	-22.4 ± 1.6	-40.8 ± 4.2	-46.8 ± 5.2	-36.8 ± 5.4	2.1 ± 0.1	0.9 ± 0.1

References

ALESSI, D. R., ANDJELKOVIC, M., CAUDWELL, B., CRON, P., MORRICE, N., COHEN, P. & HEMMINGS, B. A. (1996) Mechanism of activation of protein kinase B by insulin and IGF-1. *EMBO Journal,* 15**,** 6541-6551.

ALVAREZ DE LA ROSA, D. & CANESSA, C. M. (2003) Role of SGK in hormonal regulation of epithelial sodium channel in A6 cells. *American Journal of Physiology - Cell Physiology,* 284**,** C404-C414.

ALVAREZ DE LA ROSA, D. A., LI, H. & CANESSA, C. M. (2002) Effects of aldosterone on biosynthesis, traffic, and functional expression of epithelial sodium channels in A6 cells. *Journal of General Physiology,* 119**,** 427-442.

ANANTHARAM, A. & PALMER, L. G. (2007) Determination of epithelial Na^+ channel subunit stoichiometry from single-channel conductances. *Journal of General Physiology,* 130**,** 55-70.

ARTEAGA, M. F. & CANESSA, C. M. (2005) Functional specificity of Sgk1 and Akt1 on ENaC activity. *American Journal of Physiology - Renal Physiology,* 289**,** F90-F96.

ARTUNC, F., SANDULACHE, D., NASIR, O., BOINI, K. M., FRIEDRICH, B., BEIER, N., DICKS, E., PÖTZSCH, S., KLINGEL, K., AMANN, K., BLAZER-YOST, B. L., SCHOLZ, W., RISLER, T., KUHL, D. & LANG, F. (2008) Lack of the serum and glucocorticoid-inducible kinase SGK1 attenuates the volume retention after treatment with the PPARγ agonist pioglitazone. *Pflugers Archiv European Journal of Physiology,* 456**,** 425-436.

ATCHLEY, D. W., LOEB, R. F., RICHARDS, D. W., BENEDICT, E. M. & DRISCOLL, M. E. (1933) ON DIABETIC ACIDOSIS A Detailed Study of Electrolyte Balances Following the Withdrawal and Reestablishment of Insulin Therapy. *The Journal of Clinical Investigation,* 12**,** 297-326.

AWAYDA, M. S. (1999) Regulation of the epithelial Na+ channel by intracellular Na+. *American Journal of Physiology - Cell Physiology,* 277**,** C216-C224.

BACHHUBER, T., ALMACA, J., ALDEHNI, F., MEHTA, A., AMARAL, M. D. & SCHREIBER, R. (2008) Regulation of the epithelial Na^+ channel by the protein kinase CK2. *Journal of Biological Chemistry,* 283**,** 13225-13232.

BAIN, J., PLATER, L., ELLIOTT, M., SHPIRO, N., HASTIE, C. J., MCLAUCHLAN, H., KLEVERNIC, I., ARTHUR, J. S. C., ALESSI, D. R. & COHEN, P. (2007) The selectivity of protein kinase inhibitors: A further update. *Biochemical Journal,* 408**,** 297-315.

BARKER, P. M., NGUYEN, M. S., GATZY, J. T., GRUBB, B., NORMAN, H., HUMMLER, E., ROSSIER, B., BOUCHER, R. C. & KOLLER, B. (1998) Role of γENaC subunit in lung liquid clearance and electrolyte balance in newborn mice: Insights into perinatal adaptation and pseudohypoaldosteronism. *Journal of Clinical Investigation,* 102**,** 1634-1640.

BARNETT, S. F., DEFEO-JONES, D., FU, S., HANCOCK, P. J., HASKELL, K. M., JONES, R. E., KAHANA, J. A., KRAL, A. M., LEANDER, K., LEE, L. L., MALINOWSKI, J., MCAVOY, E. M., NAHAS, D. D., ROBINSON, R. G. & HUBER, H. E. (2005) Identification and characterization of pleckstrin-homology-domain-dependent and isoenzyme-specific Akt inhibitors. *Biochemical Journal,* 385**,** 399-408.

BENS, M., VALLET, V., CLUZEAUD, F., PASCUAL-LETALLEC, L., KAHN, A., RAFESTIN-OBLIN, M. E., ROSSIER, B. C. & VANDEWALLE, A. (1999) Corticosteroid-dependent sodium transport in a novel immortalized mouse collecting duct principal cell line. *Journal of the American Society of Nephrology,* 10**,** 923-934.

BHALLA, V., DAIDIÉ, D., LI, H., PAO, A. C., LAGRANGE, L. P., WANG, J., VANDEWALLE, A., STOCKAND, J. D., STAUB, O. & PEARCE, D. (2005) Serum- and glucocorticoid-regulated kinase 1 regulates ubiquitin ligase neural precursor cell-expressed, developmentally down-regulated protein 4-2 by inducing interaction with 14-3-3. *Molecular Endocrinology,* 19**,** 3073-3084.

BHALLA, V. & HALLOWS, K. R. (2008) Mechanisms of ENaC regulation and clinical implications. *Journal of the American Society of Nephrology,* 19**,** 1845-1854.

BIONDI, R. M., KIELOCH, A., CURRIE, R. A., DEAK, M. & ALESSI, D. R. (2001) The PIF-binding pocket in PDK1 is essential for activation of S6K and SGK, but not PKB. *EMBO Journal,* 20**,** 4380-4390.

BLAZER-YOST, B. L., COX, M. & FURLANETTO, R. (1989) Insulin and IGF I receptor-mediated Na^+ transport in toad urinary bladders. *American Journal of Physiology - Cell Physiology,* 257.

BLAZER-YOST, B. L., ESTERMAN, M. A. & VLAHOS, C. J. (2003) Insulin-stimulated trafficking of ENaC in renal cells requires PI 3-kinase activity. *American Journal of Physiology - Cell Physiology,* 284**,** C1645-C1653.

BLAZER-YOST, B. L., LIU, X. & HELMAN, S. I. (1998) Hormonal regulation of eNaCs: Insulin and aldosterone. *American Journal of Physiology - Cell Physiology,* 274**,** C1373-C1379.

BLAZER-YOST, B. L. & NOFZIGER, C. (2005) The role of the phosphoinositide pathway in hormonal regulation of the epithelial sodium channel. *Advances in Experimental Medicine and Biology,* 559**,** 359-368.

BLAZER-YOST, B. L., PĂUNESCU, T. G., HELMAN, S. I., LEE, K. D. & VLAHOS, C. J. (1999) Phosphoinositide 3-kinase is required for aldosterone-regulated sodium reabsorption. *American Journal of Physiology - Cell Physiology,* 277**,** C531-C536.

BLAZER-YOST, B. L., SHAH, N., JARETT, L., COX, M. & SMITH, R. M. (1992) Insulin and IGF1 receptors in a model renal epithelium: Receptor localization and characterization. *Biochemistry International,* 28**,** 143-153.

BLAZER-YOST, B. L., VAHLE, J. C., BYARS, J. M. & BACALLAO, R. L. (2004) Real-time three-dimensional imaging of lipid signal transduction: Apical membrane insertion of epithelial Na^+ channels. *American Journal of Physiology - Cell Physiology,* 287**,** C1569-C1576.

BOOTH, R. E., JOHNSON, J. P. & STOCKAND, J. D. (2002) Aldosterone. *American Journal of Physiology - Advances in Physiology Education,* 26**,** 8-20.

BOOTH, R. E. & STOCKAND, J. D. (2003a) Targeted degradation of ENaC in response to PKC activation of the ERK1/2 cascade. *American Journal of Physiology - Renal Physiology,* 284**,** F938-947.

BOOTH, R. E. & STOCKAND, J. D. (2003b) Targeted degradation of ENaC in response to PKC activation of the ERK1/2 cascade. *American Journal of Physiology - Renal Physiology,* 284**,** F938-F947.

BORON, W. F. & BOULPAEP, E. L. (2009a) Chapter 51. The Endocrine Pancreas, *Medical Physiology: A Cellular and Molecular Approach,* 2nd Edition, 1074-1083, Saunders Elsevier, Philadelphia.

BORON, W. F. & BOULPAEP, E. L. (2009b) Chapter 33. Organisation of the Urinary System, *Medical Physiology: A Cellular and Molecular Approach,* 2nd Edition, 749-756, Saunders Elsevier, Philadelphia.

BORON, W. F. & BOULPAEP, E. L. (2009c) Chapter 35. Transport of Sodium and Chloride, *Medical Physiology: A Cellular and Molecular Approach,* 2nd Edition, 782-796, Saunders Elsevier, Philadelphia.

BORON, W. F. & BOULPAEP, E. L. (2009d) Chapter 38. Urine Concentration and Dilution, *Medical Physiology: A Cellular and Molecular Approach,* 2nd Edition, 846-849, Saunders Elsevier, Philadelphia.

BOYD, C. & NÁRAY-FEJES-TÓTH, A. (2005) Gene regulation of ENaC subunits by serum- and glucocorticoid-inducible kinase-1. *American Journal of Physiology - Renal Physiology,* 288**,** F505-F512.

BROWN, S. G., GALLACHER, M., OLVER, R. E. & WILSON, S. M. (2008) The regulation of selective and nonselective Na^+ conductances in H441 human airway epithelial cells. *American Journal of Physiology - Lung Cellular and Molecular Physiology,* 294**,** L942-L954.

BRUNN, G. J., WILLIAMS, J., SABERS, C., WIEDERRECHT, G., LAWRENCE JR, J. C. & ABRAHAM, R. T. (1996) Direct inhibition of the signaling functions of the mammalian target of rapamycin by the phosphoinositide 3-kinase inhibitors, wortmannin and LY294002. *EMBO Journal,* 15**,** 5256-5267.

BUCKINGHAM, R. E. & HANNA, A. (2008) Thiazolidinedione insulin sensitizers and the heart: A tale of two organs? *Diabetes, Obesity and Metabolism,* 10**,** 312-328.

BUGAJ, V., POCHYNYUK, O., MIRONOVA, E., VANDEWALLE, A., MEDINA, J. L. & STOCKAND, J. D. (2008) Regulation of the epithelial Na^+ channel by endothelin-1 in rat collecting duct. *American Journal of Physiology - Renal Physiology,* 295**,** F1063-F1070.

BUGAJ, V., POCHYNYUK, O. & STOCKAND, J. D. (2009) Activation of the epithelial Na^+ channel in the collecting duct by vasopressin contributes to water reabsorption. *American Journal of Physiology - Renal Physiology,* 297**,** F1411-F1418.

BUTTERWORTH, M. B., EDINGER, R. S., FRIZZELL, R. A. & JOHNSON, J. P. (2009) Regulation of the epithelial sodium channel by membrane trafficking. *American Journal of Physiology - Renal Physiology,* 296**,** F10-F24.

BUTTERWORTH, M. B., EDINGER, R. S., JOHNSON, J. P. & FRIZZELL, R. A. (2005) Acute ENaC stimulation by cAMP in a kidney cell line is mediated by exocytic insertion from a recycling channel pool. *Journal of General Physiology,* 125**,** 81-101.

CANESSA, C. M., HORISBERGER, J. D. & ROSSIER, B. C. (1993) Epithelial sodium channel related to proteins involved in neurodegeneration. *Nature,* 361**,** 467-470.

CANESSA, C. M., SCHILD, L., BUELL, G., THORENS, B., GAUTSCHI, I., HORISBERGER, J. D. & ROSSIER, B. C. (1994) Amiloride-sensitive epithelial Na^+ channel is made of three homologous subunits. *Nature,* 367**,** 463-467.

CHALFANT, M. L., COUPAYE-GERARD, B. & KLEYMAN, T. R. (1993) Distinct regulation of Na^+ reabsorption and Cl^- secretion by arginine vasopressin in the amphibian cell line A6. *American Journal of Physiology - Cell Physiology,* 264**,** C1480-C1488.

CHANG, S. S., GRUNDER, S., HANUKOGLU, A., RÖSLER, A., MATHEW, P. M., HANUKOGLU, I., SCHILD, L., LU, Y., SHIMKETS, R. A., NELSON-WILLIAMS, C., ROSSIER, B. C. & LIFTON, R. P. (1996) Mutations in subunits of the epithelial sodium channel cause salt wasting with hyperkalaemic acidosis, pseudohypoaldosteronism type 1. *Nature Genetics,* 12**,** 248-253.

CHEN, L., YANG, B., MCNULTY, J. A., CLIFTON, L. G., BINZ, J. G., GRIMES, A. M., STRUM, J. C., HARRINGTON, W. W., CHEN, Z., BALON, T. W., STIMPSON, S. A. & BROWN, K. K. (2005) GI262570, a peroxisome proliferator-activated receptor γ agonist, changes electrolytes and water reabsorption from the distal nephron in rats. *Journal of Pharmacology and Experimental Therapeutics,* 312**,** 718-725.

CHEN, S. Y., BHARGAVA, A., MASTROBERARDINO, L., MEIJER, O. C., WANG, J., BUSE, P., FIRESTONE, G. L., VERREY, F. & PEARCE, D. (1999) Epithelial sodium channel regulated by aldosterone-induced protein sgk. *Proceedings of the National Academy of Sciences of the United States of America,* 96**,** 2514-2519.

CHEN, S. Y. U., WANG, J., LIU, W. & PEARCE, D. (1998) Aldosterone responsiveness of A6 cells is restored by cloned rat mineralocorticoid receptor. *American Journal of Physiology,* 274**,** C39-C46.

COX, M. & SINGER, I. (1977) Insulin mediated Na^+ transport in the toad urinary bladder. *American Journal of Physiology,* 232**,** F270-F277.

D'ADAMIO, F., ZOLLO, O., MORACA, R., AYROLDI, E., BRUSCOLI, S., BARTOLI, A., CANNARILE, L., MIGLIORATI, G. & RICCARDI, C. (1997) A new dexamethasone-induced gene of the leucine zipper family protects T lymphocytes from TCR/CD3-activated cell death. *Immunity,* 7**,** 803-812.

DAHLMANN, A., PRADERVAND, S., HUMMLER, E., ROSSIER, B. C., FRINDT, G. & PALMER, L. G. (2003) Mineralocorticoid regulation of epithelial Na^+ channels is maintained in a mouse model of Liddle's syndrome. *American Journal of Physiology - Renal Physiology,* 285**,** F310-F318.

DAVIES, S. P., REDDY, H., CAIVANO, M. & COHEN, P. (2000) Specificity and mechanism of action of some commonly used protein kinase inhibitors. *Biochemical Journal,* 351**,** 95-105.

DEBONNEVILLE, C., FLORES, S. Y., KAMYNINA, E., PLANT, P. J., TAUXE, C., THOMAS, M. A., MÜNSTER, C., CHRAÏBI, A., PRATT, J.

H., HORISBERGER, J. D., PEARCE, D., LOFFING, J. & STAUB, O. (2001) Phosphorylation of Nedd4-2 by Sgk1 regulates epithelial Na^+ channel cell surface expression. *EMBO Journal,* 20**,** 7052-7059.

DIAKOV, A., BERA, K., MOKRUSHINA, M., KRUEGER, B. & KORBMACHER, C. (2008) Cleavage in the γ-subunit of the epithelial sodium channel (ENaC) plays an important role in the proteolytic activation of near-silent channels. *Journal of Physiology,* 586**,** 4587-4608.

DIAKOV, A. & KORBMACHER, C. (2004) A novel pathway of epithelial sodium channel activation involves a serum- and glucocorticoid-inducible kinase consensus motif in the C terminus of the channel's α-subunit. *Journal of Biological Chemistry,* 279**,** 38134-38142.

DUONG VAN HUYEN, J. P., BENS, M., TEULON, J. & VANDEWALLE, A. (2001) Vasopressin-stimulated chloride transport in transimmortalized mouse cell lines derived from the distal convoluted tubule and cortical and inner medullary collecting ducts. *Nephrology Dialysis Transplantation,* 16**,** 238-245.

DUONG VAN HUYEN, J. P., BENS, M. & VANDEWALLE, A. (1998) Differential effects of aldosterone and vasopressin on chloride fluxes in transimmortalized mouse cortical collecting duct cells. *Journal of Membrane Biology,* 164**,** 79-90.

EDINGER, R. S., ROKAW, M. D. & JOHNSON, J. P. (1999) Vasopressin stimulates sodium transport in A6 cells via a phosphatidylinositide 3-kinase-dependent pathway. *American Journal of Physiology - Renal Physiology,* 277**,** F575-F579.

EDINGER, R. S., WATKINS, S. C., PEARCE, D. & JOHNSON, J. P. (2002) Effect of immunosuppressive agents on glucocorticoid receptor function in A6 cells. *American Journal of Physiology - Renal Physiology,* 283**,** F254-F261.

ESKANDARI, S., SNYDER, P. M., KREMAN, M., ZAMPIGHI, G. A., WELSH, M. J. & WRIGHT, E. M. (1999) Number of subunits comprising the epithelial sodium channel. *Journal of Biological Chemistry,* 274**,** 27281-27286.

FAKITSAS, P., ADAM, G., DAIDIÉ, D., VAN BEMMELEN, M. X., FOULADKOU, F., PATRIGNANI, A., WAGNER, U., WARTH, R., CAMARGO, S. M. R., STAUB, O. & VERREY, F. (2007) Early aldosterone-induced gene product regulates the epithelial sodium channel by deubiquitylation. *Journal of the American Society of Nephrology,* 18**,** 1084-1092.

FALETTI, C. J., PERROTTI, N., TAYLOR, S. I. & BLAZER-YOST, B. L. (2002) sgk: An essential convergence point for peptide and steroid hormone regulation of ENaC-mediated Na^+ transport. *American Journal of Physiology - Cell Physiology,* 282**,** C494-C500.

FAN, Q. W., KNIGHT, Z. A., GOLDENBERG, D. D., YU, W., MOSTOV, K. E., STOKOE, D., SHOKAT, K. M. & WEISS, W. A. (2006) A dual PI3 kinase/mTOR inhibitor reveals emergent efficacy in glioma. *Cancer Cell,* 9**,** 341-349.

FELDMAN, M. E., APSEL, B., UOTILA, A., LOEWITH, R., KNIGHT, Z. A., RUGGERO, D. & SHOKAT, K. M. (2009) Active-site inhibitors of

mTOR target rapamycin-resistant outputs of mTORC1 and mTORC2. *PLoS biology,* 7.

FIDELMAN, M. L., MAY, J. M., BIBER, T. U. & WATLINGTON, C. O. (1982) Insulin stimulation of Na^+ transport and glucose metabolism in cultured kidney cells. *The American journal of physiology,* 242**,** C121-C123.

FIRSOV, D., GAUTSCHI, I., MÉRILLAT, A. M., ROSSIER, B. C. & SCHILD, L. (1998) The heterotetrameric architecture of the epithelial sodium channel (ENaC). *EMBO Journal,* 17**,** 344-352.

FIRSOV, D., ROBERT-NICOUD, M., GRUENDER, S., SCHILD, L. & ROSSIER, B. C. (1999) Mutational analysis of cysteine-rich domains of the epithelium sodium channel (ENaC): Identification of cysteines essential for channel expression at the cell surface. *Journal of Biological Chemistry,* 274**,** 2743-2749.

FIRSOV, D., SCHILD, L., GAUTSCHI, I., MÉRILLAT, A. M., SCHNEEBERGER, E. & ROSSIER, B. C. (1996) Cell surface expression of the epithelial Na^+ channel and a mutant causing Liddle syndrome: A quantitative approach. *Proceedings of the National Academy of Sciences of the United States of America,* 93**,** 15370-15375.

FLORES, S. Y., DEBONNEVILLE, C. & STAUB, O. (2003) The role of Nedd4/Nedd4-like dependant ubiquitylation in epithelial transport processes. *Pflugers Archiv European Journal of Physiology,* 446**,** 334-338.

FLORES, S. Y., LOFFING-CUENI, D., KAMYNINA, E., DAIDIÉ, D., GERBEX, C., CHABANEL, S., DUDLER, J., LOFFING, J. & STAUB, O. (2005) Aldosterone-induced serum and glucocorticoid-induced kinase 1 expression is accompanied by Nedd4-2 phosphorylation and increased Na^+ transport in cortical collecting duct cells. *Journal of the American Society of Nephrology,* 16**,** 2279-2287.

FOLKES, A. J., AHMADI, K., ALDERTON, W. K., ALIX, S., BAKER, S. J., BOX, G., CHUCKOWREE, I. S., CLARKE, P. A., DEPLEDGE, P., ECCLES, S. A., FRIEDMAN, L. S., HAYES, A., HANCOX, T. C., KUGENDRADAS, A., LENSUN, L., MOORE, P., OLIVERO, A. G., PANG, J., PATEL, S., PERGL-WILSON, G. H., RAYNAUD, F. I., ROBSON, A., SAGHIR, N., SALPHATI, L., SOHAL, S., ULTSCH, M. H., VALENTI, M., WALLWEBER, H. J. A., NAN, C. W., WIESMANN, C., WORKMAN, P., ZHYVOLOUP, A., ZVELEBIL, M. J. & SHUTTLEWORTH, S. J. (2008) The identification of 2-(1H-indazol-4-yl)-6-(4-methanesulfonyl-piperazin-1- ylmethyl)-4-morpholin-4-yl-thieno[3,2-d]pyrimidine (GDC-0941) as a potent, selective, orally bioavailable inhibitor of class I PI3 kinase for the treatment of cancer. *Journal of Medicinal Chemistry,* 51**,** 5522-5532.

FRÖDIN, M., ANTAL, T. L., DÜMMLER, B. A., JENSEN, C. J., DEAK, M., GAMMELTOFT, S. & BIONDI, R. M. (2002) A phosphoserine/threonine-binding pocket in AGC kinases and PDK1 mediates activation by hydrophobic motif phosphorylation. *EMBO Journal,* 21**,** 5396-5407.

FUNDER, J. W., PEARCE, P. T., SMITH, R. & SMITH, A. I. (1988) Mineralocorticoid action: Target tissue specificity is enzyme, not receptor, mediated. *Science,* 242**,** 583-585.

GAEGGELER, H. P., GONZALEZ-RODRIGUEZ, E., JAEGER, N. F., LOFFING-CUENI, D., NORREGAARD, R., LOFFING, J., HORISBERGER, J. D. & ROSSIER, B. C. (2005) Mineralocorticoid versus glucocorticoid receptor occupancy mediating aldosterone-stimulated sodium transport in a novel renal cell line. *Journal of the American Society of Nephrology,* 16**,** 878-891.

GARCIA-ECHEVERRIA, C. & SELLERS, W. R. (2008) Drug discovery approaches targeting the PI3K/Akt pathway in cancer. *Oncogene,* 27**,** 5511-5526.

GARCÍA-MARTÍNEZ, J. M. & ALESSI, D. R. (2008) mTOR complex 2 (mTORC2) controls hydrophobic motif phosphorylation and activation of serum- and glucocorticoid-induced protein kinase 1 (SGK1). *Biochemical Journal,* 416**,** 375-385.

GARTY, H. & PALMER, L. G. (1997) Epithelial sodium channels: Function, structure and regulation. *Physiological Reviews,* 77**,** 359-396.

GELLER, D. S., RODRIGUEZ-SORIANO, J., VALLO BOADO, A., SCHIFTER, S., BAYER, M., CHANG, S. S. & LIFTON, R. P. (1998) Mutations in the mineralocorticoid receptor gene cause autosomal dominant pseudohypoaldosteronism type I. *Nature Genetics,* 19**,** 279-281.

GONIN, S., DESCHÊNES, G., ROGER, F., BENS, M., MARTIN, P. Y., CARPENTIER, J. L., VANDEWALLE, A., DOUCET, A. & FÉRAILLE, E. (2001) Cyclic AMP increases cell surface expression of functional Na,K-ATPase units in mammalian cortical collecting duct principal cells. *Molecular Biology of the Cell,* 12**,** 255-264.

GOULET, C. C., VOLK, K. A., ADAMS, C. M., PRINCE, L. S., STOKES, J. B. & SNYDER, P. M. (1998) Inhibition of the epithelial Na^+ channel by interaction of Nedd4 with a PY motif deleted in Liddle's syndrome. *Journal of Biological Chemistry,* 273**,** 30012-30017.

GRÜNDER, S., FIRSOV, D., CHANG, S. S., JAEGER, N. F., GAUTSCHI, I., SCHILD, L., LIFTON, R. P. & ROSSIER, B. C. (1997) A mutation causing pseudohypoaldosteronism type 1 identifies a conserved glycine that is involved in the gating of the epithelial sodium channel. *EMBO Journal,* 16**,** 899-907.

GUAN, Y., HAO, C., CHA, D. R., RAO, R., LU, W., KOHAN, D. E., MAGNUSON, M. A., REDHA, R., ZHANG, Y. & BREYER, M. D. (2005) Thiazolidinediones expand body fluid volume through PPARγ stimulation of ENaC-mediated renal salt absorption. *Nature Medicine,* 11**,** 861-866.

GUAN, Y., ZHANG, Y., BREYER, R. M., FOWLER, B., DAVIS, L., HÉBERT, R. L. & BREYER, M. D. (1998) Prostaglandin E_2 inhibits renal collecting duct Na^+ absorption by activating the EP_1 receptor. *Journal of Clinical Investigation,* 102**,** 194-201.

GUERTIN, D. A. & SABATINI, D. M. (2007) Defining the Role of mTOR in Cancer. *Cancer Cell,* 12**,** 9-22.

GUYTON, A. C., COLEMAN, T. G., COWLEY, A. W., SCHEEL, K. W., MANNING, R. D. & NORMAN, R. A. (1972) Arterial pressure regulation. Overriding dominance of the kidneys in long-term regulation and in hypertension. *The American Journal of Medicine,* 52**,** 584-594.

HALLOWS, K. R., WANG, H., EDINGER, R. S., BUTTERWORTH, M. B., OYSTER, N. M., LI, H., BUCK, J., LEVIN, L. R., JOHNSON, J. P. & PASTOR-SOLER, N. M. (2009) Regulation of epithelial Na^+ transport by soluble adenylyl cyclase in kidney collecting duct cells. *Journal of Biological Chemistry,* 284**,** 5774-5783.

HANDLER, J. S., PRESTON, A. S. & PERKINS, F. M. (1981a) The effect of adrenal steroid hormones on epithelia formed in culture by A6 cells. *Annals of the New York Academy of Sciences,* Vol. 372**,** 442-454.

HANDLER, J. S., PRESTON, A. S., PERKINS, F. M., MATSUMURA, M., JOHNSON, J. P. & WATLINGTON, C. O. (1981b) The effect of adrenal steroid hormones on epithelia formed in culture by A6 cells. *Ann N Y Acad Sci,* 372**,** 442-54.

HANSSON, J. H., NELSON-WILLIAMS, C., SUZUKI, H., SCHILD, L., SHIMKETS, R., LU, Y., CANESSA, C., IWASAKI, T., ROSSIER, B. & LIFTON, R. P. (1995) Hypertension caused by a truncated epithelial sodium channel γ subunit: Genetic heterogeneity of Liddle syndrome. *Nature Genetics,* 11**,** 76-82.

HARVEY, B. J., THOMAS, S. R. & EHRENFELD, J. (1988) Intracellular pH controls cell membrane Na^+ and K^+ conductances and transport in frog skin epithelium. *Journal of General Physiology,* 92**,** 767-791.

HE-PING, M., SAXENA, S. & WARNOCK, D. G. (2002) Anionic phospholipids regulate native and expressed epithelial sodium channel (ENaC). *Journal of Biological Chemistry,* 277**,** 7641-7644.

HELMAN, S. I., LIU, X., BALDWIN, K., BLAZER-YOST, B. L. & ELS, W. J. (1998) Time-dependent stimulation by aldosterone of blocker-sensitive ENaCs in A6 epithelia. *American Journal of Physiology - Cell Physiology,* 274**,** C947-C957.

HELMS, M. N., FEJES-TÓTH, G. & NÁRAY-FEJES-TÓTH, A. (2003) Hormone-regulated transepithelial Na^+ transport in mammalian CCD cells requires SGK1 expression. *American Journal of Physiology - Renal Physiology,* 284**,** F480-F487.

HERRERA, F. C. (1965) Effect of insulin on short-circuit current and sodium transport across toad urinary bladder. *The American journal of physiology,* 209**,** 819-824.

HERRERA, F. C., WHITTEMBURY, G. & PLANCHART, A. (1963) Effect of insulin on short-circuit current across isolated frog skin in the presence of calcium and magnesium. *BBA - Biochimica et Biophysica Acta,* 66**,** 170-172.

HONG, F., LARREA, M. D., DOUGHTY, C., KWIATKOWSKI, D. J., SQUILLACE, R. & SLINGERLAND, J. M. (2008) mTOR-Raptor Binds and Activates SGK1 to Regulate p27 Phosphorylation. *Molecular Cell,* 30**,** 701-711.

HONG, G. Z., LOCKHART, A., DAVIS, B., RAHMOUNE, H., BAKER, S., YE, L., THOMPSON, P., SHOU, Y. P., O'SHAUGHNESSY, K., RONCO, P. & BROWN, J. (2003) PPARγ activation enhances cell surface ENaCα via up-regulation of SGK1 in human collecting duct cells. *FASEB Journal,* 17**,** 1966-8.

HUGHEY, R. P., MUELLER, G. M., BRUNS, J. B., KINLOUGH, C. L., POLAND, P. A., HARKLEROAD, K. L., CARATTINO, M. D. & KLEYMAN, T. R. (2003) Maturation of the epithelial Na^+ channel involves proteolytic processing of the α- and γ-subunits. *Journal of Biological Chemistry,* 278**,** 37073-37082.

HUMMLER, E., BARKER, P., GALZY, J., BEERMANN, F., VERDUMO, C., SCHMIDT, A., BOUCHER, R. & ROSSIER, B. C. (1996) Early death due to defective neonatal lung liquid clearance in αENaC-deficient mice. *Nature Genetics,* 12**,** 325-328.

HUMMLER, E., BARKER, P., TALBOT, C., WANG, Q., VERDUMO, C., GRUBB, B., GATZY, J., BURNIER, M., HORISBERGER, J. D., BEERMANN, F., BOUCHER, R. & ROSSIER, B. C. (1997) A mouse model for the renal salt-wasting syndrome pseudohypoaldosteronism. *Proceedings of the National Academy of Sciences of the United States of America,* 94**,** 11710-11715.

HUMMLER, E. & HORISBERGER, J. D. (1999) Genetic disorders of membrane transport V. The epithelial sodium channel and its implication in human diseases. *American Journal of Physiology,* 276**,** G567-G571.

ICHIMURA, T., YAMAMURA, H., SASAMOTO, K., TOMINAGA, Y., TAOKA, M., KAKIUCHI, K., SHINKAWA, T., TAKAHASHI, N., SHIMADA, S. & ISOBE, T. (2005) 14-3-3 Proteins modulate the expression of epithelial Na^+ channels by phosphorylation-dependent interaction with Nedd4-2 ubiquitin ligase. *Journal of Biological Chemistry,* 280**,** 13187-13194.

INGLIS, S. K., BROWN, S. G., CONSTABLE, M. J., MCTAVISH, N., OLVER, R. E. & WILSON, S. M. (2007) A Ba^{2+}-resistant, acid-sensitive K^+ conductance in Na^+-absorbing H441 human airway epithelial cells. *American Journal of Physiology-Lung Cellular and Molecular Physiology,* 292**,** L1304-L1312.

INGLIS, S. K., GALLACHER, M., BROWN, S. G., MCTAVISH, N., GETTY, J., HUSBAND, E. M., MURRAY, J. T. & WILSON, S. M. (2009) SGK1 activity in Na^+ absorbing airway epithelial cells monitored by assaying NDRG1-$Thr^{346/356/366}$ phosphorylation. *Pflugers Archiv European Journal of Physiology,* 457**,** 1287-1301.

ITANI, O. A., LIU, K. Z., CORNISH, K. L., CAMPBELL, J. R. & THOMAS, C. P. (2002) Glucocorticoids stimulate human sgk1 gene expression by activation of a GRE in its 5'-flanking region. *American Journal of Physiology - Endocrinology and Metabolism,* 283**,** E971-E979.

JASTI, J., FURUKAWA, H., GONZALES, E. B. & GOUAUX, E. (2007) Structure of acid-sensing ion channel 1 at 1.9 Å resolution and low pH. *Nature,* 449**,** 316-323.

KAMYNINA, E., DEDONNEVILLE, C., DENS, M., VANDEWALLE, A. & STAUB, O. (2001a) A novel mouse Nedd4 protein suppresses the activity of the epithelial Na^+ channel. *FASEB Journal,* 15**,** 204-214.

KAMYNINA, E. & STAUB, O. (2002) Concerted action of ENaC, Nedd4-2, and Sgk1 in transepithelial Na^+ transport. *American Journal of Physiology - Renal Physiology,* 283**,** F377-F387.

KAMYNINA, E., TAUXE, C. & STAUB, O. (2001b) Distinct characteristics of two human Nedd4 proteins with respect to epithelial Na^+ channel regulation. *American Journal of Physiology - Renal Physiology,* 281**,** F469-F477.

KELLENBERGER, S. & SCHILD, L. (2002) Epithelial sodium channel/degenerin family of ion channels: A variety of functions for a shared structure. *Physiological Reviews,* 82**,** 735-767.

KEMENDY, A. E., KLEYMAN, T. R. & EATON, D. C. (1992) Aldosterone alters the open probability of amiloride-blockable sodium channels in A6 epithelia. *American Journal of Physiology - Cell Physiology,* 263**,** C825-C837.

KOBAYASHI, T. & COHEN, P. (1999) Activation of serum- and glucocorticoid-regulated protein kinase by agonists that activate phosphatidylinositide 3-kinase is mediated by 3-phosphoinositide-dependent protein kinase-1 (PDK1) and PDK2. *Biochemical Journal,* 339**,** 319-328.

KOEPPEN, B. M. & STANTON, B. A. (2007a) Chapter 2. Structure and Function of the Kidneys, *Renal Physiology,* 4th Edition, 19-30, Mosby Elsevier, Philadelphia.

KOEPPEN, B. M. & STANTON, B. A. (2007b) Chapter 4. Renal Transport Mechanisms: NaCl and water reabsorption along the nephron, *Renal Physiology,* Fourth Edition, 47-70, Mosby Elsevier, Philadelphia.

KOMANDER, D., FAIRSERVICE, A., DEAK, M., KULAR, G. S., PRESCOTT, A. R., DOWNES, C. P., SAFRANY, S. T., ALESSI, D. R. & VAN AALTEN, D. M. F. (2004) Structural insights into the regulation of PDK1 by phosphoinositides and inositol phosphates. *EMBO Journal,* 23**,** 3918-3928.

KOSARI, F., SHENG, S., LI, J., MAK, D. O. D., FOSKETT, J. K. & KLEYMAN, T. R. (1998) Subunit stoichiometry of the epithelial sodium channel. *Journal of Biological Chemistry,* 273**,** 13469-13474.

KOVACINA, K. S., PARK, G. Y., BAE, S. S., GUZZETTA, A. W., SCHAEFER, E., BIRNBAUM, M. J. & ROTH, R. A. (2003) Identification of a proline-rich Akt substrate as a 14-3-3 binding partner. *Journal of Biological Chemistry,* 278**,** 10189-10194.

KUNZELMANN, K., BACHHUBER, T., REGEER, R., MARKOVICH, D., SUN, J. & SCHREIBER, R. (2005) Purinergic inhibition of the epithelial Na^+ transport via hydrolysis of PIP_2. *FASEB Journal,* 19**,** 142-143.

LANG, F., ARTUNC, F. & VALLON, V. (2009) The physiological impact of the serum and glucocorticoid-inducible kinase SGK1. *Current Opinion in Nephrology and Hypertension,* 18**,** 439-448.

LEE, I. H., CAMPBELL, C. R., COOK, D. I. & DINUDOM, A. (2008) Regulation of epithelial Na^+ channels by aldosterone: Role of Sgk1. *Clinical and Experimental Pharmacology and Physiology,* 35**,** 235-241.

LEE, I. H., DINUDOM, A., SANCHEZ-PEREZ, A., KUMAR, S. & COOK, D. I. (2007) Akt mediates the effect of insulin on epithelial sodium channels by inhibiting Nedd4-2. *Journal of Biological Chemistry,* 282**,** 29866-29873.

LEHMANN, J. M., MOORE, L. B., SMITH-OLIVER, T. A., WILKISON, W. O., WILLSON, T. M. & KLIEWER, S. A. (1995) An antidiabetic thiazolidinedione is a high affinity ligand for peroxisome proliferator-

activated receptor γ (PPARγ). *Journal of Biological Chemistry,* 270**,** 12953-12956.

LIANG, X., PETERS, K. W., BUTTERWORTH, M. B. & FRIZZELL, R. A. (2006) 14-3-3 Isoforms are induced by aldosterone and participate in its regulation of epithelial sodium channels. *Journal of Biological Chemistry,* 281**,** 16323-16332.

LIFTON, R. P., GHARAVI, A. G. & GELLER, D. S. (2001) Molecular mechanisms of human hypertension. *Cell,* 104**,** 545-556.

LIN, H. H., ZENTNER, M. D., HO, H. L. L., KIM, K. J. & ANN, D. K. (1999) The gene expression of the amiloride-sensitive epithelial sodium channel α-subunit is regulated by antagonistic effects between glucocorticoid hormone and Ras pathways in salivary epithelial cells. *Journal of Biological Chemistry,* 274**,** 21544-21554.

LINGUEGLIA, E., VOILLEY, N., WALDMANN, R., LAZDUNSKI, M. & BARBRY, P. (1993) Expression cloning of an epithelial amiloride-sensitive Na^+ channel. A new channel type with homologies to Caenorhabditis elegans degenerins. *FEBS Letters,* 318**,** 95-99.

LOFFING, J. & KORBMACHER, C. (2009) Regulated sodium transport in the renal connecting tubule (CNT) via the epithelial sodium channel (ENaC). *Pflugers Archiv European Journal of Physiology,* 458**,** 111-135.

LOFFING, J., PIETRI, L., AREGGER, F., BLOCH-FAURE, M., ZIEGLER, U., MENETON, P., ROSSIER, B. C. & KAISSLING, B. (2000) Differential subcellular localization of ENaC subunits in mouse kidney in response to high- and low-Na diets. *American Journal of Physiology - Renal Physiology,* 279**,** F252-F258.

LOFFING, J., ZECEVIC, M., FÉRAILLE, E., KAISSLING, B., ASHER, C., ROSSIER, B. C., FIRESTONE, G. L., PEARCE, D. & VERREY, F. (2001) Aldosterone induces rapid apical translocation of ENaC in early portion of renal collecting system: Possible role of SGK. *American Journal of Physiology - Renal Physiology,* 280**,** F675-F682.

LOGIE, L., RUIZ-ALCARAZ, A. J., KEANE, M., WOODS, Y. L., BAIN, J., MARQUEZ, R., ALESSI, D. R. & SUTHERLAND, C. (2007) Characterization of a protein kinase B inhibitor in vitro and in insulin-treated liver cells. *Diabetes,* 56**,** 2218-2227.

LU, C., PRIBANIC, S., DEBONNEVILLE, A., JIANG, C. & ROTIN, D. (2007) The PY motif of ENaC, mutated in liddle syndrome, regulates channel internalization, sorting and mobilization from subapical pool. *Traffic,* 8**,** 1246-1264.

LU, M., WANG, J., JONES, K. T., IVES, H. E., FELDMAN, M. E., YAO, L. J., SHOKAT, K. M., ASHRAFI, K. & PEARCE, D. (2010) mTOR complex-2 activates ENaC by phosphorylating SGK1. *Journal of the American Society of Nephrology,* 21**,** 811-818.

MARUNAKA, Y., HAGIWARA, N. & TOHDA, H. (1992) Insulin activates single amiloride-blockable Na channels in a distal nephron cell line (A6). *American Journal of Physiology - Renal Fluid and Electrolyte Physiology,* 263**,** 392-400.

MASILAMANI, S., KIM, G. H., MITCHELL, C., WADE, J. B. & KNEPPER, M. A. (1999) Aldosterone-mediated regulation of ENaC α, β, and γ

subunit proteins in rat kidney. *Journal of Clinical Investigation,* 104**,** R19-R23.

MILLER, J. H. & BOGDONOFF, M. D. (1954) Antidiuresis associated with administration of insulin. *J Appl Physiol,* 6**,** 509-512.

MORA, A., KOMANDER, D., VAN AALTEN, D. M. F. & ALESSI, D. R. (2004) PDK1, the master regulator of AGC kinase signal transduction. *Seminars in Cell and Developmental Biology,* 15**,** 161-170.

MOREL, F. (1981) Sites of hormone action in the mammalian nephron. *The American journal of physiology,* 240**,** F159-F164.

MORRIS, R. G. & SCHAFER, J. A. (2002) cAMP increases density of ENaC subunits in the apical membrane of MDCK cells in direct proportion to amiloride-sensitive Na^+ transport. *Journal of General Physiology,* 120**,** 71-85.

MULLER, O. G., PARNOVA, R. G., CENTENO, G., ROSSIER, B. C., FIRSOV, D. & HORISBERGER, J. D. (2003) Mineralocorticoid effects in the kidney: Correlation between αENaC, GILZ, and Sgk-1 mRNA expression and urinary excretion of Na^+ and K^+. *Journal of the American Society of Nephrology,* 14**,** 1107-1115.

MUNE, T., ROGERSON, F. M., NIKKILA, H., AGARWAL, A. K. & WHITE, P. C. (1995) Human hypertension caused by mutations in the kidney isozyme of 11β–hydroxysteroid dehydrogenase. *Nature Genetics,* 10**,** 394-399.

MURRAY, J. T., CAMPBELL, D. G., MORRICE, N., AULD, G. C., SHPIRO, N., MARQUEZ, R., PEGGIE, M., BAIN, J., BLOOMBERG, G. B., GRAHAMMER, F., LANG, F., WULFF, P., KUHL, D. & COHEN, P. (2004) Exploitation of KESTREL to identify NDRG family members as physiological substrates for SGK1 and GSK3. *Biochemical Journal,* 384**,** 477-488.

NAGY, E., NARAY-FEJES-TOTH, A. & FEJES-TOTH, G. (1994) Vasopressin activates a chloride conductance in cultured cortical collecting duct cells. *American Journal of Physiology - Renal Fluid and Electrolyte Physiology,* 267**,** F831-F838.

NAKHOUL, N. L., HERING-SMITH, K. S., GAMBALA, C. T. & HAMM, L. L. (1998) Regulation of sodium transport in M-1 cells. *American Journal of Physiology - Renal Physiology,* 275**,** F998-F1007.

NÁRAY-FEJES-TÓTH, A., CANESSA, C., CLEAVELAND, E. S., ALDRICH, G. & FEJES-TÓTH, G. (1999) sgk is an aldosterone-induced kinase in the renal collecting duct. Effects on epithelial Na^+ channels. *Journal of Biological Chemistry,* 274**,** 16973-16978.

NÁRAY-FEJES-TÓTH, A., HELMS, M. N., STOKES, J. B. & FEJES-TÓTH, G. (2004a) Regulation of sodium transport in mammalian collecting duct cells by aldosterone-induced kinase, SGK1: Structure/function studies. *Molecular and Cellular Endocrinology,* 217**,** 197-202.

NÁRAY-FEJES-TÓTH, A., SNYDER, P. M. & FEJES-TÓTH, G. (2004b) The kidney-specific WNK1 isoform is induced by aldosterone and stimulates epithelial sodium channel-mediated Na^+ transport. *Proceedings of the National Academy of Sciences of the United States of America,* 101**,** 17434-17439.

NEW, M. I., LEVINE, L. S. & BIGLIERI, E. G. (1977) Evidence for an unidentified steroid in a child with apparent mineralocorticoid hypertension. *Journal of Clinical Endocrinology and Metabolism,* 44**,** 924-933.

NIELSEN, S., FRØKIÆR, J., MARPLES, D., KWON, T. H., AGRE, P. & KNEPPER, M. A. (2002) Aquaporins in the kidney: From molecules to medicine. *Physiological Reviews,* 82**,** 205-244.

NIZET, A., LEFEBVRE, P. & CRABBÉ, J. (1971) Control by insulin of sodium potassium and water excretion by the isolated dog kidney. *Pflugers Archiv European Journal of Physiology,* 323**,** 11-20.

NOFZIGER, C., CHEN, L., SHANE, M. A., SMITH, C. D., BROWN, K. K. & BLAZER-YOST, B. L. (2005) PPARγ agonists do not directly enhance basal or insulin-stimulated Na^+ transport via the epithelial Na^+ channel. *Pflugers Archiv European Journal of Physiology,* 451**,** 445-453.

OTULAKOWSKI, G., DUAN, W., GANDHI, S. & O'BRODOVICH, H. (2007) Steroid and oxygen effects on eIF4F complex, mTOR, and ENaC translation in fetal lung epithelia. *American Journal of Respiratory Cell and Molecular Biology,* 37**,** 457-466.

PALMER, L. G. (1992) Epithelial Na channels: Function and diversity. *Annual Review of Physiology,* 54**,** 51-66.

PARK, J., LEONG, M. L. L., BUSE, P., MAIYAR, A. C., FIRESTONE, G. L. & HEMMINGS, B. A. (1999) Serum and glucocorticoid-inducible kinase (SGK) is a target of the PI 3-kinase-stimulated signaling pathway. *EMBO Journal,* 18**,** 3024-3033.

PĂUNESCU, T. G., BLAZER-YOST, B. L., VLAHOS, C. J. & HELMAN, S. I. (2000) LY-294002-inhibitable PI 3-kinase and regulation of baseline rates of Na^+ transport in A6 epithelia. *American Journal of Physiology - Cell Physiology,* 279**,** C236-C247.

PAVLOV, T. S., LEVCHENKO, V., KARPUSHEV, A. V., VANDEWALLE, A. & STARUSCHENKO, A. (2009) Peroxisome proliferator-activated receptor γ antagonists decrease Na^+ transport via the epithelial Na^+ channel. *Molecular Pharmacology,* 76**,** 1333-1340.

PEARCE, D. & KLEYMAN, T. R. (2007) Salt, sodium channels, and SGK1. *Journal of Clinical Investigation,* 117**,** 592-595.

PEARCE, L. R., KOMANDER, D. & ALESSI, D. R. (2010) The nuts and bolts of AGC protein kinases. *Nature Reviews Molecular Cell Biology,* 11**,** 9-22.

PERROTTI, N., HE, R. A., PHILLIPS, S. A., HAFT, C. R. & TAYLOR, S. I. (2001) Activation of Serum- and Glucocorticoid-induced Protein Kinase (Sgk) by Cyclic AMP and Insulin. *Journal of Biological Chemistry,* 276**,** 9406-9412.

POCHYNYUK, O., BUGAJ, V., VANDEWALLE, A. & STOCKAND, J. D. (2008) Purinergic control of apical plasma membrane $PI(4,5)P_2$ levels sets ENaC activity in principal cells. *American Journal of Physiology - Renal Physiology,* 294**,** F38-F46.

POCHYNYUK, O., TONG, Q., STARUSCHENKO, A., MA, H. P. & STOCKAND, J. D. (2006) Regulation of the epithelial Na^+ channel (ENaC) by phosphatidylinositides. *American Journal of Physiology - Renal Physiology,* 290**,** F949-F957.

PRADERVAND, S., BARKER, P. M., WANG, Q., ERNST, S. A., BEERMANN, F., GRUBB, B. R., BURNIER, M., SCHMIDT, A., BINDELS, R. J. M., GATZY, J. T., ROSSIER, B. C. & HUMMLER, E. (1999a) Salt restriction induces pseudohypoaldosteronism type 1 in mice expressing low levels of the β-subunit of the amiloride-sensitive epithelial sodium channel. *Proceedings of the National Academy of Sciences of the United States of America,* 96**,** 1732-1737.

PRADERVAND, S., WANG, Q., BURNIER, M., BEERMANN, F., HORISBERGER, J. D., HUMMLER, E. & ROSSIER, B. C. (1999b) A mouse model for Liddle's syndrome. *Journal of the American Society of Nephrology,* 10**,** 2527-2533.

PRATT, J. H. (2005) Central role for ENaC in development of hypertension. *Journal of the American Society of Nephrology,* 16**,** 3154-3159.

PROUD, C. G. (2007) Signalling to translation: How signal transduction pathways control the protein synthetic machinery. *Biochemical Journal,* 403**,** 217-234.

RAMMINGER, S. J., RICHARD, K., INGLIS, S. K., LAND, S. C., OLVER, R. E. & WILSON, S. M. (2004) A regulated apical Na^+ conductance in dexamethasone-treated H441 airway epithelial cells. *American Journal of Physiology - Lung Cellular and Molecular Physiology,* 287**,** L411-L419.

RAYNAUD, F. I., ECCLES, S., CLARKE, P. A., HAYES, A., NUTLEY, B., ALIX, S., HENLEY, A., DI-STEFANO, F., AHMAD, Z., GUILLARD, S., BJERKE, L. M., KELLAND, L., VALENTI, M., PATTERSON, L., GOWAN, S., BRANDON, A. D. H., HAYAKAWA, M., KAIZAWA, H., KOIZUMI, T., OHISHI, T., PATEL, S., SAGHIR, N., PARKER, P., WATERFIELD, M. & WORKMAN, P. (2007) Pharmacologic characterization of a potent inhibitor of class I phosphatidylinositide 3-kinases. *Cancer Research,* 67**,** 5840-5850.

RECORD, R. D., FROELICH, L. L., VLAHOS, C. J. & BLAZER-YOST, B. L. (1998) Phosphatidylinositol 3-kinase activation is required for insulin-stimulated sodium transport in A6 cells. *American Journal of Physiology - Endocrinology and Metabolism,* 274**,** C531-C536.

REXHEPAJ, R., ARTUNC, F., GRAHAMMER, F., NASIR, O., SANDU, C., FRIEDRICH, B., KUHL, D. & LANG, F. (2006) SGK1 is not required for regulation of colonic ENaC activity. *Pflugers Archiv European Journal of Physiology,* 453**,** 97-105.

ROBERT-NICOUD, M., FLAHAUT, M., ELALOUF, J. M., NICOD, M., SALINAS, M., BENS, M., DOUCET, A., WINCKER, P., ARTIGUENAVE, F., HORISBERGER, J. D., VANDEWALLE, A., ROSSIER, B. C. & FIRSOV, D. (2001) Transcriptome of a mouse kidney cortical collecting duct cell line: Effects of aldosterone and vasopressin. *Proceedings of the National Academy of Sciences of the United States of America,* 98**,** 2712-2716.

ROKAW, M. D., WEST, M. & JOHNSON, J. P. (1996a) Rapamycin inhibits protein kinase C activity and stimulates Na^+ transport in A6 cells. *Journal of Biological Chemistry,* 271**,** 32468-32473.

ROKAW, M. D., WEST, M. E., PALEVSKY, P. M. & JOHNSON, J. P. (1996b) FK-506 and rapamycin but not cyclosporin inhibit aldosterone-stimulated

sodium transport in A6 cells. *American Journal of Physiology - Cell Physiology,* 271**,** C194-C202.

ROSSIER, B. C. & SCHILD, L. (2008) Epithelial sodium channel: Mendelian versus essential hypertension. *Hypertension,* 52**,** 595-600.

SAAD, S., AGAPIOU, D. J., CHEN, X. M., STEVENS, V. & POLLOCK, C. A. (2009) The role of Sgk-1 in the upregulation of transport proteins by PPAR-γ agonists in human proximal tubule cells. *Nephrology Dialysis Transplantation,* 24**,** 1130-1141.

SARBASSOV, D. D., GUERTIN, D. A., ALI, S. M. & SABATINI, D. M. (2005) Phosphorylation and regulation of Akt/PKB by the rictor-mTOR complex. *Science,* 307**,** 1098-1101.

SCHAFER, J. A. (2002) Abnormal regulation of ENaC: Syndromes of salt retention and salt wasting by the collecting duct. *American Journal of Physiology - Renal Physiology,* 283**,** F221-F235.

SCHAFER, J. A. & TROUTMAN, S. L. (1990) cAMP mediates the increase in apical membrane Na^+ conductance produced in rat CCD by vasopressin. *American Journal of Physiology - Renal Fluid and Electrolyte Physiology,* 259**,** F823-F831.

SCHILD, L., LU, Y., GAUTSCHI, I., SCHNEEBERGER, E., LIFTON, R. P. & ROSSIER, B. C. (1996) Identification of a PY motif in the epithelial Na channel subunits as a target sequence for mutations causing channel activation found in Liddle syndrome. *EMBO Journal,* 15**,** 2381-2387.

SHANE, M. A., NOFZIGER, C. & BLAZER-YOST, B. L. (2006) Hormonal regulation of the epithelial Na^+ channel: From amphibians to mammals. *General and Comparative Endocrinology,* 147**,** 85-92.

SHELLY, C. & HERRERA, R. (2002) Activation of SGK1 by HGF, Rac1 and integrin-mediated cell adhesion in MDCK cells: PI-3K-dependent and -independent pathways. *Journal of Cell Science,* 115**,** 1985-1993.

SHEN, J. P. & COTTON, C. U. (2003) Epidermal growth factor inhibits amiloride-sensitive sodium absorption in renal collecting duct cells. *American Journal of Physiology - Renal Physiology,* 284**,** F57-F64.

SHERK, A. B., FRIGO, D. E., SCHNACKENBERG, C. G., BRAY, J. D., LAPING, N. J., TRIZNA, W., HAMMOND, M., PATTERSON, J. R., THOMPSON, S. K., KAZMIN, D., NORRIS, J. D. & MCDONNELL, D. P. (2008) Development of a small-molecule serum- and glucocorticoid-regulated kinase-1 antagonist and its evaluation as a prostate cancer therapeutic. *Cancer Research,* 68**,** 7475-7483.

SHI, H., ASHER, C., CHIGAEV, A., YUNG, Y., REUVENY, E., SEGER, R. & GARTY, H. (2002) Interactions of β and γENaC with Nedd4 can be facilitated by an ERK-mediated phosphorylation. *Journal of Biological Chemistry,* 277**,** 13539-13547.

SHIGAEV, A., ASHER, C., LATTER, H., GART, H. & REUVENY, E. (2000) Regulation of sgk by aldosterone and its effects on the epithelial Na^+ channel. *American Journal of Physiology - Renal Physiology,* 278**,** F613-F619.

SHIMKETS, R. A., WARNOCK, D. G., BOSITIS, C. M., NELSON-WILLIAMS, C., HANSSON, J. H., SCHAMBELAN, M., GILL JR, J. R., ULICK, S., MILORA, R. V., FINDLING, J. W., CANESSA, C. M.,

ROSSIER, B. C. & LIFTON, R. P. (1994) Liddle's syndrome: Heritable human hypertension caused by mutations in the β subunit of the epithelial sodium channel. *Cell,* 79**,** 407-414.

SNYDER, P. M. (2000) Liddle's syndrome mutations disrupt cAMP-mediated translocation of the epithelial Na^+ channel to the cell surface. *Journal of Clinical Investigation,* 105**,** 45-53.

SNYDER, P. M. (2002) The epithelial Na^+ channel: Cell surface insertion and retrieval in Na^+ homeostasis and hypertension. *Endocrine Reviews,* 23**,** 258-275.

SNYDER, P. M., CHENG, C., PRINCE, L. S., ROGERS, J. C. & WELSH, M. J. (1998) Electrophysiological and biochemical evidence that DEG/ENaC cation channels are composed of nine subunits. *Journal of Biological Chemistry,* 273**,** 681-684.

SNYDER, P. M., MCDONALD, F. J., STOKES, J. B. & WELSH, M. J. (1994) Membrane Topology of the Amiloride-Sensitive Epithelial Sodium-Channel. *Journal of Biological Chemistry,* 269**,** 24379-24383.

SNYDER, P. M., OLSON, D. R., KABRA, R., ZHOU, R. & STEINES, J. C. (2004a) cAMP and serum and glucocorticoid-inducible kinase (SGK) regulate the epithelial Na^+ channel through convergent phosphorylation of Nedd4-2. *Journal of Biological Chemistry,* 279**,** 45753-45758.

SNYDER, P. M., OLSON, D. R. & THOMAS, B. C. (2002) Serum and glucocorticoid-regulated kinase modulates Nedd4-2-mediated inhibition of the epithelial Na^+ channel. *Journal of Biological Chemistry,* 277**,** 5-8.

SNYDER, P. M., STEINES, J. C. & OLSON, D. R. (2004b) Relative Contribution of Nedd4 and Nedd4-2 to ENaC Regulation in Epithelia Determined by RNA Interference. *Journal of Biological Chemistry,* 279**,** 5042-5046.

SONG, J., KNEPPER, M. A., HU, X., VERBALIS, J. G. & ECELBARGER, C. A. (2004) Rosiglitazone Activates Renal Sodium- and Water-Reabsorptive Pathways and Lowers Blood Pressure in Normal Rats. *Journal of Pharmacology and Experimental Therapeutics,* 308**,** 426-433.

SOUNDARARAJAN, R., ZHANG, T. T., WANG, J., VANDEWALLE, A. & PEARCE, D. (2005) A novel role for glucocorticoid-induced leucine zipper protein in epithelial sodium channel-mediated sodium transport. *Journal of Biological Chemistry,* 280**,** 39970-39981.

STARUSCHENKO, A., ADAMS, E., BOOTH, R. E. & STOCKAND, J. D. (2005) Epithelial Na^+ channel subunit stoichiometry. *Biophysical Journal,* 88**,** 3966-3975.

STARUSCHENKO, A., POCHYNYUK, O., VANDEWALLE, A., BUGAJ, V. & STOCKAND, J. D. (2007) Acute regulation of the epithelial Na^+ channel by phosphatidylinositide 3-OH kinase signaling in native collecting duct principal cells. *Journal of the American Society of Nephrology,* 18**,** 1652-1661.

STAUB, O., DHO, S., HENRY, P. C., CORREA, J., ISHIKAWA, T., MCGLADE, J. & ROTIN, D. (1996) WW domains of Nedd4 bind to the proline-rich PY motifs in the epithelial Na^+ channel deleted in Liddle's syndrome. *EMBO Journal,* 15**,** 2371-2380.

STAUB, O., GAUTSCHI, I., ISHIKAWA, T., BREITSCHOPF, K., CIECHANOVER, A., SCHILD, L. & ROTIN, D. (1997) Regulation of stability and function of the epithelial Na^+ channel (ENaC) by ubiquitination. *EMBO Journal,* 16**,** 6325-6336.

STOCKAND, J. D. (2002) New ideas about aldosterone signaling in epithelia. *American Journal of Physiology - Renal Physiology,* 282**,** F559-F576.

STOCKAND, J. D., BAO, H. F., SCHENCK, J., MALIK, B., MIDDLETON, P., SCHLANGER, L. E. & EATON, D. C. (2000) Differential effects of protein kinase C on the levels of epithelial Na channel subunit proteins. *Journal of Biological Chemistry,* 275**,** 25760-25765.

STOCKAND, J. D., SPIER, B. J., WORRELL, R. T., YUE, G., AL-BALDAWI, N. & EATON, D. C. (1999) Regulation of Na^+ reabsorption by the aldosterone-induced small G protein K-Ras2A. *Journal of Biological Chemistry,* 274**,** 35449-35454.

STOOS, B. A., NARAY-FEJES-TOTH, A., CARRETERO, O. A., ITO, S. & FEJES-TOTH, G. (1991) Characterization of a mouse cortical collecting duct cell line. *Kidney International,* 39**,** 1168-1175.

STRAUTNIEKS, S. S., THOMPSON, R. J., GARDINER, R. M. & CHUNG, E. (1996) A novel splice-site mutation in the γ subunit of the epithelial sodium channel gene in three pseudohypoaldosteronism type 1 families. *Nature Genetics,* 13**,** 248-250.

STUMVOLL, M. & HÄRING, H. U. (2002) Glitazones: Clinical effects and molecular mechanisms. *Annals of Medicine,* 34**,** 217-224.

SUMMA, V., MORDASINI, D., ROGER, F., BENS, M., MARTIN, P. Y., VANDEWALLE, A., VERREY, F. & FÉRAILLE, E. (2001) Short Term Effect of Aldosterone on Na,K-ATPase Cell Surface Expression in Kidney Collecting Duct Cells. *Journal of Biological Chemistry,* 276**,** 47087-47093.

SUN, X. J., ROTHENBERG, P., KAHN, C. R., BACKER, J. M., ARAKI, E., WILDEN, P. A., CAHILL, D. A., GOLDSTEIN, B. J. & WHITE, M. F. (1991) Structure of the insulin receptor substrate IRS-1 defines a unique signal transduction protein. *Nature,* 352**,** 73-77.

TANG, W. H. W. & MAROO, A. (2007) PPARγ agonists: Safety issues in heart failure. *Diabetes, Obesity and Metabolism,* 9**,** 447-454.

THOMAS, C. P., CAMPBELL, J. R., WRIGHT, P. J. & HUSTED, R. F. (2004) cAMP-stimulated Na^+ transport in H441 distal lung epithelial cells: Role of PKA, phosphatidylinositol 3-kinase, and sgk1. *American Journal of Physiology - Lung Cellular and Molecular Physiology,* 287**,** L843-L851.

THOMAS, J., DEETJEN, P., KO, W. H., JACOBI, C. & LEIPZIGER, J. (2001) $P2Y_2$ receptor-mediated inhibition of amiloride-sensitive short circuit current in M-1 mouse cortical collecting duct cells. *Journal of Membrane Biology,* 183**,** 115-124.

THOREEN, C. C., KANG, S. A., CHANG, J. W., LIU, Q., ZHANG, J., GAO, Y., REICHLING, L. J., SIM, T., SABATINI, D. M. & GRAY, N. S. (2009) An ATP-competitive mammalian target of rapamycin inhibitor reveals rapamycin-resistant functions of mTORC1. *Journal of Biological Chemistry,* 284**,** 8023-8032.

TONG, Q., BOOTH, R. E., WORRELL, R. T. & STOCKAND, J. D. (2004a) Regulation of Na^+ transport by aldosterone: Signaling convergence and cross talk between the PI3-K and MAPK1/2 cascades. *American Journal of Physiology - Renal Physiology,* 286**,** F1232-F1238.

TONG, Q., GAMPER, N., MEDINA, J. L., SHAPIRO, M. S. & STOCKAND, J. D. (2004b) Direct activation of the epithelial Na^+ channel by phosphatidylinositol 3,4,5-trisphosphate and phosphatidylinositol 3,4-bisphosphate produced by phosphoinositide 3-OH kinase. *Journal of Biological Chemistry,* 279**,** 22654-22663.

ULICK, S., LEVINE, L. S. & GUNCZLER, P. (1979) A syndrome of apparent mineralocorticoid excess associated with defects in the peripheral metabolism of cortisol. *Journal of Clinical Endocrinology and Metabolism,* 49**,** 757-764.

VALLON, V., HUMMLER, E., RIEG, T., POCHYNYUK, O., BUGAJ, V., SCHROTH, J., DECHENES, G., ROSSIER, B., CUNARD, R. & STOCKAND, J. (2009) Thiazolidinedione-induced fluid retention is independent of collecting duct αENaC activity. *Journal of the American Society of Nephrology,* 20**,** 721-729.

VAN DRIESSCHE, W. & LINDEMANN, B. (1979) Concentration dependence of currents through single sodium-Selective pores in frog skin [20]. *Nature,* 282**,** 519-520.

VASQUEZ, M. M., CASTRO, R., SEIDNER, S. R., HENSON, B. M., ASHTON, D. J. & MUSTAFA, S. B. (2008) Induction of serum- and glucocorticoid-induced kinase-1 (SGK1) by cAMP regulates increases in α-ENaC. *Journal of Cellular Physiology,* 217**,** 632-642.

VERREY, F. (1994) Antidiuretic hormone action in A6 cells: Effect on apical Cl and Na conductances and synergism with aldosterone for NaCl reabsorption. *Journal of Membrane Biology,* 138**,** 65-76.

VUAGNIAUX, G., VALLET, V., JAEGER, N. F., PFISTER, C., BENS, M., FARMAN, N., COURTOIS-COUTRY, N., VANDEWALLE, A., ROSSIER, B. C. & HUMMLER, E. (2000) Activation of the amiloride-sensitive epithelial sodium channel by the serine protease mCAP1 expressed in a mouse cortical collecting duct cell line. *Journal of the American Society of Nephrology,* 11**,** 828-834.

WALDMANN, R., CHAMPIGNY, G., BASSILANA, F., VOILLEY, N. & LAZDUNSKI, M. (1995) Molecular cloning and functional expression of a novel amiloride-sensitive Na^+ channel. *Journal of Biological Chemistry,* 270**,** 27411-27414.

WANG, H., TRAUB, L. M., WEIXEL, K. M., HAWRYLUK, M. J., SHAH, N., EDINGER, R. S., PERRY, C. J., KESTER, L., BUTTERWORTH, M. B., PETERS, K. W., KLEYMAN, T. R., FRIZZELL, R. A. & JOHNSON, J. P. (2006) Clathrin-mediated endocytosis of the epithelial sodium channel: Role of epsin. *Journal of Biological Chemistry,* 281**,** 14129-14135.

WANG, J., BARBRY, P., MAIYAR, A. C., ROZANSKY, D. J., BHARGAVA, A., LEONG, M., FIRESTONE, G. L. & PEARCE, D. (2001) SGK integrates insulin and mineralocorticoid regulation of epithelial sodium transport. *American Journal of Physiology - Renal Physiology,* 280**,** F303-F313.

WANG, J., KNIGHT, Z. A., FIEDLER, D., WILLIAMS, O., SHOKAT, K. M. & PEARCE, D. (2008) Activity of the p110-α subunit of phosphatidylinositol-3-kinase is required for activation of epithelial sodium transport. *American Journal of Physiology - Renal Physiology,* 295**,** F843-F850.

WARNOCK, D. G. & ROSSIER, B. C. (2005) Renal sodium handling: The role of the epithelial sodium channel. *Journal of the American Society of Nephrology,* 16**,** 3151-3153.

WEBSTER, M. K., GOYA, L. & FIRESTONE, G. L. (1993a) Immediate-early transcriptional regulation and rapid mRNA turnover of a putative serine/threonine protein kinase. *Journal of Biological Chemistry,* 268**,** 11482-11485.

WEBSTER, M. K., GOYA, L., GE, Y., MAIYAR, A. C. & FIRESTONE, G. L. (1993b) Characterization of sgk, a novel member of the serine/threonine protein kinase gene family which is transcriptionally induced by glucocorticoids and serum. *Molecular and Cellular Biology,* 13**,** 2031-2040.

WHITE, M. F., MARON, R. & KAHN, C. R. (1985) Insulin rapidly stimulates tyrosine phosphorylation of a M(r)-185,000 protein in intact cells. *Nature,* 318**,** 183-186.

WILLS, N. K., REUSS, L. & LEWIS, S. A. (1996) Chapter 1: Epithelia structure and function, *Epithelial Transport: A Guide to Methods and Experimental Analysis,* 1st Edition, 1-20, Chapman and Hall, Suffolk.

WILSON, S. M., MANSLEY, M. K., GETTY, J., HUSBAND, E. M., INGLIS, S. K. & HANSEN, M. K. (2010) Effects of peroxisome proliferator-activated receptor γ agonists on Na^+ transport and activity of the kinase SGK1 in epithelial cells from lung and kidney. *British Journal of Pharmacology,* 159**,** 678-688.

WULFF, P., VALLON, V., HUANG, D. Y., VÖLKL, H., YU, F., RICHTER, K., JANSEN, M., SCHLÜNZ, M., KLINGEL, K., LOFFING, J., KAUSELMANN, G., BÖSL, M. R., LANG, F. & KUHL, D. (2002) Impaired renal Na^+ retention in the sgkl-knockout mouse. *Journal of Clinical Investigation,* 110**,** 1263-1268.

WYMANN, M. P., BULGARELLI-LEVA, G., ZVELEBIL, M. J., PIROLA, L., VANHAESEBROECK, B., WATERFIELD, M. D. & PANAYOTOU, G. (1996) Wortmannin inactivates phosphoinositide 3-kinase by covalent modification of Lys-802, a residue involved in the phosphate transfer reaction. *Molecular and Cellular Biology,* 16**,** 1722-1733.

YANASE, M. & HANDLER, J. S. (1986) Activators of protein kinase C inhibit sodium transport in A6 epithelia. *American Journal of Physiology - Cell Physiology,* 250**,** C517-C522.

ZENTNER, M. D., LIN, H. H., WEN, X., KIM, K. J. & ANN, D. K. (1998) The amiloride-sensitive epithelial sodium channel α-subunit is transcriptionally down-regulated in rat parotid cells by the extracellular signal-regulated protein kinase pathway. *Journal of Biological Chemistry,* 273**,** 30770-30776.

ZHANG, H., ZHANG, A., KOHAN, D. E., NELSON, R. D., GONZALEZ, F. J. & YANG, T. (2005) Collecting duct-specific deletion of peroxisome

proliferator-activated receptor γ blocks thiazolidinedione-induced fluid retention. *Proceedings of the National Academy of Sciences of the United States of America,* 102**,** 9406-9411.